Skeletal muscle function in patients with spinal muscular atrophy

-(D)enervating studies with blocks and bikes-

Laura E. Habets

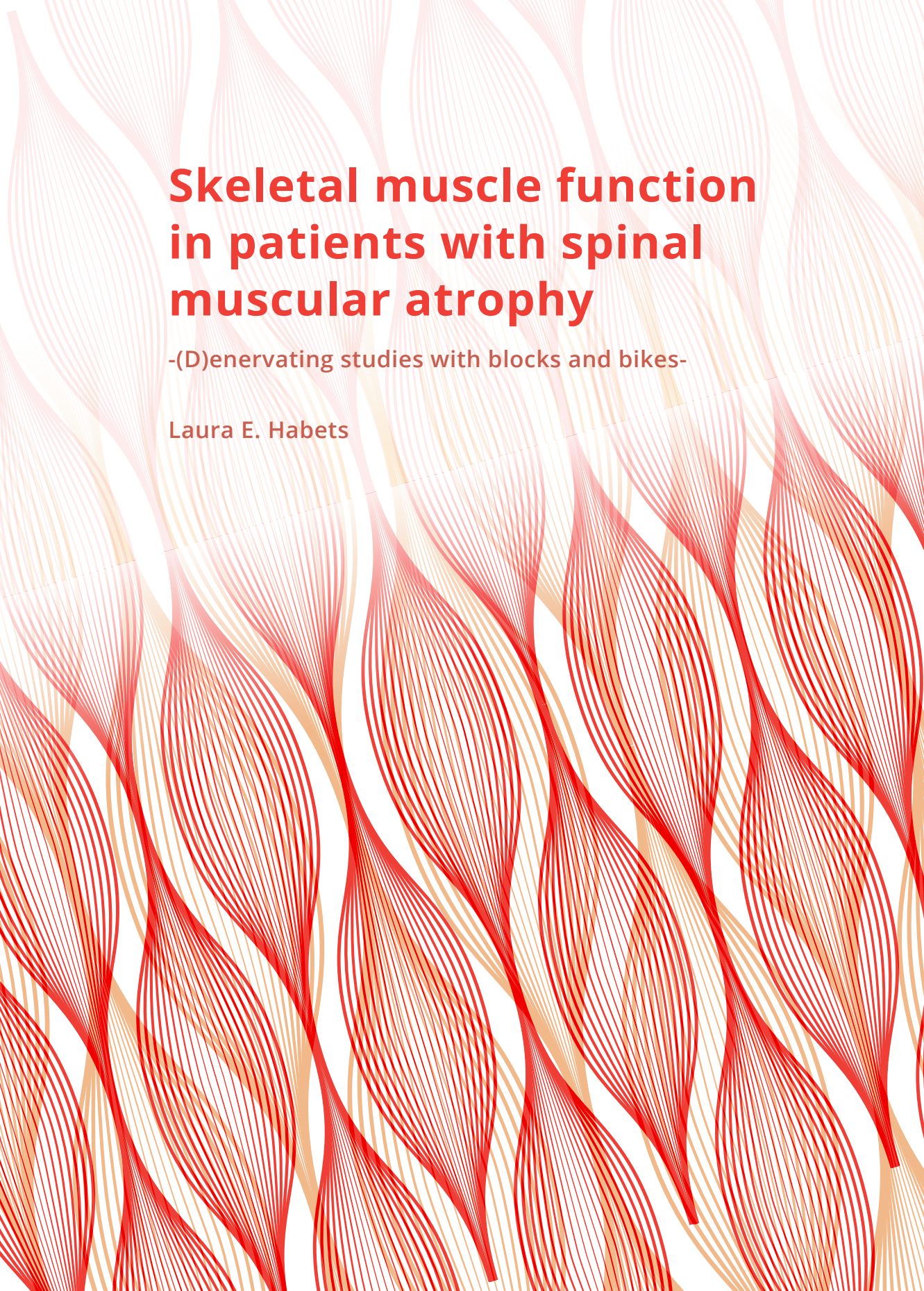

Skeletal muscle function in patients with spinal muscular atrophy

(D)enervating studies with blocks and bikes

Laura Eline Habets

Colofon

ISBN: 978-94-93270-54-1
DOI: 10.33540/727

Correspondence:
Laura E. Habets
l.e.habets@hotmail.com

Cover and printing: Guus Gijben | proefschrift-aio.nl
Layout: Laura E. Habets

The studies in this thesis were financially supported by the Prinses Beatrix Spierfonds and Stichting Spieren voor Spieren. Financial support for the publication of this thesis is gratefully acknowledged and was provided for by ChipSoft B.V. and Viatris.

Skeletal muscle function in patients with spinal muscular atrophy

(D)enervating studies with blocks and bikes

Skeletspierfunctie van patiënten met spinale musculaire atrofie

Enerverende studies met blokjes en fietsen

(met een samenvatting in het Nederlands)

Proefschrift

ter verkrijging van de graad van doctor aan de Universiteit Utrecht op gezag van de rector magnificus, prof. dr. H.R.B.M. Kummeling, ingevolge het besluit van het college voor promoties in het openbaar te verdedigen op 31 mei 2022 des middags te 4.15 uur

door

Laura Eline Habets

geboren op 3 november 1992 te Gouda

Promotoren:

Prof. dr. W.L. van der Pol

Prof. dr. E.E.S. Nieuwenhuis

Copromotoren:

Dr. B. Bartels

Dr. J.A.L. Jeneson

Table of contents

Chapter 1

General introduction

Spinal muscular atrophy

Epidemiology

Hereditary proximal spinal muscular atrophy (SMA) is an autosomal recessive neuromuscular disease with a prevalence of approximately 1-2 in 100.000 people and an incidence of 1:6000 – 1:12.000 live births.[1,2] This makes SMA, when untreated, one of the most common genetic causes of infant mortality, childhood morbidity and an important cause of childhood disability.[3] The Netherlands have a tradition to centralize treatment of rare disorders with expensive treatment. The Dutch SMA Center is part of the University Medical Center Utrecht. Its team curates the Dutch SMA patient registry that contains detailed clinical information of the large majority of patients with SMA, including natural history, biomarkers and level of functioning. The registry that was started in 2010 contains information of approximately 450 children and adults with SMA and is coupled with >5000 biobank samples. Studies described in this thesis would not have been possible without this registry and in particular without the consent and participation of all patients in this registry.

Pathophysiology

SMA is caused by the homozygous loss of function of the survival motor neuron 1 (*SMN1*) gene on chromosome 5q13.2.[1] The cause of SMA, most often a homozygous deletion of *SMN1*, was discovered in 1995.[1] This gene encodes a protein product called SMN protein. SMN protein is ubiquitous in cell types and across species and plays an important role in a large number of cell functions.[4] Complete absence of SMN protein is lethal early in embryonal development. A unique human feature is the fact that in the absence of the *SMN1* gene, residual levels of protein are produced by the highly homologous second *SMN* gene, *SMN2*. This gene crucially differs in one nucleotide in exon 7 from *SMN1*. Consequently, it is responsible for the production of low levels (±10-40%) of full length SMN protein in addition to a shortened SMN protein that lack axon 7.[4,5] The low levels of full length SMN protein produced by the *SMN2* gene ironically cause SMA since it allows embryonic development but is not sufficient to prevent α-motor neuron decline after birth.[3] The number of *SMN2* copies varies between patients, is inversely correlated with disease severity and is the most important modifier by explaining approximately 60% of variation in severity.[6–10]

SMA was for a very long time considered a lower motor neuron disorder. Recent studies challenge this concept and indicate that it is more likely a disorder that affects multiple tissues and organs, albeit with variation in severity. Abnormalities of anatomy and/or function have been reported in heart, brain, vascular system, bones, pancreas, liver, lungs, intestine and muscle of patients with SMA.[11,12] The main focus of this thesis is function of skeletal muscle tissue in patients with SMA.

Phenotype

The clinical classification system for SMA is since the 1990s based on the age of disease onset and achieved motor milestones (table 1). It originally distinguished three types that covered the severity range from severe neonatal onset to milder (later) childhood onset.[13,14] A late addition was adult onset SMA type 4.[15] Furthermore, a later modification was the distinction between SMA type 3a and 3b.[13–15] Patients with SMA type 3a often lose their ambulation in adolescence or early adulthood.[13–15] Patients with SMA type 3b often lose ambulation later in life (after the age of 40), if at all.[13–15]

Table 1. SMA classification system

SMA type	**1 (Wednig-Hoffmann syndrome)**	**2**	**3 (Kugelberg-Welander syndrome)**	**4**
Age at onset	0-6 months	6-18 months	3a: 1.5-3 years 3b: >3 years	>30 years
Incidence	50%	30%	20%	<1%
Able to sit unsupported	no	yes	yes	yes
Able to walk independently	no	no	yes	yes
Survival [15] (median)	prenatal death or several days - 17 years	majority survive into adulthood. Depending on mechanical ventilation	normal lifespan	normal lifespan

Muscle weakness

As a consequence of α-motor neuron degeneration, SMA is primarily characterized by weakness that dominates in the axial and proximal muscle groups of the extremities with a wide range of severity.[16,17] Lower extremities are more severely affected compared to upper extremities.[17] There is, however, a striking variation in vulnerability of different muscle groups.[3,17] In general, the m. diaphragm, elbow flexors, hip extensors and abductors, knee flexors and ankle dorsi- and plantar flexors are less severely affected compared to the m. intercostales, shoulder abductors, elbow extensors, hip flexors, hip adductors and knee extensors.[17–20] The exact cause is unknown, but could lie in differences in motor neuron pools in the spinal cord,[21–23] muscle fiber distribution,[24] neuromuscular junction (NMJ) dysfunction [25,26] and mitochondrial abnormalities.[27,28]

Treatment options

For a long time, SMA has been a disorder without any treatment possibilities and the standard of care mainly consisted of comfort care.[29] Since the end of 2016, three SMN-dependent pathway therapies have obtained market access. The first drug was the antisense oligonucleotide nusinersen (Spinraza) that is administered intrathecally. It increases SMN protein levels in the central nervous system via modulation of splicing of *SMN2* mRNA.[30–33] The second therapy is onasemnogene abeparvovec (Zolgensma), a single dose, AAV9 based intravenous gene-replacement therapy.[34,35] The third treatment option is the small molecule risdiplam (Evrysdi); that is administered orally [36,37] and similar to nusinersen modulates splicing of *SMN2* mRNA.[38] All three therapies increase survival in SMA type 1 and motor function in a significant fraction of patients with SMA type 1-3, but they do not provide a complete cure of SMA.[8,38–40] Nevertheless, these therapies are a huge step forward for the life of patients with SMA, especially when administered pre-symptomatically or at a young age. However, long term effects are unknown.[8,38,39,41] Patients included in the studies described in this thesis are all treatment-naïve for genetic therapies.

Besides the SMN-dependent pathway therapies several SMN-independent pathway therapies are currently under investigation, e.g. muscle enhancing drugs, drugs enhancing NMJ/ synaptic function, neuroprotectors and cell therapy.[39]

Fatigability in SMA

In addition to muscle weakness, a reduced endurance performance during repeated movements is a characteristic of SMA.[42] This includes activities of daily life such as chewing, eating with cutlery, writing, tooth brushing or walking. Patients who are physically able to perform these activities clearly experience limits in the number of repetitions which often caused them to stop. This phenomenon, fatigability, is defined as the inability to continuously perform a task on the same power output.[43] Specifically, a unified taxonomy for fatigue and fatigability in the field of neurology has been proposed since these terms were used interchangeably in the past.[43] Fatigue was divided into two main domains: 1) perceptions of fatigue and 2) performance fatigability. Subjective perceptions of fatigue are affected by homeostatic and psychological factors, e.g. the central regulation as a consequence of inflammation or hormones or motivational influences, respectively.[43] The second domain, performance fatigability, is affected by peripheral and central factors, e.g. loss of muscle function or domain specific networks, respectively (figure 1).[43] Performance fatigability in patients with SMA plays a major role in the studies described in this thesis.

Recently, fatigability in SMA has gained more attention. The first study addressing fatigability in SMA, published in 2010, used a functional performance task.[44] Ambulant patients with SMA showed reduced endurance, combined with a 17% decrease in walking speed, on the six minute walk test. It was concluded that the walking speed during a six minute walk test may be used as clinically relevant aspect of fatigability. This scale was, however, not intended to measure the construct of fatigability. Additionally, the repetitive nine hole peg test has been investigated in another study to determine upper extremity fatigability.[45] The latter revealed to be a promising outcome measure to examine fatigability in patients with SMA type 2 but its ceiling effect limited the use of this specific test in patients with good proximal arm function. Both studies highlighted the relevance of fatigability in SMA and underlined the need for development of an outcome measure to quantify fatigability in patients with SMA type 2 as well as in type 3 and 4. The possible underlying peripheral factors of fatigability (figure 1), including research methods that can be used to measure those, will be discussed in the next paragraphs.

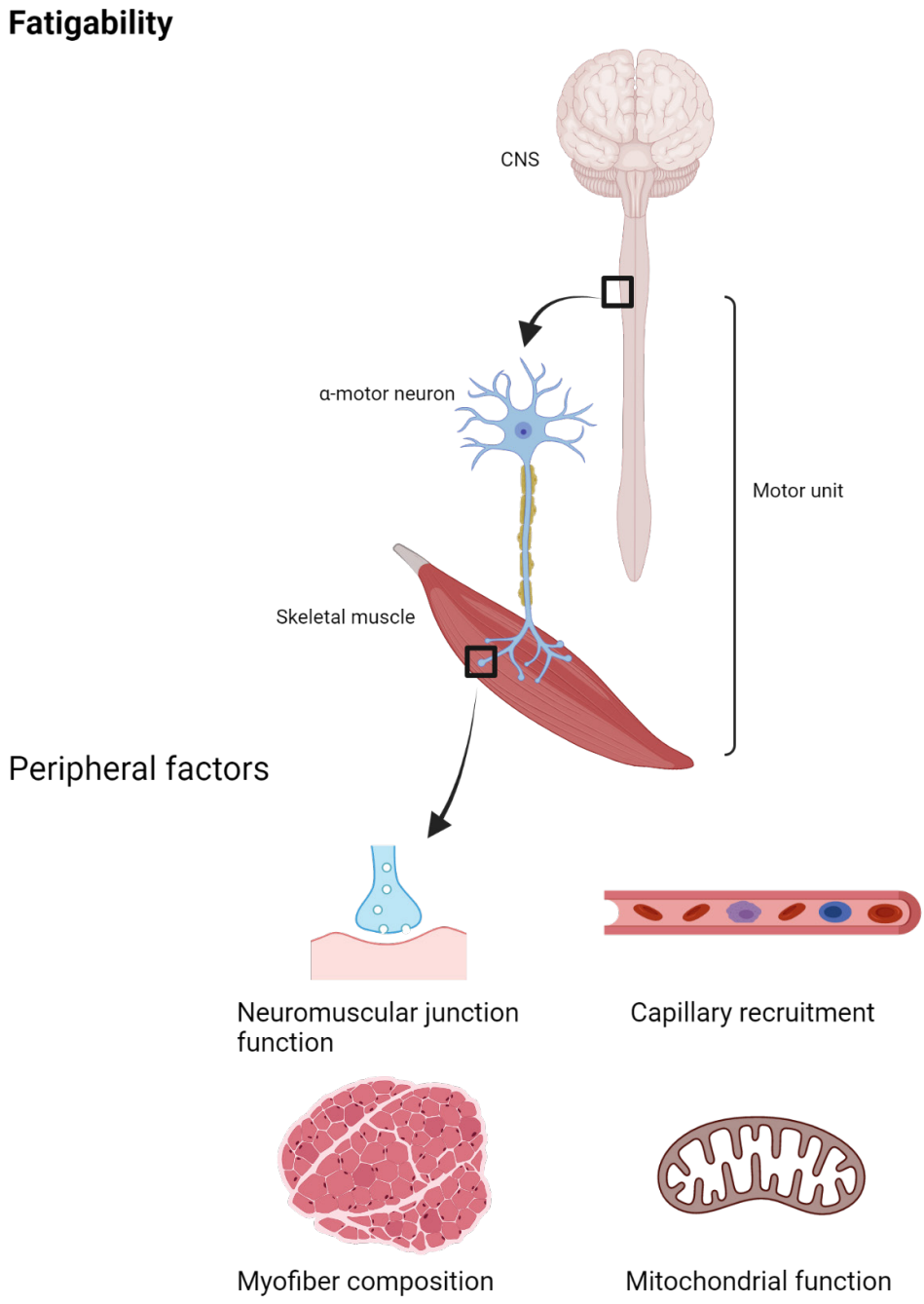

Figure 1. Schematic overview of peripheral factors possibly underlying fatigability in patients with SMA. CNS = central nervous system.

Peripheral factors of fatigability in SMA

Neuromuscular junction dysfunction

Neuromuscular junction (NMJ) dysfunction may underlie fatigability since requisite electrical signals from the central nervous system via α-motor neurons, aiming to provoke muscle contraction, may not arrive at the myofiber membrane (figure 1). Abnormal NMJ maturation in patients with SMA cause structural and functional changes in the NMJ.[25,26,46–49] Specifically, pre- and postsynaptic anatomic abnormalities may occur as a consequence of denervation. Pre-synaptic axonal neurofilament accumulation was found in severe mouse models.[25] The latter was suggested to cause abnormal organization of the cytoskelet of the synaptic terminals, which might contribute to a reduction of axonal spouting and structural postsynaptic defects.[46,50] Postsynaptic structural abnormalities include a lack of efficient NMJ maturation indicated by the presence of acetylcholine receptors,[48] abnormal clustering of acetylcholine receptors [51,52] and significantly smaller and malformed motor end plates also showing an immature state of development.[48,49,53,54]

With respect to functional changes of the NMJ reduced synaptic vesicle release, indicated by a twofold reduction in amplitudes of endplate currents, in the synaptic cleft was found in severe SMA mice.[47] This consequently reduced the probability of an action potential in the myofiber. In patients with SMA types 2 and 3 repetitive nerve stimulation studies showed pathological decrement in approximately half of the 35 included patients.[26] The found NMJ dysfunction in patients with SMA was probably primarily located at the post-synaptic side due to the absence of an increment of the signal after the Jolly test. A phase II, mono-center, placebo-controlled, double-blind cross-over trial on the efficacy and safety of pyridostigmine in patients with SMA types 2-4 showed a non-significant mean difference of 0.74% on the motor function measure (MFM) but the secondary outcome measures, i.e. risk of drop-out on endurance shuttle tests and patient reported effects of pyridostigmine on fatigability, showed significant differences between placebo and pyridostigmine.[55] Patients showed a 70% reduced risk to drop out during endurance performance.[56]

Myofiber composition

In healthy skeletal muscle, myofiber classes have different contractile properties and constitute different motor units.[57] The number of myofibers in a motor unit and the uniform contractile properties of these myofibers determine the speed and amount of force generated by that single motor unit. In that way, myofiber composition in skeletal muscle affects its performance. Distinctions in myofiber types can be made based on histochemical, biochemical, morphological or physiological characteristics (table 2).[58,59]

Table 2. Myofiber and motor unit classification based on multiple characteristics

Myofiber type classification				Motor unit classification		
Myosin ATPase	Myosin heavy chain	Biochemical	Appearance	Contractile	Fatigue	Electro-physiological
I <-->	MHCI <-->	SO	Red	Slow twitch	Fatigue resistant	Low-threshold
IC						
IIC						
IIAC						
IIA <-->	MHCIIa < - - >	FOG	Intermediate	Fast-twitch	Fatigue intermediate	
IIAB						
IIB <-->	MHCIIx/d (IIb) < - - >	FG	White	Fast-twitch	Fatigable	High-threshold

MHC = myosin heavy chain, SO = slow oxidative, FOG = fast oxidative glycolytic, FG = fast glycolytic.

The histochemical classification using pH sensitivity distinguishes myofibers based on myosin ATPase activity and the speed of muscle shortening. This results in groups of two slow type I and five fast type II myofibers.[58,59] Besides ATPase activity, myofibers can be distinguished using immunohistochemical analyses of myosin heavy chain (MHC) isoforms. Classification based on this technique correspond to the myofiber types identified using ATPase activity (table 2).[58] Next, biochemical classification is based on functional and metabolic properties of the myofiber. Specific enzymes can be analyzed that reflect the oxidative (i.e aerobic) or glycolytic (i.e. anaerobic) metabolic pathways of slow or fast myofibers, respectively.[58] Consequently, this classification results in three different myofibers: 1) slow-twitch oxidative (SO), 2) fast twitch oxidative glycolytic (FOG) and 3) fast-twitch glycolytic (FG).[58–60] Although these classification systems have important overlap, the terms cannot be used interchangeably.[58] Myofibers in this thesis are uniformly classified by their appearance since histochemical analyses were not performed and the biochemical classification system is not very often used in clinical studies. In this thesis we distinguish: 1) red myofibers with a high oxidative potential due to the presence of myoglobin and mitochondrial cytochrome oxidase,[57] 2) white myofibers with a lower oxidative but high glycolytic potential and 3) intermediate myofibers. As for myofibers, motor units can also be classified based on different characteristics, i.e. contractile, fatigue and electrophysiological characteristics.[57,58] In this thesis we distinguished motor units by their electrophysiological characteristics. Low-threshold motor units are typically made up of a lower number of red myofibers that produce low forces and are fatigue resistant compared to high-threshold motor units that are made up of larger number of white myofibers that produce higher forces and are easily fatigable.

Muscle biopsy studies in SMA

SMA muscle morphology and myofiber composition may be determined *ex vivo* in muscle samples obtained by needle biopsy.[59,61] Historically, muscle biopsies in patients suspected of neuromuscular diseases were used for diagnostics as well as for research.[61,62] Muscle biopsy studies focus on the appearance, size and structure of different myofibers and myofiber distribution within the muscle. As such, biopsy studies in patients with SMA type 3 (Kugelberg-Welander syndrome) revealed an altered special myofiber distribution away from the random pattern in healthy human muscle.[61,63–66] Neuropathic processes are an underlying cause of changes in myofiber distribution.[65] Muscle biopsies of patients with SMA are characterized by small clusters of atrophied myofibers.[62] However, inconsistent results regarding the predominant myofiber type are described in literature. For example, decreased diameters of red myofibers were reported by Dubowitz (1966), while white myofiber size was unchanged or only slightly reduced.[67] Mastaglia (1971) reported a predominance of red myofibers in the m. deltoideus while the m. biceps brachii revealed atrophy in red and white myofibers.[64] Besides atrophy, myofiber hypertrophy is found in red [68] but mostly in white myofibers.[67,69] Dubowitz suggested that the pattern of hypertrophy in a single myofiber type was mainly the cause of myofiber re-innervation.[70] Nowadays, muscle biopsies are no longer routinely performed for SMA diagnosis since molecular testing provides an alternative and patient-friendly approach.

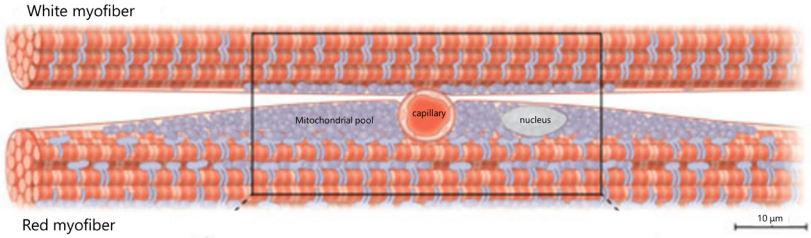

Figure 2. Schematic representation of mitochondria and capillary embedded in white and red myofibers (figure adapted from Glancy et al. [71]).

Mitochondrial abnormalities

The source of chemical free energy in all living organisms is adenosine triphosphate (ATP). Due to the high and sudden changes in cellular energy expenditure upon excitation by an action potential, muscle fibers and neurons need a high capacity for ATP synthesis, as such mitochondria, since low concentrations of ATP are available within cells at rest.[57] Mitochondrial content differs between myofiber types (figure 2).[71] Any mitochondrial abnormalities may affect skeletal muscle function and may possibly contribute to fatigability in SMA. Especially in red myofibers, responsible for low intensity endurance performance, with a high amount of mitochondria. There are several pathways to generated ATP to meet the energy requirements in healthy muscle cells (figure 3).[57,72]

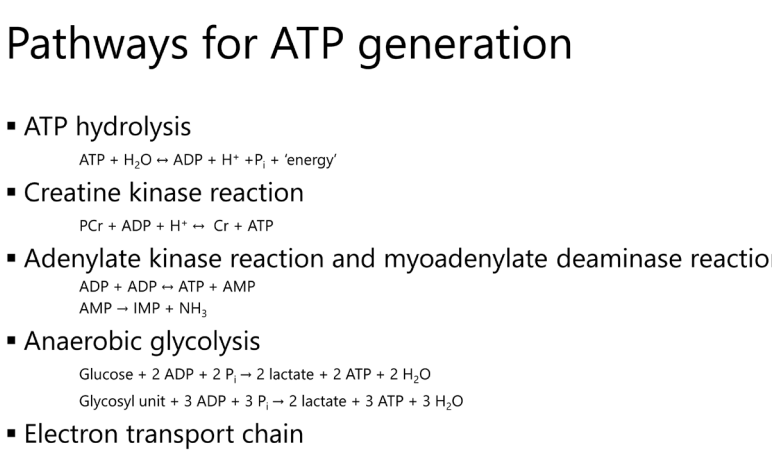

Figure 3. Pathways for ATP generation in healthy muscle cells.[57]

The first pathway is an exothermic reaction process to produce energy. Second, extremely rapid ATP production can be supplied by the high amount of the enzyme creatine kinase. At rest, creatine is mostly present in the form of PCr.[57] The third pathway consists of the rapid adenylate kinase- and myoadenylate deaminase reactions aiming to remove ADP and prevent accumulation which inhibits ATP generating reactions. The anaerobic glycolysis, which takes place in the cytoplasm of the cell, is approximately twice as fast in producing ATP compared to the creatine kinase reaction while the amount of generated ATP is similar. Glucose in blood or glycogen stored in the muscle will be converted into pyruvate. Next, pyruvate is transported to the mitochondria and decarboxylated resulting in acetylcoenzym-A. Carbohydrates, fat and amino acids are brought into the process by acetylcoenzym-A and form the main sources of energy. The tricarboxylic acid cycle produces coenzymes for the electron transport chain, the largest producer of ATP in the mitochondria. This process is more efficient compared to anaerobic production of ATP since one molecule of glucose causes 38 molecules of ATP instead of 2, respectively.[57]

Studies on mitochondrial function in SMA

At the start of the research project described in this thesis several studies reported on mitochondrial dysfunction in SMA supported by both animal studies and abnormalities observed in muscle biopsies of patients with SMA. Other studies found evidence for the role of SMN protein in cell maturation including myogenesis which is closely related to mitochondrial function.[27,28,73–76] Morphologic, biochemical and mitochondrial content abnormalities in muscle biopsies from 24 young patients with SMA 1, 2 and 3 showed altered myogenesis regulation and downregulated mitochondrial biogenesis.[27] In addition to the typical SMA neurogenic pattern, muscle biopsies showed COX negative fibers and reduced

activity of succinate dehydrogenase in complex IV and II of the electron transport chain in the mitochondria.[27] Biochemical analyses showed lower levels of citrate synthase in the tricarboxylic acid cycle and lower complex I, II, III and IV activity, most pronounced in tissue of patients with SMA type 1. Amounts of mitochondrial DNA were significantly reduced in muscles from patients with SMA type 1 and 2 and inversely related to disease severity. These results were not fully consistent in patients with SMA type 3a, although mitochondrial DNA levels were lower compared to controls. The found mitochondrial abnormalities could represent a secondary consequence of motor neuron denervation caused by SMN deficiency.[27] However, SMA mouse models seem to contradict the hypothesis that mitochondrial dysfunction appears late in the disease process.[28] Specifically, functional and structural mitochondrial deficiencies were present in presymptomatic phases of the disease, compatible with a primary role for mitochondrial function in SMA pathology.[28] Therefore, mitochondrial function needs to be examined *in vivo* in patients with SMA.

Capillary recruitment

A fourth factor that could cause fatigability in SMA is abnormal capillary recruitment.[12] Signals from the central nervous system and through the α-motor neurons to the corresponding myofibers cause muscle contractions. During exercise the muscle metabolic demand for oxygen will increase. Specifically, local muscle blood flow is controlled by spatial and temporal interactions of multiple signaling events, e.g. sympathetic neuromuscular transmission, contractile activity and metabolic mechanisms, during exercise in healthy skeletal muscle.[77–79] Progressive dilatation of distal and proximal arterioles and consequently feed arteries of the vascular system will provide the influx of oxygenated blood.[77,79] On the contrary, the sympathetic nerve system causes excretion of norepinephrine aiming for vasoconstriction regulation.[77,79] In this way these systems manage the oxygen supply for metabolic demand of skeletal muscle. In healthy muscle complete perfusion of the active muscle is suggested to be facilitated by dispersion of different motor units. In a computer model step-by-step activation of motor units was simulated which causes an increase in blood flow, even in the capillaries of still inactive myofibers.[78] Due to this safety factor activity can be increased without delay caused by diminished oxygen supply.[78] Changes in motor unit dispersion, motor unit size and recruitment strategy could dramatically reduce muscle blood flow and contribute to fatigability.[78] Animal and *in vitro* human SMA studies revealed a decreased capillary density, a 50% increased capillary caliber and a reduced capillary ramification in skeletal muscles and altered levels of a specific protein with important roles in vascular development.[80–83] *In vivo* studies on capillary recruitment in SMA during exercise have not yet been executed.

Non-invasive technologies to study muscle function and morphology

In the studies described in this thesis we wanted to investigate peripheral mechanisms possibly underlying fatigability in SMA. There are several research technologies to non-invasively measure and visualize skeletal muscle function and morphology in patients with SMA. We used surface electromyography (sEMG) to measure muscle activation and motor unit recruitment. A widely used technique to visualize muscles is magnetic resonance imaging (MRI). Quantitative MRI may provide information on the size and location of muscle, composition, fatty infiltration and inflammation. MR techniques can also be used to assess muscle mitochondrial function using ^{31}phosphorus-magnetic resonance spectroscopy (^{31}P-MRS) during dynamic exercise. To study capillary recruitment we used Near Infrared Spectroscopy (NIRS).

Surface electromyography

sEMG is a non-invasive tool to measure voluntary muscle activation by analyses of the myoelectric signals (figure 4).[84,85]

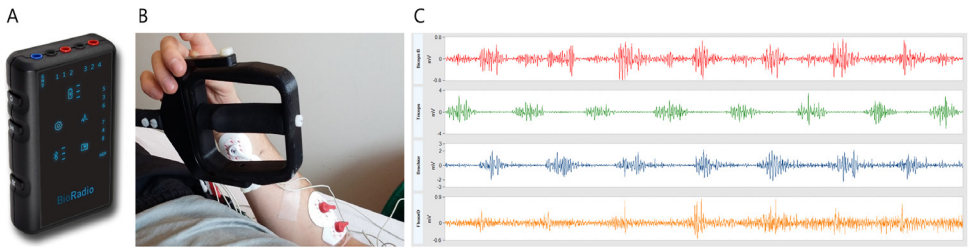

Figure 4. Surface electromyography tool (A-B) used to measure myoelectric signals (C) from the m. biceps brachii (red), m. tricep brachii (green), m. brachioradialis (blue) and m. flexor digitorum superficialis (yellow) of the arm of a healthy volunteer during arm-cycling.

Electrical signals provided by the central nervous system which arrive at the motor endplate are transferred via the NMJ and may consequently cause an electrical physiological response on the myofiber semi-permeable membrane.[84] In rest an ionic equilibrium is maintained by ion pumps between the inner and outer membrane of the myofibers, causing a potential of approximately -80 to -90 mV. When a signal, transferred by the α-motor neuron, exceeds a certain threshold, the myofiber cell depolarizes when sodium ions flow out and potassium ions flow into the cell. During this process the action potential rises to approximately +30 mV. Directly after this depolarization the myofiber repolarizes. This reaction goes along the myofiber with a velocity of 2 to 6 m/s, in both directions, away from

the motor endplate.[84] As a consequence, calcium ions will be released in the intra-cellular space necessary for shortening of the myofiber contractile elements.

At least two electrodes, attached to the skin, are needed to capture a depolarization wave along a myofiber. Due to the distance between those electrodes, a potential difference can be measured as the depolarization wave slides along the myofiber. One α-motor neuron, however, activates many myofibers, all belonging to the same motor unit. As such, the captured sEMG signal is the sum of all action potentials beneath the electrodes.[84]

In real life during voluntary muscle activation, sEMG captures the sum of motor unit action potentials of multiple active motor units; i.e. the interference pattern.[84] sEMG signals are dependent on the orientation and location of the underlying myofibers.[84–86] For example, action potentials of the more superficial myofibers have a higher contribution to the sEMG signal. Factors such as tissue characteristics (e.g. adipose tissue thickness, temperature), physiological cross talk of surrounding muscles or ECG spikes and external noise (e.g. power lines hum) may also influence sEMG signals and complicate quantitative comparisons of sEMG parameters within and between individuals.[84,86] Therefore, proper skin preparation procedures to lower the skin impedance, standardized electrode locations to lower cross talk and electrode cable fixation to prevent cable motion artefacts are crucial.[87]

sEMG outcome variables and interpretation

For quantification purposes, the root mean square (RMS) amplitude (mean power of the signal) and median frequency are two variables that can be calculated from the raw sEMG signal.[84,88] In healthy muscle, the signal density, i.e. frequency determined using Fast Fourier Transformations, lies between the 6 and 500 Hz.[84] Most frequencies, however, lie between the 20 and 150 Hz. The range in signal magnitude, i.e. amplitude, lies between +/- 5000 mV.[84] Due to the aforementioned factors that may affect the sEMG signal, absolute values of the amplitude of raw sEMG signals cannot be easily compared between individuals. The most frequently used method to overcome this problem is the use of normalization to the sEMG signal measured during a maximal voluntary contraction (MVC) of the specific muscle prior to the movement or action of interest.[84] As such, the sEMG amplitude variable may be presented as a percentage of the maximal provided amplitude during an MVC. Other procedures like mean or peak normalization and time normalization in case of repetitive movement are also possible but will not be used in the studies described in this thesis.

The sEMG signal magnitude and density may be affected by both myofiber recruitment and the fire frequency during muscle activation.[84,85,89] To study muscle fatigability, the temporal effects on median frequencies and RMS amplitudes of the sEMG signal can be investigated.[85,86,88,90] Forces to produce movement, generated by myofibers, can be provided by two strategies.[57] The first strategy is described by Henneman's size principle.[57,91] Henneman's size principle is based on a hierarchy in motor unit recruitment. In short,

lower-threshold motor units with red myofibers are recruited first to deliver low levels of force. With increasing force higher-threshold motor units are recruited in a stepwise manner (figure 5). The second strategy is by changing the stimulation frequency, i.e. rate coding.[84,89] An increase in the stimulation frequency will cause an increase in power output. The way in which both strategies are used varies between muscles.[57] As a consequence of those strategies, the amplitude of the sEMG signal will increase over time during muscle fatigue while the median frequency of the total power spectrum will show a decrease. The latter is caused by a decrease in the conduction velocity of the motor unit action potentials on the myofiber membrane.[84]

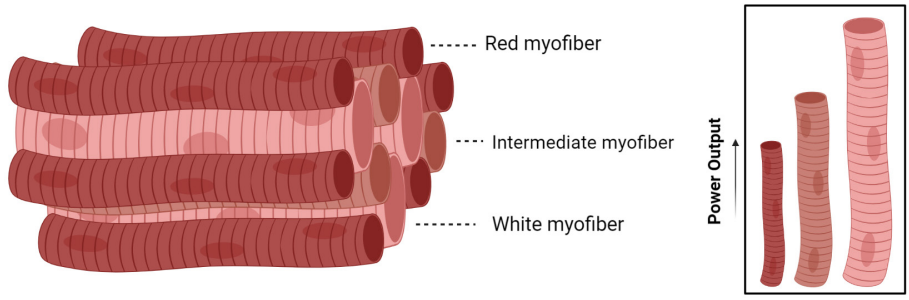

Figure 5. Stepwise recruitment of red-, intermediate- and white myofibers to increase power output.

Magnetic resonance imaging

MRI is a non-invasive tool to examine muscle anatomy *in vivo*. MR images are based on the magnetic moment of hydrogen nuclei which may interact with the magnetic field in an MR-scanner (figure 6).[92] Basically, an external magnetic field provides a turning force on the protons. After this disturbance, the scanner measures the relaxation times to their equilibrium.[92] Relaxation times depend on the attachment of the proton to water or lipid molecules and are longer in fluids compared to fatty tissue. The unit in which the magnetic flux density is expressed is tesla (T). The higher the magnetic field, the stronger the MR signals and the higher the signal to noise ratio (SNR).

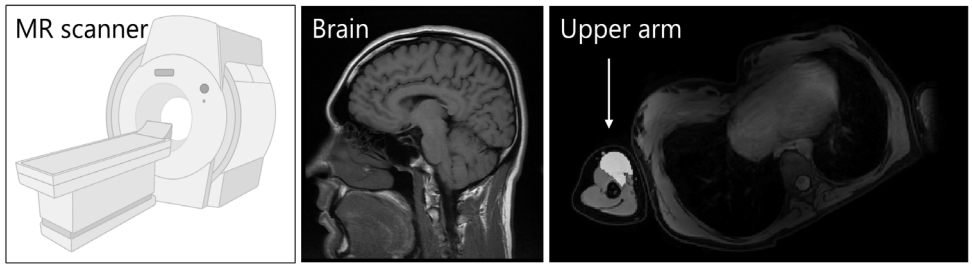

Figure 6. MR scanner and a typical example of a quantitative T2 map of the brain and upper arm of a healthy subject.

MRI outcome variables

Three quantitative MRI methods include T2 weighted sequences, Dixon and diffusion tensor imaging (DTI).[92] The first technique is quantitative T2 mapping which may gather information on inflammation and muscle anatomy based on a difference in relaxation times of water and fat. Elevated water T2 relaxation times measured in muscles of patients with neuromuscular disorders are associated with, amongst others, inflammation. Dixon MRI, a second method, gathers detailed information on muscle anatomy and fatty infiltration and is widely used as a broad measure for muscle condition in dystrophic myopathies. The third method, DTI, is a relatively new method that may provide information on the muscle microstructure based on the diffusion of water within tissues.[92–94] DTI outcome variables are three eigenvectors of the tensor (3*3 matrix) and their corresponding eigenvalues λ1, λ2 and λ3 of which the fractional anisotropy (FA) and mean diffusivity (MD) may be calculated. FA quantifies the orientation of water molecules within muscle cells and is expressed in a value between zero (isotropic movement of water molecules, e.g. fluid) and one (anisotropic movement of water molecules, e.g. myofibers). MD is the mean of the three eigenvalues and indicates the membrane density.[93] Importantly, fatty infiltration in muscles may confound T2 and DTI variables causing technical challenges especially in diseased muscles.[92,93]

Magnetic resonance spectroscopy

^{31}P-MRS is a technique to assess metabolic function of tissue *in situ*. In particular, insight on mitochondrial function may be provided since phosphorus is a main component of the energy source ATP. Nowadays ^{31}P-MRS is typically performed using high-field (4 -7 Tesla) nuclear MR (NMR) scanners but additional hardware including a reference coil for clinical MR scanners (figure 6) operating at 1.5-3 Tesla makes it possible to also examine phosphorus spectroscopy on these systems.[92] With respect to proton spectroscopy, phosphorus appears in a lower concentration in the human body. Therefore, the NMR sensitivity, expressed in the gyromagnetic ratio, is 60% lower in this technique which consequently result in smaller SNR ratios compared to proton imaging.

Muscle metabolic function

Muscle metabolic function may be investigated during rest, exercise and post-exercise recovery. ^{31}P-MRS measurements are independent from workload and could be applied during a moderate incremental exercise protocol to prevent muscle acidosis and muscle ischaemia. However, in case of suspicion of mitochondrial myopathy a maximal exercise protocol is recommended to ensure dominant mitochondrial ATP flux.[95] Measurements of mitochondrial function in human muscle *in vivo* using ^{31}P-MRS are usually done in lower extremity- and lower arm muscles due to the favorable position in the MR-scanner.[60,96] The physical ability of most patients with SMA type 3 and 4 restricted the use of a lower

extremity exercise platform. To overcome this practical problem we switched to an arm-cycling exercise platform in the studies described in this thesis.

A normal rest ^{31}P spectrum is shown in figure 7 and can be read from right to left, providing information on high energy phosphates α-, β-, γ- ATP and phosphocreatine (PCr), and on inorganic phosphate (P_i). PCr is set at the reference chemical shift of 0 ppm. Peaks between 4 and 5 ppm upfield of the PCr resonance have been typically attributed to the ATP hydrolysis product P_i (figure 3).

During exercise the main dynamics can be seen at frequencies corresponding to PCr and P_i. An example of PCr and P_i kinetics during exercise and recovery is presented in figure 8. PCr can be represented as the battery of the cell (figure 8A). As a consequence of the creatine kinase reaction (figure 3), the spiky PCr peak progressively disappears until a point of exhaustion. In other words, the battery runs down (figure 8A) and the subject can no longer continue the exercise task. Conversely, peaks at frequencies down field of PCr progressively appear (figure 8A), i.e. P_i; a direct substrate of mitochondrial oxidative ADP phosphorylation. Since PCr will be almost fully regenerated by the oxidative ATP synthesis, PCr recovery kinetics reflect the muscle mitochondrial function. This is reflected by the non-linear curve in figure 8B and can be presented by the PCr time constant τPCr or halftime $t^{1/2}$.[60,97]

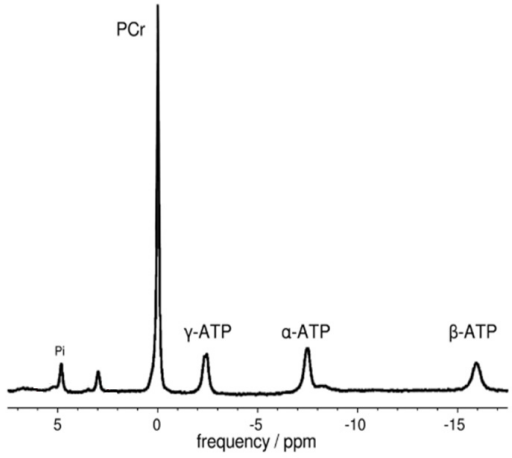

Figure 7. A typical ^{31}P-MRS spectrum of a resting muscle of a healthy volunteer acquired at 7T. P_i = inorganic phosphate, PCr = phosphocreatine, γ-/ α-/ β-ATP = γ- / α-/ β-adenosine triphosphate, ppm = parts per million.

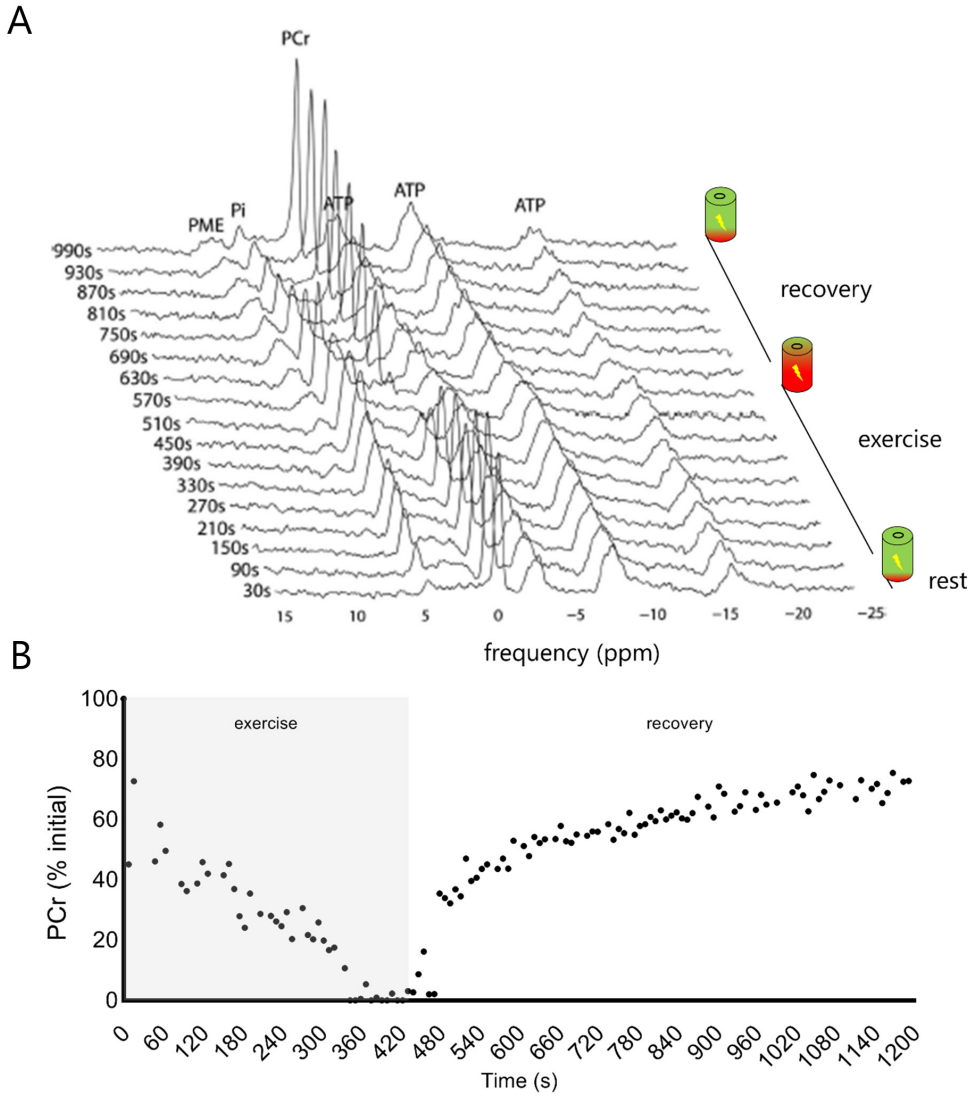

Figure 8. A) Stack plot of ^{31}P MR spectra of healthy quadriceps acquired at 1.5T during rest, exercise and recovery.[98] PCr concentrations may be referred to as the battery of the muscle. B) Phosphocreatine depletion during exercise and non-linear curve fitting of post-exercise recovery. Quadriceps PCr content was determined from ^{31}P MR spectra. P_i = inorganic phosphate, PCr = phosphocreatine, ppm = parts per million.

Myoplasmic pH

Of interest to the *in vivo* MR studies described in this thesis is the fortuitous fact that the specific resonance frequency of P_i is sensitive to myoplasmic pH (figure 9).[99]

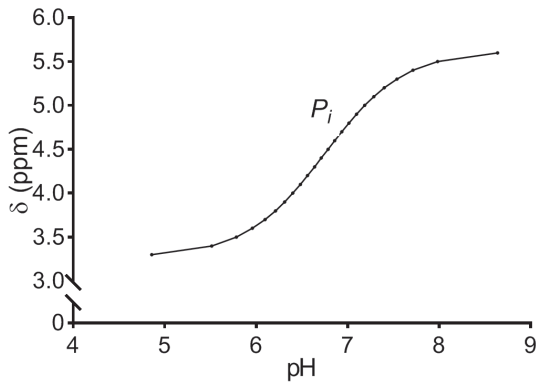

Figure 9. Correlation between myoplasmic pH and chemical shift between P_i and PCr (δ) based on the Henderson-Hasselbalch equation.

The following Henderson-Hasselbalch equation may therefore be used to estimate the intramyocellular pH :

$$pH = 6.75 + \log[(\delta - 3.27) / (5.63 - \delta)]$$

where δ is the chemical shift between P_i and PCr.[60,100] Studies on human lower arm and calf muscles in the early 90's related the multiple P_i peaks, found in single muscles, to different myofiber types based on their intracellular pH differences.[101–103] Discussions on the interpretation of these findings, back then, resulted in a blunted interest on this topic until 2016. Evidence for a relation between the intracellular pH differences in myofibers and peaks at specific frequencies measured in the m. gastrocnemius at the end state of exercise was found.[104] As such, the peak at frequencies from 5.2 to 4.6 ppm is suggested to belong to red myofibers, 4.7 to 4.3 ppm to intermediate myofibers and a peak at frequencies from 4.3 to 3.7 ppm belong to white myofibers, operating at neutral pH 7.0, intermediary-acidic pH 6.6 and acidic pH 6.2, respectively.[60,104] Separate peak area's as percentage of the total P_i peak area may be related to myofiber type volume fractions and thus provide information on the myofiber distribution. However, the latter is an assumption and need to be investigated in future research. Exact myofiber type distributions may be determined with ^{31}P-MRS in the future when two requirements are met.[104] The first is establishing estimations of myofiber type related P_i concentrations at rest and during exercise. These estimations then need to be compared with muscle biopsies at the same location to be able to design prediction models.

^{31}P-MRS studies in metabolic myopathies and neuromuscular disease

^{31}P-MRS has been previously used in metabolic myopathies, e.g. Mc Ardle disease and very long chain CoA dehydrogenase deficiency, in order to investigate mitochondrial function in relation to exercise intolerance.[105,106] In general, mitochondrial dysfunction is expressed in reduced PCr resynthesis after exercise.[60] For example, in patients with Mc Ardle disease a rapid PCr depletion and a lack of muscle acidification during exercise, combined with slow PCr recovery kinetics indicated the inhibition of the oxidative phosphorylation, most probably due to a lack of sufficient pyruvate levels.[105]

Several studies examined muscle metabolic function in patients with neuromuscular diseases, i.e. Duchenne-/ Becker muscular dystrophy and amyotrophic lateral sclerosis.[107–111] A scoping review of currently available literature on MRS studies in patients with these neuromuscular diseases can be found in table 3. These studies are, however, rare due to the in general long procedures and time-consuming data analyses.[105] Besides these technical considerations, exercise in some patient populations is often avoided because of possible negative effects on other functional outcome measures of those studies.[108] Specifically, all reported *in vivo* ^{31}P-MRS investigations of muscle in patients with Duchenne muscular dystrophy have been conducted in resting muscles.[107,108,112]

No *in vivo* ^{31}P-MRS investigations of muscles in either resting or exercising patients with SMA have previously been reported. Here, a particular obstacle may have been the practical fact that overt lower extremity muscle weakness in patients with SMA prohibits any use of in-magnet leg exercise protocols that have typically been applied in these clinical ^{31}P-MRS set-ups.[60] To overcome this practical problem we switched to an arm cycling exercise platform in the studies described in this thesis.

Table 3. Scoping review on ^{31}phosphorus magnetic resonance spectroscopy variables measured to investigate mitochondrial function in patients with muscular dystrophies and anterior horn disorders.

Article	Disease cohort	Investigated muscle(s)	Rest	Exercise	Recovery
Hájek et al. 1993	14 children and adolescents with DMD and BMD vs. controls	Calf muscles, i.e. m. gastrocnemius with contamination from m. soleus	Normal pH of 7.05. Lower PCr/P_i, PCr/PDe, PDe/beta-ATP Increased [P_i] associated with loss of muscle force. Increased [PDe] - attributed to destruction of phospholipid membranes, ageing, white myofiber atrophy or obesity.	n.a.	n.a.
Lodi et al. 1999	14 children, adolescents and adults with BMD vs. controls	Plantar flexion of right calf muscle	Higher pH Lower [PCr] Higher [ADP]	During exercise: Lower fall in pH Higher rise in [ADP] End-exercise: Higher [PCr] Increased pH Increased [ADP]	Normal initial [PCr] recovery. Normal maximum rate of ATP synthesis and ADP recovery $t_{1/2}$.
Sharma et al. 2003	DMD muscle biopsies	m. vastus lateralis ($^1H^+$-MRS)	Lower [glucose], [lactate], lutamate],[Cr+PCr], [acetate], [GPC/PC/ Car], [Cho]	n.a.	n.a.
Torriani et al. 2011	9 children and adolescents with DMD	m. tibialis anterior m. soleus	m. tibialis anterior: Higher pH Lower [PCr] m. soleus: Lower [PCr/P_i]	Not performed to avoid negative effects on other functional measures of the study	n.a.

Tosetti et al. 2011	9 adults with BMD vs. controls	Plantar flexors	Higher pH	End-exercise: Lower [PCr] consumption for degree of acidification	[PCr] recovery similar to controls
Sassani et al. 2020	20 adults with ALS vs. controls	m. tibialis anterior	Reduced delta G_{ATP} Higher [P_i], [PME], pH		Slower PCr/P_i recovery
Sharma et al. 1995	5 adults with ALS vs. controls	m. tibialis anterior		No significant differences	Normal [PCr], [P_i] and pH recovery
Kent-Braun et al. 2000	7 adults with ALS vs. controls	m. tibialis anterior		End-exercise: Less [PCr] depletion Similar pH values	n.a.
Grehl et al. 2007	10 adults with ALS vs. 38 controls	m. gastrocnemius	Higher PCr/ATP Similar PCr/P_i	Lower [PCr] depletion	Similar [PCr] recovery

ADP = adenosine diphosphate, ALS = amyotrophic lateral sclerosis, ADP = adenosine diphosphate, ATP = adenosine triphosphate, BMD = Becker muscular dystrophy, DMD = Duchenne muscular dystrophy, G_{ATP} = Gibbs free energy of ATP, $^{1}H^{+}$-MRS = proton MRS, n.a. = not applicable, PCr = phosphocreatine, P_i = inorganic phosphate, PME = phosphomonoesters [107–115].

Near infrared spectroscopy

NIRS is a non-invasive method to investigate capillary recruitment in muscle during dynamic exercise (figure 10).[116–118]

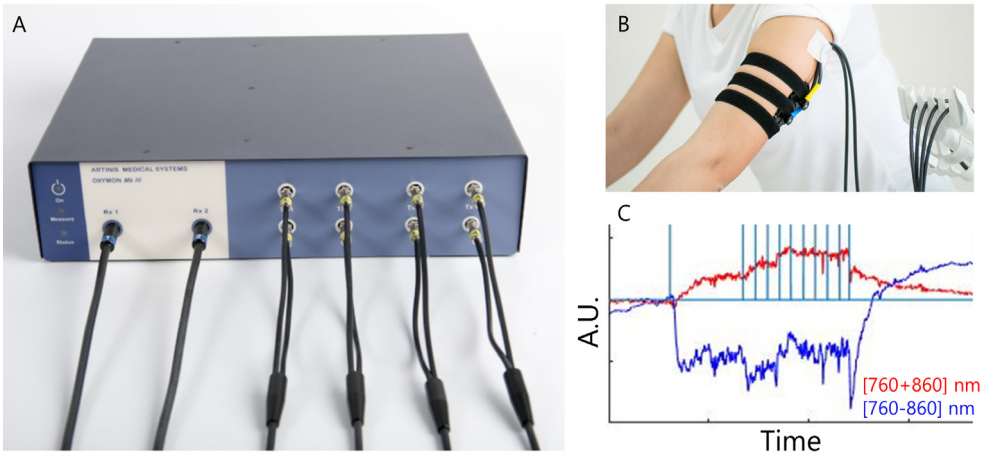

Figure 10. Example of a continuous wave near infrared spectroscopy (CW-NIRS) tool used to measure capillary recruitment during arm-cycling from the m. triceps brachii of a healthy subject. A-B: OXYMON (Artinis, The Netherlands, https://www.artinis.com/oxymon) CW-NIRS system, C: example of CW-NIRS signals, i.e. [760 + 860] nm and [760 - 860] nm, expressed in arbitrary units.

NIRS, based on continuous wave (CW) spectrophotometers, uses light emitted by a laser diode or light emitting diode.[119] The emitted light is captured by a photomultiplier, photodiode or avalanche photodiode detector.[119] In 1977, Jöbsis used CW-NIRS for the first time in cats to measure *in vivo* brain oxygenation.[116] Other NIRS techniques are based on time-resolved or intensity-modulated instruments.[119] CW-NIRS measures changes in concentrations of different chromophores.[116] Specifically, oxygenated hemoglobin ([HbO2]), hemoglobin ([Hb]) and cytochrome oxidase ([CtOx]). Oxygen, bounded to [Hb], is transported via the blood to the organs, e.g. to muscle tissue for oxidative metabolism. CtOx is an enzyme in mitochondria which is involved in the process of oxidative metabolism.[119,120] The change in concentration of these chromophores can be measured using infrared light and their difference in rate of absorption.[121] The emitted light is, however, not only absorbed by chromophores, scattering of the light as a consequence of the surrounding tissue also causes a decrease in the light captured by the detector. The amount of scattering depends on the structure of the underlying tissue and differs slightly between individuals.[119] Therefore, it is important to know the factor in which the optical path length will be increased due to scattering in general, i.e. pathlength factor (DPF). In skeletal muscle tissue this DPF is set at 4.[122]

NIRS outcome parameters and interpretation

Infrared light with a wavelength of approximately 760 nm will mostly be absorbed by [Hb], whereas wavelengths of approximately 860 nm will mostly be absorbed by [HbO2]. As mentioned before, [CtOx] also absorbs part of the emitted light in the range of both wavelengths. Moreover, part of the measured absorption at both wavelengths is also a result of the other two components. Specifically, the absorption at one wavelength is always the sum of these three components which is an important aspect of NIRS and complicates the interpretation of the signals.

The optical density on both wavelengths can be calculated by the sum of the extinction coefficients of all three chromophore components at a specific wavelength (figure 11). The optical density at both wavelengths can be used to provide information on total blood volume ([760+860] nm) and relative [HbO2] saturation ([760-860] nm) .

In healthy muscle a normal physiological response during heavy exercise causes a decrease in the [760 - 860] nm signal, indicating a decrease in oxygenated hemoglobin (figure 11C).[117] The [760+860] nm signal remains more or less at the same level. Increasing [760 + 860] nm signals are also reported, meaning that the total blood volume increases during exhaustive exercise.[123] During the recovery following heavy exercise, [760-860] nm signals will extensively increase until the normal resting values are reached.

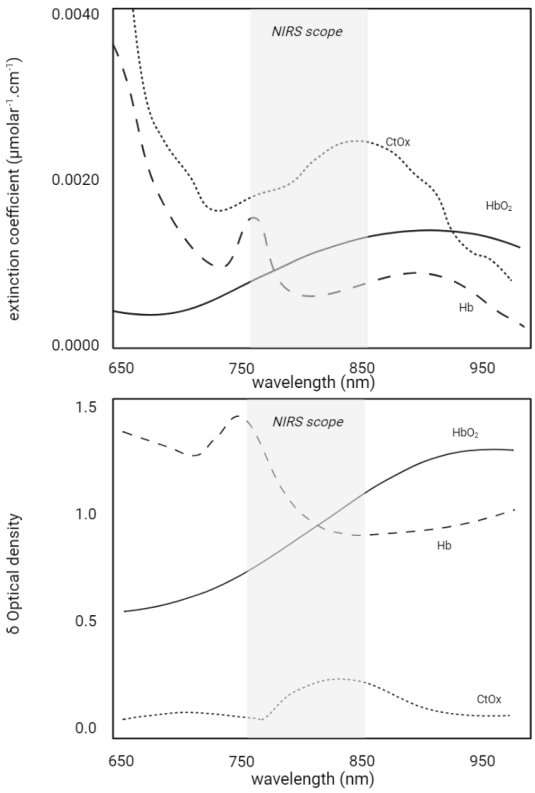

Figure 11. Schematic representation of extinction coefficients and δ optical density of oxygenated hemoglobin ([HbO2]), hemoglobin ([Hb]) and cytochrome oxidase ([CtOx]) at different wavelengths.

General aims and outline

The main objective of this thesis is to gain more insight in peripheral factors possibly underlying fatigability of skeletal muscles of patients with SMA. For the research projects described in this thesis, the three formulated aims were to:

1. develop outcome measures to quantify fatigability in patients with SMA across the clinical spectrum.

   In **chapter 2**, we define the construct of fatigability to explore the design, development and validation of endurance shuttle tests to measure fatigability in all patients with SMA. The endurance shuttle tests are subsequently tested in three pilot studies.

2. examine the presence of and the possibility to improve motor unit recruitment capacity in patients with SMA.

   In **chapter 3**, we assess motor unit reserve capacity in upper and lower extremity muscles during performance of the endurance shuttle tests using surface electromyography. Because we intent to develop endurance tests, representing submaximal activities of daily life, we additionally study the level of muscle activation per group of patients with different types of SMA.

   In **chapter 4**, we use surface electromyography signals of upper extremities during endurance shuttle tests to assess the effect of pyridostigmine, a drug that enhances the neuromuscular transmission, on muscle activation.

3. investigate skeletal muscle morphology, mitochondrial function and capillary recruitment in patients with SMA.

   In **chapter 5**, we explore the use of quantitative magnetic resonance techniques to image proximal upper arm musculature in patients with SMA.

   In **chapter 6**, we focus on myofiber composition and mitochondrial function of upper arm musculature in patients with SMA during dynamic arm-cycling performance until exhaustion, quantified by magnetic resonance spectroscopy parameters.

   In **chapter 7**, we assess oxidative capacity and motor unit- and capillary recruitment during maximal voluntary arm-cycling exercise aiming to further explore fatigability.

References

1. Lefebvre S, Brglen L, Reboullet S, et al. Identification and characterization of a spinal muscular atrophy-determining gene. Cell. 1995;80(1):155-165.
2. Verhaart IEC, Robertson A, Wilson IJ, et al. Prevalence, incidence and carrier frequency of 5q-linked spinal muscular atrophy - A literature review. Orphanet J Rare Dis. 2017;12(1):1-15.
3. Lunn MR, Wang CH. Spinal muscular atrophy. Lancet. 2008;371(9630):2120-2133.
4. Farrar MA, Kiernan MC. The Genetics of Spinal Muscular Atrophy: Progress and Challenges. Neurotherapeutics. 2015;12(2):290-302.
5. Lauria F, Bernabò P, Tebaldi T, et al. SMN-primed ribosomes modulate the translation of transcripts related to spinal muscular atrophy. Nat Cell Biol. 2020;22(10):1239-1251.
6. Chabanon A, Seferian AM, Daron A, et al. Prospective and longitudinal natural history study of patients with Type 2 and 3 spinal muscular atrophy: Baseline data NatHis-SMA study. PLoS One. 2018;13(7):1-28.
7. Wadman RI, Stam M, Gijzen M, et al. Association of motor milestones, SMN2 copy and outcome in spinal muscular atrophy types 0-4. J Neurol Neurosurg Psychiatry. 2017;88(4):364-367.
8. Talbot K, Tizzano EF. The clinical landscape for SMA in a new therapeutic era. Gene Ther. 2017;24(9):529-533.
9. Feldkötter M, Schwarzer V, Wirth R, Wienker TF, Wirth B. Quantitative analyses of SMN1 and SMN2 based on real-time lightcycler PCR: Fast and highly reliable carrier testing and prediction of severity of spinal muscular atrophy. Am J Hum Genet. 2002;70(2):358-368.
10. Wadman RI, Jansen MD, Stam M, et al. Intragenic and structural variation in the SMN locus and clinical variability in spinal muscular atrophy. Brain Commun. 2020;2(2):1-13.
11. Hamilton G, Gillingwater TH. Spinal muscular atrophy: Going beyond the motor neuron. Trends Mol Med. 2013;19(1):40-50.
12. Yeo CJJ, Darras BT. Overturning the Paradigm of Spinal Muscular Atrophy as just a Motor Neuron Disease. Pediatr Neurol. 2020;109:12-19.
13. Munsat TL, Davies KE. International SMA Consortium Meeting (26-28 June 1992, Bonn, Germany). Neuromuscul Disord. 1992;2(5-6):423-428.
14. Dubowitz V. Chaos in the classification of SMA: A possible resolution. Neuromuscul Disord. 1995;5(1):3-5.
15. Wijngaarde CA, Stam M, Otto LAM, et al. Population-based analysis of survival in spinal muscular atrophy. Neurology. 2020;94(15):E1634-E1644.
16. Mercuri E, Bertini E, Iannaccone ST. Childhood spinal muscular atrophy: Controversies and challenges. Lancet Neurol. 2012;11(5):443-452.
17. Wadman RI, Wijngaarde CA, Stam M, et al. Muscle strength and motor function throughout life in a cross-sectional cohort of 180 patients with SMA types 1c-4. Eur J Neurol. 2018;25(3):512-518.
18. Deymeer F, Serdaroglu P, Poda M, Gülşen-Parman Y, Özçelik T, Özdemir C. Segmental distribution of muscle weakness in SMA III: Implications for deterioration in muscle strength with time. Neuromuscul Disord. 1997;7(8):521-528.

19. Durmus H, Yilmaz R, Gulsen-Parman Y, et al. Muscle magnetic resonance imaging in spinal muscular atrophy type 3: Selective and progressive involvement. Muscle and Nerve. 2017;55(5):651-656.
20. Montes J, Dunaway S, Garber CE, Chiriboga CA, De Vivo DC, Rao AK. Leg muscle function and fatigue during walking in spinal muscular atrophy type 3. Muscle Nerve. 2014;50(1):34-39.
21. Mentis GZ, Blivis D, Liu W, et al. Early Functional Impairment of Sensory-Motor Connectivity in a Mouse Model of Spinal Muscular Atrophy. Neuron. 2011;69(3):453-467.
22. Ling KKY, Gibbs RM, Feng Z, Ko CP. Severe neuromuscular denervation of clinically relevant muscles in a mouse model of spinal muscular atrophy. Hum Mol Genet. 2012;21(1):185-195.
23. Rodriguez-Torres R, Fabiano J, Goodwin A, et al. Neuroanatomical Models of Muscle Strength and Relationship to Ambulatory Function in Spinal Muscular Atrophy. J Neuromuscul Dis. 2020;7(4):459-466.
24. Kingma DW, Feeback DL, Marks WA, Bobele GB, Leech RW, Brumback RA. Selective Type II Muscle Fiber Hypertrophy in Severe Infantile Spinal Muscular Atrophy. J Child Neurol. 1991;6(4):329-334.
25. Murray LM, Comley LH, Thomson D, Parkinson N, Talbot K, Gillingwater TH. Selective vulnerability of motor neurons and dissociation of pre- and post-synaptic pathology at the neuromuscular junction in mouse models of spinal muscular atrophy. Hum Mol Genet. 2008;17(7):949-962.
26. Wadman RI, Vrancken AFJ, Van den Berg LH, Van der Pol WL. Dysfunction of the neuromuscular junction in patients with spinal muscular atrophy type 2 and 3. Neurology. 2012;79:2050-2055.
27. Ripolone M, Ronchi D, Violano R, et al. Impaired Muscle Mitochondrial Biogenesis and Myogenesis in Spinal Muscular Atrophy. JAMA Neurol. 2015;72(6):1-10.
28. Miller N, Shi H, Zelikovich A., Ma Y-C. Motor Neuron Mitochondrial Dysfunction in Spinal Muscular Atrophy. Hum Mol Genet. 2016;25(16):3395-3406.
29. Finkel RS, Fischbeck KH. Maybe too much of a good thing in gene therapy. Nat Neurosci. 2021;24(July):8-9.
30. Darras B, Chiriboga CA, Iannaccone ST, et al. Nusinersen in later-onset spinal muscular atrophy: Long-term results from the phase 1/2 studies. Neurology. 2019;92(21):e2492-e2506.
31. Finkel RS, Mercuri E, Darras BT, et al. Nusinersen versus sham control in infantile-onset spinal muscular atrophy. N Engl J Med. 2017;377(18):1723-1732.
32. Finkel RS, Chiriboga CA, Vajsar J, et al. Treatment of infantile-onset spinal muscular atrophy with nusinersen: a phase 2, open-label, dose-escalation study. Lancet. 2016;388(10063):3017-3026.
33. Hoy SM. Nusinersen: A Review in 5q Spinal Muscular Atrophy. CNS Drugs. 2018;32(7):689-696.
34. Mendell JR, Al-Zaidy S, Shell R, et al. Single-dose gene-replacement therapy for spinal muscular atrophy. N Engl J Med. 2017;377(18):1713-1722.
35. Finkel R, Day J, Darras B, et al. Phase 1 study of intrathecal administration of AVXS-101 gene-replacement therapy (GRT) for spinal muscular atrophy type 2 (SMA2) (STRONG). Neurology. 2019;92(15 Supplement):P1.6-059.
36. Ratni H, Ebeling M, Baird J, et al. Discovery of Risdiplam, a Selective Survival of Motor Neuron-2 (SMN2) Gene Splicing Modifier for the Treatment of Spinal Muscular Atrophy (SMA). J Med Chem. 2018;61(15):6501-6517.
37. Ratni H, Karp GM, Weetall M, et al. Specific Correction of Alternative Survival Motor Neuron 2 Splicing by Small Molecules: Discovery of a Potential Novel Medicine to Treat Spinal Muscular Atrophy. J Med Chem. 2016;59(13):6086-6100.

38. Wirth B, Karakaya M, Kye MJ, Mendoza-Ferreira N. Twenty-Five Years of Spinal Muscular Atrophy Research: From Phenotype to Genotype to Therapy, and What Comes Next. Annu Rev Genomics Hum Genet. 2020;21:231-261.
39. Chen TH. New and developing therapies in spinal muscular atrophy: From genotype to phenotype to treatment and where do we stand? Int J Mol Sci. 2020;21(9):1-20.
40. Bowerman M, Becker CG, Yáñez-Muñoz RJ, et al. Therapeutic strategies for spinal muscular atrophy: SMN and beyond. DMM Dis Model Mech. 2017;10(8):943-954.
41. Tizzano EF, Finkel RS. Spinal muscular atrophy: A changing phenotype beyond the clinical trials. Neuromuscul Disord. 2017;27(10):883-889.
42. Bartels B, Groot JF De, Habets LE, et al. Fatigability in spinal muscular atrophy : validity and reliability of endurance shuttle tests. Orphanet J Rare Dis. 2020;2:1-9.
43. Kluger BM, Krupp LB, Enoka RM. Fatigue and fatigability in neurologic illnesses: Proposal for a unified taxonomy. Neurology. 2013;80(4):409-416.
44. Montes J, McDermott MP, Martens WB, et al. Six-minute walk test demonstrates motor fatigue in spinal muscular atrophy. Neurology. 2010;74(10):833-838.
45. Stam M, Wadman RI, Bartels B, et al. A continuous repetitive task to detect fatigability in spinal muscular atrophy. Orphanet J Rare Dis. 2018;13(1):1-7.
46. Goulet B, Kothary R, Parks R. At the "Junction" of Spinal Muscular Atrophy Pathogenesis: The Role of Neuromuscular Junction Dysfunction in SMA Disease Progression. Curr Mol Med. 2013;13(7):1160-1174.
47. Kong L, Wang X, Choe DW, et al. Impaired synaptic vesicle release and immaturity of neuromuscular junctions in spinal muscular atrophy mice. J Neurosci. 2009;29(3):842-851.
48. Kariya S, Park GH, Maeno-Hikichi Y, et al. Reduced SMN protein impairs maturation of the neuromuscular junctions in mouse models of spinal muscular atrophy. Hum Mol Genet. 2008;17(16):2552-2569.
49. Bowerman M, Murray LM, Beauvais A, Pinheiro B, Kothary R. A critical smn threshold in mice dictates onset of an intermediate spinal muscular atrophy phenotype associated with a distinct neuromuscular junction pathology. Neuromuscul Disord. 2012;22(3):263-276.
50. Cifuentes-Diaz C, Nicole S, Velasco ME, et al. Neurofilament accumulation at the motor endplate and lack of axonal sprouting in a spinal muscular atrophy mouse model. Hum Mol Genet. 2002;11(12):1439-1447.
51. Arnold AS, Gueye M, Guettier-Sigrist S, et al. Reduced expression of nicotinic AChRs in myotubes from spinal muscular atrophy I patients. Lab Invest. 2004;84(10):1271-1278.
52. Braun S, Croizat B, Lagrange M, Warter J, Poindron P. Constitutive muscular abnormalietis in culture in spinal muscular atrophy. Lancet. 1995;345:694-695.
53. Houdebine L, D'Amico D, Bastin J, et al. Low-Intensity Running and High-Intensity Swimming Exercises Differentially Improve Energy Metabolism in Mice With Mild Spinal Muscular Atrophy. Front Physiol. 2019;10(October):1-21.
54. Biondi O, Grondard C, Lécolle S, et al. Exercise-induced activation of NMDA receptor promotes motor unit development and survival in a type 2 spinal muscular atrophy model mouse. J Neurosci. 2008;28(4):953-962.
55. Stam M, Wadman RI, Wijngaarde CA, et al. Protocol for a phase II, monocentre, double-blind, placebo-controlled, cross-over trial to assess efficacy of pyridostigmine in patients with spinal muscular atrophy types 2-4 (SPACE trial). BMJ Open. 2018;8(7):1-9.

56. Stam M, Wijngaarde C, Bartels B, et al. Space trial. A phase 2, monocenter, double-blind, placebo-controlled, cross-over trial to assess efficacy of pyridostigmine in patients with spinal muscular atrophy types 2,3 and 4. In: Cure SMA June 30 2019; 2019.
57. Jones D, Round J, de Haan A. Skeletal Muscle from Molecules to Movement. Elsevier Ltd; 2005.
58. Scott W, Stevens J, Binder–Macleod SA. Human Skeletal Muscle Fiber Type Classifications. Phys Ther. 2001;81(11):1810-1816.
59. Schiaffino S, Reggiani C. Fiber types in Mammalian skeletal muscles. Physiol Rev. 2011;91(4):1447-1531.
60. Meyerspeer M, Boesch C, Cameron D, et al. 31P magnetic resonance spectroscopy in skeletal muscle: Experts' consensus recommendations. NMR Biomed. 2020;(August 2019):1-22.
61. Joyce NC, Oskarsson B, Jin LW. Muscle biopsy evaluation in neuromuscular disorders. Phys Med Rehabil Clin N Am. 2012;23(3):609-631.
62. Arnold WD, Kassar D, Kissel JT. Spinal muscular atrophy: Diagnosis and management in a new therapeutic era. Muscle Nerve. 2015;51(February):157-167.
63. Roth R, Graziani L, Terry R, Scheinberg L. Muscle fine structure in the kugelberg-welander syndrome chronic spinal muscular atrophy. J Neuropath exp Neurol. 1965;24:444-454.
64. Mastaglia FL, Walton JN. Histological and histochemical changes in skeletal muscle from cases of chronic juvenile and early adult spinal muscular atrophy (the Kugelberg-Welander syndrome). J Neurol Sci. 1971;12(1):15-44.
65. Johnson MA, Sideri G, Weightman D, Appleton D. A comparison of fibre size, fibre type constitution and spatial fibre type distribution in normal human muscle and in muscle from cases of spinal muscular atrophy and from other neuromuscular disorders. J Neurol Sci. 1973;20(4):345-361.
66. Salort-campana E, Quijano-roy S. Clinical features of spinal muscular atrophy (SMA) type 3 (Kugelberg-Welander disease). Arch Pédiatrie. 2020;27(7):7S23-7S28.
67. Dubowitz V. Enzyme histochemistry of skeletal muscle. 3. Neurogenic muscular atrophies. J Neurol Neurosurg Psychiatry. 1966;29(1):23-28.
68. Anderson JR. Atlas of skeletal muscle pathology. In: Gresham GA, ed. Atlas of Skeletal Muscle Pathology. 9th ed. MTP Press Limited; 1985:46-52.
69. Hausmanowa-Petrusewicz I, Askanas W, Badurska B, et al. Infantile and juvenile spinal muscular atrophy. J Neurol Sci. 1968;6(2):269-287.
70. Dubowitz V. Pathology of experimentally re-innervated skeletal muscle. J Neurol Neurosurg Psychiatry. 1967;30(2):99-110.
71. Glancy B, Hsu LY, Dao L, et al. In Vivo microscopy reveals extensive embedding of capillaries within the sarcolemma of skeletal muscle fibers. Microcirculation. 2014;21(2):131-147.
72. McArdle WD, Katch FI, Katch VL. EXERCISE PHYSIOLOGY - Nutrition, Energy, and Human Performance. 7th ed. Wolters Kluwer| Lippincott Williams & Wilkins; 2010.
73. Hausmanowa-Petrusewicz I, Vrbová G. Spinal muscular atrophy: A delayed development hypothesis. Neuroreport. 2005;16(7):657-661.
74. Boyer JG, Deguise MO, Murray LM, et al. Myogenic program dysregulation is contributory to disease pathogenesis in spinal muscular atrophy. Hum Mol Genet. 2014;23(16):4249-4259.

75. Hayhurst M, Wagner AK, Cerletti M, Wagers AJ, Rubin LL. A cell-autonomous defect in skeletal muscle satellite cells expressing low levels of survival of motor neuron protein. Dev Biol. 2012;368(2):323-334.
76. Bricceno K V., Martinez T, Leikina E, et al. Survival motor neuron protein deficiency impairs myotube formation by altering myogenic gene expression and focal adhesion dynamics. Hum Mol Genet. 2014;23(18):4745-4757.
77. Segal SS, Kurjiaka DT. Coordination of blood flow control in the resistance vasculatur of skeletal muscle. Med Sci Sports Exerc. 1995;27(8):1158-1164.
78. Fuglevand AJ, Segal SS. Simulation of motor unit recruitment and microvascular unit perfusion: Spatial considerations. J Appl Physiol. 1997;83(4):1223-1234.
79. Thomas GD, Segal SS. Neural control of muscle blood flow during exercise. J Appl Physiol. 2004;97(2):731-738.
80. Nobutoki T, Ihara T. Early disruption of neurovascular units and microcirculatory dysfunction in the spinal cord in spinal muscular atrophy type I. Med Hypotheses. 2015;85(6):842-845.
81. Shababi M, Habibi J, Ma L, Glascock JJ, Sowers JR, Lorson CL. Partial restoration of cardio-vascular defects in a rescued severe model of spinal muscular atrophy. J Mol Cell Cardiol. 2012;52(5):1074-1082.
82. Somers E, Stencel Z, Wishart TM, Gillingwater TH, Parson SH. Density, calibre and ramification of muscle capillaries are altered in a mouse model of severe spinal muscular atrophy. Neuromuscul Disord. 2012;22(5):435-442.
83. Zhou H, Ying H, Scoto M, Brogan P, Parson S, Muntoni F. Microvascular abnormality in spinal muscular atrophy and its response to antisense oligonucleotide therapy. Neuromuscul Disord. 2015;25(2015):S193.
84. Konrad P. The ABC of EMG: A Practical Introduction to Kinesiological Electromyography. Noraxon INC. USA; 2005. http://www.noraxon.com/docs/education/abc-of-emg.pdf
85. Al-Mulla MR, Sepulveda F, Colley M. A review of non-invasive techniques to detect and predict localised muscle fatigue. Sensors. 2011;11(4):3545-3594.
86. Farina D. Interpretation of the Surface Electromyogram in Dynamic Contractions. Exerc Sport Sci Rev. Published online 2006:121-127.
87. Hermens HJ, Freriks B, Disselhorst-Klug C, Rau G. Development of recommendations for SEMG sensors and sensor placement procedures. J Electromyogr Kinesiol. 2000;10:361-374.
88. Dimitrova NA, Dimitrov G V. Interpretation of EMG changes with fatigue: Facts, pitfalls, and fallacies. J Electromyogr Kinesiol. 2003;13(1):13-36.
89. Felici F. Neuromuscular responses to exercise investigated through surface EMG. J Electromyogr Kinesiol. 2006;16(6):578-585.
90. Bonato P, Roy SH, Knaflitz M, Luca CJ De. Time-frequency parameters of the surface myoelectric signal for assessing muscle fatigue during cycling dynamic contractions. IEEE Trans Biomed Eng. 2001;48(July):745-754.
91. Henneman E, Clamann HP, Gillies JD, Skinner RD. Rank order of motoneurons within a pool: law of combination. J Neurophysiol. 1974;37(6):1338-1349.
92. McRobbie DW, Moore EA, Graves MJ, Prince MR. MRI from Picture to Proton. second. Cambride University Press; 2006.
93. Oudeman J, Nederveen AJ, Strijkers GJ, Maas M, Luijten PR, Froeling M. Techniques and applications of skeletal muscle diffusion tensor imaging: A review. J Magn Reson Imaging. 2016;43(4):773-788.

94. Budzik JF, Balbi V, Verclytte S, Pansini V, Le Thuc V, Cotten A. Diffusion tensor imaging in musculoskeletal disorders. Radiographics. 2014;34(3):56-73.
95. Jeneson JAL, Westerhoff H V., Kushmerick MJ. A metabolic control analysis of kinetic controls in ATP free energy metabolism in contracting skeletal muscle. Am J Physiol - Cell Physiol. 2000;279(3 48-3):813-832.
96. Jeneson JAL, Schmitz JPJ, Hilbers PAJ, Nicolay K. An MR-compatible bicycle ergometer for in-magnet whole-body human exercise testing. Magn Reson Med. 2010;63(1):257-261.
97. Meyer RA. A linear model of muscle respiration explains monoexponential phosphocreatine changes. Am J Physiol - Cell Physiol. 1988;254(4):C548–553.
98. van Brussel M, van Oorschot JWM, Schmitz JPJ, et al. Muscle Metabolic Responses During Dynamic In-Magnet Exercise Testing: A Pilot Study in Children with an Idiopathic Inflammatory Myopathy. Acad Radiol. 2015;22(11):1443-1448.
99. Roberts JKM, Wade-Jardetzky N, Jardetzky O. Intracellular pH Measurements by 31P Nuclear Magnetic Resonance. Influence of Factors Other Than pH on 31P Chemical Shifts. Biochemistry. 1981;20(19):5389-5394.
100. Moon RB, Richards JH. Determination of Intracellular pH by 31P Magnetic Resonance*. J Biol Chem. 1973;248(No. 20, Issue of Octover 25):7276-7278.
101. Vandenborne K, McCully K, Kakihira H, et al. Metabolic heterogeneity in human calf muscle during maximal exercise. Proc Natl Acad Sci U S A. 1991;88(13):5714-5718.
102. Vandenborne K, Walter G, Leigh JS, Goelman G. pH heterogeneity during exercise in localized spectra from single human muscles. Am J Physiol - Cell Physiol. 1993;265(5 34-5).
103. Mizuno M, Justesen LO, Bedolla J, Friedman DB, Secher NH, Quistorff B. Partial curarization abolishes splitting of the inorganic phosphate peak in 31P-NMR spectroscopy during intense forearm exercise in man. Acta Physiol Scand. 1990;139(4):611-612.
104. Rzanny R, Stutzig N, Hiepe P, Gussew A, Thorhauer HA, Reichenbach JR. The reproducibility of different metabolic markers for muscle fiber type distributions investigated by functional 31P-MRS during dynamic exercise. Z Med Phys. 2016;26(4):323-338.
105. Tonon C, Gramegna LL, Lodi R. Magnetic resonance imaging and spectroscopy in the evaluation of neuromuscular disorders and fatigue. Neuromuscul Disord. 2012;22(SUPPL. 3):S187-S191.
106. Diekman EF, Visser G, Schmitz JPJ, et al. Altered energetics of exercise explain risk of rhabdomyolysis in very long-chain acyl-coa dehydrogenase deficiency. PLoS One. 2016;11(2):1-19.
107. Hájek M, Grosmanov A, Horsk A, Urban P. Spectroscopy Comparison of the clinical state and its changes in patients with Duchenne and Becker muscular dystrophy with results of in vivo 31p magnetic resonance spectroscopy. Eur Radiol. 1993;3:499-506.
108. Torriani M, Townsend E, Thomas BJ, Bredella MA, Ghomi RH, Tseng BS. Lower leg muscle involvement in Duchenne muscular dystrophy: An MR imaging and spectroscopy study. Skeletal Radiol. Published online 2011.
109. Tosetti M, Linsalata S, Battini R, et al. Muscle metabolic alterations assessed by 31-phosphorus magnetic resonance spectroscopy in mild becker muscular dystrophy. Muscle Nerve. 2011;44(5):816-819.

110. Lodi R, Kemp GJ, Muntoni F, et al. Reduced cytosolic acidification during exercise suggests defective glycolytic activity in skeletal muscle of patients with Becker muscular dystrophy. An in vivo 31P magnetic resonance spectroscopy study. Brain. 1999;122(1):121-130.
111. Sassani M, Alix JJ, McDermott CJ, et al. Magnetic resonance spectroscopy reveals mitochondrial dysfunction in amyotrophic lateral sclerosis. Brain. 2020;143(12):3603-3618.
112. Sharma U, Atri S, Sharma M., Sarkar C, Jagannathan N. Skeletal muscle metabolism in Duchenne muscular dystrophy (DMD): an in-vitro proton NMR spectroscopy study. Magn Reson Imaging. 2003;21(2):145-153.
113. Sharma KR, Kent-Braun J a, Majumdar S, et al. Physiology of fatigue in amyotrophic lateral sclerosis. Neurology. 1995;45(4):733-740.
114. Kent-Braun JA, Miller RG. Central fatigue during isometric exercise in amyotrophic lateral sclerosis. Muscle and Nerve. 2000;23(6):909-914.
115. Grehl T, Fischer S, Müller K, Malin JP, Zange J. A prospective study to evaluate the impact of 31P-MRS to determinate mitochondrial dysfunction in skeletal muscle of ALS patients. Amyotroph Lateral Scler. 2007;8(1):4-8.
116. Jöbsis FF. Noninvasive , Infrared Monitoring of Cerebral and Myocardial Oxygen Sufficiency and Circulatory Parameters Author (s): Frans F . Jöbsis. Am Assoc Adv Sci. 1977;198(4323):1264-1267.
117. Mancini DM, Bolinger L, Li H, Kendrick K, Chance B, Wilson JR. Validation of near-infrared spectroscopy in humans. J Appl Physiol. 1994;77(6):2740-2747.
118. Piantadosi CA, Hemstreet TM, Jöbsis-Vandervliet FF. Near-infrared spectrophotometric monitoring of oxygen distribution to intact brain and skeletal muscle tissues. Crit Care Med. 1986;14(8):698-706.
119. Delpy DT, Cope M. Quantification in tissue near-infrared spectroscopy. Philos Trans R Soc B Biol Sci. 1997;352(1354):649-659.
120. Jobsis FF, Keizer H, Lamanna JC, Carolina N. Reflectance cytochrome spectrophotometry aa t in vivo of. J Appl Physiol. 1977;43(858):858-872.
121. Hamaoka T, McCully KK, Quaresima V, Yamamoto K, Chance B. Near-infrared spectroscopy/imaging for monitoring muscle oxygenation and oxidative metabolism in healthy and diseased humans. J Biomed Opt. 2007;12(6):062105.
122. Duncan A, Meek J, Clemence M, et al. Optical pathlength measurements on adult head, calf and forearm and the head of the newborn infant using phase resolved optical spectorscopy. Phys Med Biol. 1995;(40):295-304.
123. Habers GEA, De Knikker R, Van Brussel M, et al. Near-infrared spectroscopy during exercise and recovery in children with juvenile dermatomyositis. Muscle Nerve. 2013;47(1):108-115.

Chapter 2

Assessment of fatigability in patients with spinal muscular atrophy: development and content validity of a set of endurance tests

B. Bartels
L.E. Habets
M. Stam
R.I. Wadman
C.A. Wijngaarde
M.A.G.C. Schoenmakers
T. Takken
E.H. Hulzebos
W.L. van der Pol
J.F. de Groot

BMC Neurology 2019; 19 (1)

Abstract

Background

Fatigability has emerged as an important dimension of physical impairment in patients with Spinal Muscular Atrophy (SMA). At present reliable and valid outcome measures for both mildly and severely affected patients are lacking. Therefore the primary aim of this study is the development of clinical outcome measures for fatigability in patients with SMA across the range of severity.

Methods

We developed a set of endurance tests using five methodological steps as recommended by the COnsensus-based Standards for the selection of health Measurement INstruments (COSMIN). In this iterative process, data from multiple sources were triangulated including a scoping review of scientific literature, input from a scientific and clinical multidisciplinary expert panel and three pilot studies including healthy persons (N=9), paediatric patients with chronic disorders (N=10) and patients with SMA (N=15).

Results

Fatigability in SMA was operationalised as the decline in physical performance. The following test criteria were established; one method of testing for patients with SMA type 2-4, a set of outcome measures that mimic daily life activities, a submaximal test protocol of repetitive activities over a longer period; external regulation of pace. The scoping review did not generate suitable outcome measures. We therefore adapted the Endurance Shuttle Walk Test for ambulatory patients and developed the Endurance Shuttle Box and Block Test and the - Nine Hole Peg Test for fatigability testing of proximal and distal arm function. Content validity was established through input from experts and patients. Pilot testing showed that the set of endurance tests are comprehensible, feasible and meet all predefined test criteria.

Conclusions

The development of this comprehensive set of endurance tests is a pivotal step to address fatigability in patients with SMA.

Background

Hereditary proximal Spinal Muscular Atrophy (SMA) is an autosomal recessive neurodegenerative disease caused by homozygous loss of function of the survival motor neuron 1 (*SMN1*) gene 1. SMA is characterised by a wide range of disease severity ranging from neonatal respiratory insufficiency and death (SMA type 1), ability to sit without support but inability to walk independently (SMA type 2), problems with or the loss of ambulation (SMA type 3a-b) to relatively mild impairments due to proximal muscle weakness in patients with adult onset disease (SMA type 4).[2] All four SMA types are characterised by progressive muscle weakness and secondary loss of motor abilities over time.[3] In addition to muscle weakness, fatigability has emerged as a rather common but often overlooked complaint among patients with SMA.[4,5] The current taxonomy defines 'fatigability' as the magnitude or rate of change in a performance criterion relative to a reference over a given time of task performance or measure of mechanical output and is the opposite of ´endurance´, which involves the prolonged maintenance of constant or self-regulated power or velocity.[6,7] Patients with SMA refer that they easily fatigue during repetitive activities of daily living such as lifting an arm during eating or walking even short distances. A possible explanation comes from SMA animal models and post-mortem studies that showed abnormal development and maturation of the neuromuscular junction. Neuromuscular dysfunction has been found in at least half of the patients with SMA, suggesting that this may contribute to complaints of fatigability.[5,8–12] Since outcome measures sensitive to change in fatigability are lacking, their development is a pivotal step in a better understandig of fatigabillity in SMA.[13,14] This study aimed to provide the framework for the development of novel clinical outcome measures for fatigability in patients with SMA type across the range of severity. We determined content validity following the COnsensus-based Standards for the selection of health Measurement INstruments (COSMIN)-guidelines and recommendations by European and American regulatory authorities.[15,16]

Methods

A set of outcome measures for fatigability was developed according to five methodological steps as recommended by COSMIN (table 1).[17,18] In this iterative process data from multiple sources were triangulated. Sources included a scoping review of scientific literature, input from a scientific and clinical multidisciplinary expert panel and three pilot studies including healthy persons (N=9), paediatric patients with chronic disorders (N=10) and patients with SMA (N=15). The expert panel consisted of ten clinicians and researchers including paediatric physical therapists (BB, MS), clinical exercise physiologists and movement

scientists (JG, LH, HH,TT) and neurologists or neurology residents with ample experience in caring for children and adults with SMA (MS, CW, RW, WP). Three round table discussions took place with different group compositions.

Table 1. Methodological steps COSMIN*

Methodological steps	Questions to be answered	Sources
Step 1: Definition and elaboration of the construct	1. Definition of fatigability? 2. Target population? 3. Purpose of the outcome measure?	Key papers on fatigability assessment
Step 2: Choice of measurement method	1. Existing measurement that responds closely to construct to be measured? 2. Level of measurement? 3. Single or multiple measures?	Scoping review of scientific literature Expert panel (round table discussion 1)
Step 3: Selecting and formulating items	1. Which activities cause most problems? 2. Which available measures reflect these activities?	Patient report outcome (pilot sample 3) Expert panel (round table discussion 2)
Step 4: Scoring issues	1. Application in research or clinical practice 2. Measurement level?	Expert panel (round table discussion 3)
Step 5: Pilot testing	1. Comprehensibility? 2. Feasibility? 3. Relevance?	Pilot sample 1 (healthy subjects) Pilot sample 2 (pediatric patients with chronic diseases) Pilot sample 3 (patients with SMA)

* COSMIN = 'COnsensus-based Standards for the selection of health Measurement Instruments.

Definition and elaboration of the construct intended to be measured

The first step in the development of a new outcome measure consisted of the operationalization of the theoretical construct in SMA. This included a clear definition of fatigability, a description of the target population and the purpose of the outcome measure and the composition of specific test criteria. The taxonomy for fatigue and fatigability as proposed by Kluger et al was used as a starting point from which a construct for fatigability assessment in SMA was described. Fatigability was defined as the magnitude or rate of change in a performance criterion relative to a reference over a given time of task performance or measure of mechanical output.[7] Several other key papers on fatigability

that used a similar definition and described test methodology were selected to complement the framework.[19–25]

Choice of measurement method

During the second step we combined the results from a scoping review on available measures for fatigability in patients with SMA with the experiences with fatigability testing by our research group.

Scoping review of the literature

Given the fact that SMA has been associated with fatigability only recently, it was anticipated that a systematic review would not generate significantly more information than a scoping literature search. Peer-reviewed experimental articles written in English were retrieved from Pubmed and Trial.gov up to the first of October 2014. The following search strings was used: ((“muscular atrophy, spinal”[MeSH Terms] OR (“muscular”[All Fields] AND “atrophy”[All Fields] AND “spinal”[All Fields]) OR “spinal muscular atrophy”[All Fields] OR (“spinal”[All Fields] AND “muscular”[All Fields] AND “atrophy”[All Fields])) OR (“Stat Methods Appt”[Journal] OR “sma”[All Fields])) AND (((Fatigability[All Fields] OR Endurance[All Fields]) OR Stamina[All Fields]) OR (“fatigue”[MeSH Terms] OR “fatigue”[All Fields])). At first, papers were selected that described the measurement of fatigability or endurance in patients with SMA. Secondly, outcome measures were assessed to what extent they complied with the definition and test criteria defined within this study. In the case that no suitable outcome measure were retrieved, the expert panel discussed in the first round table discussion whether other appropriate outcome measure were available that met the clinimetric requirements and could be validated for SMA.

Selecting and formulating items

During the third step, questionnaires were taken from the pilot sample of patients with SMA to determine which activities of daily living (ADLs) provoked fatigability. In adults, the questionnaire by Straver et al. was used which was originally validated for peripheral nervous system disorders.[26] A similar questionnaire was developed for children based on clinical experience from the expert panel and items from the Child Health Assessment Questionnaire, a validated questionnaire for ADLs in other clinical populations.[27] Patient-reported activities that caused fatigability were clustered into three different functional domains, namely leg function, upper arm function and hand function. The expert panel assessed in the second round table discussion whether all domains were relevant to SMA and should be included in the development of the set of outcome measures for fatigability.

Scoring issues

During the fourth step, the expert panel discussed about the composition of the tests, taking into account the application setting (research, clinical practise) and the patient group, and selecting primary outcome parameters. For example, tests are usually shorter in clinical practise, due to time constraints.[17]

Pilot testing

Patients with SMA were recruited from the Dutch SMA registry (www.treatnmd.eu/patientregistries).[28] This registry contains detailed clinical information of over 300 children and adults with SMA. To minimize selection bias, all eligible patients listed in this register were offered the possibility to participate. All patients had a confirmed homozygous deletion of the ***SMN1*** gene or a heterozygous ***SMN1*** deletion in combination with a point mutation on the second ***SMN1*** allele. In order to be eligible to participate in this study, a subject had to meet all of the following additional criteria: age 8-60 years; ability to follow test instructions and no exercise restrictions. Two patients with SMA declined participation due to frequent hospital visits in the recent past and fear of increased fatigue. Patient controls were recruited from a school for special education in Utrecht. Healthy controls were recruited from the University of Applied Sciences and the University Medical Center Utrecht. The outcome measures for fatigability were pilot-tested on 'comprehensibility' ('Are test instructions to participants unambiguous and well understood?') and 'feasibility' (measurement completion, acceptability and perceived burden) in three consecutive pilot samples of healthy controls (pilot sample 1), paediatric patients with chronic diseases (pilot sample 2) and patients with SMA (pilot sample 3). 'Measurement completion rate' was defined as the number of participants able to complete the test without premature discontinuation caused by motivational issues or a-specific physical complaints.[17] 'Acceptability' was defined as the willingness to perform the test again in the future and was assessed with a 'Visual Analogue Scale'.[29] Perceived burden was assessed with the OMNI scale for perceived exertion.[30] The third round table discussion was used to discuss pilot data and if necessary to make small adjustments to the protocol.

Results

Definition and elaboration of the construct intended to be measured

Fatigability is subdivided in 'physical fatigability' and 'cognitive fatigability' which are measured in different ways.[7,21,24,31] Physical fatigability is primarily measured by quantifying the decline in one or more aspects of motor performance such as peak force, power, speed and accuracy while cognitive fatigability is measured by quantifying the decline in processing speed and sustained attention over time during a sustained complex information processing task. Given the fact that patients with SMA complain about sustaining physical activities, we decided to focus on physical fatigability defined as a decline in performance such as peak force, power, speed and accuracy. A number of methods have been described to measure fatigability during different types of performances including:

1) Continuous performance of a prolonged task:[19,21]
   a) Intermitted submaximal exercise protocol which mimics activities such as walking or cycling in which fatigability develops over a longer period
   b) Continuous maximal protocol which mimics activities such as lifting heavy objects or sprinting
2) Comparing performance on a probe task before and immediately after prolonged performance of a separate fatigue inducing task.[32]

Fatigability is experienced by patients with SMA as the inability to perform prolonged repetitive tasks during activities of daily life. These complaints are reminiscent of those of patients with myasthenic syndromes, which are caused by reduced efficiency of neuromuscular junction.[33] Moreover, SMA is characterised by structural and physiological abnormalities of the neuromuscular junction as shown by post-mortem studies and the presence of pathological decrement upon repetitive nerve stimulation supporting the hypothesis that neuromuscular junction dysfunction is associated with fatigability in SMA and should be the focus of fatigability test development. The extent of fatigability may vary according to the method of testing.[22,24] Therefore, test protocols should be used that mimic daily life activities that provoke fatigability in patients. Consequently a set of predefined test-criteria were composed (table 2).

Table 2. Test criteria for SMA and candidate outcome measures

	Methodology	**Type**	**Protocol**	**Standardization**	**Intensity**	**Test duration**	**External regulation of pace**
Pre-defined test criteria	Generic applicable	Mimic daily life activities	Repetitive tasks	Yes	Submaximal	75 sec*	yes
RNHPT	+/-	+	+	+	+	+	-
Sustained MVC during 60 seconds	-	-	-	+	-	+	-
Sustained MVC during 15 seconds	+	+/-	-	+	-	-	-
Masticatory function	-	-	-	+	-		
6MWT	-	+	+	+/-	+	+	-
ESWT	-	+	+	+	+	+	+

RNHPT = Repeated Nine Hole Peg Test, MVC = Maximal Voluntary Contraction, 6MWT = 6 Minute Walk Test, ESWT = Endurance Shuttle Walk Test, Mn = Mean value, *Gastin et al. 2010 [64].

Choice of measurement method

The scoping review search performed on the 1st of October 2014 retrieved 109 records in Pubmed and no additional records in trial.gov. All records were screened on title and abstract. Seven papers were included describing 4 different methods to assess fatigability in SMA (Appendix 1): Sustained maximal voluntary contraction for 60 seconds, [34] Sustained maximal voluntary contraction for 15 seconds,[35] Masticatory endurance [36] and the Six Minute Walk Test (6MWT). [37–40] We recently reported our experience with the repeated Nine Hole Peg Test (rNHPT) as a measure for fatigability of arm and hand function in patients with SMA. Given the promising results, the r9HPT was included in the assessment of potential outcome measures derived from the review. Recently, this study was published.[41]

Evaluation of selected outcome measures

All five different outcome measures from the methods above, defined fatigability as the decrease in physical performance, which was in accordance with the definition used in this study. There was however a large difference in methods of testing with regards to target muscles, type of exercise, intensity and duration (table 2). The rNHPT and the 6MWT, both

submaximal repetitive tasks, met most predefined criteria and provided proof of principle that including an endurance element holds promise as a mode to measure fatigability objectively in patients with SMA. The authors of the 6MWT and the rNHPT use similar methodology in which subjects are instructed to deliver maximal performance and change in velocity or distance is assessed as primary outcome measure. The simple instruction and relatively short test period (1.5-6 minutes) make them particularly useful to detect fatigability in the individual patient with SMA. There were, however, several intrinsic clinical properties of both tests which made them less appropriate to assess the construct of fatigability as defined in this study: The intensity was not standardized and might fluctuate between maximal and submaximal intensity within and between subjects depending on disease severity and motivation;[42,43] The change in velocity as primary outcome measure did not directly reflect the inability to sustain prolonged repetitive task during ADLs such as frequently reported by patients; Both tests did not cover the subgroup of non-ambulatory patients with antigravity function of the arms, who primarily experience problems with repetitively lifting the arm while drinking or eating. The expert panel discussed whether potential non-validated outcome measure for fatigability were available that were more standardized on performance and used meaningful outcome parameters for endurance capacity. The methodology of the Endurance Shuttle Walk Test (ESWT) was proposed by one of the experts with experience in chronic pulmonary disease.

The Endurance Shuttle Walk Test

Revill et al. developed an externally controlled constant paced walking test to assess endurance capacity in patients with chronic obstructive pulmonary disease [44] (Appendix 1). The expert panel judged the methodology of ESWT as superior to all other outcome measures with regards to external regulation of pace, test duration and standardization of intensity. Since the ESWT could only be used in ambulatory patients, it was concluded that alternative outcome measures using the same methodology should be ideally used for endurance testing in non-ambulatory patients. Since no such outcome measure were available, it was decided to select existing scales that corresponded well with reported activities by patients and incorporate them in to the methodology of the ESWT.

Selecting and formulating items

Patients with SMA reported a great number of different activities on the domains of leg function, upper arm function and hand function (table 3). The expert panel therefore decided that all domains should be included in the development of the set of outcome measures for fatigability. The ESWT was selected to cover the activities related to leg muscles. The upper arm domain mainly comprehended activities lifting an object while the hand function domain mainly included activities performed at the table while moving

around the lower arm and hand. To cover activities of the upper arm and hand function, the expert panel decided to apply the methodology of the ESWT to the Nine Hole Peg Test and the Box and Block Test resulting in the Endurance Shuttle Nine Hole Peg test (ESNHPT) and the Endurance Shuttle Box and Block Test (ESBBT). The Nine Hole Peg Test, originally developed to assess distal arm function demonstrated good feasibility and sensitivity to detect fatigability in patients with SMA type 2.[41,45,46] The Box and Block Test, a measure for upper limb motor function, represented antigravity activities of the arms such as brushing teeth, eating a sandwich and lifting a cup.[47,48]

Table 3. Daily life activities provoking fatigability clustered per functional domain

Leg function	Proximal arm function	Hand function
Walking	Lifting a cup	Writing
Climbing stairs	Brushing teeth	Eating a sandwich
Cycling	Throwing a ball	Typing
Swimming	Fishing	Riding a power driven wheelchair
Showering	Holding phone to ear	Cutting (scissors)
Playing soccer	Washing hair	Drawing
Running	Carrying a bag	Painting
Putting clothes in the washing machine	Shoe polishing	Playstation
	Dish washing	Using cutlery
	Using cutlery	Driving car with mini joystick
	Showering	
		Moving things on the table
	Cooking	Using Mousepad
	Vacuum cleaning	Taking money out of wallet
	Washing clothes	Clapping hands
	Riding a hand driven wheelchair	Fixing screws
	Swimming	Putting on make-up
	Hanging clothes to dry	Moving objects on wheelchair table

Scoring issues

In accordance with the original ESWT, Time to Limitation (Tlim (sec)) was chosen by the expert panel as the primary outcome measure of all three endurance tests (round table discussion 3). With the aim to eventually use the set of tests both in research and clinical practise time constraints in the latter had to be taken in account.[17] To improve both motivation for and

feasibility of tests, maximum test duration was shortened from 20 minutes to 10 minutes. Based on clinical experience, it was expected that 10 minutes would be a sufficient time period to measure fatigability.

Pilot testing

Pilot-test sample 1 and 2

Eight healthy adults and one adolescent (mean age = 28.7, 50% female) performed all three endurance tests. Respectively 30% and 44% of the subjects could not continue at an intensity level of 85% for at least 10 minutes during the ESWT and ESBBT. Early termination was primarily caused by subtle coordinative errors due to the high velocity at which the motor task was performed. Therefore, intensity level of 85% was not considered valid for the assessment of fatigability in patients with SMA. Assessment at a 65% intensity level was considered too easy. It was therefore decided to set the intensity level at 75% for all tests. Consecutively a second pilot study was performed in 10 children with neuromuscular diseases and other motor disabilities (Developmental Coordination Disorder (N=1), Cerebral Palsy (N=2), SMA (N=2), Duchenne Muscular Dystrophy (N=2), Spina Bifida (N=1), Acquired Brain Injury (N=1) and Spinal Cord Injury (N=1)) to determine the feasibility of the endurance tests. All participants showed good comprehensibility and acceptability of the tests without any adverse events. Three children (SMA (n=2), Spinal Cord Injury (n=1) demonstrated a decreased time to limitation.

Pilot-test sample 3

Fifteen patients with SMA type 2 (n=8), type 3a (n=5) and type 3b (n=3) aged 10-49 and with a broad range in clinical severity (Hammersmith Functional Motor Scale Expanded score = 0-66) (table 4) performed 1,2 or 3 of the endurance shuttle tests (i.e. ESNHPT, ESBBT, ESWT) tests depending on their level of motor function. The comprehensibility, acceptability and measurement completion of all three tests were excellent despite moderate to severe self-reported muscle fatigue. All subjects were strongly motivated to perform well on the test and willing to do the test again in the context of future studies. Beforehand, it was expected that at least 50% of the subjects would end the test prematurely because of fatigability. Although most subjects did show signs of fatigability at the end of the test reflected by decrease in coordination, compensatory movements and perceived exertion, the drop–out rate was lower than expected on the ESNHPT (31%), ESBBT (45%) and ESWT (50%). The ESWT showed a trend towards ceiling effect (Tlim (Mn) = 462/600 seconds). It was observed that during the ESBBT subjects were actively compensating for fatigability by leaning on the box.

The Endurance Shuttle Tests: materials and procedures

To improve the validity of the tests, the protocol was modified on two important aspects. First, the maximal test duration was lengthened to 20 minutes for all tests (in accordance with the original ESWT procedure). Second, we decided that compensatory movements (e.g. leaning on the box during the performance of the box and block test) was no longer allowed. Materials and procedures for the set of endurance tests were described (Appendix 2).

Table 4. Pilot sample 3

	ESWT	**ESBBT**	**ESNHPT**
Sample size	4	9	13
SMA type			
2	0	3	6
3a	1	3	4
3b	3	3	3
Age			
yrs (min.-max.)	26.2 (10-37)	20.8 (10-37)	23.9 (10-49)
Gender			
Male	2	6	8
Female	1	3	5
HFMSE			
0-66	52 (44-66)	31 (4-66)	22 (1-66)
Time to Limitation			
0-600	555 (462-600)	373 (83-600)	457 (52-600)
Reduced time to limitation			
Yes	50%	44,4%	30,8%
No	50%	55,6%	69,2%
Measurement completion			
Yes	100%	100%	100%
No	0%	0%	0%
Comprehensibility			
Yes	100%	100%	100%
No	0%	0%	0%
Acceptability			
0-10 (min. – max.)	9.2 (7.4-10)	9.6 (7.9-10)	8.9 (4.9-10)
Perceived burden			
Muscle fatigue	7 (6-9)	4.9 (3-9)	4.5 (1-10)

ESWT = Endurance Shuttle Walk Test, ESBBT = Endurance Shuttle Box and Block Test,
ESNHPT = Endurance Shuttle Nine Hole Peg Test.

Discussion

This study aimed to provide the framework for the development of novel clinical outcome measures for fatigability in patients with SMA across the range of severity. The major strength of this study includes the use of the methodological steps as recommended by the COSMIN guidelines to systematically develop a set of endurance tests for patients with SMA with a specific emphasis on content validity.[17] Content validity is the degree to which the content of an instrument is an adequate reflection of the construct to be measured and without it, it is difficult to select appropriate outcome measures for trials or other types of interventions.[49] It is therefore recommended by the US Food and Drug Administration and the European Medicines Agency to establish content validity before evaluating other measurement properties.[15,16] The content validity of the endurance shuttle tests was established by combining evidence from scientific literature with patient reported outcome and the expertise from health care professionals and scientists, which will potentially lead to both valid and clinically meaningful outcome measures.

An important aim of this study was to develop one methodology for a broad clinical spectrum that would enable comparison between severely and mildly affected patients and with that facilitate future study trial inclusion. The methodology of the ESWT, originally validated for pulmonary disease was adjusted and applied to other motor tasks to meet with the specific disease characteristics of SMA. The ESWT speed was originally derived from a time consuming four component process including a second ISWT and a regression equation including maximal predicted oxygen uptake. Although Hill et al. simplified this method by directly using maximal walking speed it still included a second exercise test.[50] We questioned the validity of this method because of the risk of inducing fatigability prior to the test and therefore decided to use muscle power as the parameter to determine exercise intensity in SMA. Time in which 10 meter, 9 pegs or 10 blocks could be transferred were taken as maximal performance measure. It was decided not to adjust for the weight of the blocks and pegs or body weight, since both materials were very light and body weight is fixed in daily life activities as well. The convergent validity of this modified method with the original procedures and the comparability between patients with mild and severe muscle weakness need to be further analysed in future studies.

We decided to include motor tasks because we wanted to generate clinical relevant outcome measures and patients with SMA generally have normal coordinative function. The use of motor task within endurance tests potentially causes validity issues. For example, a subject might drop out because of motor coordination difficulties rather than fatigability. To confirm construct validity, it will be important to monitor other parameters of fatigability such as perceived exertion, motor behaviour and change in strength and electromyography response.[38,40,51,52]

Besides the clinimetric properties, the practical application of a new measurement test is an important aspect in the development of outcome measures for clinical practice. Ideally, an outcome measure is suitable for both day-to-day clinic purposes and clinical trials. For this purpose, an instrument needs to be easy to use in a limited time period, acceptable and feasible for the individual subject, while at the same time, applicable to a large part of the study population. The endurance tests have demonstrated to be comprehensible and acceptable for both healthy subjects and patients with a wide range of severity in an age range of 10-49 years. Based on our clinical experience and an upcoming large study on validity and reliability,[53] we expect the endurance tests to be suitable for subjects aged 6 years and older for those being able to move around their dominant hand on their wheelchair table as minimal motor function. The additional burden and time consumption in the context of endurance tests as part of the already extensive trial assessments asks for a clear rationale about the efficacy in terms of function accompanied by the selection of the most appropriate tests. In order to be able to measure clinically relevant improvement in endurance, endurance tests that mimic long-term activities are required.

In the current literature, the concept of fatigability and fatigue are often used interchangeably with different terms such as fatigue,[25] fatigability,[7] neuromuscular fatigue,[54] perceived fatigability,[55] physiological fatigue,[56] physiological fatigability,[19] physical fatigue,[20] peripheral fatigue,[22] muscle fatigue [21,57,58] and so on. The lack of standard definitions and the inconsistency of terminology hamper the advancement in our understanding of the pathophysiological background of fatigability in SMA and the development of appropriate outcome measures. The taxonomy used in this study was particularly suitable to standardize definitions and clarify the different concepts and means of measurements as a prelude to the development of an outcome measure for fatigability in SMA. The taxonomy makes an important distinction between ´perception´ and ´performance´, which are measured at a different level. Perception of fatigue is defined as the subjective sensations of weariness, increasing sense of effort, mismatch between effort expended and actual performance or exhaustion while fatigability is about decline in either physical or mental performance. Although there is a clear distinction in definitions and means of measure, endurance performance is regulated by an interaction between fatigability and perceptions of fatigue and influenced by physchological factors, peripheral limitations and central factors.[6,58–60] Therefore, a psychophsyiological approach is needed when interpreting the outcome of endurance testing in patients with SMA. Based on both pre-clinical and clinical data it was hypothesised that fatigability would be associated with neuromuscular junction dysfunction in at least half of the patients with SMA and therefore, similar to the approach in myasthenic syndromes, best provoked with a repetitive submaximal prolonged motor task. Although SMA is primary characterised by loss of motor neurons, involvement of other systems such as autonomic dysfunction and altered muscle metabolism is reported and might demand

additional methods of testing to capture fatigability in SMA.[61,62] Fatigability in SMA could also be related to an increased energy cost of movement due to progressive muscle weakness and secondary deconditioning.[20,23] Therefore, the individual disease course and physical activity levels should be taken in account when measuring fatigability and its change in time.

Limitations

We decided to limit our search for existing outcome measures to a scoping review in SMA although a systematic review in the entire range of neuromuscular diseases could have generated other endurance measures. Based on experience by the expert panel and the specific characteristics of SMA regarding clinical variability and complaints of fatigability, it was anticipated that a time consuming systematic review would give very limited additional information as hardly any endurance testing has been developed in neuromuscular diseases. The involvement of patients in rare disease clinical trial design is increasingly becoming a priority.[63] Although established methods such as face-to-face meeting and focus groups were not applied yet, extensive questionnaires provided a valuable insight in the patient perspective on fatigability. In the further development of the endurance tests, patients will continue to play an important role.

Conclusions

Fatigability has emerged as an important dimension of physical impairment in patients with SMA. The development of a comprehensive set of endurance tests is a pivotal next step to facilitate intervention studies on fatigability and address this important complaint in patients with SMA. We developed a set of endurance tests for both non-ambulatory and ambulatory children and adults with SMA which meet predefined specific criteria to achieve three main objectives: 1) quantify endurance; 2) generate clinical relevant outcome parameters and; 3) cover a large part of the clinical spectrum of SMA. Reliability and construct validity need to be investigated in future studies.

Abbreviations

6MWT	Six Minute Walk Test
ADLs	Activities of Daily Living
COSMIN	COnsensus-based Standards for the selection of health Measurement INstruments
ESBBT	Endurance Shuttle Box and Block Test
ESNHPT	Endurance Shuttle Nine Hole Peg Test
ESWT	Endurance Shuttle Walk Test
ISWT	Incremental Shuttle Walk Test
r9HPT	repeated Nine Hole Peg Test
SMA	Spinal Muscular Atrophy
Tlim	Time to Limitation

Declarations

Ethics approval and consent to participate

The Medical Ethics Committee of the University Medical Centre Utrecht in the Netherlands approved the research protocol. Written informed consent was obtained from all subjects and their parents.

Consent for publication

Written consent for publication was obtained from all subjects and their parents with regards to images used.

Funding

This study was funded by Prinses Beatrix Spierfonds, Stichting Spieren voor Spieren and de Vriendenloterij by means of salary costs of author Bart Bartels and Laura Habets during the course of the study. Author Ludo van der Pol has received support from Prinses Beatrix Spierfonds, Stichting Spieren voor Spieren and de Vriendenloterij. The funding parties were not involved in the design of the study, collection, analysis and interpretation of the data and in writing the manuscript.

Acknowledgements

The authors thank all patients and healthy controls who participated in this study.

References

1. Lefebvre S, Brglen L, Reboullet S, et al. Identification and characterization of a spinal muscular atrophy-determining gene. Cell. 1995;80(1):155-165.
2. Mercuri E, Bertini E, Iannaccone ST. Childhood spinal muscular atrophy: Controversies and challenges. Lancet Neurol. 2012;11(5):443-452.
3. Wadman RI, Wijngaarde CA, Stam M, et al. Muscle strength and motor function throughout life in a cross-sectional cohort of 180 patients with SMA types 1c-4. Eur J Neurol. 2018;25(3):512-518.
4. Noto Y, Misawa S, Mori M, et al. Prominent fatigue in spinal muscular atrophy and spinal and bulbar muscular atrophy: evidence of activity-dependent conduction block. Clin Neurophysiol. 2013;124(9):1893-1898.
5. Wadman RI, Vrancken AFJ, Van den Berg LH, Van der Pol WL. Dysfunction of the neuromuscular junction in patients with spinal muscular atrophy type 2 and 3. Neurology. 2012;79:2050-2055.
6. Pageaux B, Lepers R. Fatigue Induced by Physical and Mental Exertion Increases Perception of Effort and Impairs Subsequent Endurance Performance. Front Physiol. 2016;7:587.
7. Kluger BM, Krupp LB, Enoka RM. Fatigue and fatigability in neurologic illnesses: Proposal for a unified taxonomy. Neurology. 2013;80(4):409-416.
8. Kariya S, Park GH, Maeno-Hikichi Y, et al. Reduced SMN protein impairs maturation of the neuromuscular junctions in mouse models of spinal muscular atrophy. Hum Mol Genet. 2008;17(16):2552-2569.
9. Kong L, Wang X, Choe DW, et al. Impaired synaptic vesicle release and immaturity of neuromuscular junctions in spinal muscular atrophy mice. J Neurosci. 2009;29(3):842-851.
10. Arnold AS, Gueye M, Guettier-Sigrist S, et al. Reduced expression of nicotinic AChRs in myotubes from spinal muscular atrophy I patients. Lab Invest. 2004;84(10):1271-1278.
11. Goulet B, Kothary R, Parks RJ. At the junction of Spinal Muscular Atrophy Pathogenesis: The Role of Neuromuscular Junction Dysfunction in SMA Disease Progression. Curr Mol Med . 2013;13(1-15).
12. Pera MC, Luigetti M, Pane M, et al. 6MWT can identify type 3 SMA patients with neuromuscular junction dysfunction. Neuromuscul Disord. 2017;27(10):879-882.
13. Stam M, Wadman RI, Wijngaarde CA, et al. Protocol for a phase II, monocentre, double-blind, placebo-controlled, cross-over trial to assess efficacy of pyridostigmine in patients with spinal muscular atrophy types 2-4 (SPACE trial). BMJ Open. 2018;8(7):1-9.
14. Safety and Efficacy Study of Pyridostigmine on Patients With Spinal Muscular Atrophy Type 3 (EMOTAS). https://clinicaltrials.gov/show/NCT02227823
15. U.S. Department of Health and Human Services FDA Center for Drug Evaluation and Research USD of H and HSFC for BE and R, Health USD of H and HSFC for D and R. Guidance for industry: patient-reported outcome measures: use in medical product development to support labeling claims: draft guidance. Heal Qual Life Outcomes. 2006;4:79.
16. Committee for medicinal products for human use (CHMP). Reflection Paper on the Regulatory Guidance for the Use of Health-Related Quality of Life (HRQL) Measures in the Evaluation of Medicinal Products.; 2005.

https://www.ema.europa.eu/en/documents/scientific-guideline/reflection-paper-regulatory-guidance-use-healthrelated-quality-life-hrql-measures-evaluation_en.pdf

17. de Vet HC, terwee CB, Mokkink LB, Knol DL. Measurement in Medicine: Practical Guides to Biostatistics and Epidemiology . 4th ed. Cambride University Press; 2011.
18. Mokkink LB, Terwee CB, Knol DL, et al. Protocol of the COSMIN study: COnsensus-based Standards for the selection of health Measurement INstruments. BMC Med Res Methodol. 2006;6:2.
19. Lou J-S. Techniques in assessing fatigue in neuromuscular diseases. Phys Med Rehabil Clin N Am. 2012;23:11-22.
20. Alexander NB, Taffet GE, Horne FM, et al. Bedside-to-Bench conference: research agenda for idiopathic fatigue and aging. J Am Geriatr Soc. 2010;58(5):967-975.
21. Vollestad NK. Measurement of human fatigue. J Neurosci Methods. 1997;74:219/227.
22. Finsterer J. Biomarkers of peripheral muscle fatigue during exercise. BMC Musculoskelet Disord. 2012;13:218.
23. Bar-Or O. Role of exercise in the assessment and management of neuromuscular disease in children. Med Sci Sport Exerc. 1996;28(4):421-427.
24. Jones D, Round J, de Haan A. Skeletal Muscle from Molecules to Movement. Elsevier Ltd; 2005.
25. Féasson L, Camdessanché JP, El Mhandi L, Calmels P, Millet GY. Fatigue and neuromuscular diseases. Ann Réadaptation Médecine Phys. 2006;49(6):375-384.
26. Straver CG, van den Berg LH, van Doorn PA, Franssen H. Symptoms of activity induced weakness in peripheral nervous system disorders. J Peripher Nerv Syst. 2011;16:108-112.
27. van Mater H a, Williams JW, Coeytaux RR, Sanders GD, Kemper AR. Psychometric characteristics of outcome measures in juvenile idiopathic arthritis: A systematic review. Arthritis Care Res (Hoboken). 2012;64(4):554-562.
28. Wadman RI, Stam M, Gijzen M, et al. Association of motor milestones, SMN2 copy and outcome in spinal muscular atrophy types 0-4. J Neurol Neurosurg Psychiatry. 2017;88(4):364-367.
29. Bowen DJ, Kreuter M, Spring B, et al. How we design feasibility studies. Am J Prev Med. 2009;36(5):452-457.
30. Utter AC, Robertson RJ, Nieman DC, Kang J. Children's OMNI scale of perceived exertion: walking/running evaluation . Med Sci Sport Exerc. 2002;34(1):139-144.
31. Moller MC, Nygren de Boussard C, Oldenburg C, Bartfai A. An investigation of attention, executive, and psychomotor aspects of cognitive fatigability. J Clin Exp Neuropsychol. 2014;36(7):716-729.
32. Hart R, Ballaz L, Robert M, et al. Impact of Exercise-Induced Fatigue on the Strength, Postural Control, and Gait of Children with a Neuromuscular Disease. Am J Phys Med Rehabil. Published online 2014.
33. Meriggioli MN, Sanders DB. Autoimmune myasthenia gravis: emerging clinical and biological heterogeneity. Lancet Neurol. 2009;8(5):475-490.
34. Milner-Brown HS, Miller RG. Increased muscular fatigue in patients with neurogenic muscle weakness: quantification and pathophysiology. Arch Phys Med Rehabil. 1989;70(5):361-366.
35. Iannaccone ST, White M, Browne R, Russman B, Buncher R, Samaha FJ. Muscle fatigue in spinal muscular atrophy. J Child Neurol. 1997;12:321-326.
36. Granger MW, Buschang PH, Throckmorton GS, Iannaccone ST. Masticatory muscle function in patients with spinal muscular atrophy. Am J Orthod Dentofac Orthop. 1999;115(6):697-702.

37. Montes J, McDermott MP, Martens WB, et al. Six-minute walk test demonstrates motor fatigue in spinal muscular atrophy. Neurology. 2010;74(10):833-838.
38. Montes J, Dunaway S, Montgomery MJ, et al. Fatigue leads to gait changes in spinal muscular atrophy. Muscle Nerve. 2011;43(4):485-488.
39. Montes J, Blumenschine M, Dunaway S, et al. Weakness and fatigue in diverse neuromuscular diseases. J Child Neurol. 2013;28(10):1277-1283.
40. Montes J, Dunaway S, Garber CE, Chiriboga CA, De Vivo DC, Rao AK. Leg muscle function and fatigue during walking in spinal muscular atrophy type 3. Muscle Nerve. 2014;50(1):34-39.
41. Stam M, Wadman RI, Bartels B, et al. A continuous repetitive task to detect fatigability in spinal muscular atrophy. Orphanet J Rare Dis. 2018;13(1):1-7.
42. Lammers AE, Diller GP, Odendaal D, Tailor S, Derrick G, Haworth SG. Comparison of 6-min walk test distance and cardiopulmonary exercise test performance in children with pulmonary hypertension. Arch Dis Child. 2011;96(2):141-147.
43. Dunaway Young S, Montes J, Kramer SS, et al. Six-minute walk test is reliable and valid in spinal muscular atrophy. Muscle Nerve. 2016;54(5):836-842.
44. Revill SM, Morgan MDL, Singh SJ, Williams J, Hardman AE. The endurance shuttle walk test: a new field exercise test for the assessment of endurance capacity in chronic obstructive pulmonary disease. Thorax. 1999;54:213-222.
45. Grice KO, Vogel KA, Le V, Mitchell A, Muniz S, Vollmer MA. Adult norms for a comercially available Nine Hole Peg Test for finger dexterity. Am J Occup Ther. 2003;57:570-573.
46. Poole JL, Burtner PA, Torres TA, et al. Measuring dexterity in children using the Nine-hole Peg Test. J Hand Ther. 2005;18(3):348-351.
47. Mathiowetz V, Federman S, Wiemer D. Box and Block Test of Manual Dexterity Norms for 6-19 years old. Can J Occup Ther . 1985;52(5).
48. Mathiowetz V, Volland G, Kashman N, Weber K. Adult norms for the Box and Block Test of manual dexterity. Am J Occup Ther. 1985;39(6):386-391.
49. Terwee CB, Prinsen CAC, Chiarotto A, et al. COSMIN methodology for evaluating the content validity of patient-reported outcome measures: a Delphi study. Qual Life Res. 2018;27(5):1159-1170.
50. Hill K, Dolmage TE, Woon L, Coutts D, Goldstein R, Brooks D. A simple method to derive speed for the endurance shuttle walk test. Respir Med. 2012;106(12):1665-1670.
51. Qin J, Lin J-H, Buchholz B, Xu X. Shoulder muscle fatigue development in young and older female adults during a repetitive manual task. Ergonomics. 2014;57(June):1201-1212.
52. Qin J, Lin JH, Faber GS, Buchholz B, Xu X. Upper extremity kinematic and kinetic adaptations during a fatiguing repetitive task. J Electromyogr Kinesiol. 2014;24(3):404-411.
53. Bartels B, Groot JF De, Habets LE, et al. Fatigability in spinal muscular atrophy : validity and reliability of endurance shuttle tests. Orphanet J Rare Dis. 2020;2:1-9.
54. Conceicao A, Silva AJ, Barbosa T, Karsai I, Louro H. Neuromuscular fatigue during 200 m breaststroke. J Sport Sci Med. 2014;13(1):200-210.

55. Enoka RM, Duchateau J. Translating Fatigue to Human Performance. Med Sci Sports Exerc. 2016;48(11):2228-2238.
56. Schillings ML, Kalkman JS, Janssen HM, van Engelen BG, Bleijenberg G, Zwarts MJ. Experienced and physiological fatigue in neuromuscular disorders. Clin Neurophysiol. 2007;118(2):292-300.
57. Taylor JL, Amann M, Duchateau J, Meeusen R, Rice CL. Neural Contributions to Muscle Fatigue: From the Brain to the Muscle and Back Again. Med Sci Sport Exerc. 2016;48(11):2294-2306.
58. Allen DG, Lamb GD, Westerblad H. Skeletal muscle fatigue: cellular mechanisms. Physiol Rev. 2008;88(1):287-332.
59. Gandevia SC. Spinal and supraspinal factors in human muscle fatigue. Physiol Rev. 2001;81(4):1725-1789.
60. Van Cutsem J, Marcora S, De Pauw K, Bailey S, Meeusen R, Roelands B. The Effects of Mental Fatigue on Physical Performance: A Systematic Review. Sport Med. 2017;47(8):1569-1588.
61. Ripolone M, Ronchi D, Violano R, et al. Impaired Muscle Mitochondrial Biogenesis and Myogenesis in Spinal Muscular Atrophy. JAMA Neurol. 2015;72(6):1-10.
62. Shababi M, Lorson CL, Rudnik-Schöneborn SS. Spinal muscular atrophy: A motor neuron disorder or a multi-organ disease? J Anat. 2014;224(1):15-28.
63. Gaasterland CMW, Jansen-van der Weide MC, Vroom E, et al. The POWER-protocol: recommendations for involving patient representatives in choosing relevant outcome measures during rare diseases clinical trial design. J Heal Policy. 2018;accepted.
64. Gastin PB. Energy system interaction and relative contribution during maximal exercise. Sport Med. 2001;31(10):725-741.

Appendix 1

Description of outcome measures considered for selection

Sustained maximal voluntary contraction for 60 seconds

Milner-Brown studied fatigability of knee extensors and ankle dorsiflexors in 15 patients with neurogenic muscle weakness including five patients with SMA aged 16-55 years and 20 healthy controls aged 18-55 years. Subjects were asked to exert maximum force against a electromechanical device incorporating a force transducer and maintain maximum effort for one minute. Fatigue Index (FI) was expressed as the percentage decrease in maximal force at the end of 60 seconds. The mean FI of both ankle dorsiflexion (50 % ± 15 versus 34% ± 13) and knee extensors (62% ± 17 versus 46% ± 15%) of patients was significantly greater than in controls ($p < 0.01$) and characterised by a steep decrease in performance by patients from 30 to 60 seconds.

Sustained maximal voluntary contraction for 15 seconds

Iannacone et al. studied fatigability of knee flexors, knee extensors, elbow flexors and elbow extensors in 72 ambulatory and non-ambulatory patients with SMA aged 5-57 years and 24 healthy controls aged 5-32 years. Subjects were asked to push or pull against a fixed myometer as hard as possible and hold for 15 seconds, while given audio feedback. The maximal voluntary contraction times 15 seconds represented 100% of endurance or no fatigability. Endurance was expressed as the area under the curve for each maximal voluntary contraction. The authors found a large variability in endurance (AUC of 50-90%) with a similar response in patient and controls.

Masticatory endurance

Granger et al. studied masticatory muscle endurance in 15 patients with juvenile onset SMA aged 6-20 years and 15 age- and sex-matched healthy controls. Subjects were asked to hold a 60% sub-maximum bite force level for as long as possible while being timed. Patients with SMA (11.1 seconds) fatigued faster than controls (17.9 seconds) ($p = 0.03$).

The six minute walk test (6MWT)

Montes et al. studied fatigability during ambulation in patients with SMA type 3 aged 4-49 year in 4 separate studies. Subjects were instructed to walk as far as possible along a 25-m course during 6 minutes. Encouragements during the test were standardized according to the American Thoracic Society (ATS) – guidelines. Distance walked each minute and time to complete each 25-m segment were recorded. Montes et al. found a range of 11-21% decrease in walking distance between the 6th and the 1st minute.

The Repeated Nine Hole Peg Test (r9HPT)

Stam et al. studied fatigability of the arm and hand in fifty two patients aged 7-72 years with SMA type 2-4, 17 healthy aged 6-73 years and 29 disease controls aged 8-76 years. Subjects were asked to perform five consecutive rounds of the Nine-Hole Peg Test as fast as possible without a break.[41] The time required to complete each round was recorded and compared to the first round. Time needed to complete each round during the five-round task increased in 65% of patients with SMA type 2, 36% of type 3a, 22% of type 3b/4, 31% of disease controls and 6% of healthy controls. Patients with SMA type 2 performed the test significantly more slowly (+27%) than all other groups ($p<0.005$). This study was published recently and given the promising results, the r9HPT was included in the assessment of potential outcome measures

The Endurance Shuttle Walk Test

Subjects walked at 85% intensity, derived from the walking speed at 85% of peak VO_2 uptake during a separate Incremental Shuttle Walk Test (ISWT). Subject were instructed to continue walking on a 10 meters shuttle course until too tired or breathless to continue with a cut off time of 20 minutes. Subjects were given no indication of how long they were walking and were not informed of the 20 minutes limit. Walking speed was externally regulated by a beep signal and the test was terminated prematurely when subjects failed two times in a row to reach the other side within time. The ESWT demonstrated good test-retest reliability and sensitivity to change after a seven week rehabilitation program.

Appendix 2

The Endurance Shuttle Tests: materials and procedures

	ESWT	ESBBT	ESNHPT
		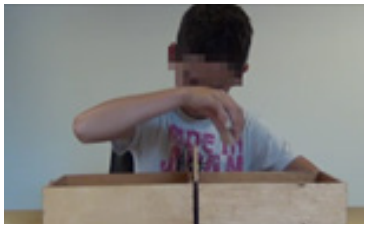	
Test Material	• Straight corridor • 10 meter walking course • 4 cones • Metronome	• Box and Block Test • 200 blocks • Adjustable table • Metronome	• Nine Hole Peg Test • Adjustable table • Metronome
Maximal performance estimation	• Walk as fast as possible and turn at the line between the cones before the beep • 5-10 trials, 30 seconds breaks • Fastest time out of three attempts < 10% difference	• Transfer 10 blocks over the partition as fast as possible before the beep • 5-10 trials, 30 seconds breaks • Fastest time out of three attempts < 10% difference	• Place and return the nine pegs as fast as possible before the beep • 5-10 trials, 30 seconds breaks • Fastest time out of three attempts < 10% difference
Intensity level	75% individual intensity (s) = maximal time(s)/0.75 and then converted into the matching metronome number	75% individual intensity (s) = maximal time(s)/0.75 and then converted into the matching metronome number	75% individual intensity (s) = maximal time(s)/0.75 and then converted into the matching metronome number
Maximal duration	20 minutes	20 minutes	20 minutes
Instruction Assessor	• Cover each time 10 meters before the beep • Continue as long as possible within safety margins • Try to speed up in case of one failure	• Transport each time 10 blocks before the beep • Continue as long as possible • Try to speed up in case of one failure	• Place and return 9 pegs each time before the beep • Continue as long as possible • Try to speed up in case of one failure

Chapter 3

Motor unit reserve capacity in spinal muscular atrophy during fatiguing endurance performance

L.E. Habets
B. Bartels
J.F. de Groot
W.L. van der Pol
J.A.L. Jeneson
F. Asselman
R.P.A. van Eijk
D.F. Stegeman

Clinical Neurophysiology 2021; 132:3

Abstract

Objective

To investigate the availability of any motor unit reserve capacity during fatiguing endurance testing in patients with spinal muscular atrophy (SMA).

Methods

We recorded surface electromyography (sEMG) of various muscles of upper- and lower extremities of 70 patients with SMA types 2-4 and 19 healthy controls performing endurance shuttle tests (ESTs) of arm and legs. We quantitatively evaluated the development of fatigability and motor unit recruitment using time courses of median frequencies and amplitudes of sEMG signals. Linear mixed effect statistical models were used to evaluate group differences in median frequency and normalized amplitude at onset and its time course.

Results

Normalized sEMG amplitudes at onset of upper body ESTs were significantly higher in patients compared to controls, yet submaximal when related to maximal voluntary contractions, and showed an inverse correlation to SMA phenotype. sEMG median frequencies decreased and amplitudes increased in various muscles during execution of ESTs in patients and controls.

Conclusions

Decreasing median frequencies and increasing amplitudes reveal motor unit reserve capacity in individual SMA patients during ESTs at submaximal performance intensities.

Significance

Preserving, if not expanding motor unit reserve capacity may present a potential therapeutic target in clinical care to reduce fatigability in individual patients with SMA.

Introduction

Spinal muscular atrophy (SMA) is caused by a deficiency of survival motor neuron (SMN) protein due to the homozygous deletion of the *SMN 1* gene.[1] SMA has a broad spectrum of severity, ranging from neonatal respiratory insufficiency and death (type 1), inability to walk independently (type 2) and problems with or loss of ambulation (type 3), to mild impairments in adults (type 4).[2] Degeneration of α-motor neurons is the pathological hallmark of the disease, but other components of the motor unit, such as the neuromuscular junction and the myofiber itself, are also affected.[3–5] With respect to the former, studies in rodent models and humans have reported aberrant neuromuscular junction development and abnormal function of postsynaptic acetylcholine receptors, resulting in neuromuscular transmission impairments.[6–10] With respect to the myofiber, human muscle biopsies and SMA mouse models revealed altered skeletal muscle differentiation, growth and metabolism.[4,11,12] The most prominent clinical characteristic of SMA is progressive muscle weakness leading to limitations in motor function.[13–15] In addition, fatigability, defined as a decline in physical endurance performance during repetitive motor tasks, has emerged as a common, but sparsely examined, symptom.[16–19]

A repetitive upper and lower body motor task, tailored specifically to test fatigability in SMA (endurance shuttle tests (ESTs) [17]), recently demonstrated abnormal fatigability during walking, proximal- and distal arm function in up to 85% of patients with SMA, compared to no fatigability in healthy controls.[20] Importantly, significantly higher endurance in disease controls (Limb girdle muscular dystrophy, Becker muscular dystrophy and Duchenne muscular dystrophy), compared to SMA, found in this previous study, indicated that fatigability was not secondary to weakness, but a specific feature of SMA.[20]

Surface electromyography (sEMG) recordings from muscles during endurance testing may provide insight into the mechanisms underlying fatigability in physical performance.[21–28] Specifically, fatigability is evidenced by a shift towards lower median frequencies of the sEMG signal, concomitant with a decline in the amplitude (root mean square (RMS)) of the sEMG signal.[29–31] A transient rise in RMS, preceding the decline in RMS, is typically observed in healthy subjects.[29,31] This phenomenon is commonly thought to reflect recruitment of motor unit reserve capacity to prevent task failure. This reserve capacity can be present both in terms of still unrecruited (usually larger) motor units,[32] as well as in terms of 'rate coding', i.e. the possibility to increase the firing rate of active motor units.[33] Montes et al. (2014) previously reported that there is little or no such reserve capacity in SMA.[41]

Here, we further investigated motor unit reserve capacity in SMA using continuous sEMG recording from upper and lower extremity muscles during ESTs execution in patients with SMA types 2-4 and healthy controls. We tested two specific hypotheses: 1) patients with SMA would perform the ESTs at higher levels of muscle electrical activation, but submaximal

to maximal voluntary contractions (MVC), compared to healthy controls, and 2) patients with SMA show reserve capacity during fatiguing ESTs. Rejection of the latter hypothesis would reveal failing use of existing reserve capacity as performance limiting factor, identifying a potential patient-specific therapeutic target in SMA.

Methods

Subjects

Data were collected as part of a cross-sectional study on fatigability in SMA.[20] We invited patients with SMA types 2, 3a, 3b, and 4, registered in the Dutch SMA registry (www.treatnmd.eu/patientregistries), to participate in this study. The SMA classification system (i.e. type 1-4) is based on the age of onset and the best of two achieved motor milestones reported in medical records or by patient reports. All had a confirmed homozygous deletion of the *SMN1* gene. We recruited healthy controls through the HU University of Applied Sciences, the University Medical Center Utrecht, and the subject's social network of family, friends, and schoolmates. Inclusion criteria were: 1) aged between 8 and 60 years, 2) able to follow test instructions, and 3) able to perform and repeat, at least once, the physical tasks involved in execution of each of the ESTs described below. Exclusion criteria were: 1) history of a disorder which affects the neuromuscular junction function, 2) use of medication that affects neuromuscular junction function, and 3) other medical problems that could influence ESTs results.

Standard Protocol Approvals, Registrations and Patient Consent

All participants and their parents (if they were under 18 years of age) signed informed consent. The study was approved by the Medical Ethics Committee of the University Medical Center Utrecht in the Netherlands (NL48715.041.14).

Study design

The study consisted of three visits within approximately 6 weeks. At the first visit, we documented baseline characteristics and subjects performed a practice test.[20] At the second and third visits, participants performed ESTs and retests at the participant's home, or at the exercise laboratory in our hospital, depending on the subject's preference. Visits two and three were separated by at least one week of rest.[20]

Endurance shuttle tests

We used three different, recently validated endurance shuttle tests to assess fatigability: the endurance shuttle nine hole peg test (ESNHPT) for distal arm function, the endurance

shuttle box and block test (ESBBT) for proximal arm function, and the endurance shuttle walk test (ESWT) for leg function.[17,20] The execution of these ESTs has been described in detail elsewhere.[17] Briefly, we first determined the individual's maximum test intensity level by asking him/her to perform one cycle of an endurance test at maximum speed (i.e. one cycle of: putting nine pins in holes for the ESNHPT, transporting 10 blocks from a bin over a partition into an adjacent bin for the ESBBT, walking 10 meters for the ESWT).[17] During execution of the ESTs, participants repeated the cycle at 75% of their maximum speed until they twice consecutively failed to complete a cycle within the defined time period, paced by auditory signals. Participants were not informed about the maximal duration of the test. During the pilot phase of the development of the ESTs, the maximal duration was 10 minutes.[17] Thereafter, this was adjusted to 20 minutes. Participants performed at least one of the ESTs, always keeping the sequence of tests in the same order: ESNHPT, ESBBT and ESWT. A resting period of at least 30 minutes was taken between two tests to allow full recovery.

Maximal voluntary contractions

We measured MVCs of muscles (figure 1A, 1B) prior to each EST using a handheld dynamometer (CT 3001; C.I.T. Technics, Groningen, The Netherlands) in combination with the break test, according to standardized procedures.[34] We used manual muscle testing in patients with overt muscle weakness (Medical Research Council (MRC) score for muscle strength <5).[35] Contractions lasted for approximately three seconds. We maintained standardized starting positions in a fixed sequence, proximal to distal.

sEMG registration

We used sEMG at visit 2 during the ESNHPT and ESBBT and at visit 3 during the ESWT. Muscle electrical activation was continuously measured with wireless Bio Radio (Great Lakes Neurotechnologies, Cleveland, Ohio, USA) bipolar four channel sEMG during both MVCs and the ESTs. Each cycle performed during an EST was marked manually online in the sEMG signal.

Electrode placement

We used self-adhesive Ag/AgCl Discs (3M™Red Dot™, 0.9 mm electrode, 1.8 mm gel, 50 mm disc) with 20 mm inter-electrode distance. Skin preparation procedures included removal of hair, if necessary, and rubbing and cleaning the skin with alcohol (70% denatured ethanol incl. 5% isopropanol). We placed standard electrodes on muscles of upper and lower extremities using standard guidelines.[36,37] For the ESNHPT/ESBBT: m. deltoideus pars anterior (one finger distal and anterior to the acromion), m. biceps brachii (1/3 on the line from fossa cubit to medial acromion), m. flexor digitorum superficialis (1/4 between wrist

and elbow on the area where the greatest movement is felt while the subject flexes his/her fingers), and m. extensor digitorum superficialis (1/4 between wrist and elbow on palpable muscle mass while the subject extends his/her fingers). For the ESWT: m. rectus femoris (1/2 on the line from anterior spina iliaca superior to the superior part of the patella), m. biceps femoris (1/2 on the line from ischial tuberosity to the lateral epicondyle of the tibia), m. tibialis anterior (1/3 on the line from the tip of the fibula to the medial malleolus), and m. gastrocnemius (1/3 on the line from the head of the fibula to the heel). Electrodes were placed on the dominant side of the body parallel to the direction of the fibers. Reference electrodes were placed on the spina scapulae and spina iliaca anterior superior for the ESNHPT and ESBBT, and ESWT, respectively. Wires were secured to the skin with tape to prevent cable movement artifacts.

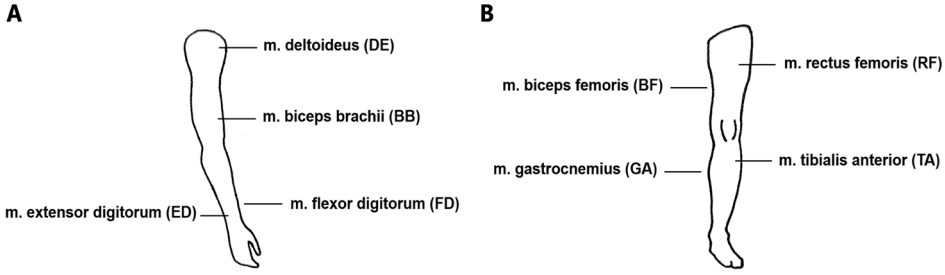

Figure 1. Schematic muscle representation A: Schematic representation of upper extremity muscle, B: Schematic representation of lower extremity muscle, DE = m. deltoideus, BB = m. biceps brachii, FD = m. flexor digitorum, ED = m. extensor digitorum, RF = m. rectus femoris, BF = m. biceps femoris, TA = m. tibialis anterior, GA = m. gastrocnemius.

Signal acquisition and processing

We used Biocapture software, at a sampling rate of 1000 samples/s and amplified with a gain of 1000, to measure real time muscle electrical activation during the ESTs. The sampling resolution was 6 μV per least significant bit. An anti-aliasing filter, set to 250 Hz, was implemented in the recording system. Raw sEMG data were detrended offline, high pass filtered bidirectionally with a fourth order Butterworth filter at 20 Hz, and filtered with a 50 Hz notch filter to remove power line noise. Lastly, the sEMG signal was rectified using custom programs written in MATLAB R2016b. Markers were manually checked for presence and position. The mean root mean square (RMS) amplitude per cycle was calculated over an overlapping moving window (100 samples). We calculated the median frequency of the power spectrum, determined in Hertz (Hz), using Fast Fourier Transformation for every single cycle of the ESTs. Maximum RMS amplitudes of the MVCs were calculated for an overlapping moving window of 500 samples. RMS amplitudes per cycle were normalized to the MVC of

the corresponding muscle to determine exercise intensity over the EST. Performances at intensities below 100% are referred to as submaximal. Raw RMS amplitudes were used to determine time-related changes.

Statistical analysis

The first ten minutes of all sEMG signals were analyzed. First, we aimed to assess the overall group differences between patients with SMA type 2, type 3a, type 3b/4, and controls performing ESNHPT and ESBBT. Due to a smaller sample size, the overall group difference between all patients with SMA and controls performing ESWT was assessed. Mean differences in muscle electrical activation, as quantified by the median frequencies or the natural logarithm of RMS (lnRMS) amplitudes, were estimated using linear mixed effects models for the four muscles described above for the ESNHPT, ESBBT, and the four muscles for the ESWT. lnRMS amplitudes were processed as described by Duan (1983) to reduce back-transformation bias.[38] The relationship between lnRMS amplitudes and group (SMA type 2, type 3a, type 3b, and controls) was assessed, for every muscle, by Spearmans's correlation. Secondly, we assessed whether muscle electrical activation changed over time (i.e. over the course of the 10-minute endurance test) and whether the effect over time differed between patients with SMA and controls. We constructed a linear mixed effect model with group, time, and their interaction as fixed effects, and a random intercept and slope for time per individual. An unstructured covariance type was chosen. All statistical analyses were performed using SPSS and the level of significance was set at 0.05.

Results

In total, 70 patients with SMA and 19 healthy controls participated in this study. Participant characteristics per EST are summarized in table 1. Age and gender were similar in patients with SMA and healthy controls: 1) ESNHPT: age: p=0.173, gender: p=0.712, 2) ESBBT: age: p=0.198, gender: p=0.287, and 3) ESWT: age: p=0.206, gender: p=0.241). Test drop-out rate in subgroups of SMA, during all ESTs, varied between 17% in SMA type 3b/4 during ESNHPT, and 93% in SMA type 2 during ESBBT (table 1). Results of muscle electrical activation measured with sEMG in different muscles are described per EST below.

Table 1. Participant characteristics

	ESNHPT		ESBBT		ESWT	
Characteristics	**SMA (n=66)**	**Controls (n=19)**	**SMA (n=45)**	**Controls (n=16)**	**SMA (n=17)**	**Controls (n=16)**
SMA subtype (n)		-		-		-
type 2:	34		14		0	
type 3a:	14		13		2	
type 3b:	18		17		14	
type 4:	0		1		1	
Gender (m:f)	28:38	9:10	24:21	6:10	12:5	8:8
Age, y, mean (SD)	26.9 (14.0)	23.0 (9.6)	26.8 (13.7)	23.2 (7.8)	28.8 (11.9)	24.0 (9.8)
HFMSE, mean (SD)	18.5 (22.0)	-	29.6 (22.8)	-	54.8 (7.2)	-
Strength (n): median (N)	DE (30): 40.5 (2.0-38.5)	DE: 132.0 (40-243.5)	DE (33): 41.5 (6.5-122.0)	DE: 136.5 (40.0-244.0)	RF (17): 25.5 (16.5-201.0)	RF (13): 359 (262-437)
(min-max)	BB (65): 22.5 (3.5-47.0)	BB: 213.5 (83.0-361.5)	BB (45): 39.0 (12.0-356.0)	BB: 219.8 (76.5-386.0)	BF (17): 117.0 (26.5-237.0)	BF (13): 275 (123-343)
	FD (63): 15.0 (1.0-167.0)	FD: 167.0 (57.5-274.5)	FD (45): 40.0 (1.5-171.5)	FD: 147.5(53.5-297.5)	TA (17): 215.5 (52.5-319.0)	TA (13): 316 (213-364)
	ED (65): 7.5 (0.5-149.0)	ED: 127.0 (46.5-196.0)	ED (45): 17.0 (3.5-149.5)	ED: 117.0(46.0-186.0)	GA (17): MRC 5	GA (17): MRC 5
Test drop-out rate (%)		0		13		0
type 2:	71		93		-	
type 3a:	50		85		50	
type 3b/4	17		44		36	
Time to limitation (n):	P1 (10): 600 (548)	P1 (13): 600 (0)	P1 (6): 272 (412)	P1 (13): 600 (0)	P1 (2): 600 (0)	P1 (11): 600 (0)
median (s) (IQR)	P2 (56): 639 (1001)	P2 (6): 1200 (0)	P2 (39): 194 (1096)	P2 (3): 579 (-)	P2 (15): 861 (846)	P2 (5): 1200 (-)
Excluded RMS-MVC (n) *	24	4	5	1	5	5

ESNHPT= endurance shuttle nine hole peg test, ESBBT= endurance shuttle box and block test, ESWT= endurance shuttle walk test, SMA= spinal muscular atrophy; subtype 3a: clinical symptoms <3yrs; subtype 3b: clinical symptoms >3yrs, HFMSE = Hammersmith functional motor scale expanded, DE= m. deltoideus, BB= m. biceps brachii, FD= m. flexor digitorum, ED= m. extensor digitorum, RF= m. rectus femoris, BF= m. biceps femoris, TA= m. tibialis anterior, GA= m. gastrocnemius, MRC = Medical Research Council score for muscle strength, IQR= interquartile range, P1=protocol 600 seconds, P2=protocol 1200 seconds, RMS-MVC= root mean square amplitude normalized to maximal voluntary contraction , *Number of muscles excluded due to inadequate MVC measurement.

Median frequency dynamics

Significantly higher median frequencies in SMA compared to controls may indicate that larger motor units are recruited at onset of an EST.[29–31] A subsequent decrease in median frequencies during test performance would indicate: 1) muscle acidification, associated with fatiguing, fast-twitch, anaerobic muscle fibers, already recruited at onset; and 2) synchronization of motor unit firings.[29–31] Results of the linear mixed model analyses are listed in supplementary tables S1, S2, S3.

ESNHPT We found significantly higher median frequencies of m. extensor digitorum in patients with SMA types 2 and 3a compared to healthy controls (figure 2A). Median frequencies decreased in m. deltoideus of all patient groups, whereas healthy controls showed an increase in median frequencies (figure 2B).

ESBBT We found significantly higher median frequencies of m. biceps brachii, m. flexor digitorum and m. extensor digitorum in patients with SMA types 2 and type 3b/4, compared to healthy controls (figure 3A). Similar findings are shown in m. biceps brachii and m. extensor digitorum of patients with SMA type 3a (figure 3A). Median frequencies showed a stronger decrease in various muscles of all patient groups, compared to healthy controls (figure 3B).

ESWT Median frequencies of sEMG recordings from m. rectus femoris, m. biceps femoris, m. tibialis anterior and m. gastrocnemius, at onset of the ESWT, were similar in patients with SMA and in controls (figure 4A). We found a smaller decrease in median frequency of m. biceps femoris and m. tibialis anterior, and an increase for m. gastrocnemius over time, in patients with SMA compared to controls (figure 4B).

RMS amplitude dynamics

RMS amplitudes, normalized to the highest amplitude determined during MVC of the corresponding muscle, indicate the level of exercise intensity on a scale from 0 to 100%. Significantly higher amplitudes in SMA, compared to controls, would indicate the recruitment of larger motor units at onset to perform an EST.[29–31] An increase in RMS amplitude during test performance would indicate increased firing rates, motor unit synchronization, and recruitment of additional larger motor units not activated at onset of the task, to prevent task failure as a result of fatigability.[29–31] Results of the linear mixed model analyses are listed in supplementary tables S1, S2, S3.

ESNHPT All subjects performed the ESNHPT at an intensity submaximal to their MVC (8-60% MVC) (figure 2C). These exercise intensities were strongly inversely correlated to SMA phenotype in all muscles, $r_S(1269) = -0.764$ (m. deltoideus), $r_S(1396) = -0.775$ (m. biceps brachii), $r_S(1358) = -0.803$ (m. flexor digitorum), and $r_S(1322) = -0.811$ (m. extensor digitorum), all $p<0.001$. Patients with SMA type 3a showed a significant increase in RMS

amplitude of m. deltoideus and m. flexor digitorum over time, compared to a decrease in controls (figure 2D).

ESBBT All subjects performed the ESBBT at an intensity submaximal to their MVC (13-53% MVC) (figure 3C). These exercise intensities were again inversely correlated to SMA phenotype, $r_S(2062) = -0.549$ (m. deltoideus), $r_S(2117) = -0.645$ (m. biceps brachii), $r_S(2001) = -0.693$ (m. flexor digitorum), and $rS(2057) = -0.773$ (m. extensor digitorum), all $p<0.001$. We found a significantly larger increase in RMS amplitude over time in m. biceps brachii, m. flexor digitorum, and m. extensor digitorum of various patients with SMA, compared to healthy controls (figure 3D).

ESWT All patients performed the ESWT at an intensity submaximal to their MVC (41-82% MVC) (figure 4C). Patients with SMA showed an equal or smaller decrease in RMS amplitude of the sEMG signal from, respectively, m. rectus femoris, m. gastrocnemius and m. tibialis anterior, compared to controls (figure 4D). At the individual level, we observed both patients and healthy controls with increasing or decreasing RMS amplitudes over time (Supplementary figure S4).

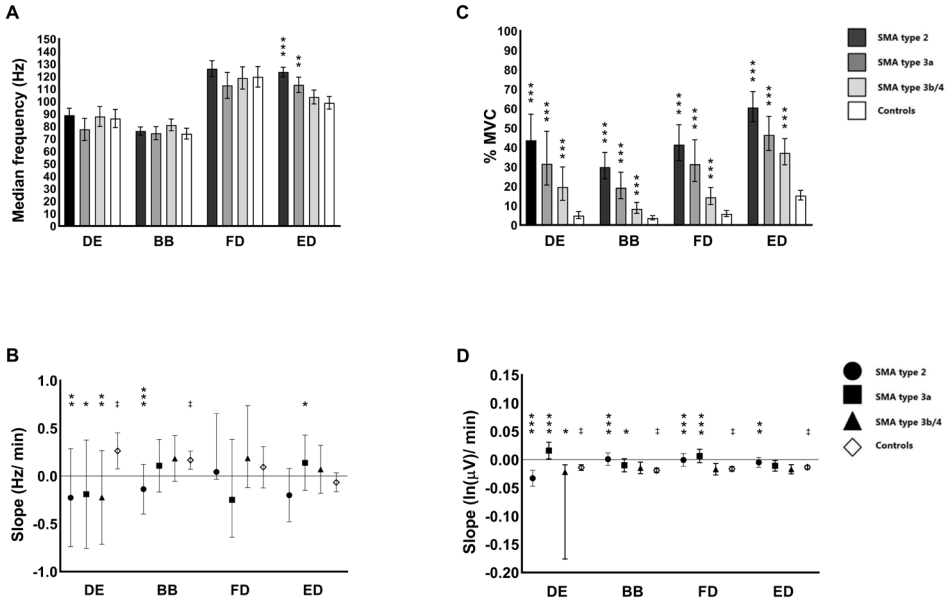

Figure 2. Endurance shuttle nine hole peg test (ESNHPT) A: Median frequency at onset, B: Slope median frequency over time, C: Exercise intensity at onset, D: Slope amplitudes over time, error bars indicate upper and lower limits, */**/*** = significantly different from controls (p<.05/p<.01/p<.001), ‡ = significantly different from zero (p<.05), DE = m. deltoideus, BB = m. biceps brachii, FD = m. flexor digitorum, ED = m. extensor digitorum.

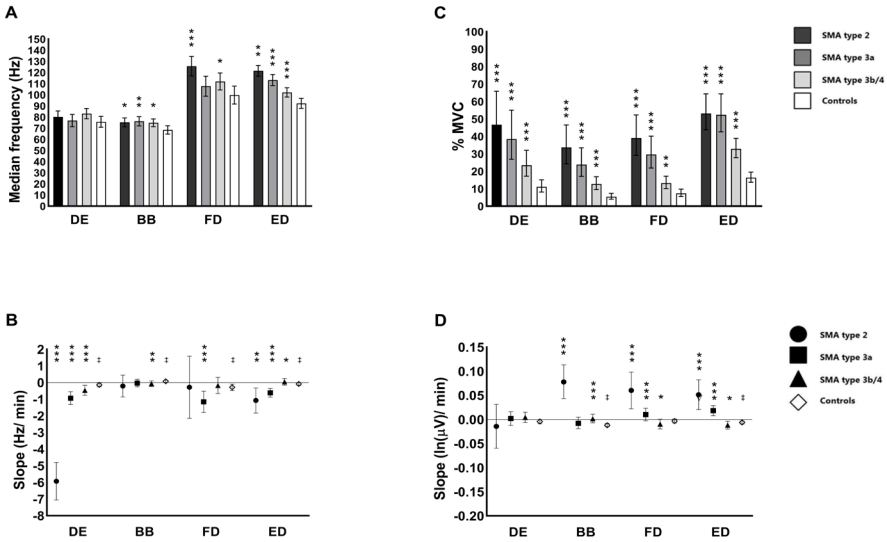

Figure 3. Endurance shuttle box and block test (ESBBT) A: Median frequency at onset, B: Slope median frequency over time, C: Exercise intensity at onset, D: Slope amplitudes over time, error bars indicate upper and lower limits, */**/*** = significantly different from controls (p<.05/p<.01/p<.001), ‡ = significantly different from zero (p<.05), DE = m. deltoideus, BB = m. biceps brachii, FD = m. flexor digitorum, ED = m. extensor digitorum.

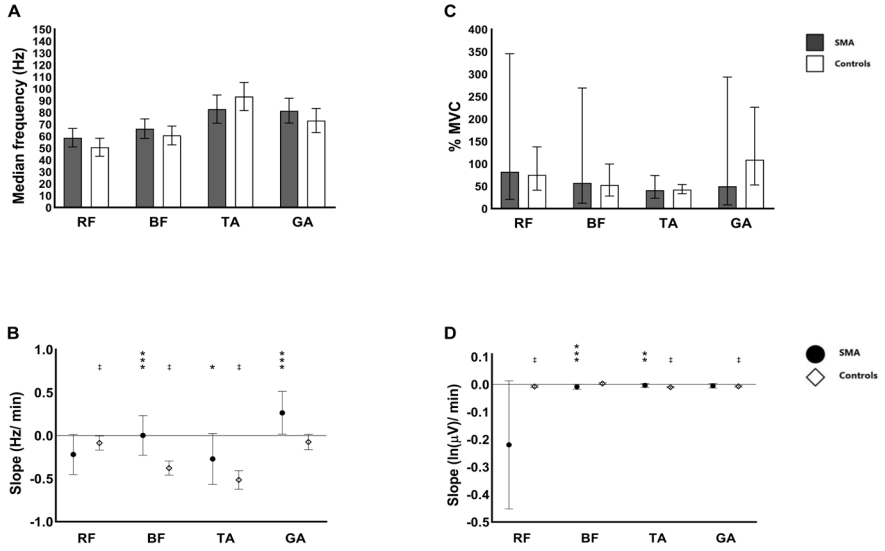

Figure 4. Endurance shuttle walk test (ESWT) A: Median frequency at onset, B: Slope median frequency over time, C: Exercise intensity at onset, D: Slope amplitudes over time, error bars indicate upper and lower limits, */**/*** = significantly different from controls (p<.05/p<.01/p<.001), ‡ = significantly different from zero (p<.05), RF = m. rectus femoris, BF = m. biceps femoris, TA = m. tibialis anterior, GA = m. gastrocnemius.

Discussion

This study applied sEMG to investigate motor unit reserve capacity during execution of three quantitative endurance shuttle tests in patients with SMA types 2-4. Our results show decreasing median frequencies and rising RMS amplitudes during fatiguing submaximal endurance performance in some, but not all, patients with SMA, indicating the availability of motor unit reserve capacity in upper and lower extremities in individual patients. Current therapeutic approaches in SMA are principally aimed at restoring survival motor neuron (SMN) protein expression to prevent motor neuron loss.[4] However, others have argued that therapy design in SMA should also consider targeting other components of the motor units – i.e., the neuromuscular junction and skeletal muscle itself.[3,4,39] Our current finding of motor unit reserve capacity in SMA suggests that boosting this reserve, for example, using exercise training, may be a target for such combined treatment approaches.

All ESTs were executed at submaximal intensity, normalized to MVCs (figure 2C, 3C, 4C). As such, the original EST design criterion of "a submaximal test protocol of repetitive activities over a longer period",[17] was met in all subjects. The relative exercise intensities of ESNHPT and ESBBT were found to be inversely related to SMA phenotype. This finding is in agreement with a recent study that measured trunk muscle electrical activation during unsupported sitting in patients with SMA.[40] Specifically, the authors reported three-fold higher activation levels in trunk muscles of patients with SMA types 2 and 3, during execution of a reaching task or a daily task, compared to controls.

Our sEMG recordings from muscles of the arm and leg in patients, during EST execution, showed a range of (patho)physiological trends in the time courses of median frequencies and RMS amplitudes. Progressive decrement in median frequency of the sEMG signal during execution of a physical task is commonly thought to be indicative of muscle acidification.[28] We observed such a decrease in median frequency over time in sEMG recordings of m. deltoideus of the shoulder during ESNHPT, of m. deltoideus, m. flexor digitorum and m. extensor digitorum of the arm during ESBBT, and of m. rectus femoris and m. tibialis anterior of the leg during ESWT execution. Conversely, any concomitant progressive increase in RMS amplitude would be indicative of motor unit reserve capacity progressively recruited to prevent task failure.[29,31] This phenomenon was indeed observed in sEMG recordings of m. deltoideus and m. flexor digitorum during ESNHPT, and of the m. biceps brachii, m. flexor digitorum and m. extensor digitorum during ESBBT execution, respectively. As such, these results support the hypothesis under investigation, that patients with SMA types 2-4 are able to recruit motor unit reserve capacity during fatiguing motor tasks.

Montes et al. (2014) previously observed a decrease in RMS amplitude of sEMG signals recorded from leg muscles in SMA type 3 patients performing the six-minute walking test, and attributed their finding to a limited, if not absent, motor unit reserve capacity in SMA.[41]

Here, we observed a similar manifestation of fatigability of the leg muscles in patients with SMA performing the ESWT, with an overall mean decrease in median frequency and RMS amplitude in m. rectus femoris and m. tibialis anterior. However, at the individual level, increases in RMS amplitudes over time were found in some lower extremity muscles, indicating the availability of motor unit reserve capacity in leg muscles during the ESWT in individual patients (Supplementary figure S4).

We found the largest changes in median frequencies and RMS amplitudes over time in patients with SMA type 2 during the ESBBT (figure 3B-D). For example, we measured a change in median frequency of 6 Hz per minute in m. deltoideus of these patients. Although experimental setup and subject conditions are not fully comparable, a previous study, examining muscle fatigue and shoulder injury in the physically demanding car industry, reported a change of this magnitude in median frequency only after more than 120 minutes of executing a repetitive task.[42] Since no reference values for fatigability during cyclic dynamic tasks exist in the literature, the absolute magnitude of change in median frequency and RMS amplitude over time should be interpreted with caution.

MVC determination for muscle of the human leg, using a handheld dynamometer, is generally considered to be reliable and valid; i.e. in m. rectus femoris in young healthy subjects.[43] However, we had difficulty accurately determining MVC of leg muscles in healthy controls, and in the m. gastrocnemius of the lower leg in patients. Here, maximal recorded strength may well have reflected physical strength of the individual handling the dynamometer rather than maximal strength of the leg muscle of the test subject.[44] This may have led to underestimation of MVC, and thereby to overestimation of exercise intensity of ESWT for these muscles in these subjects. Another complication for true normalization of effort of leg muscles, is the fact that MVC determination and ESWT execution were performed in a different body position (i.e. supine/sitting vs. upright); for example, a study in healthy subjects reports diverse EMG-length relations for the m. rectus femoris muscle at varying knee-joint angles.[45] This may have contributed further to variance of strength and sEMG activation during ESWT. The large range of estimated exercise intensities in m. rectus femoris and m. biceps femoris muscles in patients with SMA (figure 4C), may additionally reflect variation in muscle strength between individuals (table 1).

This study has confirmed exercise intolerance at submaximal exercise intensity in patients with SMA types 2-4, while sEMG recordings showed pattern heterogeneities over time between individuals. Such variability suggests that a multifactorial causal base underlies fatigability in SMA types 2-4. A possible cause of fatigability may be dysfunction of the neuromuscular junction, with a prevalence of 40-50% in patients with SMA.[6] If this is the case, one might expect to find constant sEMG median frequencies, concomitant with decreasing amplitudes in every other patient. However, our results did not show this, a possible explanation being individual compensational strategies during ESNHPT and ESBBT

execution. Movements, such as lateral bending of the trunk and elevation of the shoulder, were allowed. The reported patterns of muscle electrical activation should, therefore, be interpreted as a component of executing a complex motor task rather than as an indication of isolated muscle performance.

Lastly, oxidative capacity of skeletal muscle in SMA may also contribute to the clinical presentation of early fatigability. Various mouse and human studies have reported evidence of mitochondrial dysfunction in SMA.[11,12,46] Specifically, Miller et al. (2016) analysed the transcriptome of spinal motor neurons in a transgenic pre-symptomatic SMA mouse model and found altered mitochondrial function.[11] Ripolone et al. (2015) reported down-regulated mitochondrial biogenesis in quadriceps and paraspinal muscle biopsy samples from patients with SMA types 1-3.[12] Clearly, more research into this particular subject matter is warranted, to establish whether or not oxidative abnormalities, found in SMA mouse models and muscle biopsies, may contribute to exercise intolerance in human SMA. Dynamic *in vivo* ^{31}P Magnetic Resonance Spectroscopy of muscles, engaged in execution of a physical task, offers a well-established and non-invasive method for evaluating in vivo muscle mitochondrial function in neuromuscular diseases.[47]

Conclusion

In the present study, individual patients with SMA types 2, 3 and 4 demonstrate some motor unit reserve capacity during execution of fatiguing endurance tasks, yet present with exercise intolerance during submaximal activities in daily life. Preserving, if not expanding this reserve capacity, may, therefore, present a potential therapeutic target in clinical care for some patients with SMA types 2-4.

Abbreviations

ESBBT	Endurance shuttle box and block test
ESNHPT	Endurance shuttle nine hole peg test
ESTs	Endurance shuttle tests
ESWT	Endurance shuttle walk test
MVC	Maximal voluntary contraction
RMS	Root mean square
sEMG	Surface electromyography
SMA	Spinal muscular atrophy
SMN	Survival motor neuron

Declarations

Conflict of Interest Statement

Bart Bartels obtained research grants from Prinses Beatrix Spierfonds and Stichting Spieren voor Spieren, both non-profit foundations. His employer receives fees for SMA-related consultancy activities. W. Ludo van der Pol obtained grants from Prinses Beatrix Spierfonds, Stichting Spieren voor Spieren and Vriendenloterij. All other authors reported no conflict of interest.

Human and animal rights

"We confirm that we have read the Journal's position on issues involved in ethical publication and affirm that this report is consistent with those guidelines."

Funding

The study was funded by Prinses Beatrix Spierfonds, Stichting Spieren voor Spieren and Vriendenloterij. These funding sources had no involvement in data collection, data analysis and interpretation, writing of the report nor in the decision to submit the article for publication.

Acknowledgment

We thank all participants in this study for their willingness and commitment.

References

1. Lefebvre S, Brglen L, Reboullet S, et al. Identification and characterization of a spinal muscular atrophy-determining gene. Cell. 1995;80(1):155-165.
2. D'Amico A, Mercuri E, Tiziano FD BE. Spinal muscular atrophy. Orphanet J Rare Dis. 2011;6(71).
3. Shababi M, Lorson CL, Rudnik-Schöneborn SS. Spinal muscular atrophy: A motor neuron disorder or a multi-organ disease? J Anat. 2014;224(1):15-28.
4. Yeo CJJ, Darras BT. Overturning the Paradigm of Spinal Muscular Atrophy as just a Motor Neuron Disease. Pediatr Neurol. 2020;109:12-19.
5. Mercuri E, Bertini E, Iannaccone ST. Childhood spinal muscular atrophy: Controversies and challenges. Lancet Neurol. 2012;11(5):443-452.
6. Wadman RI, Vrancken AFJ, Van den Berg LH, Van der Pol WL. Dysfunction of the neuromuscular junction in patients with spinal muscular atrophy type 2 and 3. Neurology. 2012;79:2050-2055.
7. Kong L, Wang X, Choe DW, et al. Impaired synaptic vesicle release and immaturity of neuromuscular junctions in spinal muscular atrophy mice. J Neurosci. 2009;29(3):842-851.
8. Arnold AS, Gueye M, Guettier-Sigrist S, et al. Reduced expression of nicotinic AChRs in myotubes from spinal muscular atrophy I patients. Lab Investig. 2004;84(10):1271-1278.
9. Kariya S, Park GH, Maeno-Hikichi Y, et al. Reduced SMN protein impairs maturation of the neuromuscular junctions in mouse models of spinal muscular atrophy. Hum Mol Genet. 2008;17(16):2552-2569.
10. Goulet B, Kothary R, Parks R. At the "Junction" of Spinal Muscular Atrophy Pathogenesis: The Role of Neuromuscular Junction Dysfunction in SMA Disease Progression. Curr Mol Med. 2013;13(7):1160-1174.
11. Miller N, Shi H, Zelikovich A., Ma Y-C. Motor Neuron Mitochondrial Dysfunction in Spinal Muscular Atrophy. Hum Mol Genet. 2016;25(16):3395-3406.
12. Ripolone M, Ronchi D, Violano R, et al. Impaired Muscle Mitochondrial Biogenesis and Myogenesis in Spinal Muscular Atrophy. JAMA Neurol. 2015;72(6):1-10.
13. Wadman RI, Wijngaarde CA, Stam M, et al. Muscle strength and motor function throughout life in a cross-sectional cohort of 180 patients with SMA types 1c-4. Eur J Neurol. 2018;25(3):512-518.
14. Chabanon A, Seferian AM, Daron A, et al. Prospective and longitudinal natural history study of patients with Type 2 and 3 spinal muscular atrophy: Baseline data NatHis-SMA study. PLoS One. 2018;13(7):1-28.
15. Mercuri E, Finkel R, Montes J, et al. Patterns of disease progression in type 2 and 3 SMA: Implications for clinical trials. Neuromuscul Disord. 2016;26(2):126-131.
16. Kluger BM, Krupp LB, Enoka RM. Fatigue and fatigability in neurologic illnesses: Proposal for a unified taxonomy. Neurology. 2013;80(4):409-416.
17. Bartels B, Habets LE, Stam M, et al. Assessment of fatigability in patients with spinal muscular atrophy: Development and content validity of a set of endurance tests. BMC Neurol. 2019;19(1):1-10.
18. Montes J, McDermott MP, Martens WB, et al. Six-minute walk test demonstrates motor fatigue in spinal muscular atrophy. Neurology. 2010;74(10):833-838.

19. Stam M, Wadman RI, Bartels B, et al. A continuous repetitive task to detect fatigability in spinal muscular atrophy. Orphanet J Rare Dis. 2018;13(1):1-7.
20. Bartels B, Groot JF De, Habets LE, et al. Fatigability in spinal muscular atrophy : validity and reliability of endurance shuttle tests. Orphanet J Rare Dis. 2020;2:1-9.
21. Bonato P, Roy SH, Knaflitz M, Luca CJ De. Time-frequency parameters of the surface myoelectric signal for assessing muscle fatigue during cycling dynamic contractions. IEEE Trans Biomed Eng. 2001;48(July):745-754.
22. Qin J, Lin J-H, Buchholz B, Xu X. Shoulder muscle fatigue development in young and older female adults during a repetitive manual task. Ergonomics. 2014;57(June):1201-1212.
23. Beck TW, Stock MS, Defreitas JM. Shifts in EMG spectral power during fatiguing dynamic contractions. Muscle Nerve. 2014;50(1):95-102.
24. Bosch T, de Looze MP, van Dieën JH. Development of fatigue and discomfort in the upper trapezius muscle during light manual work. Ergonomics. 2007;50(2):161-177.
25. Bosch T, de Looze MP, Kingma I, Visser B, van Dieën JH. Electromyographical manifestations of muscle fatigue during different levels of simulated light manual assembly work. J Electromyogr Kinesiol. 2009;19(4):246-256.
26. Travis LA, Arthmire SJ, Baig AM, Goldberg A, Malek MH. Intersession reliability of the electromyographic signal during incremental cycle ergometry: Quadriceps femoris. Muscle Nerve. 2011;44(December):937-946.
27. Rogers DR, MacIsaac DT. A comparison of EMG-based muscle fatigue assessments during dynamic contractions. J Electromyogr Kinesiol. 2013;23(5):1004-1011.
28. Linssen WHJP, Stegeman DF, Joosten EMG, van 't Hof MA, Binkhorst RA, Notermans SLH. Variability and interrelationships of surface EMG parameters during local muscle fatigue. Muscle Nerve. 1993;16(August):849-856.
29. Dimitrova NA, Dimitrov G V. Interpretation of EMG changes with fatigue: Facts, pitfalls, and fallacies. J Electromyogr Kinesiol. 2003;13(1):13-36.
30. Fitts RH. Cellular mechanisms of skeletal muscle fatigue. Pysiological Rev. 1994;74(1):49-81.
31. Konrad P. The ABC of EMG: A Practical Introduction to Kinesiological Electromyography. Noraxon INC. USA; 2005. http://www.noraxon.com/docs/education/abc-of-emg.pdf.
32. Henneman E, Clamann HP, Gillies JD, Skinner RD. Rank order of motoneurons within a pool: law of combination. J Neurophysiol. 1974;37(6):1338-1349.
33. González-Izal M, Malanda A, Gorostiaga E, Izquierdo M. Electromyographic models to assess muscle fatigue. J Electromyogr Kinesiol. 2012;22(4):501-512.
34. Beenakker EAC, Van der Hoeven JH, Fock JM, Maurits NM. Reference values of maximum isometric muscle force obtained in 270 children aged 4-16 years by hand-held dynamometry. Neuromuscul Disord. 2001;11(5):441-446.
35. Hislop H, Montgomery J. Daniels and Worthingham (1986) Muscle Testing: Techniques of Manual Examination. 7th ed. Saunders; 2002. http://www.getcited.org/pub/102461099.
36. Hermens HJ, Freriks B, Disselhorst-Klug C, Rau G. Development of recommendations for SEMG sensors and sensor placement procedures. J Electromyogr Kinesiol. 2000;10:361-374.
37. Criswell E. Cram's Introduction to Surface Electromyography. Jones Bartlett Publ. 2011:338-371.
38. Duan N. Smearing estimate: A nonparametric retransformation method. J Am Stat Assoc. 1983;78(383):605-610.

39. Zhou H, Meng J, Malerba A, et al. Myostatin inhibition in combination with antisense oligonucleotide therapy improves outcomes in spinal muscular atrophy. J Cachexia Sarcopenia Muscle. 2020;11(3):768-782.
40. Peeters LHC, Janssen MMHP, Kingma I, van Dieën JH, de Groot IJM. Patients with spinal muscular atrophy use high percentages of trunk muscle capacity to perform seated tasks. Am J Phys Med Rehabil. 2019:1.
41. Montes J, Dunaway S, Garber CE, Chiriboga CA, De Vivo DC, Rao AK. Leg muscle function and fatigue during walking in spinal muscular atrophy type 3. Muscle Nerve. 2014;50(1):34-39.
42. Ferguson SA, Allread WG, Le P, Rose J, Marras WS. Shoulder muscle fatigue during repetitive tasks as measured by electromyography and near-infrared spectroscopy. Hum Factors. 2013;55(6):1077-1087.
43. Lee TH, Park KS, Lee DG, Lee NG. Concurrent validity by comparing EMG activity between manual muscle testing, handheld dynamometer, and stationary dynamometer in testing of maximal isometric quadriceps contraction. J Phys Ther Sci. 2012;24(12):1219-1223.
44. Marmon AR, Pozzi F, Alnahdi AH, Zeni JA. The validity of plantarflexor strength measures obtained through hand-held dynamometry measurements of force. Int J Sports Phys Ther. 2013;8(6):820-827.
45. Hahn D. Lower extremity extension force and electromyography properties as a function of knee angle and their relation to joint torques: implications for strength diagnostics. J Strenght Cond Res. 2011;25(6):1622-1631.
46. Boyd PJ, Tu WY, Shorrock HK, et al. Bioenergetic status modulates motor neuron vulnerability and pathogenesis in a zebrafish model of spinal muscular atrophy. PLoS Genet. 2017;13(4):1-27.
47. Meyerspeer M, Boesch C, Cameron D, et al. 31P magnetic resonance spectroscopy in skeletal muscle: Experts' consensus recommendations. NMR Biomed. 2020;(August 2019):1-22.

Supplementary material

Supplementary table S1. Results of the linear mixed model analyses: Endurance Shuttle Nine Hole Peg Test

Variable	Median frequency				RMS amplitude			
	β	95% CI		p	β	95% CI		p
		lower bound	upper bound			lower bound	upper bound	
m. deltoideus								
Time*contols (ref.)	0.263984	0.075689	0.45228	0.006	-0.01418	-0.019	-0.009054	0.000
Time*SMA type 2	-0.48937	-0.813804	-0.164943	0.003	-0.01877	-0.028	-0.009828	0.000
Time*SMA type 3a	-0.45299	-0.830694	-0.075288	0.019	0.030081	0.0204	0.039812	0.000
Time*SMA type 3b/4	-0.48652	-0.788872	-0.184169	0.002	-0.00788	-0.157	-0.000006	0.050
m. biceps brachii								
Time*contols (ref.)	0.167395	0.072386	0.262405	0.001	-0.019	-0.023	-0.015	0.000
Time*SMA type 2	-0.30352	-0.469219	-0.137824	0.000	0.0198	0.0127	0.0268	0.000
Time*SMA type 3a	-0.05827	-0.238123	0.121584	0.525	0.009	0.0013	0.0166	0.023
Time*SMA type 3b/4	0.017593	-0.128401	0.163588	0.813	0.0044	-0.002	0.0106	0.169
m. flexor digitorum								
Time*contols (ref.)	0.062972	-0.073115	0.199059	0.364	-0.01635	-0.020419	-0.01229	0.000
Time*SMA type 2	n.a.	n.a.	n.a.	n.a.	0.015841	0.008747	0.022935	0.000
Time*SMA type 3a	n.a.	n.a.	n.a.	n.a.	0.022848	0.015127	0.03057	0.000
Time*SMA type 3b/4	n.a.	n.a.	n.a.	n.a.	-0.00062	-0.006869	0.005621	0.845
m. extensor digitorum								
Time*contols (ref.)	-0.06519	-0.164081	0.033693	0.196	-0.01361	-0.016872	-0.01035	0.000
Time*SMA type 2	-0.13336	-0.31305	0.046333	0.146	0.008755	0.003064	0.014446	0.003
Time*SMA type 3a	0.204905	0.014554	0.395256	0.035	0.002611	-0.003584	0.00885	0.409
Time*SMA type 3b/4	0.136575	-0.01538	0.288529	0.078	-0.00339	-0.008398	0.001623	0.185

CI = confidence interval, ref. = reference group, RMS, = root mean square, SMA=spinal muscular atrophy, n.a.=not applicable.

Supplementary table S2. Results of the linear mixed model analyses: Endurance Shuttle Box and Block Test

Variable	Median frequency				RMS amplitude			
	β	95% CI		p	β	95% CI		p
		lower bound	upper bound			lower bound	upper bound	
m. deltoideus								
Time*contols (ref.)	-0.138514	-0.256197	-0.020830	0.021	-0.00039	-0.003430	0.002700	0.802
Time*SMA type 2	-5.787041	-6.797315	-4.776767	0.000	n.a.	n.a.	n.a.	n.a.
Time*SMA type 3a	-0.795716	-1.065029	-0.526403	0.000	n.a.	n.a.	n.a.	n.a.
Time*SMA type 3b/4	-0.324759	-0.504743	-0.144774	0.000	n.a.	n.a.	n.a.	n.a.
m. biceps brachii								
Time*contols (ref.)	0.080307	0.011914	0.148700	0.021	-0.012	-0.015000	-0.008000	0.000
Time*SMA type 2	0.282358	-0.871123	0.306406	0.347	0.0898	0.0583	0.1213	0.000
Time*SMA type 3a	-0.106274	-0.262943	0.050395	0.184	0.0041	-0.004	0.0125	0.342
Time*SMA type 3b/4	-0.146505	-0.251142	-0.041869	0.006	0.0135	0.0078	0.0191	0.000
m. flexor digitorum								
Time*contols (ref.)	-0.282722	-0.477585	-0.087859	0.004	-0.00325	-0.007225	0.000718	0.108
Time*SMA type 2	0.005321	-1.665913	1.676554	0.995	0.063431	0.029316	0.097547	0.000
Time*SMA type 3a	-0.867433	-1.313012	-0.421854	0.000	0.013308	0.004173	0.022444	0.004
Time*SMA type 3b/4	0.112689	-0.185164	0.410543	0.458	-0.0063	-0.012397	-0.000194	0.043
m. extensor digitorum								
Time*contols (ref.)	-0.080811	-0.159356	-0.002266	0.044	-0.00617	-0.009379	-0.002964	0.000
Time*SMA type 2	-0.991974	-1.668339	-0.315609	0.004	0.057583	0.030019	0.085146	0.000
Time*SMA type 3a	-0.531236	-0.71118	-0.351293	0.000	0.024428	0.017049	0.031807	0.000
Time*SMA type 3b/4	0.127151	0.006978	0.247325	0.038	-0.00545	-0.010381	-0.000526	0.030

CI = confidence interval, ref. = reference group, RMS, = root mean square, SMA=spinal muscular atrophy, n.a.=not applicable.

Supplementary table S3. Results of the linear mixed model analyses: Endurance Shuttle Walk Test

Variable	Median frequency				RMS amplitude			
	β	95% CI		p	β	95% CI		p
		lower bound	upper bound			lower bound	upper bound	
m. rectus femoris								
Time*contols (ref.)	-0.12671	-0.195651	-0.057765	0.000	-0.0083	-0.011559	-0.005042	0.000
Time*SMA	n.a.	n.a.	n.a.	n.a.	n.a.	n.a.	n.a.	n.a.
m. biceps femoris								
Time*contols (ref.)	-0.37743	-0.458728	-0.296121	0.000	0.002906	-0.000424	0.006237	0.087
Time*SMA	0.379775	0.231705	0.527845	0.000	-0.01183	-0.017895	-0.005768	0.000
m. tibialis anterior								
Time*contols (ref.)	-0.51474	-0.621758	-0.407728	0.000	-0.01017	-0.012595	-0.00775	0.000
Time*SMA	0.243734	0.054209	0.43326	0.012	0.006417	0.002007	0.010826	0.004
m. gastrocnemius								
Time*contols (ref.)	-0.07364	-0.161936	0.014657	0.102	-0.00638	-0.008785	-0.003974	0.000
Time*SMA	0.338543	0.177778	0.499308	0.000	n.a.	n.a.	n.a.	n.a.

CI = confidence interval, ref. = reference group, RMS, = root mean square, SMA=spinal muscular atrophy, n.a.=not applicable.

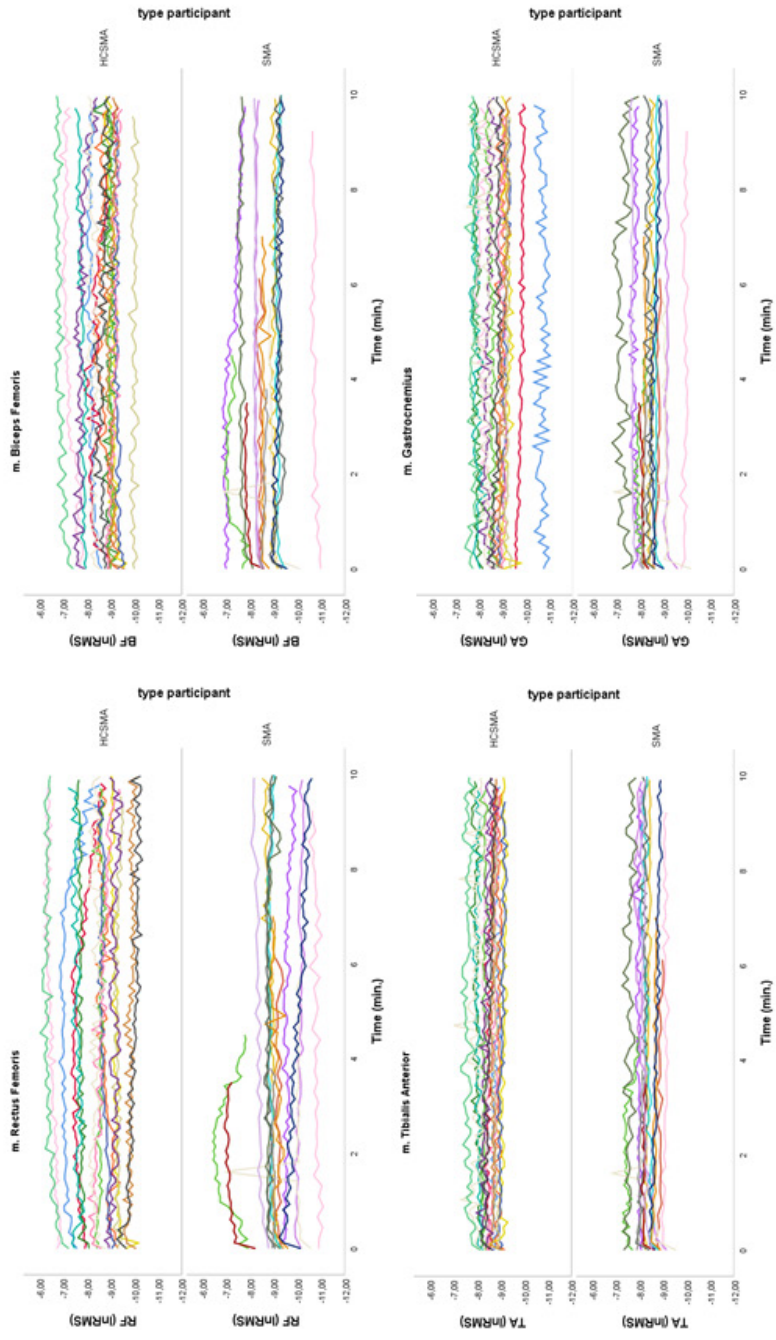

Supplementary figure S4. Individual muscle electrical activation (ln root mean square (RMS) amplitudes) per cycle of endurance shuttle walk test (ESWT) in four muscles of patients with spinal muscular atrophy (SMA) and healthy controls (HCSMA).

Chapter 4

Enhanced low-threshold motor unit capacity during endurance tasks in patients with spinal muscular atrophy using pyridostigmine

L.E. Habets
B. Bartels
J.A.L. Jeneson
F. Asselman
M. Stam
C.A. Wijngaarde
R.I. Wadman
R.P.A. van Eijk
D.F. Stegeman
W.L. van der Pol

Abstract

Objective

To investigate the electrophysiological basis of pyridostigmine enhancement of endurance performance documented earlier in patients with spinal muscular atrophy (SMA).

Methods

We recorded surface electromyography (sEMG) in four upper extremity muscles of 31 patients with SMA types 2 and 3 performing endurance shuttle tests (EST) and maximal voluntary contraction (MVC) measurements during a randomized, double blind, cross-over, phase II trial. Linear mixed effect models (LMM) were used to assess the effect of pyridostigmine on (i) time courses of median frequencies and of root mean square (RMS) amplitudes of sEMG signals and (ii) maximal RMS amplitudes during MVC measurements. These EMG changes over time indicate levels of peripheral muscle fatigue and recruitment of new motor units, respectively.

Results

In comparison to a placebo, patients with SMA using pyridostigmine had fourfold smaller decreases in frequency and twofold smaller increases in amplitudes of sEMG signals in some muscles, recorded during ESTs ($p < .05$). We found no effect of pyridostigmine on MVC RMS amplitudes.

Conclusions

sEMG parameters indicate enhanced low-threshold (LT) motor unit (MU) function in upper-extremity muscles of patients with SMA treated with pyridostigmine. This may underlie their improved endurance.

Significance

Our results suggest that enhancing LT MU function may constitute a therapeutic strategy to reduce fatigability in patients with SMA.

Introduction

Hereditary proximal spinal muscular atrophy (SMA) is caused by homozygous deletion of the survival motor neuron 1 (*SMN 1*) gene. Insufficient SMN protein expression in tissues leads to abnormalities at multiple levels of the motor unit (MU), including α-motor neuron degeneration, abnormal anatomy and function of the neuromuscular junction (NMJ), and atrophy and fatty infiltration of the associated musculature.[1–4] Muscle weakness is most pronounced in proximal muscle groups of the extremities and in the more severe and early onset types in axial, respiratory and bulbar muscle groups. In addition, limited endurance for repetitive motor tasks, i.e. fatigability, has been identified as an important characteristic.[5–8]

Pyridostigmine is a neuromuscular excitation enhancer[9] and first-line of treatment for Myasthenia Gravis (MG).[10] Approximately half of the patients with SMA present with similar electrophysiological abnormalities as patients with MG during repetitive nerve stimulation, i.e. a pathological decrement.[1,11] Therefore, we recently examined the efficacy of pyridostigmine in patients with SMA types 2-4 in a placebo-controlled, double-blind, cross-over trial.[5] We found a significant positive effect on endurance performance, while muscle strength and motor function remained stable.[12] Specifically, patients showed a 70% reduced risk of endurance shuttle test (EST) failure under pyridostigmine. However, the electrophysiological basis of this finding remains unclear.

Surface electromyography (sEMG) is a widely used, non-invasive, research tool to study real-time electrophysiological events associated with muscle activation. As such, its use may advance our understanding of the mechanisms responsible for increased fatigability in patients with SMA.[13–21] We recently reported MU reserve capacity in some, but not all, treatment naïve patients with SMA performing ESTs.[22] The MU reserve capacity was estimated as the potential to increase activity of low-threshold (LT) and high-threshold (HT) MUs consecutively. LT MUs are small, more easily recruited and the most fatigue resistant units, used for relatively low forces over a prolonged time.[23] HT MU are larger, faster and rapidly fatigable units, recruited for high force contractions or after exhaustion of LT units.[23] The use of motor unit reserve capacity to prevent task failure is reflected in an increase of the sEMG amplitude during ongoing exercise.[22] In addition, a decrease of the median sEMG frequency can be used as an index of developing muscle acidification,[22] as soon as HT MUs are recruited. Importantly, both manifestations are representations of a muscle's attempt to prolong an ongoing task, but may appear independent from each other.[23]

Here, we performed sEMG recording from working muscles in patients with SMA treated with pyridostigmine or placebo during execution of ESTs, to study electrophysiological processes determining fatigability. We hypothesized augmented reserve capacity of activated MUs during ESTs in patients with SMA using pyridostigmine.

Methods

Study design

Data was collected as part of a clinical trial on the efficacy of pyridostigmine in SMA.[5] This investigator-initiated, mono-center, placebo-controlled study had a cross-over, double blinded design. The protocol consisted of five study visits within a timeframe of 22 weeks (Supplementary Figure 1). The screening visit was performed at the outpatient clinic of the University Medical Center Utrecht, The Netherlands, while follow-up visits took place either at the hospital or at home, depending on the participant's preference.

Subjects

We included patients with SMA types 2, 3a (onset of symptoms between 18 and 36 months) and 3b (onset after 36 months), ≥12 years of age, registered in the Dutch SMA registry.[24] The inclusion and exclusion criteria for this study have been previously described in detail. In short, we included patients with genetically confirmed SMA with predefined minimal and maximal motor scores to allow assessments of meaningful changes during treatment, without other relevant disorders, contraindications for the use of pyridostigmine or use of SMN-augmenting therapies.[5]

Standard protocol approvals, registrations and patient consents

All participants and, in case of minors, their parents signed informed consent. The study was approved by the Medical Ethics Committee of the University Medical Center Utrecht and by the national Central Committee on Research Involving Human Subjects in the Netherlands. Trial registration number NCTO2941328 and EudraCT number 2011-004369-34.

Intervention procedures

Study medication (pyridostigmine or placebo) was taken four times per day and the dose was gradually increased in the first week to minimize side-effects. The maximum dose, reached after one week, was 6 mg/kg/day. In case this dose was not well tolerated the highest achievable dose was continued. Randomization and intervention procedures are described in detail elsewhere.[5]

Endurance shuttle tests

To examine the effect of pyridostigmine use on muscle activation we used two ESTs: the endurance shuttle box and block test (ESBBT) for patients with proximal arm function and the endurance shuttle nine hole peg test (ESNHPT) for patients with only distal arm function 6,7 (Supplementary video SV1). The design and validation of the EST protocols have been published previously.[6,7] In short, we first determined the individual's maximum test intensity

level by asking the subject to perform one cycle of an EST at maximum speed. Subjects then repeated the cycle of an EST at 75% of their maximum speed until they consecutively twice failed to complete a cycle within the defined time period, paced by auditory signals. Subjects were blinded for the maximal test duration of 20 minutes. We documented time to limitation (s) for each EST patients performed and compared this outcome to assess differences between pyridostigmine and placebo use.

Maximal voluntary contraction

We measured maximal voluntary contraction (MVC) force of four muscle groups of the dominant arm (shoulder abduction, elbow flexion, wrist extension and hand grip) before the EST using a handheld dynamometer (CT 3001; C.I.T. Technics, Groningen, The Netherlands) following standardized procedures.[25] We performed manual muscle testing of the same muscle groups in patients with overt muscle weakness (Medical Research Council (MRC) score for muscle strength <4).[26]

Surface Electromyography

sEMG registration and electrode placement

We continuously recorded four bipolar sEMG signals during MVCs and ESTs at study visits 2 and 4, using a wireless Bio Radio (Great Lakes Neurotechnologies, Cleveland, Ohio, USA). We have previously described the sEMG registration and electrode placement procedures 22. We used self-adhesive Ag/AgCl Discs (3M™ Red Dot™, 9 mm electrode, 18 mm gel, 50 mm disk), attached in overlap, with 34 mm center-to-center inter-electrode distance. Skin preparation procedures included removal of hair if necessary and rubbing and cleaning of the skin with alcohol (70% denatured ethanol incl. 5% isopropanol). We placed standard electrodes in a bipolar montage on four muscles, i.e. m. deltoideus pars anterior (shoulder abduction), m. biceps brachii (elbow flexion), m. flexor digitorum superficialis (hand grip), m. extensor digitorum superficialis (wrist extension), on the dominant side of the body, in parallel to myofiber direction using standard guidelines.[27,28] We placed a reference electrode on the spina scapulae. Electrode wires were secured with tape on the skin to prevent cable motion artefacts.

Signal acquisition and processing

We used Biocapture software to measure real time muscle activation and raw sEMG data was processed using custom programs written in MATLAB R2016b.[22] The sampling rate was 1000 samples/s and sampling resolution was 6μV per least significant bit. We used a 250 Hz anti-aliasing filter and a 4th order Butterworth high pass bidirectional filter at 20 Hz. A 50 Hz notch filter removed power line noise of the signal. sEMG outcome parameters were

median frequencies (Hz) and mean root mean square (RMS) amplitudes (V) determined per cycle of an EST.[29] The median frequency of a cycle was determined using the Fast Fourier Transformation. The mean RMS amplitude per cycle was determined over an overlapping moving window (100 samples). The sEMG outcome parameter of an MVC measurement was the maximal RMS amplitude (V), determined over 500 samples overlapping moving windows of the recorded signal.

Statistical analysis

We used a Wilcoxon signed rank test with continuity correction to analyze differences in time to limitation on the ESTs under pyridostigmine and placebo. RMS amplitude intercepts of the four muscles during performance of the two different ESTs (ESNHPT and ESBBT) were similar, meaning that both tests were performed at the same intensity. Therefore, we combined the sEMG outcome parameters measured during the ESNHPT and ESBBT for further analyses. RMS amplitudes were not normally distributed and therefore ln-transformed to meet assumptions for statistical analyses. For analyses of the sEMG parameters measured during the EST we first used linear models to provide individual slopes for the median frequencies (Hz) and the natural logarithm of RMS amplitudes (ln(V)) over time (s). Second, we used linear mixed effects models (LMM) to determine the effect of treatment period (1 or 2) adjusted for treatment (placebo or pyridostigmine) (fixed effect) on intra-individual clustering of median frequency slopes (Hz/s), and RMS amplitude slopes (ln(V)/s)). The random part was modelled with a random intercept per individual and an unstructured covariance matrix. Differences between treatment periods on MVC forces are examined using related-samples Wilcoxon signed rank tests. For the analyses of the MVC measurements we used LMM to determine the effect of treatment period (1 or 2) adjusted for treatment (placebo or pyridostigmine) (fixed effect) on intra-individual clustering of maximal RMS amplitudes (ln(V)). We used R statistics (R-3.4.3 for Windows with RStudio v1.1.414) for all statistical analyses, with the "lme4" package for LMM 30. P-values of < 0.05 were considered significant.

Results

Thirty-two patients completed all study visits; in 31 high-quality sEMG data was collected. Of these, 16 performed the ESNHPT, 15 performed the ESBBT. Participant characteristics are summarized in table 1. Time to limitation was more than two-fold longer on pyridostigmine compared to placebo (389 s (94-971) versus 149 s (96-467), respectively; median and IQR, $p = 0.003$), similar to previously reported results.[12]

Table 1. Baseline characteristics

Characteristics	EST (n=31)
SMA sub-type, n	
Type 2:	15
Type 3a:	12
Type 3b:	4
Gender, m/f	9/22
Age, y, mean (SD)	35.2 (14.1)
MFM, mean (SD)	58.4 (19.5)
MVC force, N, median (IQR)	
m. deltoideus	17 (9-40)
m. biceps brachii	16 (11.5-25)
m. flexor digitorum	8 (6-14.5)
m. extensor digitorum	8 (4-22.5)
Missing sEMG data per visit (n-subjects)	
Visit 2	1
Visit 4	6

SMA = spinal muscular atrophy, subtype 3a: onset of clinical symptoms <3yrs; subtype 3b: onset of clinical symptoms >3yrs, ESBBT = endurance shuttle box and block test, ESNHPT = endurance shuttle nine hole peg test, sEMG = surface electromyography, MFM = motor function measure, MVC = maximal voluntary contraction.

Efficacy of pyridostigmine on muscle activation

Median frequency slopes

We found a significant difference in rate of decrease in median frequencies of the m. biceps brachii between the placebo and pyridostigmine period (figure 1a and Supplementary Table 1). No significant effect of treatment period was found on the rate of decrease in median frequencies of the other muscles examined during the tests (figure 1a and Supplementary Table 1). The decrease in median frequencies of the m. biceps brachii was significantly smaller over time under pyridostigmine ($-14*10^{-3}$ Hz/s, 95% CI: [$-86*10^{-3}$ $58*10^{-3}$]) compared to placebo ($-58*10^{-3}$ Hz/s), 95% CI: [$-94*10^{-3}$ $23*10^{-3}$]), p = 0.018 (figure 1b). An example dataset of median frequencies during the two treatment periods measured at the m. biceps brachii of an individual patient is shown in figure 1c.

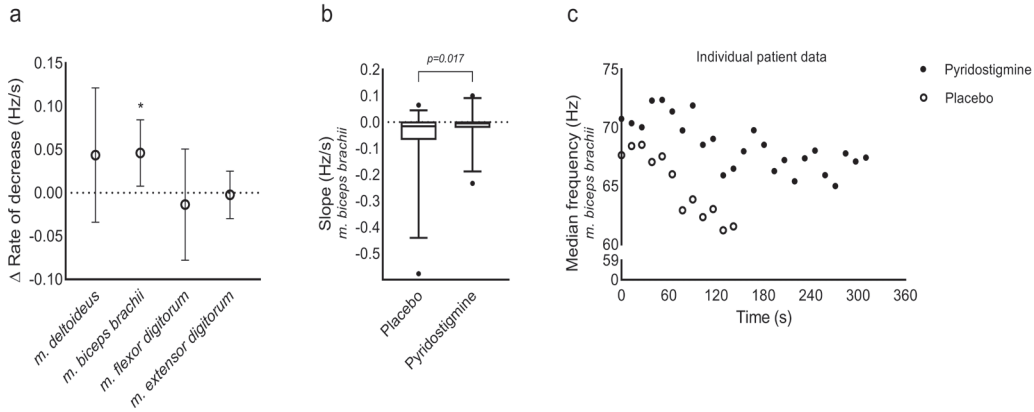

Figure 1. Median frequency slopes measured during ESTs performed by patients with SMA under treatment of placebo or pyridostigmine. a) Mean differences (pyridostigmine-placebo) and 95% confidence intervals in rate of decrease in median frequencies (Hz/s) of four muscles, *p < 0.05. Median frequencies measured in m. biceps brachii decreased significantly slower under pyridostigmine compared to placebo. b) Significant difference in median frequency slopes (Hz/s) of the m. biceps brachii between the placebo and pyridostigmine period. The boxplot shows the median, interquartile range and min/ max of the median frequency slopes. c) Slower decrease in median frequencies calculated from the sEMG signal of the m. biceps brachii combined with a longer exercise duration under pyridostigmine (solid dots) in an individual patient with SMA compared to placebo (open dots).

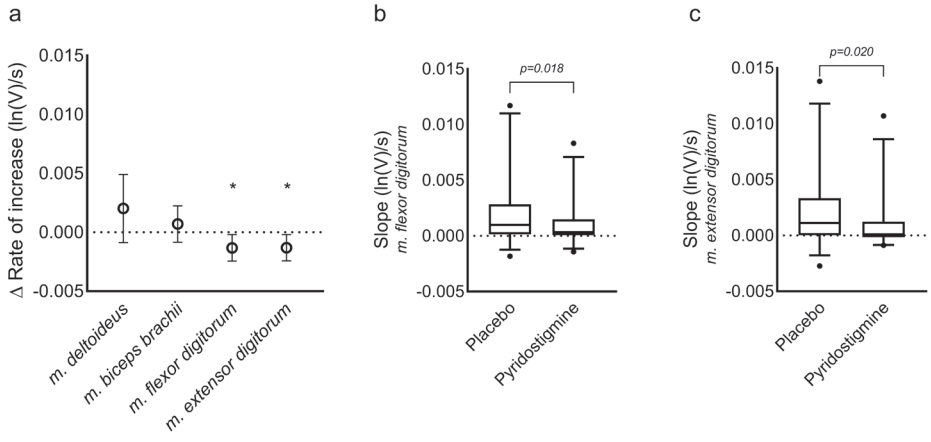

Figure 2. RMS amplitude slopes measured during ESTs performed by patients with SMA under treatment of placebo or pyridostigmine. a) Mean differences (pyridostigmine-placebo) and 95% confidence intervals in rate of increase in RMS amplitudes (ln(V)/s) of four muscles, *p < 0.05. RMS amplitudes measured in m. flexor- and m. extensor digitorum increased significantly slower under pyridostigmine compared to placebo. b-c) Significant difference in RMS amplitude slopes (ln(V)/s) of the m. flexor digitorum and m. extensor digitorum between the placebo and pyridostigmine period. The boxplot shows the median, interquartile range and min/ max of the median frequency slopes.

RMS amplitude slopes

We found a significant difference in rate of increase in RMS amplitudes of the m. flexor- and extensor digitorum between the placebo and pyridostigmine period (figure 2a and Supplementary Table 1). No significant effect of treatment period was found on the rate of increase in RMS amplitudes of the other two muscles examined during the tests (figure 2a and Supplementary Table 1).The increase in RMS amplitudes of the m. flexor digitorum was significantly smaller over time under pyridostigmine ($11*10^{-4}$ ln(V)/s, 95% CI: [$-10*10^{-4}$ $32*10^{-4}$]) compared to placebo ($24*10^{-4}$ ln(V)/s, 95% CI: [$-13*10^{-4}$ $34*10^{-4}$]), p = 0.018 (Figure 2b). Similarly, the increase in RMS amplitudes of m. extensor digitorum was significantly smaller over time under pyridostigmine ($9*10^{-4}$ ln(V)/s, 95% CI: [$-12*10^{-4}$ $31*10^{-4}$]) compared to placebo ($22*10^{-4}$ ln(V)/s, 95% CI: [$11*10^{-4}$ $33*10^{-4}$]), p = 0.021 (Figure 2c). Individual effects of treatment on all muscles for both sEMG parameters are shown in Supplementary figure 2.

Efficacy of pyridostigmine on MVC forces

Maximal voluntary contraction forces of all muscle groups were not significantly different between the placebo and pyridostigmine period, p > 0.05 (Table 2). In all four muscle groups, maximal RMS amplitudes measured during MVC force examination under pyridostigmine were similar to maximal RMS amplitudes measured during these examinations under placebo, p > 0.05 (Supplementary Table 2).

Table 2. Non-parametric related samples Wilcoxon signed rank test to examine difference between placebo and pyridostigmine period on maximal voluntary contraction force.

	MVC force (N)		
	Placebo	**Pyridostigmine**	
Muscle	**Median (IQR)**	**Median (IQR)**	**p-value**
m. deltoideus (n=7)	13 (33)	15 (25)	0.176
m. biceps brachii (n=29)	16 (15)	18 (14)	0.078
m. flexor digitorum (n=29)	8 (9)	9 (7)	0.890
m. extensor digitorum (n=28)	7.5 (17)	7.5 (15)	0.930

MVC = maximal voluntary contraction, sEMG = surface electromyography, IQR = Interquartile range.

Discussion

This study employed sEMG to examine the physiological mechanism of pyridostigmine on muscle activation during EST performance in patients with SMA types 2 and 3. Our results significantly show a smaller down going slope of the median frequency and a smaller up going slope of the RMS amplitude over time measured in part of interrogated upper extremity muscles. These effects both are explained by an enhanced performance of LT MUs during treatment, in accordance with the twofold longer endurance time on pyridostigmine compared to placebo. As expected, we found no significant effect of pyridostigmine on short time MVC. These findings reaffirm pyridostigmine efficacy on endurance performance, but not strength in patients with SMA.[12]

Understanding the effect of pyridostigmine on endurance performance

Pyridostigmine is a commonly prescribed drug for patients with MG.[10] Case studies and clinical experience, report a short term symptom relief as a consequence of daily intake of pyridostigmine in newly diagnosed patients and in patients with a mild form of MG.[10,31] There is, however, no evidence from placebo-controlled randomized clinical trials that support the beneficial effect of pyridostigmine in these patients.[10,31] The precise mechanism of action through which pyridostigmine reduces fatigability is unknown. A decrement during repetitive nerve stimulation, with an absence of incrementing signals, was previously found in patients with SMA suggesting postsynaptic abnormalities of the excitation response at the NMJ.[1]

Here, pyridostigmine enhancement of endurance performance in SMA[12] was hypothesized to improve NMJ functionality and, as such, LT MU recruitment in SMA. Our sEMG results offer two possible explanations for the beneficial effect of pyridostigmine on endurance performance. First, a decline in median frequencies is typically indicative of decreased myofiber propagation velocity associated with muscle acidification.[13,32] We found a fourfold smaller decrease in median frequency in the m. biceps brachii under pyridostigmine (Figure 1) indicating less recruitment of HT MUs associated with glycolytic myofibers to perform the physical task at the same power output.[33] Secondly, we found a twofold smaller increase in RMS amplitude in the m. flexor- and extensor digitorum under pyridostigmine (Figure 2) indicating that neither activation of unrecruited HT MUs nor increasing firing rates of active MUs was necessary to perform the physical task (EST) for a longer duration.[34,35] These findings may be explained either by delayed onset of fatigue in the activated MUs or the availability of unrecruited LT MUs during the task enabling MU rotation[36] in the presence of pyridostigmine.

In summary, we found evidence for pyridostigmine enhancement of neuromuscular excitation capacity, specifically in LT MUs. Additionally, visual inspection of individual patient

data revealed that pyridostigmine affected sEMG parameter slopes in an important fraction of patients while no effect was found in others (Supplementary Figure 2). This observation is in agreement with the previously reported effect of pyridostigmine on endurance[12] and makes a strong case for personalized rather than one-size-fits-all therapeutic use of pyridostigmine suppletion.

Understanding the effect of pyridostigmine on muscle strength

We did not find any effect of pyridostigmine on MVC force. As discussed in the above, enhanced function of LT MUs appeared to be mainly responsible for the improved endurance performance under pyridostigmine, while the combined number and function of LT and HT MUs is more closely associated with muscle strength.[37] Current studies exploring muscle-directed therapy in SMA are mainly focussed on rescuing muscle strength because of the apparent higher vulnerability of HT MUs and associated white myofibers in SMA.[38–40] Our present findings suggest that additional abnormalities in excitation capacity at the neuromuscular junction of LT MUs in SMA may be rescued by pyridostigmine suppletion. Pyridostigmine thus presents a potential therapy to complement muscle-directed therapies and existing SMN upregulatory therapies. Further research is needed to examine this hypothesis and to study the exact working mechanism of pyridostigmine on the NMJ in MUs of different myofiber types.

Applicability of sEMG as an outcome measure

The results of this study confirm the need for novel biomarkers to develop and expand the multisystemic treatment approach in SMA.[41,42] SEMG results add to understanding functional changes in muscle activation. Here it adds to the finding of neurotransmission abnormalities in SMA already indicated by repetitive nerve stimulation.[1] Importantly, clinical applicability of the latter methodology in SMA appeared to be less than straightforward, particularly in patients with contractures and excessive muscle weakness.[43] We therefore believe that sEMG in combination with physical tests, such as the ESTs, contribute to gaining further insight in the mechanisms underlying fatigability in SMA.

Limitations

In this explorative study, we used sEMG in a relatively small number of patients. Although the results provide more insight in the effect of pyridostigmine on muscle activation, future studies that encompass a larger number of patients have the potential to additionally provide a more complete picture of the differences between different types of SMA during separate ESTs, i.e. ESNHPT and ESBBT. In general, patients with SMA type 2 performed the ESNHPT and patients with SMA type 3a/b performed the ESBBT. Previous research[1] showed a trend, but not a significant correlation, between NMJ dysfunction and SMA subtype.

Patients with SMA type 2 and 3a showed an abnormal decrement in 60% of the patients compared to 33% in SMA type 3b. In line with these findings, larger effects of pyridostigmine in patients performing the ESNHPT may be expected in future studies.

The sEMG parameters explored in this study showed the effects of pyridostigmine in some, but not all, examined muscles. Median frequency and RMS amplitude slopes varied between muscles, which raises the question which underlying factors may influence these differences. Patients were allowed to use compensational strategies, to temporarily relieve certain muscles, because the ESTs were designed to represent daily activities. We suggest that this may have led to underestimations of our results. From experience we learned that patients used compensational strategies to relieve for example the m. deltoideus, in which no significant effects of pyridostigmine on sEMG parameters were found. To examine the working mechanism of pyridostigmine on specific muscle groups further, we suggest the use of low intensity movements with a smaller amount of degrees of freedom.

Conclusion

Patients with SMA treated with pyridostigmine reveal increased capacity of LT MUs, partly because of MU rotation resulting in improved endurance. No significant effects on sEMG variables during maximal muscle strength were detected, suggesting that pyridostigmine selectively affects LT MUs, associated with endurance performance. Improving LT MU capacity should further be explored as a therapeutic target in clinical care to reduce fatigability in patients with SMA.

Abbreviations

ESBBT	Endurance shuttle box and block test
ESNHPT	Endurance shuttle nine hole peg test
ESTs	Endurance shuttle tests
HT	High-threshold
LT	Low-threshold
MG	Myasthenia Gravis
MU	Motor unit
MVC	Maximal voluntary contraction
NMJ	Neuromuscular junction
RMS	Root mean square
sEMG	Surface electromyography
SMA	Spinal muscular atrophy
SMN	Survival motor neuron

Declarations

Conflict of Interest Statement

BB obtained research grants from Prinses Beatrix Spierfonds and Stichting Spieren voor Spieren, both non-profit foundations. He is a member of the scientific advisory board of Scholar Rock. His employer receives fees for SMA-related consultancy activities. JALJ obtained a research grant from Prinses Beatrix Spierfonds, a non-profit foundation. WLP obtained grants from Prinses Beatrix Spierfonds, Stichting Spieren voor Spieren and Vriendenloterij. He is a member of the scientific advisory board of SMA Europe and has served as an ad hoc member of the scientific advisory boards of Biogen and Avexis and as a member of data monitoring committee for Novartis. All other authors report no conflicts of interest.

Human and animal rights

"We confirm that we have read the Journal's position on issues involved in ethical publication and affirm that this report is consistent with those guidelines."

Funding

The study is supported by grants from Spieren voor Spieren, Prinses Beatrix Spierfonds, Rotary Bussum and VriendenLoterij. The investigators have full access to the data and have the right to publish this data separate and apart from any sponsor.

Acknowledgment

We thank all patients with SMA in this study for their willingness and commitment.

References

1. Wadman RI, Vrancken AFJ, Van den Berg LH, Van der Pol WL. Dysfunction of the neuromuscular junction in patients with spinal muscular atrophy type 2 and 3. Neurology. 2012;79:2050-2055.
2. Lefebvre S, Brglen L, Reboullet S, et al. Identification and characterization of a spinal muscular atrophy-determining gene. Cell. 1995;80(1):155-165.
3. Otto LAM, van der Pol WL, Schlaffke L, et al. Quantitative MRI of skeletal muscle in a cross-sectional cohort of patients with spinal muscular atrophy types 2 and 3. NMR Biomed. 2020;(March):1-13.
4. Goulet B, Kothary R, Parks R. At the "Junction" of Spinal Muscular Atrophy Pathogenesis: The Role of Neuromuscular Junction Dysfunction in SMA Disease Progression. Curr Mol Med. 2013;13(7):1160-1174.
5. Stam M, Wadman RI, Wijngaarde CA, et al. Protocol for a phase II, monocentre, double-blind, placebo-controlled, cross-over trial to assess efficacy of pyridostigmine in patients with spinal muscular atrophy types 2-4 (SPACE trial). BMJ Open. 2018;8(7):1-9.
6. Bartels B, Habets LE, Stam M, et al. Assessment of fatigability in patients with spinal muscular atrophy: Development and content validity of a set of endurance tests. BMC Neurol. 2019;19(1):1-10.
7. Bartels B, Groot JF De, Habets LE, et al. Fatigability in spinal muscular atrophy : validity and reliability of endurance shuttle tests. Orphanet J Rare Dis. 2020;2:1-9.
8. Montes J, McDermott MP, Martens WB, et al. Six-minute walk test demonstrates motor fatigue in spinal muscular atrophy. Neurology. 2010;74(10):833-838.
9. Robb SA, Sewry CA, Dowling JJ, et al. Impaired neuromuscular transmission and response to acetylcholinesterase inhibitors in centronuclear myopathies. Neuromuscul Disord. 2011;21(6):379-386.
10. Maggi L, Mantegazza R. Treatment of myasthenia gravis: Focus on pyridostigmine. Clin Drug Investig. 2011;31(10):691-701.
11. Meriggioli MN, Sanders DB. Autoimmune myasthenia gravis: emerging clinical and biological heterogeneity. Lancet Neurol. 2009;8(5):475-490.
12. Stam M, Wijngaarde C, Bartels B, et al. Randomised, double-blind cross-over, phase II trial of pyridostigmine versus placebo in spinal muscular atrophy types 2, 3 and 4. PLoS ONE, *under submission* 2021.
13. Linssen WHJP, Stegeman DF, Joosten EMG, van 't Hof MA, Binkhorst RA, Notermans SLH. Variability and interrelationships of surface EMG parameters during local muscle fatigue. Muscle Nerve. 1993;16(August):849-856.
14. Bonato P, Roy SH, Knaflitz M, Luca CJ De. Time-frequency parameters of the surface myoelectric signal for assessing muscle fatigue during cycling dynamic contractions. IEEE Trans Biomed Eng. 2001;48(July):745-754.
15. Bosch T, de Looze MP, van Dieën JH. Development of fatigue and discomfort in the upper trapezius muscle during light manual work. Ergonomics. 2007;50(2):161-177.
16. Bosch T, de Looze MP, Kingma I, Visser B, van Dieën JH. Electromyographical manifestations of muscle fatigue during different levels of simulated light manual assembly work. J Electromyogr Kinesiol. 2009;19(4):246-256.
17. Beck TW, Stock MS, Defreitas JM. Shifts in EMG spectral power during fatiguing dynamic contractions. Muscle Nerve. 2014;50(1):95-102.

18. Rogers DR, MacIsaac DT. A comparison of EMG-based muscle fatigue assessments during dynamic contractions. J Electromyogr Kinesiol. 2013;23(5):1004-1011.
19. Qin J, Lin J-H, Buchholz B, Xu X. Shoulder muscle fatigue development in young and older female adults during a repetitive manual task. Ergonomics. 2014;57(June):1201-1212.
20. Peeters LHC, Janssen MMHP, Kingma I, van Dieën JH, de Groot IJM. Patients with spinal muscular atrophy use high percentages of trunk muscle capacity to perform seated tasks. Am J Phys Med Rehabil. Published online 2019:1.
21. Eken MM, Brændvik SM, Bardal EM, Houdijk H, Dallmeijer AJ, Roeleveld K. Lower limb muscle fatigue during walking in children with cerebral palsy. Dev Med Child Neurol. 2019;61(2):212-218.
22. Habets LE, Bartels B, de Groot JF, et al. Motor unit reserve capacity in spinal muscular atrophy during fatiguing endurance performance. Clin Neurophysiol. 2021;132(3):800-807.
23. Jones D, Round J, de Haan A. Skeletal Muscle from Molecules to Movement. Elsevier Ltd; 2005.
24. Wadman RI, Stam M, Gijzen M, et al. Association of motor milestones, SMN2 copy and outcome in spinal muscular atrophy types 0-4. J Neurol Neurosurg Psychiatry. 2017;88(4):364-367.
25. Beenakker EAC, Van der Hoeven JH, Fock JM, Maurits NM. Reference values of maximum isometric muscle force obtained in 270 children aged 4-16 years by hand-held dynamometry. Neuromuscul Disord. 2001;11(5):441-446.
26. Hislop H, Montgomery J. Daniels and Worthingham (1986) Muscle Testing: Techniques of Manual Examination. 7th ed. Saunders; 2002. http://www.getcited.org/pub/102461099
27. Hermens HJ, Freriks B, Disselhorst-Klug C, Rau G. Development of recommendations for SEMG sensors and sensor placement procedures. J Electromyogr Kinesiol. 2000;10:361-374.
28. Criswell E. Cram's Introduction to Surface Electromyography. Jones Bartlett Publ. Published online 2011:338-371.
29. Konrad P. The ABC of EMG: A Practical Introduction to Kinesiological Electromyography. Noraxon INC. USA; 2005. http://www.noraxon.com/docs/education/abc-of-emg.pdf
30. Bates D, Mächler M, Bolker BM, Walker SC. Fitting linear mixed-effects models using lme4. J Stat Softw. 2015;67(1).
31. Skeie GO, Apostolski S, Evoli A, et al. Guidelines for treatment of autoimmune neuromuscular transmission disorders. Eur J Neurol. 2010;17(7):893-902.
32. Schmitz JPJ, Van Dijk JP, Hilbers PAJ, Nicolay K, Jeneson JAL, Stegeman DF. Unchanged muscle fiber conduction velocity relates to mild acidosis during exhaustive bicycling. Eur J Appl Physiol. 2012;112(5):1593-1602.
33. Ertl P, Kruse A, Tilp M. Detecting fatigue thresholds from electromyographic signals: A systematic review on approaches and methodologies. J Electromyogr Kinesiol. 2016;30:216-230.
34. Henneman E, Clamann HP, Gillies JD, Skinner RD. Rank order of motoneurons within a pool: law of combination. J Neurophysiol. 1974;37(6):1338-1349.
35. González-Izal M, Malanda A, Gorostiaga E, Izquierdo M. Electromyographic models to assess muscle fatigue. J Electromyogr Kinesiol. 2012;22(4):501-512.
36. Bawa P, Murnaghan C. Motor unit rotation in a variety of human muscles. J Neurophysiol. 2009;102(4):2265-2272.
37. Fitts RH. Cellular mechanisms of skeletal muscle fatigue. Pysiological Rev. 1994;74(1):49-81.

38. Long KK, O'Shea KM, Khairallah RJ, et al. Specific inhibition of myostatin activation is beneficial in mouse models of SMA therapy. Hum Mol Genet. 2019;28(7):1076-1089.
39. Pirruccello-Straub M, Jackson J, Wawersik S, et al. Blocking extracellular activation of myostatin as a strategy for treating muscle wasting. Sci Rep. 2018;8(1):1-15.
40. Houdebine L, D'Amico D, Bastin J, et al. Low-Intensity Running and High-Intensity Swimming Exercises Differentially Improve Energy Metabolism in Mice With Mild Spinal Muscular Atrophy. Front Physiol. 2019;10(October):1-21.
41. Smeriglio P, Langard P, Querin G, Biferi MG. The identification of novel biomarkers is required to improve adult SMA patient stratification, diagnosis and treatment. J Pers Med. 2020;10(3):1-23.
42. Yeo CJJ, Darras BT. Overturning the Paradigm of Spinal Muscular Atrophy as just a Motor Neuron Disease. Pediatr Neurol. 2020;109:12-19.
43. Bartels B, de Groot JF, Habets LE, et al. Correlates of fatigability in patients with spinal muscular atrophy. Neurology. 2021;96(6):845-852.

Supplementary material

Supplementary table 1. Linear mixed effects statistical model of treatment effect on median frequency and RMS amplitude

sEMG parameter	**Median frequency slope (Hz/s)**					
Muscle	**Slope placebo**	**Slope pyridostigmine**	**Slope difference**	**95% CI**		**p-value**
				Lower bound	**Upper bound**	
m. deltoideus	-0.076	-0.031	0.043	-0.029	0.116	0.229
m. biceps brachii	-0.058	-0.014	0.045	0.008	0.080	0.018*
m. flexor digitorum	-0.020	-0.039	-0.019	-0.070	0.032	0.457
m. extensor digitorum	-0.029	-0.031	-0.002	-0.028	0.024	0.877
sEMG parameter	**RMS amplitude (ln(V)/s)**					
m. deltoideus	$-1.51*10^{-3}$	$-5.17*10^{-5}$	$1.46*10^{-3}$	$-1.26*10^{-3}$	$4.15*10^{-3}$	0.286
m. biceps brachii	$2.59*10^{-4}$	$9.40*10^{-4}$	$6.81*10^{-4}$	$-7.60*10^{-4}$	$2.12*10^{-3}$	0.343
m. flexor digitorum	$2.38*10^{-3}$	$1.09*10^{-3}$	$-1.29*10^{-3}$	$-2.34*10^{-3}$	$-2.37*10^{-3}$	0.018*
m. extensor digitorum	$2.21*10^{-3}$	$9.42*10^{-4}$	$-1.27*10^{-3}$	$-2.32*10^{-3}$	$-2.10*10^{-4}$	0.021*

sEMG = surface electromyography, RMS amplitude = root mean square amplitude of the sEMG signal, 95%CI = 95% confidence interval, * = p<.05.

Supplementary table 2. Linear mixed effects statistical model on treatment effect on maximal RMS amplitudes measured during MVCs

sEMG parameter	**Maximal RMS amplitude (ln(V))**		
Muscle	**Placebo Estimate [95% CI]**	**Pyridostigmine Estimate [95% CI]**	**p-value**
m. deltoideus	-8.55 [-9.14 -7.96]	-8.43 [-9.65 -7.21]	0.6987
m. biceps brachii	-8.20 [-8.77 -7.62]	-7.53 [-8.81 -6.25]	0.0632
m. flexor digitorum	-8.04 [-8.68 -7.40]	-7.94 [-9.51 -6.44]	0.8183
m. extensor digitorum	-8.14 [-8.61 -7.67]	-7.94 [-9.01 -6.86]	0.4919

MVC = maximal voluntary contraction, sEMG = surface electromyography, RMS amplitude = root mean square amplitude of the sEMG signal, 95%CI = 95% confidence interval.

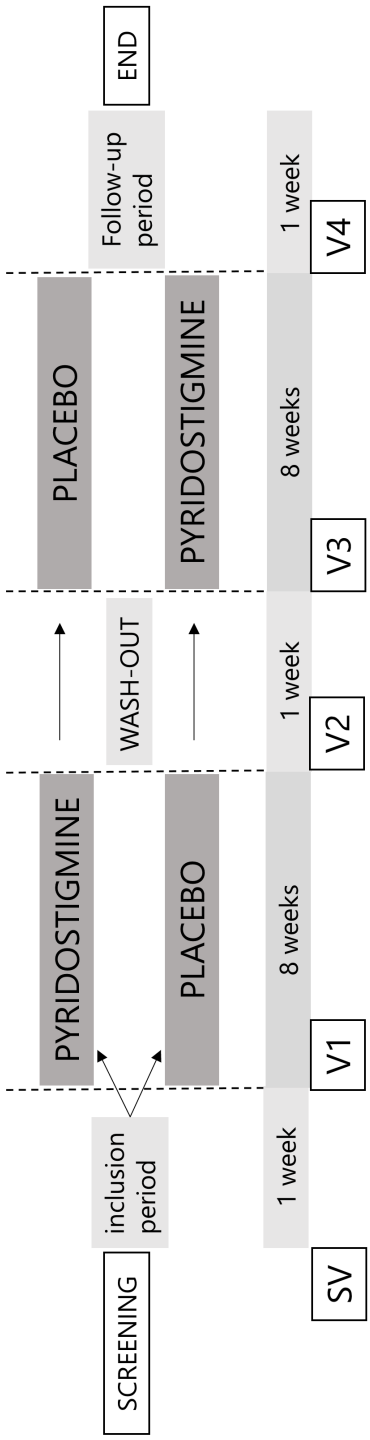

Supplementary Figure 1. Study protocol flow chart. sEMG signals are measured during endurance performance at visit 2 and 4. SV = screening visit, V1-4 = visit 1-4.

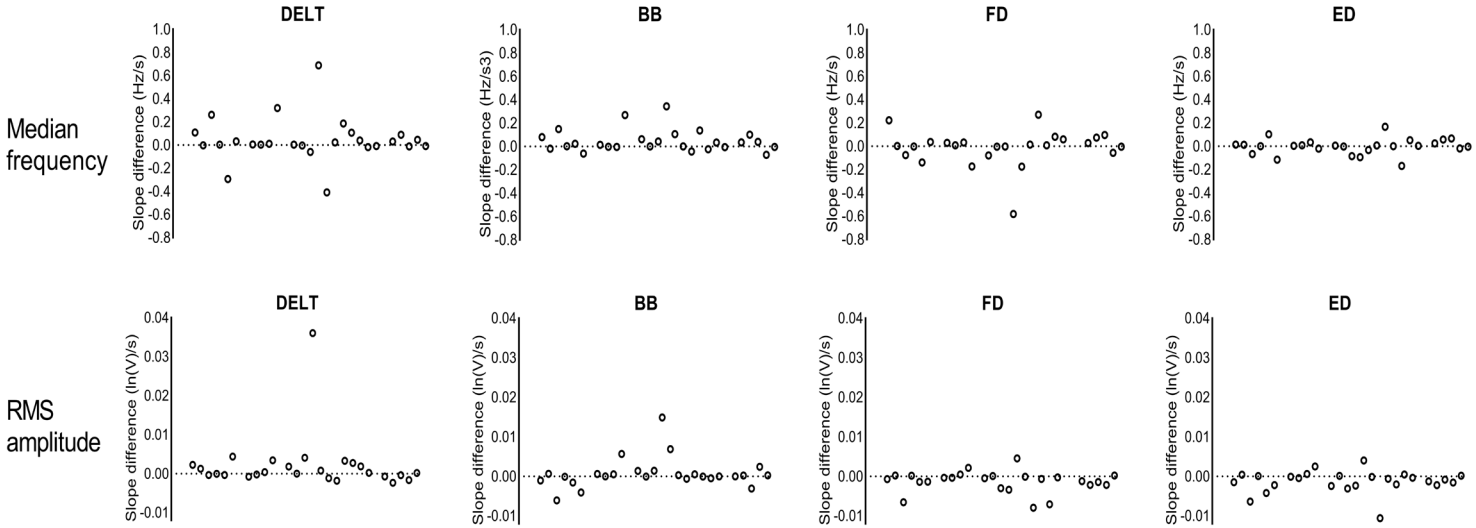

Supplementary figure 2. Individual slope differences (pyridostigmine – placebo) of median frequencies (Hz) and RMS amplitudes ln(V) over time (s) during EST performance. Open circles represent individual patients. DELT = m. deltoideus , BB = m. biceps brachii, FD = m. flexor digitorum, ED = m. extensor digitorum.

Chapter 5

Multi-modal MR imaging of the upper arm muscles of patients with spinal muscular atrophy

M.T. Hooijmans
L.E. Habets
S. van den Berg
M. Froeling
F. Asselman
G. J. Strijkers
J.A.L. Jeneson
B. Bartels
A.J. Nederveen
W.L. van der Pol

NMR in Biomedicine 2022

Abstract

Quantitative Magnetic Resonance Imaging (qMRI) is frequently used to map disease state and disease progression in lower extremity muscles of patients with Spinal Muscular Atrophy (SMA). This is in stark contrast with the almost complete lack of data on the upper extremity muscles which are essential for meaningful activities of daily living. The aim of this study was therefore to assess disease state in upper arm muscles of patients with SMA in comparison to controls by quantitative assessment of fat fraction, diffusion indices and water T2 relaxation times and to relate these measures to muscle force. We evaluated 13 patients with SMA and 15 controls with a 3T MRI protocol consisting of DIXON, DTI, and T2 sequences. qMRI measures were compared between groups and related to muscle force measured with quantitative myometry. Fat Fraction was significantly increased in all upper arm muscles of the patients with SMA compared to controls and correlated negatively with muscle force. Additionally, fat fraction was heterogeneously distributed within the Triceps Brachii (TB) and Brachialis (BR) muscle but not in the Biceps Brachii (BB) muscle. Diffusion indices and water T2 relaxation times were similar between patients with SMA and healthy controls but we did find a slightly reduced MD, λ1 and λ3 in the TB of patients with SMA. Furthermore, MD positively correlated with muscle force in the TB of patients with SMA. The variation in fat fraction further substantiates the selective vulnerability of muscles. The reduced DTI indices along with the positive correlation of MD with muscle force point to myofiber atrophy. Our results show the feasibility of qMRI to map disease state in the upper arm muscles of patients with SMA. Longitudinal data in a larger cohort is needed to further explore qMRI to map disease progression and to capture possible effects of therapeutic interventions.

Introduction

Spinal Muscular Atrophy (SMA) is caused by homozygous loss of function of the *SMN1* gene.[1,2] The deficiency of survival motor neuron (SMN) protein results in extensive changes in the motor unit, including loss of alpha-motor neurons, abnormal anatomy of the neuromuscular junction and progressive muscle wasting and is characterized by predominant axial and proximal muscle weakness.[1,3,4] SMA has a wide range of severity from lethal neonatal to adult symptom onset. This variation is reflected in the clinical classification system that distinguishes four types based on the achieved motor milestones, sitting and walking, and the age of disease onset.[5,6] An increasing number of genetic therapies that increase cellular SMN protein levels have obtained market authorization.[7,8] With these already available therapeutic strategies and emerging second-generation therapies that also directly target muscle, quantitative outcome measures are of increasing importance. Ideally, these outcome measures have a broad dynamic range and reflect disease state and progression over a wide range of disease stages.[9]

Quantitative Magnetic Resonance Imaging (qMRI) has been used to map the natural disease progression in neuromuscular disorders, including SMA.[10–12] The majority of imaging studies in SMA focused on characterizing the progressive replacement of muscle tissue by fat, using both qualitative and quantitative mapping strategies.[13–18] Fat fraction, primarily assessed in the leg muscles, correlates with disease progression and functional outcomes in SMA.[13,14,19] A few studies have also explored other pathophysiological processes, including inflammation using T2 mapping and changes in muscle microstructure using Diffusion Tensor Imaging (DTI).[11,12,19,20] This is in contrast with the almost complete lack of studies that aimed to assess the disease state and progression in arm muscles of patients with SMA. This is likely due to challenges inherent to imaging of the upper extremity muscles, such as respiratory motion, body positioning difficulties and field inhomogeneity due to the off-center location of the upper arm. However, muscles of the shoulder and upper arm are essential for activities of daily living such as eating and personal care and remain preserved longer over time compared to leg muscles.[21,22] Consequently, quantitative measures of the upper extremity muscles are critical for meaningful disease markers across a wide range of disease stages.

Imaging data in patients with SMA, specifically fat fraction, is commonly represented as an average over multiple central slices or a specific region, even though it is not known how fat is distributed within muscles. Recent studies in other neuromuscular diseases, including Duchenne Muscular Dystrophy (DMD), Becker Muscular Dystrophy (BMD) and Facioscapulohumeral Muscular Dystrophy (FSHD),[23–26] showed that fat fraction varies both within and between individual muscles. Hence, evaluation of the fat distribution in patients

with SMA is required to generate insight into the selective vulnerability of extremity muscles in this patient population.

The primary aim of this study was to quantitatively assess fat fraction, diffusion indices and water T2 relaxation time in upper arm muscles of patients with SMA in comparison to controls. Furthermore, we investigated the distribution of fat fraction within individual upper arm muscles in both patients with SMA and controls. Lastly, we explored the associations of these quantitative MR outcome measures with functional measures in patients with SMA.

Methods

Study population

Patients were recruited from the Dutch SMA registry (www.treatnmd.eu/patientregistries). All patients with SMA had a confirmed homozygous deletion of the *SMN1* gene or a heterozygous *SMN1* deletion in combination with a disabling point mutation on the second *SMN1* allele. We used the current SMA classification system with minor modifications as described previously.[27] Inclusion criteria for this study were: 1) age >12 years, 2) ability to perform active arm cycling movements, 3) ability to follow test instructions, 4) Biceps Brachii (BB) muscle Medical Research Council (MRC) score for muscle strength ≥ 4 and Triceps Brachii (TB) muscle MRC score ≥ 2. Exclusion criteria were: 1) contraindications concerning MRI assessment, 2) risk factors for exercise testing registered by a Dutch version of the Preparticipation Questionnaire (American College of Sports Medicine and American Heart Association), 3) mental retardation, 4) comorbidities affecting exercise tolerance, 5) being under examination for non-diagnosed disease at the time of the investigation. The measurements described in this study were part of a larger data-collection, also investigating exercise intolerance, hence some of the inclusion criteria.[28] We recruited control participants with the help of the patients' social network of family, friends and via social media. The study was approved by the medical ethical committee of the University Medical Center of Utrecht (NL62792.041.17) and all participants, and if necessary, the parents, signed written informed consent.

Study set-up & functional measures

The study consisted of two visits. During the first visit, we documented baseline characteristics including Hammersmith Functional Motor Scale Expanded (HFMSE), the Medical Research Council (MRC) score for muscle strength of the Biceps Brachii (BB)/ Brachialis (BR) and Triceps Brachii (TB) muscle and maximal voluntary contraction force (MVCF) of the flexor muscles (BB/ BR) and TB muscle. The HFMSE is an assessment tool of physical abilities in type 2 & 3 SMA, consisting of 33 items with a total achievable score of 66. The MRC scale

assesses muscle strength from grade 0 (no visible contraction) to grade 5 (normal). MVCF was measured with a handheld dynamometer using the break test with the elbow in 90° flexion and supination of the lower arm (MicroFET2, Hoggan Health Industries, Salt Lake City, USA). MR datasets were acquired during the second visit. The two visits were preferably scheduled 2-8 weeks apart to prevent fatigue as a consequence of a maximal arm cycling task which was also part of the same study.[28]

MR Examination

MR datasets were acquired in the right upper arm on a 3 tesla MR System (Philips, Ingenia, Best, the Netherlands) using a 16-element receiver coil (anterior) and the 12-element receiver coil built into the patient table (posterior). Participants were positioned on their right side head-first in the MR scanner to position the right upper arm in the most central location of the bore. Sand bags were placed next to the upper and lower arm to stabilize the position next to the upper body. The neck, back and legs of the participant were supported based on individual preferences. The anterior coil was placed on top of the participant and covered the full upper arm and shoulder region. The data were acquired in a transverse stack with a field of view (FOV) of 480x276 mm^2. The total duration of the imaging protocol was 20 minutes and contained four sequences:

1. 4-point Dixon sequence to determine muscle fat fraction (MS-FFE; TR/TE/ΔTE = 210/2.3/0.76; 4 echoes; acquisition matrix = 184x320; voxel size = 1.5x1.5x6 mm^3, no gap, number of slices = 33; SENSE 2; duration = 02:37).
2. Spin-echo echo planar imaging (SE-EPI) sequence with diffusion weighting to quantify diffusion indices (TR/TE = 6600/57ms; number of gradient directions = 56; b-values 0 (1), 1 (8), 5 (3), 10 (3), 20 (3), 50 (3), 100 (3), 200 (10), 400 (10), 600 (12) s/mm^2; number of signal averages = 1; acquisition matrix = 92x160; voxel size = 3x3x6, number of slices = 33; no slice gap, SENSE = 1.9; combination of three fat suppression techniques: SPectral Adiabatic Inversion Recovery (SPAIR) and Slice Selected Gradient Reversal (SSGR) for the main aliphatic fat peak and an SPIR pulse for the olefinic fat peak; Partial Fourier factor = 0.73; duration = 04:50).
3. Noise acquisition to determine Signal-to-Noise Ratio (SNR) of the diffusion data (SE-EPI, TR/TE = 6200/56; b = 0 + dynamic noise; acquisition matrix = 92x160; voxel size = 3x3x6 mm^3; no gap; number of slices = 33; SPAIR/SSGR/SPIR; SENSE = 1.9; Partial Fourier factor = 0.73; duration = 01:27).
4. Multi-Echo Spin Echo (MESE) sequence to measure water T2 relaxation times (TSE; TR/TE/ΔTE = 4000/7.7/7.6; number of echoes = 17; acquisition matrix = 92x160; voxel size = 3x3x6 mm^3; number of slices = 17; slice gap = 6 mm; Flip angle/Refocusing angle = 90°/180°; SENSE = 2; duration = 06:24).

The middle of the slice stack of each of the sequences was positioned mid-humerus level perpendicular to the humerus bone.

MR data-analysis

MR datasets were processed using QMRITools (https://github.com/mfroeling/QMRITools) for Wolfram Mathematica 11.3. The Dixon data were reconstructed using an iterative decomposition of water and fat with echo asymmetry and least-squares estimation (IDEAL) using eight reference fat peaks and considering a single T2* decay.[29] Fat fraction (FF) was calculated as the signal intensity (SI) fat/ (SI fat+ SI water))*100. Contractile muscle volume (cVolume) was calculated as muscle volume * (100 - fat fraction).

Diffusion data were de-noised using a principal component analysis (PCA) noise algorithm and spatially registered to correct for motion and eddy current induced displacements using an open-source registration tool (http://elastix.isi.uu.nl).[30] Furthermore, the diffusion data were registered to anatomical space using a rigid registration and a B-spline registration to correct for EPI distortions. The diffusion tensor was calculated using an Intra Voxel Incoherent Motion (IVIM) based iterative Weighted-Linear-Least-Squares (iWLLS) algorithm.[31] The tensor was diagonalized generating three eigenvectors and the corresponding eigenvalues (λ1, λ2 and λ3) per voxel. Fractional Anisotropy (FA) and Mean Diffusivity (MD) were calculated per voxel, based on the three eigenvalues, using standard equations. SNR levels were calculated per voxel based on the local average signal divided by the local noise sigma. DTI signal was determined on the b=0 image while the noise sigma was based on the DTI noise acquisition. Datasets with SNR-levels <10 or fat fraction > 50% were excluded from the analysis.[32,33]

Water T2 relaxation times were calculated using an Extended Phase Graph fitting approach, considering different T2 relaxation times for a single water and single fat component. The fat calibration was performed per subject using 1000 random points automatically selected from the subcutaneous fat. The water T2 relaxation time, the fat fraction and the transmit field (B1+) were fitted on a voxel-by-voxel basis using a dictionary method. Pixels with a fat fraction > 50%, based on the reconstructed fat fraction map were excluded from the analysis as these pixels have been shown to impact the stability of the EPG fit.[34,35]

Regions-of-Interest (ROI) were manually drawn on the reconstructed water image of the four-point Dixon sequence for the TB, BB and BR muscle. ITK-snap (www.itksnap.org),[36] was used for the segmentation on the slices where the muscles were visible. Fat fraction, cVolume, water T2, MD,FA, λ1, λ2 and λ3 are reported as mean values of all pixels in the ROI averaged over the full segmented volume. Additionally, the three upper arm muscles were divided into a distal, middle and proximal segment (according to an equal number of

slices per segment) to assess any potential differences in fat fraction along the length of the individual upper arm muscles.

Statistical Analysis

Statistical analyses were performed using IBM SPSS (Version 23, IBM corp., Armonk, NY). Due to the low number of subjects and non-normal distributions nonparametric tests were used for all analysis. Differences between controls and patients with SMA for fat fraction, cVolume, water T2, MD, FA, λ1, λ2, λ3 and MVCF were assessed using a Mann-Whitney U test. The level of statistical significance was corrected for multiple testing and set at $p \leq 0.0055$ (9 measures; 0.05/9=0.0055). Furthermore, differences between the SMA types are described and visualized but not tested due to the small group sizes. Differences in fat fraction between muscle segments were evaluated using a Friedman test. The level of statistical significance was corrected for multiple comparisons and set at $p \leq 0.008$ (6 comparisons; 0.05/6 =0.0083). A Wilcoxon signed-rank test was used as post-hoc analysis to determine which of the muscle segments differed. Lastly, a Kendall tau's correlation was used to explore the association between function measures, i.e. MVCF and HFMSE score, with four of the MR outcome measures, Fat Fraction, MD, FA and water T2 relaxation time in the patients with SMA. MVCF is measured for flexion and extension of the elbow. Elbow flexion MVCF is therefore associated with an average qMRI measure of the BR and BB muscle, as both muscles contribute to flexion force. The strengths of the associations are based on the Kendall tau's coefficient and classified as very weak ($\tau < 0.3$), weak ($0.3 < \tau > 0.5$), moderate ($0.5 < \tau > 0.7$) and strong ($\tau > 0.7$).

Results

Study population

A total of 13 patients with SMA (median age: 47 years; range:12-63 years; m/w: 5/8) and 15 healthy controls (median age: 38 years; range: 13-63 years; m/w: 6/9) participated in this study. The patient group consisted of patients with SMA type 3a (n: 4; median age: 31 years; range: 12-57 years), type 3b & type 4 (n: 9; median age: 54 years; range: 19-63 range years). Due to the very low number (one patient) of patients with SMA type 4 in our study population, patients with SMA type 3b and type 4 were grouped, when describing differences in qMRI outcome parameters between SMA types. All control and patient characteristics and function measures are reported in Table 1. Notable is the wide range of MVCF in the flexor muscles of the patients with SMA. MVCF was significantly lower in the flexor muscles ($Z = -3.7$; $p<0.0001$) and TB muscle ($Z= -3.7$; $p<0.0001$) in patients with SMA compared to controls.

Table 1. Patient Characteristics

	SMA (n=13)	**Controls (n=15)**
Age in years, median (min-max)	47 (12-63)	38 (13-63)
Sex (M/F)	5/8	6/9
MRC score BB, median (min-max)	4 (4-5)	5 (5-5)
MRC score TB, median (min-max)	4 (2-5)	5 (5-5)
HFMSE, median (min-max)	42 (11-65)	n.a.
MVCF flexor muscles, median (min-max)	119.6 (16-351.9)*	189.5 (114.3-437.3)
MVCF TB muscle, median (min-max)	29.1 (8.8-128.1)*	129.9 (95.2-250.4)

MRC Medical Research Council for muscle strength (right BB/BR and TB muscle); range between 0-5, HFMSE Hammersmith Functional Motor Scale Expanded; MVCF Maximal Voluntary Contraction Force, measured in Newton (N), significant differences between patients and controls are marked with an asterisk (*).

Data quality & exclusion

For the DTI-data, a total of 17 muscles were excluded (SMA 12; HC 5). Of those 17 muscles, 7 muscles (of 4 subjects) were excluded since their fat fraction was above 50% (SMA TB 4; BB 3). Additionally, DTI data sets of 4 muscles (of 3 subjects) were excluded due to insufficient SNR(<10) (SMA TB 1; BB 1; BR 1; HC BB 1;) and 6 muscles (of 3 subjects) were excluded due to fat artefacts (SMA TB 1; BB 0; BR 1; HC TB 1; BB 2; BR 1). All Dixon datasets were included for analysis and one T2 patient dataset was excluded due to data export problems.

Fat Fractions, cVolume, Diffusion Indices & Water T2 relaxation times

Multi-parametric axial images of a representative patient with SMA are shown in Figure 1. The median, min and max values for MVCF and MR outcome measures are summarized per group on a muscle-by-muscle basis in Table 2. Muscle fat fraction was significantly higher in all upper arm muscles of the patients with SMA compared to the control muscles ($Z > -2.76$; p-value ≤ 0.006) (Figure 2). cVolume was significantly lower in the TB muscle of patients with SMA compared to controls ($Z=-3.4$; $p=0.0003$) while non-significant but slightly lower cVolumes were seen in BB ($Z=-2.004$; $p=0.046$) and BR ($Z=-2.69$; $p=0.007$) muscle of patients with SMA compared to controls (Table 2). No differences between groups were detected for water T2 relaxation time (Figure 2) or any of the diffusion indices for all the upper arm muscles (Figure 3). However, slightly lower values for $\lambda 1$ ($Z = -2.5$; $p = 0.01$), $\lambda 3$ ($Z = -2.14$; $p = 0.031$) and MD ($Z = 2.35$; $p = 0.016$) were seen in the TB muscle of patients with SMA compared to controls (Figure 3). Based on visual inspection only, there were some variations detectable between SMA types across the muscles. Average fat fractions were highest in SMA type 3a, followed by type 3b & 4 (Figure 4a). This effect was most apparent in the TB muscle. Across the individual muscles, there were no uniform differences in water T2 relaxation times for the SMA types (Figure 4b). A small effect was seen in the diffusion indices between the SMA types across the muscles, with the highest FA values in patients with SMA type 3a (Figure 4c-d).

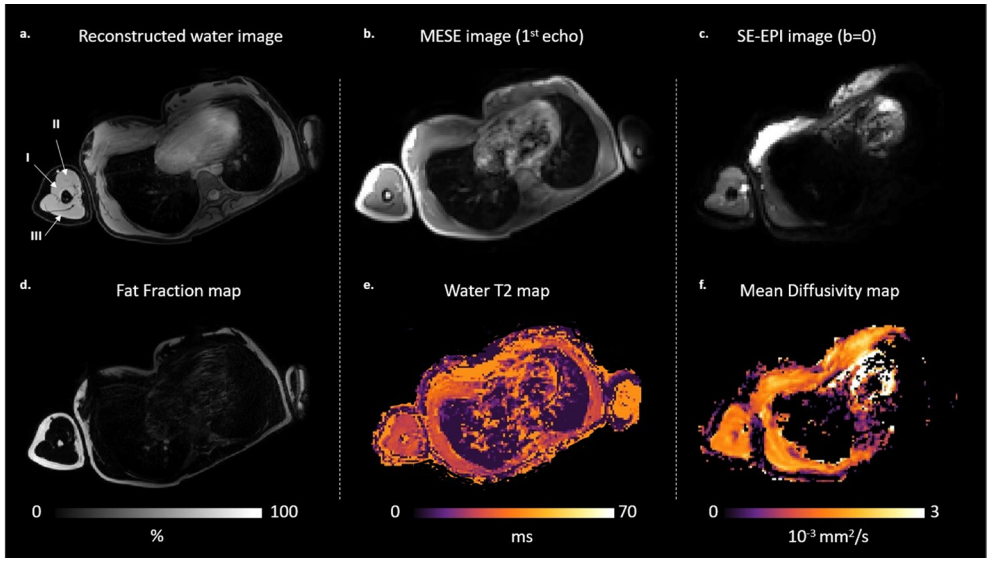

Figure 1. Multi-parametric axial images of the upper arm of a patient with SMA; An offline reconstructed water map of the Dixon scan on which the Brachialis (I), Biceps Brachii (II) and Triceps Brachii (III) muscle are indicated (a); 1st echo of a multi-spin-echo image (b) and a SE-EPI image without diffusion weighting (b = 0 s/mm2) (c); a reconstructed fat fraction map (d), a reconstructed water T2 map (e) and a reconstructed Mean Diffusivity (MD) map (f).

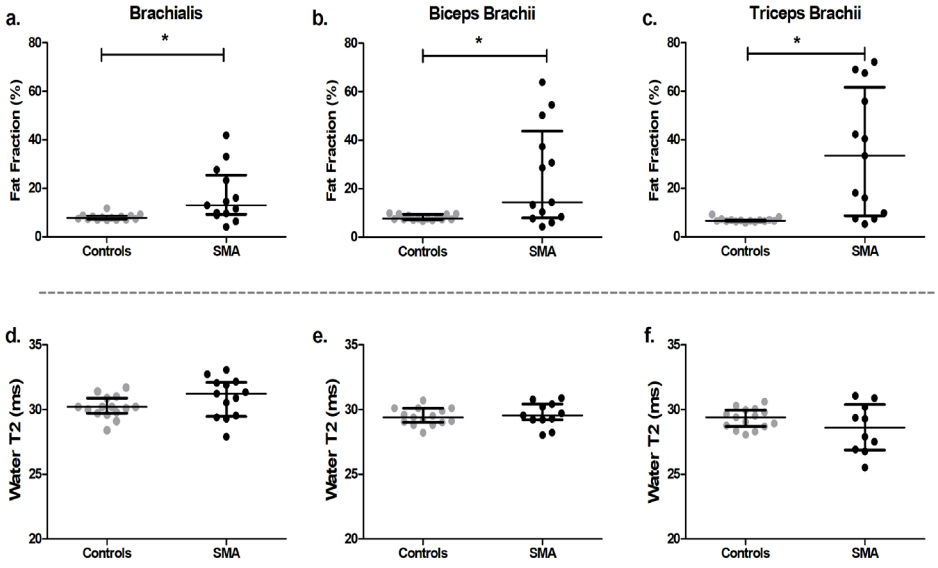

Figure 2. Scatter plots showing the individual data points, median and Inter Quartile Range for fat fraction and water T2 relaxation times in healthy controls (black rounds) and patients with SMA (gray rounds) for the Brachialis (a, d), Biceps Brachii (b, e) and Triceps Brachii (c, f) muscle. *Significant group differences; p< 0.0055.

Table 2. qMRI outcome measures

Muscle	Parameter	SMA	Controls	p-value
Brachialis		N (FF/qT2) = 13/12	N=15	
	Fat fraction (%)	13 (4.1-41.9)*	7.8 (6.8-11.8)	0.004
	Water T2 (ms)	31.5 (27.8 -33.5)	30.2 (28.4-31.7)	0.067
	cVolume (cm^3)	44.1(15.2-260.1)	70.1 (42.7-147)	0.007
		N=11	N=14	
	λ1 (*10^{-3} mm^2/s)	2.06 (1.61-2.44)	2.12 (2.01-2.39)	0.31
	λ2 (*10^{-3} mm^2/s)	1.45 (1.06-1.68)	1.43 (1.31-1.67)	0.83
	λ3 (*10^{-3} mm^2/s)	1.22 (0.91-1.35)	1.22 (1.08-1.36)	0.37
	MD (*10^{-3} mm^2/s)	1.59 (1.21-1.78)	1.59 (1.49-1.82)	0.66
	FA (-)	0.28 (0.22-0.35)	0.28 (0.23-0.38)	0.85
Biceps Brachii		N (FF/qT2) = 13/12	N=15	
	Fat fraction (%)	14.4 (4.3–63.9)*	7.6 (6.6-9.9)	0.009
	Water T2 (ms)	29.9 (28.0-34.7)	29.4 (28.2–30.7)	0.063
	cVolume (cm^3)	107 (15.2-245)	153 (79-218)	0.05
		N=9	N=12	
	λ1 (*10^{-3} mm^2/s)	1.96 (1.77-2.25)	2.06 (1.81-2.17)	0.29
	λ2 (*10^{-3} mm^2/s)	1.37 (1.23-1.64)	1.38 (1.23-1.53)	0.78
	λ3 (*10^{-3} mm^2/s)	1.18 (0.77-1.3)	1.19 (1.09-1.32)	0.433
	MD (*10^{-3} mm^2/s)	1.51 (1.26-1.7)	1.55 (1.44-1.66)	0.70
	FA (-)	0.28 (0.23-0.37)	0.29 (0.23-0.34)	0.75
Triceps Brachii		N (FF/qT2) = 13/12	N=15	
	Fat fraction (%)	33.4 (5.3 – 72.2)*	6.6 (5.9 – 9.3)	0.0001
	Water T2 (ms)	30 (27.9 -39.8)	29.4 (28.1 -30.6)	0.56
	cVolume (cm^3)	124 (26.8-270.9)	297.9 (161-568.7)	0.0003
		N=7	N = 14	
	λ1 (*10^{-3} mm^2/s)	1.95 (1.84 -2.09)#	2.13 (1.91 -2.35)	0.012
	λ2 (*10^{-3} mm^2/s)	1.53 (1.12 -1.61)	1.56 (1.41 –1.7)	0.16
	λ3 (*10^{-3} mm^2/s)	1.18(0.65 -1.61)#	1.31 (1.21- 1/37)	0.032
	MD (*10^{-3} mm^2/s)	1.58 (1.24 – 1.67)#	1.68 (1.54 -1.86)	0.019
	FA (-)	0.26 (0.2 – 0.47)	0.25 (0.21 -0.28)	0.57

Median and Range for Fat Fraction, water T2 relaxation times, contractile Volume and Diffusion Indices in patients with SMA and controls. Significant differences between patients and controls are marked with an asterisk (*) and trends are indicated with a number sign (#). (cVolume = contractile muscle volume, MD = mean diffusivity, FA = fractional anisotropy and λ1, λ2 and λ3 = the three eigenvalues).

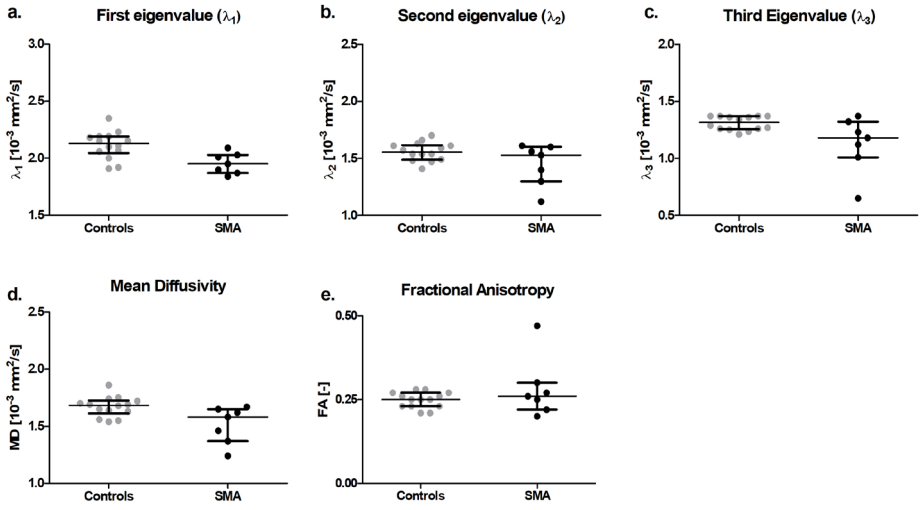

Figure 3. Scatter plots showing the individual data points, median and Inter Quartile Range for Mean Diffusivity (MD) (d), Fractional Anisotropy (FA) (e), and the three eigenvalues (a-c) in healthy controls (black rounds) and patients with SMA (gray rounds) for the Triceps Brachii muscle. *Significant group differences; $p < 0.0055$. Note the trend for a reduction in the first eigenvalue, third eigenvalue and MD.

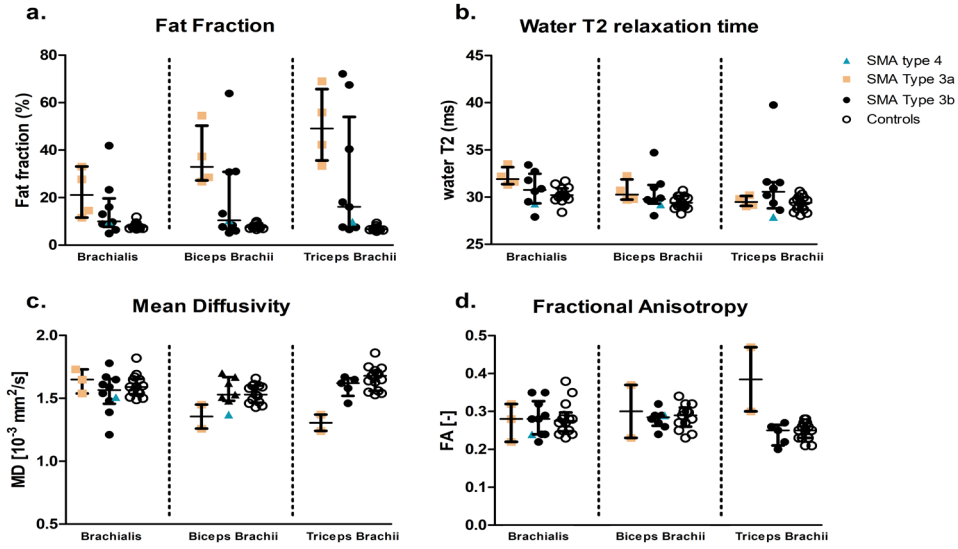

Figure 4. Box and whisker plots for the fat fraction (a), water T2 relaxation time (b), Mean Diffusivity (MD) (c) and Fractional Anisotropy (FA) (d) for the SMA types and controls. SMA type 3a (orange squares); SMA type 3b (black rounds) & 4 (blue triangle) and controls (open rounds). For SMA type 3a, only two diffusion datasets are available of the Triceps Brachii muscle resulting in the median being the average of the two data-points. The individual data points are presented as red dots.

Fat Fraction distributions within muscles

Variations in fat fraction along the length of the muscle are visualized for a control subject, a patient with SMA with low fat fractions, a patient with SMA with intermediate fat fractions and a patient with SMA with high fat fractions in Figure 5. Fat fractions were homogeneously distributed in the BB muscle for patients with SMA (chi-square = 5.5; p = 0.06) as well as controls (chi-square = 6; p = 0.05) (Figure 6). In the BR muscle of patients with SMA, we found higher fat fractions proximally compared to the middle (Z = -3.2; p = 0.001) and distal segment (Z = -3.2; p = -0.001) whereas in the controls a small but significant gradual decline was seen from proximal to distal (dist-mid Z = -3.2, p = 0.001; prox-dist Z = -2.73, p = 0.006). In the TB muscle of the patients with SMA fat fraction gradually increased from distal to middle to proximal, where all segments differed (dist-mid Z = -2.5; dist-prox Z = -2.6; mid-prox Z = -2.3; p < 0.02), while in controls fat fractions were homogeneously distributed (chi-square = 5.3; p = 0.071).

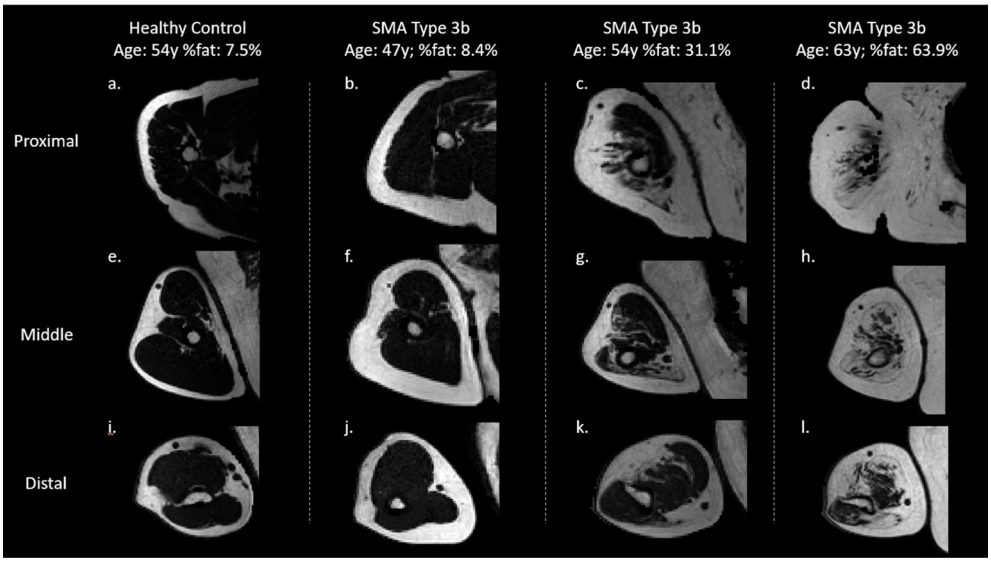

Figure 5. Overview of fat distributions within the individual upper arm muscles. Showing a distal i-l), middle (e-h) and proximal (a-d) slice for a healthy control subject (a, e, i), a SMA patient with low fat fractions (b ,f, j), a patient with SMA with intermediate fat fractions (c, g, k) and a patient with SMA with high fat fractions (d, h, l).

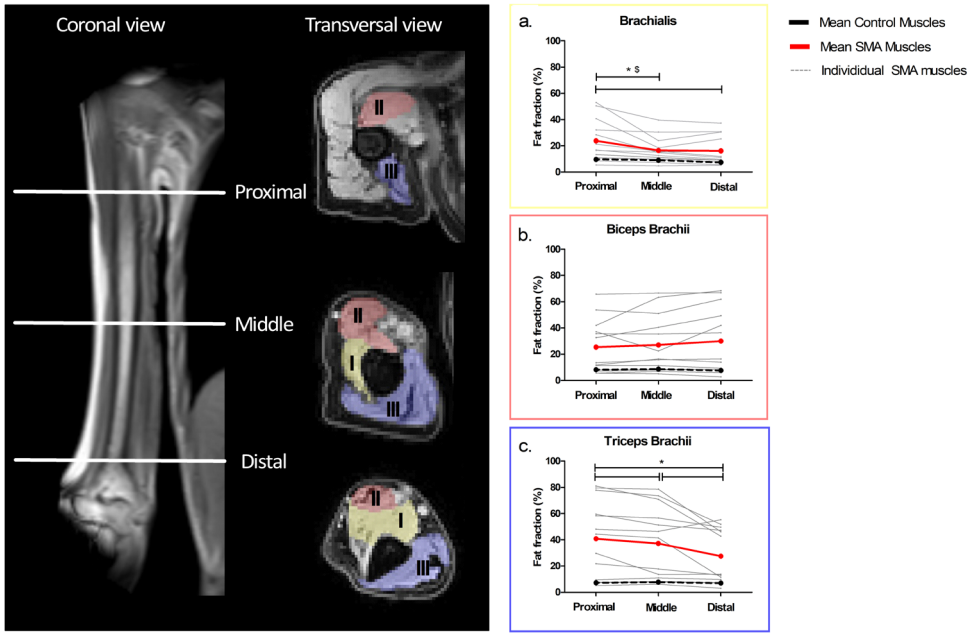

Figure 6. Fat distributions within the individual upper arm muscles. The images in the two left columns show a coronal view of the placement of the Dixon FOV used for fat quantification together with axial images representing a distal, middle and proximal slice with the manual drawn ROI's for the Brachialis (ROI #I – yellow), Biceps Brachii (ROI #II – red) and Triceps Brachii (ROI #III – blue) muscle. The line graphs are presented on a muscle-by-muscle basis showing fat fraction in the distal, middle and proximal segments. Individual patients with SMA are plotted in gray, the median value of the SMA patient group is plotted in red and the median value of the control group in black. Significant differences between segments are indicated with an asterisk (*) for patients with SMA and Controls with a dollar sign ($); p-value: 0.0083.

Associations of MR outcome measures with MVCF and HFMSE in patients with SMA

We found a weak-to-moderate negative association for both MVCF and HFMSE score with fat fraction in flexor (BR & BB) and TB muscles (Figure 7-8). A strong positive association was found between MVCF and MD in the TB muscle but not in the flexor (BR & BB) muscles or with FA (Figure 7). Furthermore, we found a strong positive association of MD and a strong negative association of FA with HFMSE score in the TB muscle (Figure 8). Water T2 relaxation time was negatively associated with HFMSE score in the BR and BB muscle but not in the TB muscle or with MVCF (Figure 8). Lastly, we found no association between fat fraction and age in the patients with SMA (Figure S1).

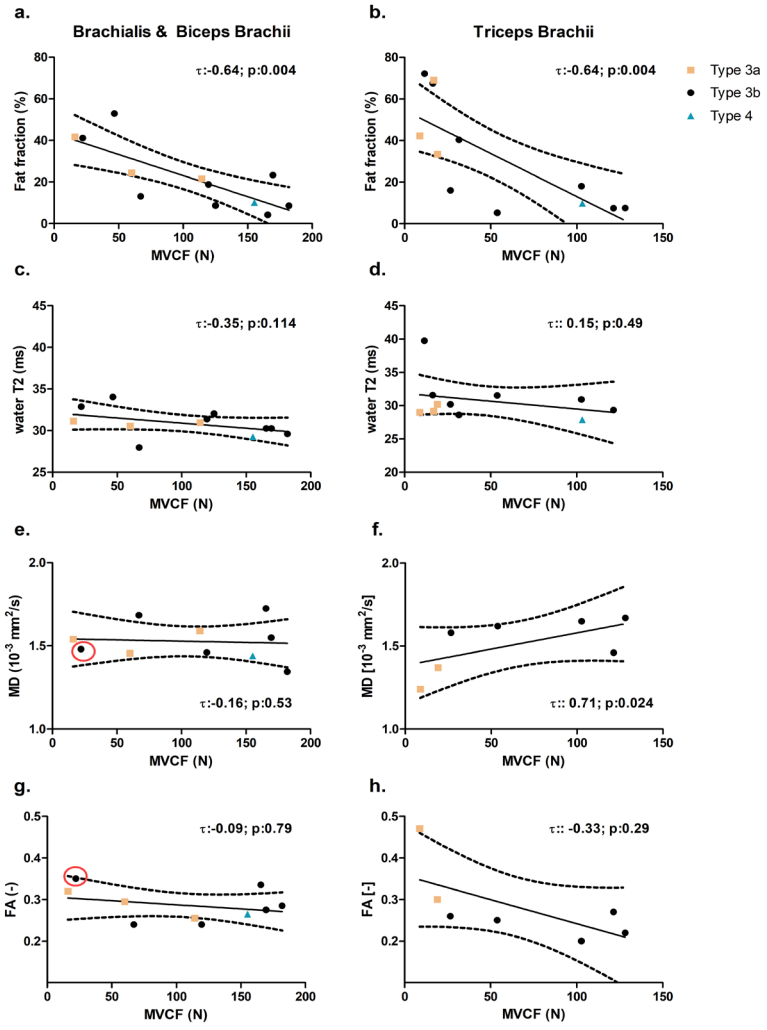

Figure 7. The associations between qMRI measures and MVCF in patients with SMA. Fat fraction (a-b), Mean Diffusivity (MD) (c-d), Fractional Anisotropy (FA) (e-f) and water T2 relaxation times (g-h) are plotted against maximal voluntary contraction force (MVCF) of the flexor muscles (Brachialis and Biceps Brachii muscle) together (a, c, e, g) and Triceps Brachii muscle (b, d, f, h). For the flexor muscles, the qMRI measures are an average of the Biceps Brachii and Brachialis for each patient. Linear regression lines with the 95% confidence intervals are plotted in black solid and dotted lines. SMA types are identified by color and sign, i.e. SMA type 3a – orange square, SMA type 3b – black round, SMA type 4 – blue triangle. For one of the subjects, we only have diffusion indices in the Brachialis muscle due to high fat fraction in the Biceps Brachii muscle. The association between MVCF and the diffusion indices for this subject is indicated with a red circle. The Kendall's tau correlation coefficient and the p-value are shown per plot.

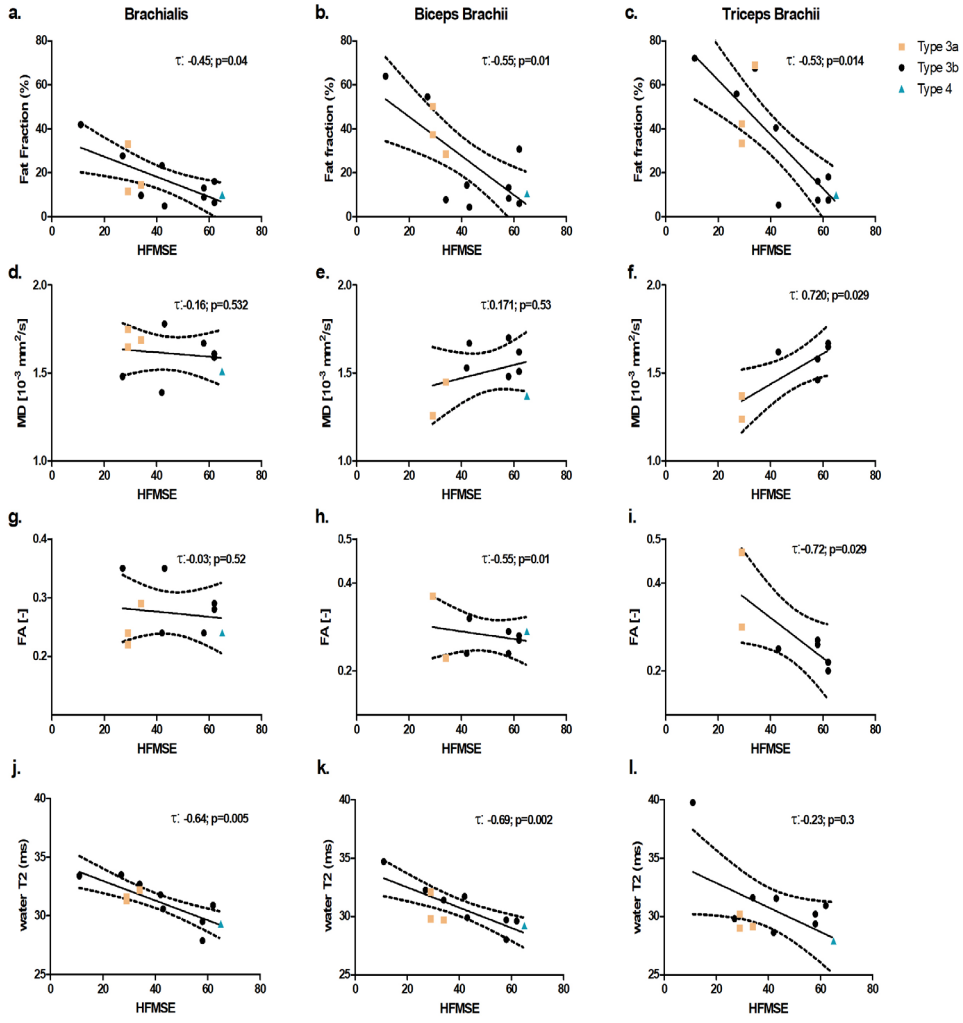

Figure 8. The association between qMRI measures and Hammersmith Functional Motor Scale Expanded (HFMSE) sum score in patients with SMA. Fat fraction (a-c), Mean Diffusivity (MD) (d-f), Fractional Anisotropy (FA) (g-i) and water T2 relaxation time (j-l) are plotted against HFMSE score for the Brachialis (a, d, g, j), Biceps Brachii (b, e, h, k) and Triceps Brachii (c, f, i, l) muscle. The linear regression lines with the 95% confidence intervals are plotted in black solid and dotted lines. SMA types are identified by color and sign, i.e. SMA type 3a – orange square, SMA type 3b – black round, SMA type 4 – blue triangle. The Kendall's tau correlation coefficient and the p-value are shown per plot.

Discussion

We used a multi-modal qMR approach to assess fat fraction, diffusion indices and water T2 relaxation time in upper arm muscles of patients with SMA and controls. Our results showed that fat fractions were significantly higher in all upper arm muscles of the patients with SMA compared to controls and were negatively associated with function measures. Additionally, in patients with SMA fat fractions were heterogeneously distributed within the TB and BR muscle whereas fat fractions were homogeneously distributed in the BB muscle. We did not find differences between patients with SMA and controls based on the DTI indices or water T2 relaxation time.

Fat Fraction between and within individual arm muscles

Fat fraction was higher in patients with SMA compared to controls in all upper arm muscles, with the highest fat fractions in the TB muscle, followed by the BB and BR muscle. We also found variations in fat fraction between SMA types, with the highest fat fraction in SMA type 3a followed by type 3b & 4, which is in line with the clinical presentation of the SMA phenotype. The observed pattern of selective involvement of individual upper arm muscles is in agreement with previous observations.[13,15,37–39] This selective involvement of muscles is a hallmark of SMA, of which the underlying mechanism is not completely understood. Nevertheless, various hypothesis exists on the role of specific biomechanical or anatomical features in this selective vulnerability.[5,40–42] We also observed variations in fat fraction within individual upper arm muscles of patients with SMA. In two of the muscles, i.e. TB and BR muscle, the highest fat fractions were detected proximally whereas the BB muscle showed a homogeneous distribution.[5,43] This phenomenon has not been reported before in SMA, but has been described in DMD[23,44], BMD and FSHD.[25] These diseases showed different distributions, i.e. in DMD higher fat fractions were seen in the muscle end segments compared to the muscle belly, in BMD whereas in FSHD a gradual increase was seen from proximal to distal. Interestingly, in DMD and FSHD, all muscles showed a similar distribution pattern while we observed between muscle variations in fat fraction distributions along the length of the muscle in SMA. We have no explanation for this heterogeneity between and within muscles. As a next step, it would be of interest to investigate whether this distribution of the fat fractions is also visible in other muscles or muscle groups and ultimately to investigate the underlying mechanism. Fat fraction measurements have been proven valuable for characterizing muscle involvement and thereby disease status in patients with SMA. Recent longitudinal studies even showed that it is possible to map the slow progressiveness of the disease, reflected by increased fat fractions, over 6-12 months period.[11,16,20] However, the irreversible nature of the replacement of muscle tissue by fat makes this measure more appropriate for evaluations of future interventions aimed at

preserving rather than improving muscle tissue. Other outcome parameters that can reflect the quality of remaining or non-fatty replaced muscle tissue such as DTI, T2 mapping and Phosphorous Spectroscopy (^{31}P-MRS) might be more suitable for this.

Diffusion Indices

The mean reported values for the diffusion indices are in the range of values normally expected in skeletal muscle.[45,46] After correction for multiple comparisons and exclusion of datasets with artefacts, low SNR levels and high fat fractions (>50%), we did not find significant changes in diffusion indices between patients with SMA and controls. However, in our small cohort, we observed a trend towards a reduction in the first eigenvalue, third eigenvalue and MD in the TB muscle of patients with SMA compared to controls. We suggest that the latter may be explained by a more advanced disease stage in the TB muscle, indicated by high levels of fat fraction, likely associated with higher levels of myofiber atrophy. The absence of differences in the diffusion indices in the other arm muscles may be explained by a mixture of atrophic and hypertrophic fibers previously observed in muscle biopsy studies in SMA.[47] Fiber atrophy and hypertrophy have opposing effects on water diffusivity and could therefore average out an effect on the diffusion indices. Our DTI observations in the arm muscles are partly in line with recent work in thigh muscles of patients with SMA, showing a reduction in MD and an increase in FA in comparison to controls which has been attributed to myofiber atrophy.[12] Since the DTI assessment by Otto and colleagues focused on MD and FA, a comparison of the eigenvalues is unfortunately not possible. The more pronounced changes detected in the thigh muscles may be due to superior statistical power caused by a combination of larger sample size in the previous cohort study and the approach to analyze muscle groups rather than individual muscles. Our results suggest convergence with previous findings in thigh muscles and underline the potential of DTI for mapping disease progression in the remaining and/or non-fatty replaced muscle tissue. Studies with larger sample size and the distinction between non-fatty replaced muscle and low fat muscles, like the study of Rehmann and colleagues in patients with Pompe disease,[48] are needed to fully explore the potential of DTI as outcome measure in neuromuscular diseases, including in SMA.

Water T2 relaxation time

We did not detect differences in water T2 relaxation time in any of the upper arm muscles of patients with SMA compared to healthy controls. This is partly in line with our expectation as inflammatory changes are not a hallmark of SMA in contrast to other neuromuscular disorders such as DMD.[49-51] However, water T2 relaxation times are not solely sensitive to inflammation but also to other pathophysiological processes but no effect was found. Nonetheless, global T2 relaxation times and water T2 relaxation times have been previously

measured in patients with SMA in the lower leg, upper leg and upper arm muscles.[12,19,20] In these studies, a variety of post-processing algorithms have been used for the calculation of global T2 and water T2 relaxation times, which complicates comparison of values between studies.[52] Longer water T2 relaxation times (ranging from 33.4-36.7 ms) were measured by Chabanon and colleagues in the upper arm muscles of patients with SMA using a tri-exponential model for T2 calculation while Otto and colleagues used the same EPG approach in a study on thigh muscles and found slightly shorter water T2 relaxation times.[12,19] These shorter relaxation times in highly fat infiltrated muscles have also been detected in other neuromuscular disorders using spectroscopy and have been attributed to partial volume effects caused by the amount of fat infiltration.[34,53] Not finding clear group differences in our study in combination with mixed findings in previous studies suggest that water T2 relaxation time is not a meaningful outcome measure for mapping disease status in the arm muscles of patients with SMA.

Associations of qMRI parameters with MVCF and HFMSE in patients with SMA

We found the strongest association between fat fraction and MVCF in the most severely affected muscle, i.e. TB muscle. This is in line with previous studies in patients with SMA and suggest a clear relationship between muscle function and fat fraction.[15,19] The relation between fat and function in this patient cohort has been investigated in more detail in Habets 2021 showing a strong positive correlation between cCSA and MVCF in the TB and BB muscle which did not vary between controls and patients with SMA.[29] This suggest that the force generating capacity of the remaining muscle tissue is unaffected in patients with SMA. Furthermore, comparable relations between CSA, cCSA and %fat have been observed in the lower extremity muscles of patients with SMA.[12] Remarkable is the large variation we found in MVCF in the flexor muscles in patients with SMA type 3a but not in the TB muscle or in the HFMSE score. The latter emphasizes the importance to investigate muscle-specific parameters, complementary to overall muscle function. We also observed strong negative correlations for MD with MVCF and HFMSE score in the TB muscle, but not in the other two arm muscles. This finding is partly in line with correlations found in thigh muscles[12] and indicates the potential of diffusion indices as an outcome measure reflecting changes in the remaining muscle tissue. The lack of association between diffusion indices and function measures in the other arm muscles may be explained by the overall lower vulnerability of these muscles in SMA. A moderate negative association of water T2 relaxation time with HFMSE score was observed in the BR and BB muscle but not in the TB muscle or with MVCF. We have no explanation for the latter, however, it suggests a potential relationship with overall function which should be explored in future studies with larger cohorts.

Limitations

The small number of patients with SMA participating in this explorative observational study was highly heterogeneous in age and disease severity, which precludes definite conclusions. Some of the DTI datasets had to be discarded due to insufficient quality as a result of extensive fat replacement, fat artefacts and low SNR. This has resulted in some bias to less severely affected muscles and could explain absence of significant difference in DTI indices. For future applications, other shimming strategies and positions for the upper arm could be explored to improve shimming which could benefit the fat suppression. In addition, more averages can be obtained for higher SNR but the longer scan times will reduce the clinical applicability of the measurement. These strategies may benefit data-acquisition in controls, slightly and intermediately affected patients. However, in severely affected patients it is unavoidable that some data must be excluded, because of low SNR/high fat as in these cases almost no muscle tissue is left. The Dixon FOV did not cover the full length of the upper arm muscles. Therefore, variations seen along the length of the individual upper arm muscles could have been slightly under- or overestimated. Nevertheless, our study showed the feasibility of upper arm qMRI in SMA and indicates its potential. Future studies should aim to obtain data of complete muscle volumes, in order to verify any observations of heterogeneity in the fat fraction of individual muscles. We also need to collect longitudinal data to confirm and further explore the use of qMRI to map disease state, progression and to detect early effects of interventions.

Conclusion

Our multi-modal MR approach showed that it is feasible to quantitatively map disease state in the upper arm muscles of patients with SMA over a wide range of disease phases. Two- to five-fold higher fat fractions were measured in the upper arm muscles of patients with SMA compared to controls, with clear differences between and within individual muscles. No differences were detected in water T2 relaxation times while DTI indices showed potential for mapping of changes in the remaining muscle tissue. Additionally, fat fraction in all three upper arm muscles and MD in the TB muscle, were associated with function measures in patients with SMA.

Abbreviations

BB	Biceps Brachii muscle
BR	Brachialis muscle
DMD	Duchenne Muscular Dystrophy
DTI	Diffusion Tensor Imaging
FA	Fractional Anisotropy
FF	Fat Fraction
FSHD	Facioscapulohumeral Muscular Dystrophy
HFMSE	Hammersmith Functional Motor Scale Expanded
MD	Mean Diffusivity
MRC	Medical Research Council
MVCF	Maximal Voluntary Contraction Force
SMA	Spinal Muscular Atrophy
SMN	Survival Motor Neuron
SNR	Signal-to-Noise Ratio
SPAIR	SPectral Adiabatic Inversion Recovery
SPIR	Spectral Presaturation with Inversion Recovery
SSGR	Slice Selective Gradient Reversal
qMRI	Quantitative Magnetic Resonance Imaging
qT2	quantitative T2
λ1	Eigenvalue 1
λ2	Eigenvalue 2
λ3	Eigenvalue 3
TB	Triceps Brachii muscle

Funding

Prinses Beatrix Spierfonds (W.OR17-05); Stichting Spieren voor Spieren; Zwaluwen Jeugd Actie.

References

1. Lefebvre S, Brglen L, Reboullet S, et al. Identification and characterization of a spinal muscular atrophy-determining gene. Cell. 1995;80(1):155-165.
2. D'Amico A, Mercuri E, Tiziano FD BE. Spinal muscular atrophy. Orphanet J Rare Dis. 2011;6(71).
3. Goulet B, Kothary R, Parks R. At the "Junction" of Spinal Muscular Atrophy Pathogenesis: The Role of Neuromuscular Junction Dysfunction in SMA Disease Progression. Curr Mol Med. 2013;13(7):1160-1174.
4. Wadman RI, Wijngaarde CA, Stam M, et al. Muscle strength and motor function throughout life in a cross-sectional cohort of 180 patients with SMA types 1c-4. Eur J Neurol. 2018;25(3):512-518.
5. Wadman RI, Stam M, Gijzen M, et al. Association of motor milestones, SMN2 copy and outcome in spinal muscular atrophy types 0-4. J Neurol Neurosurg Psychiatry. 2017;88(4):364-367.
6. Munsat TL, Davies KE. International SMA Consortium Meeting (26-28 June 1992, Bonn, Germany). Neuromuscul Disord. 1992;2(5-6):423-428.
7. Mercuri E, Darras BT, Chiriboga CA, et al. Nusinersen versus Sham Control in Later-Onset Spinal Muscular Atrophy. N Engl J Med. 2018;378(7):625-635.
8. Groen EJN, Talbot K, Gillingwater TH. Advances in therapy for spinal muscular atrophy: promises and challenges. Nat Rev Neurol. 2018;14(4):214-224.
9. Yeo CJJ, Darras BT. Overturning the Paradigm of Spinal Muscular Atrophy as just a Motor Neuron Disease. Pediatr Neurol. 2020;109:12-19.
10. Strijkers GJ, Araujo ECA, Azzabou N, et al. Exploration of New Contrasts, Targets, and MR Imaging and Spectroscopy Techniques for Neuromuscular Disease - A Workshop Report of Working Group 3 of the Biomedicine and Molecular Biosciences COST Action BM1304 MYO-MRI. J Neuromuscul Dis. 2019;6(1):1-30.
11. Otto LA., Froeling M, van Eijk RP., et al. Quantification of disease progression in spinal muscular atrophy with muscle MRI – a pilot study. NMR Biomed. Published online 2021:1-11.
12. Otto LAM, van der Pol WL, Schlaffke L, et al. Quantitative MRI of skeletal muscle in a cross-sectional cohort of patients with spinal muscular atrophy types 2 and 3. NMR Biomed. 2020;(March):1-13.
13. Brogna C, Cristiano L, Verdolotti T, et al. MRI patterns of muscle involvement in type 2 and 3 spinal muscular atrophy patients. J Neurol. 2020;267(4):898-912.
14. Brogna C, Cristiano L, Verdolotti T, et al. Predominant distal muscle involvement in spinal muscular atrophy. Neuromuscul Disord. 2019;29(11):910-911.
15. Durmus H, Yilmaz R, Gulsen-Parman Y, et al. Muscle magnetic resonance imaging in spinal muscular atrophy type 3: Selective and progressive involvement. Muscle and Nerve. 2017;55(5):651-656.
16. Sproule DM, Montgomery MJ, Punyanitya M, et al. Thigh muscle volume measured by magnetic resonance imaging is stable over a 6-month interval in spinal muscular atrophy. J Child Neurol. 2011;26(10):1252-1259.
17. Sproule DM, Punyanitya M, Shen W, et al. Muscle volume estimation by magnetic resonance imaging in spinal muscular atrophy. J Child Neurol. 2011;26(3):309-317.
18. Leroy-Willig A, Willig TN, Henry-Feugeas MC, et al. Body composition determined with MR in patients with Duchenne muscular dystrophy, spinal muscular atrophy, and normal subjects. Magn Reson Imaging. 1997;15(7):737-744.

19. Chabanon A, Seferian AM, Daron A, et al. Prospective and longitudinal natural history study of patients with Type 2 and 3 spinal muscular atrophy: Baseline data NatHis-SMA study. PLoS One. 2018;13(7):1-28.
20. Bonati U, Holiga Š, Hellbach N, et al. Longitudinal characterization of biomarkers for spinal muscular atrophy. Ann Clin Transl Neurol. 2017;4(5):292-304.
21. Kruitwagen-Van Reenen ET, Wadman RI, Visser-Meily JM, van den Berg LH, Schroder C, van der Pol WL. Correlates of health related quality of life in adult patients with spinal muscular atrophy. Muscle Nerve. 2016;54(5):850-855.
22. Kruitwagen-van Reenen ET, van der Pol L, Schroder C, et al. Social participation of adult patients with spinal muscular atrophy: Frequency, restrictions, satisfaction, and correlates. Muscle Nerve. 2018;58(6):805-811.
23. Hooijmans MT, Niks EH, Burakiewicz J, et al. Non-uniform muscle fat replacement along the proximodistal axis in Duchenne muscular dystrophy. Neuromuscul Disord. 2017;27(5):458-464.
24. Chrzanowski SM, Baligand C, Willcocks RJ, et al. Multi-slice MRI reveals heterogeneity in disease distribution along the length of muscle in Duchenne muscular dystrophy. Acta Myol. 2017;36(3):151-162.
25. Janssen BH, Voet NB, Nabuurs CI, et al. Distinct disease phases in muscles of facioscapulohumeral dystrophy patients identified by MR detected fat infiltration. PLoS One. 2014;9(1):e85416.
26. van de Velde NM, Hooijmans MT, Sardjoe Mishre ASD, et al. Selection Approach to Identify the Optimal Biomarker Using Quantitative Muscle MRI and Functional Assessments in Becker Muscular Dystrophy. Neurology. Aug 3 2021;97(5):e513-e522.
27. Wijngaarde CA, Stam M, Otto LAM, et al. Muscle strength and motor function in adolescents and adults with spinal muscular atrophy. Neurology. 2020;95(14):e1988-e1998.
28. Habets LE, Bartels B, Asselman FL, et al. Magnetic resonance reveals mitochondrial dysfunction and muscle remodelling in spinal muscular atrophy. Brain. 2021.
29. Reeder SB, Pineda AR, Wen Z, et al. Iterative decomposition of water and fat with echo asymmetry and least-squares estimation (IDEAL): application with fast spin-echo imaging. Magn Reson Med. 2005;54(3):636-644.
30. Klein S, Staring M, Murphy K, Viergever MA, Pluim JP. elastix: a toolbox for intensity-based medical image registration. IEEE Trans Med Imaging. 2010;29(1):196-205.
31. De Luca A, Bertoldo A, Froeling M. Effects of perfusion on DTI and DKI estimates in the skeletal muscle. Magn Reson Med. 2017;78(1):233-246.
32. Froeling M, Nederveen AJ, Nicolay K, Strijkers GJ. DTI of human skeletal muscle: the effects of diffusion encoding parameters, signal-to-noise ratio and T2 on tensor indices and fiber tracts. NMR Biomed. 2013;26(11):1339-1352.
33. Williams SE, Heemskerk AM, Welch EB, Li K, Damon BM, Park JH. Quantitative effects of inclusion of fat on muscle diffusion tensor MRI measurements. J Magn Reson Imaging. 2013;38(5):1292-1297.
34. Keene KR, Beenakker JM, Hooijmans MT, et al. T2 relaxation-time mapping in healthy and diseased skeletal muscle using extended phase graph algorithms. Magn Reson Med. Published online 2020.
35. Marty B, Baudin PY, Reyngoudt H, et al. Simultaneous muscle water T2 and fat fraction mapping using transverse relaxometry with stimulated echo compensation. NMR Biomed. 2016;29(4):431-443.
36. Yushkevich PA, Piven J, Hazlett HC, et al. User-guided 3D active contour segmentation of anatomical structures: Significantly improved efficiency and reliability. Neuroimage. 2006;31(3):1116-1128.

37. Liu GC, Jong YJ, Chiang CH, Yang CW. Spinal muscular atrophy: MR evaluation. Pediatr Radiol. 1992;22(8):584-586.
38. Mercuri E, Pichiecchio A, Allsop J, Messina S, Pane M, Muntoni F. Muscle MRI in inherited neuromuscular disorders: past, present, and future. J Magn Reson Imaging. 2007;25(2):433-440.
39. Quijano-Roy S, Avila-Smirnow D, Carlier RY, group W-M muscle study. Whole body muscle MRI protocol: pattern recognition in early onset NM disorders. Neuromuscul Disord. 2012;22 Suppl 2:S68-84.
40. Piepers S, van der Pol WL, Brugman F, Wokke JH, van den Berg LH. Natural history of SMA IIIb: muscle strength decreases in a predictable sequence and magnitude. Neurology. 2009;72(23):2057-2058.
41. Mentis GZ, Blivis D, Liu W, et al. Early Functional Impairment of Sensory-Motor Connectivity in a Mouse Model of Spinal Muscular Atrophy. Neuron. 2011;69(3):453-467.
42. Deymeer F, Serdaroglu P, Poda M, Gulsen-Parman Y, Ozcelik T, Ozdemir C. Segmental distribution of muscle weakness in SMA III: implications for deterioration in muscle strength with time. Neuromuscul Disord. 1997;7(8):521-528.
43. Piepers S, Van Den Berg LH, Brugman F, et al. A natural history study of late onset spinal muscular atrophy types 3b and 4. J Neurol. 2008;255(9):1400-1404.
44. Spitali P, Hettne K, Tsonaka R, et al. Tracking disease progression non-invasively in Duchenne and Becker muscular dystrophies. J Cachexia Sarcopenia Muscle. 2018;9(4):715-726.
45. Monte JR, Hooijmans MT, Froeling M, et al. The repeatability of bilateral diffusion tensor imaging (DTI) in the upper leg muscles of healthy adults. Eur Radiol. 2020;30(3):1709-1718.
46. Schlaffke L, Rehmann R, Rohm M, et al. Multi-center evaluation of stability and reproducibility of quantitative MRI measures in healthy calf muscles. NMR Biomed. 2019;32(9):1-14.
47. Dubowitz V. Muscle Biopsy. 3rd editio. Saunders Elsevier; 2007.
48. Rehmann R, Froeling M, Rohm M, et al. Diffusion tensor imaging reveals changes in non-fat infiltrated muscles in late onset Pompe disease. Muscle Nerve. 2020;62(4):541-549.
49. Forbes SC, Willcocks RJ, Triplett WT, et al. Magnetic resonance imaging and spectroscopy assessment of lower extremity skeletal muscles in boys with Duchenne muscular dystrophy: a multicenter cross sectional study. PLoS One. 2014;9(9):e106435.
50. Hooijmans MT, Niks EH, Burakiewicz J, Verschuuren JJ, Webb AG, Kan HE. Elevated phosphodiester and T2 levels can be measured in the absence of fat infiltration in Duchenne muscular dystrophy patients. NMR Biomed. 2017;30(1).
51. Wood CL, Hollingsworth KG, Hughes E, et al. Pubertal induction in adolescents with DMD is associated with high satisfaction, gonadotropin release and increased muscle contractile surface area. Eur J Endocrinol. Jan 2021;184(1):67-79.
52. Carlier PG. Global T2 versus water T2 in NMR imaging of fatty infiltrated muscles: different methodology, different information and different implications. Neuromuscul Disord. 2014;24(5):390-392.
53. Schlaeger S, Weidlich D, Klupp E, et al. Decreased water T2 in fatty infiltrated skeletal muscles of patients with neuromuscular diseases. NMR Biomed. 2019;32(8):e4111.

Supplementary material

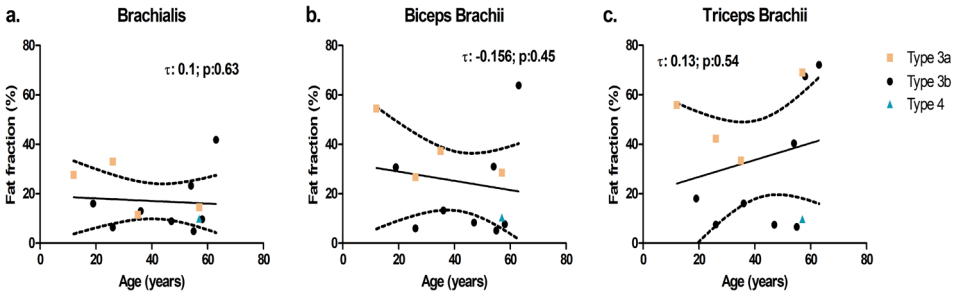

Figure S1: The association between fat fraction and age in patients with SMA for the Brachialis (a), Biceps Brachii (b) and Triceps Brachii (c) muscle. The linear regression lines with the 95% confidence intervals are plotted in black solid and dotted lines. SMA types are identified by color and sign, i.e. SMA type 3a – orange square, SMA type 3b – black round, SMA type 4 – blue triangle. The Kendall's tau correlation coefficient and the p-value are shown per plot for the significant correlations.

Chapter 6

Magnetic resonance reveals mitochondrial dysfunction and muscle remodeling in spinal muscular atropy

L.E. Habets
B. Bartels
F. Asselman
M.T. Hooijmans
S. van den Berg
A.J. Nederveen
W.L. van der Pol*
J.A.L. Jeneson*

*authors contributed equally

Brain 2021

Abstract

Genetic therapy has changed the prognosis of hereditary proximal spinal muscular atrophy, although treatment efficacy has been variable. There is a clear need for deeper understanding of underlying causes of muscle weakness and exercise intolerance in patients with this disease to further optimize treatment strategies. Animal models suggest that in addition to motor neuron and associated musculature degeneration, intrinsic abnormalities of muscle itself including mitochondrial dysfunction contribute to the disease etiology.

To test this hypothesis in patients, we conducted the first in vivo clinical investigation of muscle bioenergetics. We recruited 15 patients and 15 healthy age and gender-matched control subjects in this cross-sectional clinico-radiological study. MRI and ^{31}phosphorus magnetic resonance spectroscopy, the modality of choice to interrogate muscle energetics and phenotypic fiber type makeup, was performed of the proximal arm musculature in combination with fatiguing arm-cycling exercise and blood lactate testing. We derived bioenergetic parameter estimates including: blood lactate, intramuscular pH and inorganic phosphate accumulation during exercise, and muscle dynamic recovery constants. Linear correlation was used to test for associations between muscle morphological and bioenergetic parameters and clinico-functional measures of muscle weakness.

MRI showed significant atrophy of triceps but not biceps muscles in patients. Maximal voluntary contraction force normalized to muscle cross-sectional area for both arm muscles was 1.4-fold lower in patients than in controls, indicating altered intrinsic muscle properties other than atrophy contributed to muscle weakness in this cohort. *In vivo* ^{31}phosphorus magnetic resonance spectroscopy identified white-to-red remodeling of residual proximal arm musculature in patients on basis of altered intramuscular inorganic phosphate accumulation during arm-cycling in red versus white and intermediate myofibers. Blood lactate rise during arm-cycling was blunted in patients and correlated with muscle weakness and phenotypic muscle makeup. Post-exercise metabolic recovery was slower in residual intramuscular white myofibers in patients demonstrating mitochondrial ATP synthetic dysfunction in this particular fiber type.

This study provides first *in vivo* evidence in patients that degeneration of motor neurons and associated musculature causing atrophy and muscle weakness in 5q spinal muscular atrophy type 3 and 4 is aggravated by disproportionate depletion of myofibers that contract fastest and strongest. Our finding of decreased mitochondrial ATP synthetic function selectively in residual white myofibers provides both a possible clue to understanding the apparent vulnerability of this particular fiber type in 5q spinal muscular atrophy type 3 and 4 as well as a new biomarker and target for therapy.

Introduction

5q Spinal muscular atrophy (5qSMA) is an important genetic cause of infant mortality, severe and progressive physical disability in children and adults and is caused by homozygous loss of function of the survival motor neuron 1 gene.[1] Deficiency of the ubiquitously expressed survival motor neuron protein interferes with a range of basic cellular processes, including splicing and ribosomal translation of mRNA.[2] In α-motor neurons survival motor neuron protein deficiency is associated with progressive destabilization of axonal end-plates and ultimately denervation and atrophy of associated skeletal musculature.[3]

Large and fast-conducting motor neurons and their associated pools of fast-twitch glycolytic 'white' myofibers appear to be particularly vulnerable to neuronal survival motor neuron protein deficiency.[4,5] This hypothesis is supported by the prevalence of the most prominent symptom in 5qSMA, muscle weakness,[6,7] as well as by *ex vivo* and *in vitro* examinations of muscle biopsy samples from patients with 5qSMA and SMA mouse models,[8–10] respectively. Abnormal muscular fatigability is, however, also common in 5qSMA.[11–14] Since fatigue resistance of any muscle scales with contractile energetic efficiency and ATP synthetic capacity,[15] this particular symptom suggests that the functionality of motor units comprising oxidative myofiber phenotypes (i.e., slow-twitch oxidative 'red' and fast-twitch oxidative glycolytic 'intermediate' myofibers, respectively)[4,5,16] is also affected in 5qSMA. Indeed, there is evidence that intrinsic abnormalities in muscle itself may contribute to the disease phenotype.[17,18] For example, several studies of SMA have found mitochondrial abnormalities in animal models and muscle *ex vivo* that may cause energetic failure of excitation-contraction coupling preservation during muscular work.[15,18–23] Moreover, results of a recent investigation in an SMA mouse model suggest that mitochondrial ATP synthetic capacity is dysfunctional specifically in white myofibers.[22] Any mechanistic link between survival motor neuron protein depletion and abnormal muscular phenotypic traits in 5qSMA is yet to be identified.[17,18]

Various studies have used Magnetic Resonance imaging (MRI) to investigate muscle morphology in 5qSMA.[24–27] *In vivo* ^{31}Phosphorus MR spectroscopy (^{31}P MRS) is a complementary, non-invasive method to additionally study metabolic phenotypic traits of muscle including *in vivo* mitochondrial function.[16] Of particular interest to 5qSMA, integration of ^{31}P MRS with in-magnet voluntary exercise paradigms can capture and distinguish metabolic manifestations of functional innervation of intramuscular pool of red, intermediate and white myofibers, respectively, in a muscle.[28,29] Here, we apply the power of these in vivo methodologies to study muscle morphology and metabolic phenotypic traits in relation to function in adolescent and adult patients with 5qSMA type 3 and 4. Our work provides *in vivo* evidence that both neurogenic as well as intrinsic muscular abnormalities contribute to the clinical phenotype of the disease.

Materials and methods

Participants

We recruited patients with 5qSMA type 3a, 3b and 4 registered in the Dutch SMA registry (www.treatnmd.eu/patientregistries) for this study. All patients had a confirmed homozygous deletion of the *SMN1* gene. We used the clinical classification system based upon age of onset and acquired motor milestones to distinguish between 5qSMA types 2-4.[30] In case of discrepancies between age at symptom onset and highest achieved motor milestones, the latter determined classification. Patients with 5qSMA type 3a, 3b and 4 show clinical symptoms before the age of three, after the age of three and during adult life, respectively. Age and gender matched control participants were recruited with the help of the patient's social network of family and friends and via social media. Inclusion criteria were: 1) age ≥ 12, 2) ability to perform active supine arm cycling movements, 3) ability to follow test instructions, 4) m. biceps brachii (BB) Medical Research Council score for muscle strength ≥ 4 and m. triceps brachii (TB) Medical Research Council score ≥ 2. Exclusion criteria were: 1) contraindications concerning MR assessment, 2) risk factors for exercise testing registered by a Dutch version of the Preparticipation Questionnaire (American College of Sports Medicine and American heart Association), 3) mental retardation, 4) comorbidities affecting exercise tolerance, 5) being under examination for non-diagnosed disease at the time of investigation. The Medical Ethics Committee of the University Medical Centre Utrecht in the Netherlands approved the study (NL62792.041.17). All participants (and their parents) signed appropriate informed consent.

Study design

This cross-sectional clinical investigation consisted of two visits separated by at least 1 week to minimize the influence of exercise induced fatigue (Fig. 1A). The first visit took place at the Centre for Child Development, Exercise and Physical Literacy at the University Medical Centre Utrecht, The Netherlands. First, participants performed maximal voluntary contractions measured with a handheld dynamometer using the break test (MicroFET2, Hoggan Health Industries, Salt Lake City, UT, USA), as described elsewhere.[31] Thereafter a supine arm-cycling test outside MR-scanner was performed. We measured capillary blood lactate, caught in lithium heparin micro cups (Greiner Bio-One B.V., Alphen aan den Rijn, The Netherlands, catalog number: 450550) prior and directly after cycling using a finger stick. Lactate is a metabolic product of anaerobic glycolysis and is rapidly exchanged with the extracellular milieu.[32] As such, any increase in blood lactate during exercise is generally viewed on metabolic activity of white myofibers in active muscles.[33] The second visit took place at the Amsterdam University Medical Centre, location AMC. After an MRI of the upper

arm, participants were asked to perform an incremental supine arm-cycling test twice at the same day. A resting period of 20-30 minutes separated the two moments of exercise.

Supine arm-cycling test

A previously described MR-compatible mechanically braked bicycle ergometer adjusted for asynchronous arm-cycling with two length-adjustable carbon skipoles (Leki, Italy) with custom made 3D printed carbon handles was used for physical exercise of the upper arm muscles (Fig. 1B).[34,35] Pole handles were additionally fitted with adjustable gloves from cross-country skipoles (Leki, Italy) to minimize involvement of muscles of the forearm during execution of the cycling task (Supplementary Fig. 9). Lastly, the platform was fitted with a mounting system for the mobile Lode MR ergometer carrier (Lode, Groningen, The Netherlands) allowing flexible positioning over the patient bed of the MR scanner (Fig. 1B). The supine arm cycling test was performed with an angle of 90º elbow flexion at the neutral starting position of vertical cranks. After 5 minutes of rest, participants were asked to cycle until exhaustion to ensure myofiber recruitment across the spectrum according to Henneman's size principle.36 Lower arms moved between -45º and +45º in the z-direction at 90 rpm.

The rate of 90 rpm was indicated by an audio cue. Two patients with 5qSMA cycled on a rate of 45 rpm. The test started with six minutes of cycling at 5 Watt on the MR compatible ergometer. Subsequently a mechanical brake aggravated the protocol to 10 Watt for one minute. A weight of 0.2 kg for women and 0.3 kg for men was added to increase the resistance every minute thereafter. Post exercise recovery was monitored for 10 to 20 minutes. The BB was measured during the first, and the TB during the second cycling test at the second visit (Fig. 1A). We measured acceptability of the study visits and perceived fatigue in participants on a visual analogue scale and OMNI scale of perceived exertion on a range between zero and ten, respectively.

Magnetic Resonance Imaging

MRI data acquisition

MR images were obtained to provide insight in upper arm muscle morphology of patients with 5qSMA and controls. All MR experiments were conducted on the 70 cm wide-bore diameter 3 Tesla Ingenia multinuclear MR system (Philips Healthcare, Best, The Netherlands). Participants were positioned on their right side and head first into the scanner. Neck, back and legs were supported based on individual preferences. Sand bags fixated the right upper and lower arm which was positioned to the center of the bench as much as possible. Datasets were acquired from the right upper arm using a 16-channel Anterior Receive coil positioned on the torso of the participant covering the whole arm and 12-channel coil located in the

patient table. The imaging protocol consisted of survey scans used for accurate placement of the Dixon sequence and a 4-point Dixon sequence (TR/TE/ΔTE 210/2.6/0.76ms; Flip angle 8°; Field-Of-View 480x276x198mm; Acquisition voxel size 1.5x1.5x6 mm^2; reconstruction voxel size 1.5x1.5x6mm; no gap; number of slices 33; SENSE 2;) for fat quantification and muscle volume assessments.[37]

MRI Data-analysis

MR images were analyzed using QMRITools for Mathematica (https://mfroeling.github.io/QMRITools). Dixon data was processed using iterative decomposition of water and fat with echo asymmetry and least squares estimation (IDEAL) using eight reference fat peaks and considering a single T2* decay. Muscle morphology was described by fat percentage and contractile cross-sectional area of the muscle. Fat fractions were calculated as the signal intensity (SI) fat/ (SI fat+ SI water))*100 and contractile cross-sectional area was calculated by the following equation: contractile cross-sectional area = CSA * (100-%fat). Regions of Interest (ROIs) for the BB and TB were manually drawn on the reconstructed water image of the Dixon scan using ITK-SNAP (www.itksnap.org)[38] on the slice with the largest CSA. First, largest CSA was determined for each muscle individually using visual assessment. After which ROIs were drawn on those slices, specifically and used to derive the CSA, percentage of fat and the contractile cross-sectional area of BB and TB separately.

Muscle ^{31}Phosphorus Magnetic Resonance Spectroscopy

MRS data acquisition

A 6 cm diameter single turn ^{31}P surface coil (Rapid Biomedical, Germany) was fastened over either the BB or TB, respectively, of the right upper arm. Head and knees were supported on individual preferences. Upper arms were stabilized with a cushion to prevent movement during the preparation phase of MRS data acquisition. Participants were moved into the magnet center and a scout image was acquired to direct shimming. ^{31}P MR spectra from upper arm muscles were collected at rest, during arm-cycling and subsequent metabolic recovery (block pulse, flip angle 45°; TR: 4000 ms; NSA 2; 2048 data points; bandwidth 3000 Hz). The bottom bracket of the platform approached the bore no more than 50 cm to prevent influence of the magnetic field on the cycling resistance. Data acquisition during arm-cycling was synchronized with the cycling rate as described elsewhere.[35]

MRS data analysis

Datasets were analyzed blindly by one observer (JALJ). FIDs were analyzed using AMARES time domain fitting (www. jMRUI.org) with customized starting value- and prior knowledge files. Myofiber pH was derived from the chemical shift difference between the inorganic

phosphate (P_i) and phosphocreatine (PCr) resonances.[35] Myofiber phenotypes were attributed by 1) phenotypic fingerprint at end state of exercise and 2) by PCr and P_i 95% recovery times. Phenotypic fingerprint, expressed in the fraction of P_i signals from recruited myofibers, was examined in participants showing a PCr depletion of >90% at the point of exhaustion. We included two patients with a PCr depletion between 80-90% and we excluded one patient with a PCr depletion <80%. The latter showed decrement (>10%) of the m. trapezius during repetitive nerve stimulation of the n. accessorius. Post-exercise metabolic recovery kinetics (Fig. 4C-D) were determined by nonlinear curve fitting of mono- or double-exponential functions.[39] P_i and PCr 95% recovery times in minutes were calculated by the following equation: 0.95*(3*tau(min.)).

Statistical analysis

We used two tailed parametric t-tests to examine differences in contractile cross-sectional area and PCr 95% recovery times between patients with 5qSMA and healthy controls. We used non-parametric Mann-Whitney U tests to examine differences in maximal voluntary contractions, Δ capillary blood lactate, fat infiltration, phenotypic fingerprint and $P_{i\ (red,\ intermediate,\ white)}$ 95% recovery time between patients with 5qSMA and healthy controls. An allometric function was used to fit associations between MRI parameters. We used Pearson's correlations to assess the relationship between maximal voluntary contraction force and contractile cross-sectional area of both muscles. We used Spearman's correlations to assess the relationship between maximal voluntary contraction force and Δ capillary blood lactate, Δ capillary blood lactate and $P_{i\ Intermediate+White}$. The level of significance was set at $P < .05$.

Data availability

The data that support the findings of this study are available form the corresponding author (JALJ) upon reasonable request.

Results

Experimental paradigm to assess upper arm muscle

To probe the relation between function and muscle quality and quantity, our experimental design featured functional testing (maximal voluntary contraction and dynamic voluntary exercise), morphological (1H MRI) and metabolic studies (blood sampling and *in vivo* ^{31}P MRS) in a cohort of treatment naïve patients with genetically confirmed 5qSMA (Fig. 1A; Materials and Methods). To overcome the communal practical problem of proximal muscle weakness and lower body disability in this patient group, we switched from a leg-cycling to an arm-cycling exercise platform (Fig. 1B and Supplementary Video 1).[40,41] We recruited a total of 15 patients with 5qSMA and 15 age- and gender-matched healthy controls (Table 1 and Supplementary Table 1). Of our 15 patients with 5qSMA, six were classified as 5qSMA type 3a (4 non-ambulant patients; Supplementary Table 1 case no. 4, 6, 11, 15), eight as type 3b and one as type 4. Patient acceptability of the MR exercise intervention, measured on a visual analogue scale ranging from zero to ten indicating willingness to repeat this test in any future clinical study, was excellent in patients (mean (SD): 9.1 (1.3)) and controls (8.3 (2.3)). One control subject dropped out after the first visit.

MVC force of BB and TB muscles in patients was significantly lower compared to controls reflecting muscle weakness, the hallmark symptom of 5qSMA (Fig. 1C); $P = 0.002$, $p < 0.001$, respectively. Blood lactate increase in response to arm-cycling exercise was significantly lower in patients compared to controls (Fig. 1D)($P = 0.004$) and uncorrelated to cycling time in the large majority of patients (Supplementary Fig. 1). Cycling time between bouts in the second visit was highly reproducible in both groups, but significantly shorter in patients compared to controls (BB (mean (SD)): 3.1 (1.9), TB: 3.0 (2.1) min. versus BB: 7.4 (1.3), TB: 7.2 (2.4) min., respectively; $P < 0.001$) recapitulating previous observations of exercise intolerance and premature fatigability in 5qSMA.[13] Perceived fatigue was similar in patients compared to controls (BB (median (IQR)): 9.0 (2.0), TB: 9.0 (4.0) versus BB: 9.0 (5.0),TB: 9.0 (7.0), respectively; $P > 0.05$).

Table 1. Cohort demographic characteristics

Demographic	Age, y	% male	5qSMA type 3a/3b/4 (n)	SMN copy no. 3/4 (n)	HFMSE	MRC score BB (range)	MRC score TB (range)
Controls (n=14)	40 ± 17	36	n.a.	n.a.	n.a.	5	5
5qSMA (n=15)	40 ± 17	33	6/8/1	3/12	40 ± 18	4-5	3-5

Values are expressed as mean ± SD, subtype 3a clinical symptoms <3yrs, subtype 3b clinical symptoms >3yrs, HFMSE Hammersmith Functional Motor Scale Expanded, MRC Medical Research Council score for muscle strength, n.a. = not applicable.

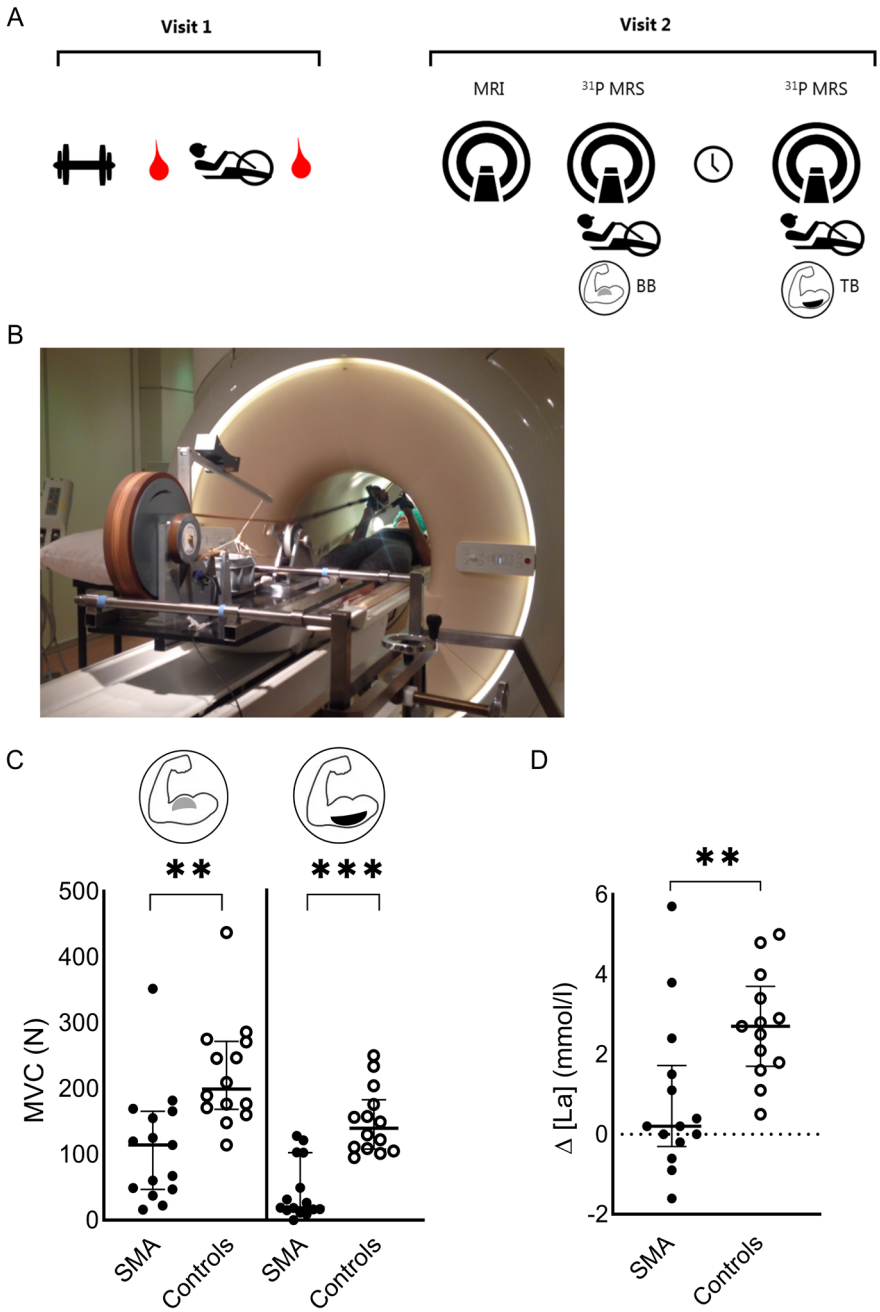

Figure 1. Experimental design and first visit results. (A) Study design. (B) The experimental set-up used for supine arm-cycling inside the bore of a 3T multinuclear MRI scanner (Ingenia scanner with 70 cm bore diameter, Philips Healthcare). (C) Median, interquartile range (IQR) and individual maximal voluntary contraction (MVC) force (N) of patients with 5qSMA and controls measured in the BB ($P = 0.002$) and TB ($P < 0.001$) muscle. (D) Median, IQR and individual Δ capillary blood lactate ([La]) (mmol/l) measured in patients with 5qSMA and controls ($P = 0.004$). ** = $P < 0.01$, *** = $P < 0.001$.

Morphology of upper arm muscles in adolescent and adult 5qSMA

We acquired MR images of the upper arm to examine fat infiltration and atrophy of the BB and TB muscles of the right arm of patients with 5qSMA (n = 13) and controls (n = 14) using a 4-point Dixon sequence. Two patients with 5qSMA had contraindications concerning MRI assessment. A set of typical transverse images of the upper arm of a patient versus a healthy control are shown in Fig. 2A, with BB and TB indicated in red. Visual inspection of the images indicated that fat infiltration and loss of muscle mass as previously reported for leg muscles in patients with 5qSMA were also present in the upper arm muscles of patients.[24] To objectify this trend, we performed quantitative image analyses using QMRITools for Mathematica (Materials and Methods) and found that fat percentages of both BB as well as TB were significantly higher in patients than controls (Fig. 2B); $P = 0.007$, $P < 0.001$, respectively. Our findings mirror the 11.9-15.5% fatty infiltration in the BB muscle of patients with 5qSMA type 3 reported previously.[25] On the other hand we found a higher fat percentage in the TB muscle of patients in our cohort than the previously reported 12.9-20.3%.[25] Contractile cross-sectional area of the TB muscle, defined as gross CSA adjusted for fatty infiltration, was significantly reduced in patients compared to controls (Fig. 2C); $P < 0.001$. BB contractile cross-sectional area was not different in patients and controls (Fig. 2C)($P = 0.309$) suggesting this muscle of the upper arm was more preserved than its antagonist in this particular cohort. Fat infiltration negatively correlated with the contractile cross-sectional area for both BB and TB ($r = -0.71$ and -0.80, $P < 0.0001$, respectively; Fig. 2D-E).

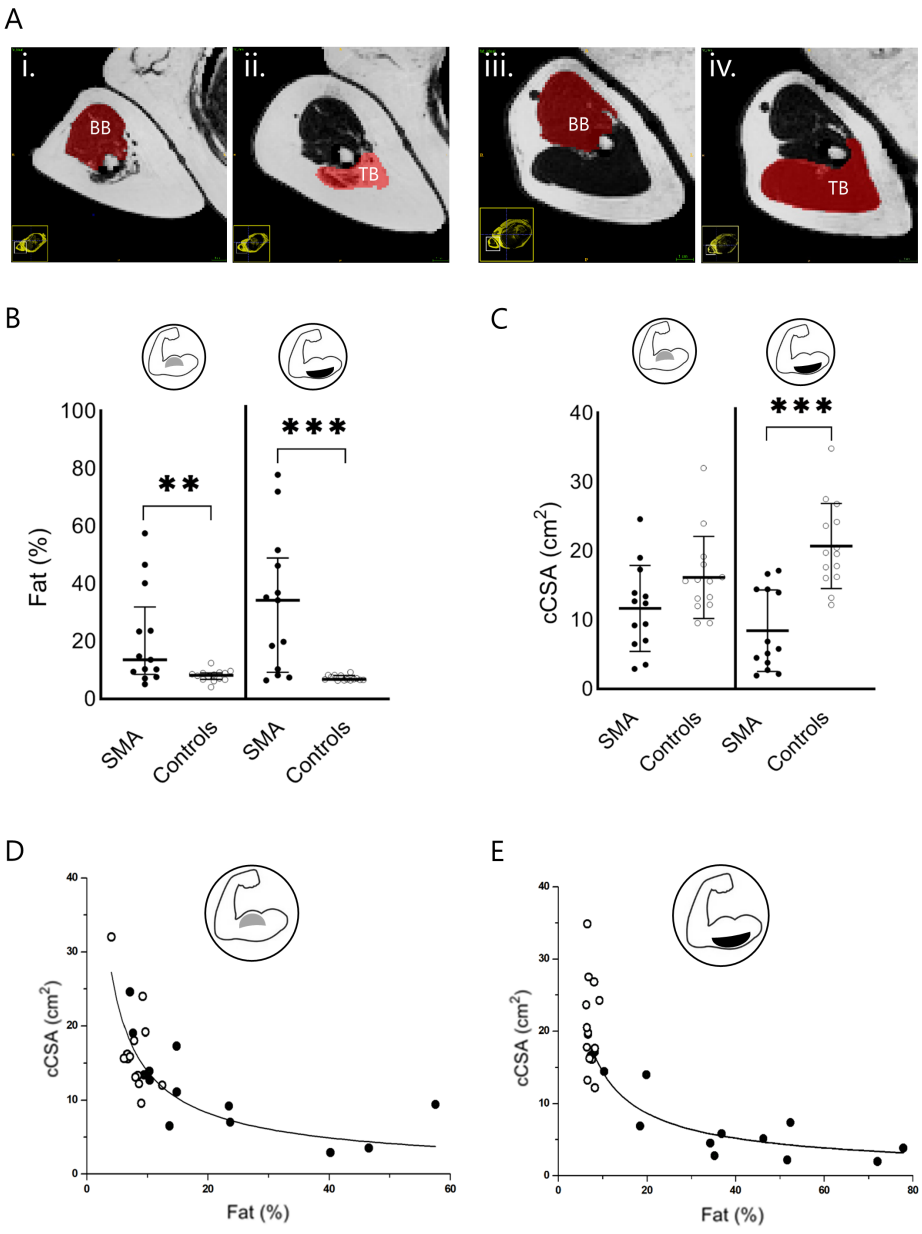

Figure 2. Morphologic examination of upper arm musculature of patients with 5qSMA and controls using quantitative MRI. (A) MR images with BB and TB ROI of a patient with 5qSMA (i,ii) and a healthy control (iii,iv). (B) Median, interquartile range and individual BB ($P = 0.007$) and TB ($P < 0.001$) fat infiltration (%) in 5qSMA and controls. (C) Mean, standard deviation and individual BB and TB ($P < 0.001$) contractile cross-sectional area (cCSA) (cm2) in 5qSMA and controls. (D-E) Allometric correlation between fat infiltration and cCSA in SMA (open dots) and controls (solid dots); BB: $r = -0.71$, TB: $r = -0.80$. ** = $P < 0.01$, *** = $P < 0.001$.

Metabolic phenotypic profiling of upper arm muscles in adolescent and adult 5qSMA

Integration of ^{31}P MRS with in-magnet voluntary exercise paradigms for human lower limb muscles has been shown to capture and distinguish metabolic manifestations of working red, intermediate and white myofiber pools, respectively.[28,29] To test if this methodology can be used to evaluate residual functional innervation of each of these fiber type pools in upper arm muscles of patients with 5qSMA, we first performed dynamic recording of *in vivo* ^{31}P MR spectra from the BB muscle in a healthy subject performing the arm-cycling trial. We observed multiple distinct peaks between 5.2 and 3.7 ppm in *in vivo* ^{31}P MR spectra from this working muscle (Fig. 3A) that exhibited extraordinary temporal dynamics as exercise continued until exhaustion (Supplementary Fig. 2). A point of note is that these spectral dynamics presented early into exercise in the presence of high total muscle content of the myofibrillar ATP buffer PCr (0.0 ppm). Previous studies in human lower limb muscles reported such observations only late into exercise in the presence of large PCr depletion.[28,39,42] Similar observations were made in the TB muscle (Supplementary Fig. 3). On basis of previous work we attributed the detected ^{31}P MR resonances between 5.2 and 3.7 ppm to P_i, a metabolic product of ATP hydrolysis, accumulating in red, intermediate and white myofibers operating at distinct cytoplasmic pH values ranging between pH 7 and 6 (Fig. 3A-B and Supplementary Fig. 4).[28,39,42]

We next hypothesized that the observed rich P_i and pH dynamics in working BB and TB muscles captured motor unit recruitment in action on the premise that arm-cycling represents an uncommon motor task in daily life and has been associated with short-term motor skill learning in naïve subjects.[34,43] As such, once all available MUs have been recruited, the particular *in vivo* ^{31}P MR spectral BB and TB fingerprint at that time should inform on the relative abundance of red, intermediate and white myofiber pools with functional innervation in these muscles. We then estimated these fractions for each myofiber type on basis of numerically fitted fractional amplitudes of P_i resonances at 5 ppm (pH 7; red fibers), 4.6-4.2 ppm (pH 6.6 ± 0.1; intermediate fibers) and 4 ppm (pH 6; white fibers), respectively (Materials and Methods; Supplementary Fig. 5) as described previously.[39] Assuming the condition of complete motor unit recruitment is adequately satisfied when total muscle PCr is 90% or more depleted,[42,44] we verified in a healthy subject that analysis of the ^{31}P MR spectrum of the BB muscle at fatigue recorded in two separate arm-cycling trials yielded reproducible estimates of its functional phenotypic myofiber makeup in this individual (Supplementary Table 2). The resulting outcome of a predominantly fast-twitch white myofiber phenotype is in good agreement with histological studies of the BB muscle of healthy adults.[45–47]

We next collected *in vivo* ^{31}P MR spectra of the BB and TB muscles during exhaustive arm-cycling in patients (n = 15) and controls (n = 14) to compare the relative abundance of red, intermediate and white myofibers with functional innervation, respectively, in these muscles. Time to PCr depletion was four- to eightfold shorter in 5qSMA than in controls (BB:

64s, 32-92 versus 288s, 144-328 (median, IQR), P = 0.055, respectively, TB: 48, 28-128; 320, 120-352, P = 0.029). Comparison of the group medians of the fractional size of functional red versus intermediate and white myofiber pools in the BB and TB muscles in 5qSMA versus controls (Fig. 3C-D) identified a trend towards a white-to-red shift in functional myofiber makeup for the TB muscle of patients compared to controls (Fig. 3D; P = 0.101). This white-to-red shift was significant for the BB muscle of patients (Fig. 3C; P = 0.0045).

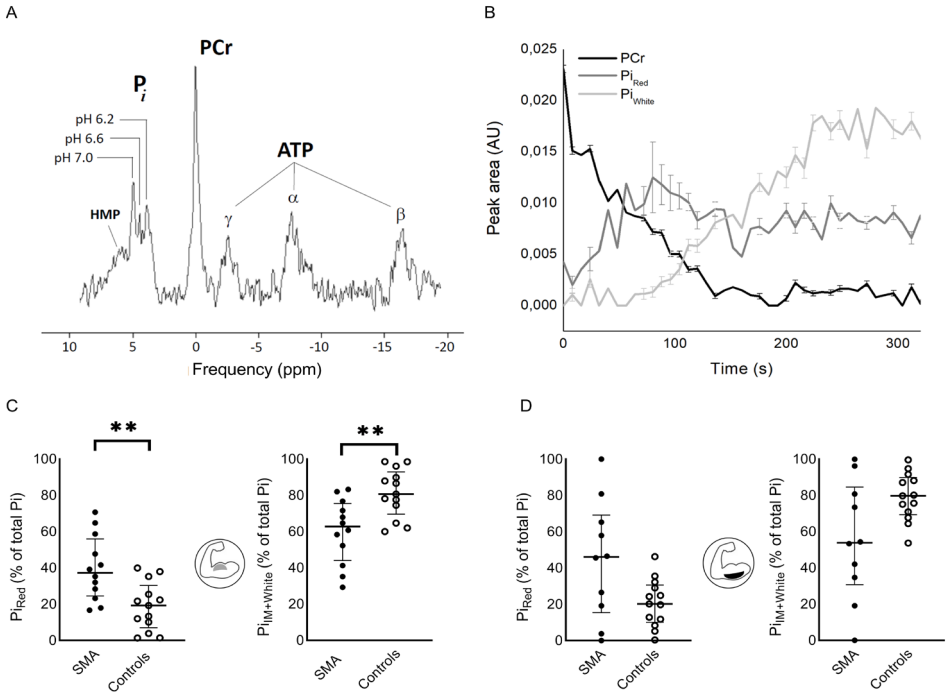

Figure 3. Phenotypic fingerprinting of proximal arm musculature of patients with 5qSMA and healthy controls using dynamic *in vivo* ^{31}P MRS. (A) *In vivo* ^{31}P MR spectrum acquired from BB muscle of a healthy control subject, 60 seconds after onset of supine arm-cycling exercise at 90 rpm. (B) Time course of PCr (black) and P_i in red myofibers operating at pH 7 (dark gray) versus P_i in white fiber operating at pH 6 (light gray) of the BB muscle of an individual patient with 5qSMA performing the arm-cycling at 90 rpm until exhaustion (Supplementary Table 1 Case no. 10). Error bars represent Cramer-Rao bounds of AMARES fit of ^{31}P MR spectra and inform on goodness of fit. The time course of P_i in intermediate (IM) fibers operating at pH 6.6 is omitted for clarity of presentation (see Supplementary Fig. 4). (C-D) Median, interquartile range (IQR) and individual fractional peak area of P_i in red, IM and white myofibers (% of total peak area) in the *in vivo* ^{31}P MR spectrum recorded at exhaustion from BB (P = 0.004) and TB (P = 0.101) muscles of patients with 5qSMA and controls. ** = P < 0.01.

In vivo mitochondrial function in arm muscle in adolescent and adult 5qSMA

Restoration of the resting energetic state of myofibers following muscular work is principally driven by mitochondrial ATP synthesis.[44,48] Therefore, we continued recording *in vivo* ^{31}P MR spectra from BB and TB muscles after arm-cycling had stopped to test our hypothesis that this ATP synthesis in muscle is compromised in 5qSMA.[19,20] We found that full recovery of PCr and Pi levels to pre-exercise concentrations may take up to 10 minutes in patients with 5qSMA (Fig. 4A-B) and that the divergence in myoplasmic pH between red, intermediate and white fiber types developed during the preceding exercise, persisted during all this time (Supplementary Fig. 6). This uniquely afforded tracking and quantification of P_i recovery times for each myofiber phenotype (Fig. 4C) in addition to the standard approach of tracking total muscular PCr content (Fig. 4D).[16]

In the control group, mean 95% recovery time for P_i in red and intermediate fiber types was the same within each muscle (Fig. 4C) but significantly faster in BB muscle compared to TB (Fig. 4C; P = 0.013). Median P_i 95% recovery time for white myofibers in this group was five-fold slower (Fig. 4C) compared to red myofibers and similar in both muscles. This 1:1:5 ratio for P_i 95% recovery time in human red, intermediate and white myofiber phenotypes, respectively, mirrors the ratio of in vivo initial rates of post-exercise P_i recovery in these fiber types reported previously for leg muscle of healthy individuals.[42] This outcome fits well with findings of 5-fold lower measures of mitochondrial density and 6-fold fewer embedded capillaries for white compared to red myofibers,[49,50] respectively, in rodent muscles. Likewise, mean 95% recovery time for total PCr in BB and TB muscles (Fig. 4D) matched previous reports of PCr recovery times following strenuous exercise.[51,52]

In the patient group, median P_i 95% RTs for red and intermediate myofibers of BB and TB muscles were identical to controls (Fig. 4C). In contrast, median 95% recovery time for P_i in white myofibers of BB muscles was almost twofold longer than in controls (Fig. 4C);P = 0.031. P_i recovery in white myofibers of the TB muscle of patients was similarly prolonged in two of four available datasets from this group (Fig. 4C). These results indicate that mitochondrial ATP synthetic function is compromised in white, but not red or intermediate myofibers of arm muscle in the patient group. Our findings that post-exercise recovery of total muscular PCr in patients was either not prolonged (BB muscle; P = 0.764) or even faster (TB muscle; P = 0.025) compared to controls (Fig. 4D) both fit this conclusion and confirm white-to-red muscle remodeling in the patient group.

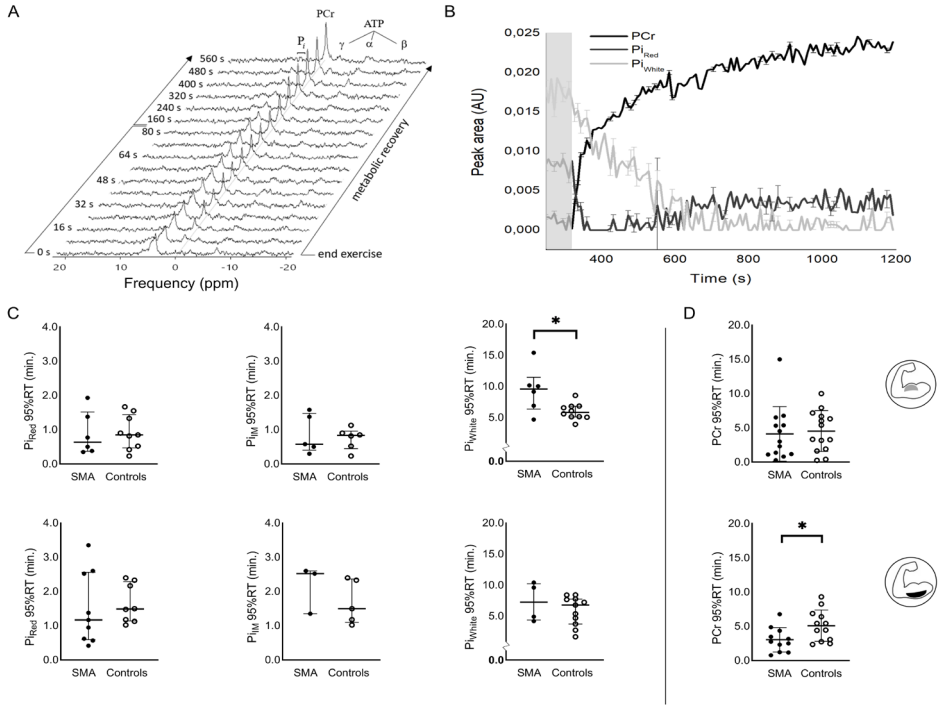

Figure 4. *In vivo* assay of mitochondrial ATP synthetic function in red, intermediate and white myofibers of upper arm muscles of patients with 5qSMA and controls on basis of dynamic *in vivo* ^{31}P MR spectroscopic recordings from BB and TB muscles of patients versus healthy controls post-exercise. (A) Stack plot of *in vivo* ^{31}P NMR spectra acquired serially from BB in a patient with 5qSMA starting at the point of exhaustion from preceding arm-cycling exercise and subsequent metabolic recovery. (B) Time course of PCr (black) and P_i in red myofibers operating at pH 7 (dark gray) versus P_i in white fiber operating at pH 6 (light gray) of the BB muscle of an individual patient with 5qSMA in final seconds of arm-cycling (shaded area) and subsequent rest (Supplementary Table 1 Case no. 10). Error bars represent Cramer-Rao bounds of AMARES fit of ^{31}P MR spectra and inform on goodness of Lorentzian model fit. The time course of P_i in intermediate (IM) fibers operating at pH 6.6 is omitted for clarity of presentation. (C) Median, IQR and individual P_i (red, IM and white) 95% recovery time (RT) (min.) in the BB and TB muscle; BB P_i white: p = 0.031. (D) Mean, standard deviation and individual PCr 95% RT (min.) in the BB (P = 0.764) and TB (P = 0.025) muscle. * = P < 0.05.

Relationship between muscle ultrastructure, phenotypic traits and function in 5qSMA

Our study has revealed associations between function (Fig. 1C), morphological (Fig. 2) and metabolic phenotypic traits (Fig. 3 and 4) of upper arm musculature in 5qSMA. Next, we investigated whether it was possible for each of these traits to predict residual function of these muscles in patients. First, we tested the hypothesis that muscles with a larger functional mass generate more power. Indeed, we found strong positive correlations between maximal voluntary contraction force and contractile cross-sectional area for both the BB and TB muscles in patients with 5qSMA and controls ($r = 0.89$, 95%CI: 0.77-0.95 and $rs(130)=0.96$, respectively, $P < 0.001$; Fig. 5A-B). Combining these functional and morphological datasets we compared force per contractile cross-sectional area between patients and controls. For both the BB and TB muscles this parameter was 1.4 fold reduced in the patient group ($p < 0.01$ for BB; Supplementary Fig. 7). Next, we hypothesized that the reduced power of the BB and TB muscles of patients was associated with a lower abundance of white and intermediate myofibers with functional innervation compared to controls (Fig. 4C-D). We then tested a first corollary that any increase in capillary blood lactate in response to arm-cycling would be blunted in patients compared to controls (Materials and Methods). A strong positive correlation was found between maximal voluntary contraction force and capillary blood lactate changes during the exercise trial in patients with 5qSMA for both BB and TB ($rs(90)=0.80$, $P < 0.001$, $rs(86)=0.76$, $P = 0.002$, respectively, Fig. 5C). We next investigated in the patient group the correlation of capillary blood lactate changes during arm-cycling with of ^{31}P MRS estimates of the fractional intermediate and white myofiber content of their BB and TB muscles. Significant positive correlations were found for both muscles ($rs(112)=0.61$, $P = 0.040$, $rs(54)=0.67$, $P = 0.039$, respectively, Fig. 5D). Lastly, we explored if there is any meaningful association between P_i 95% recovery time in white myofibers and the white-to-red myofiber shift in the patient group. For this limited cohort we lacked statistical power to support any predictive potential at this time but we found for the BB muscle that the majority of patients demonstrated above-average (>median score of the control group) on both parameters. (Fig. 5E). We also tested any predictive power of the more facile and commonly used parameter PCr 95% recovery time with respect to white-to-red myofiber shift in the BB muscle but no significant correlation was found (Supplementary Fig. 8).[16]

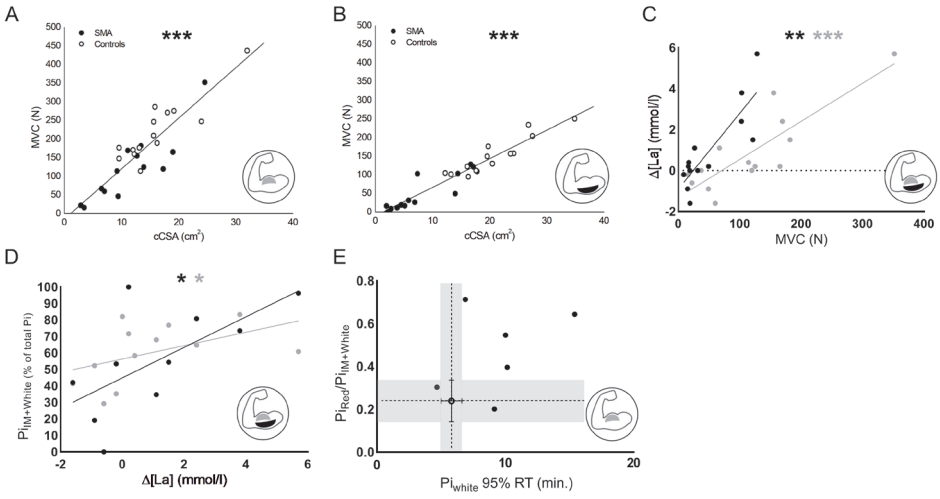

Figure 5. Relationship between muscle ultrastructure, phenotypic traits and function in 5qSMA. (A-B) Linear correlations between contractile cross-sectional area (cCSA) (cm2) and maximal voluntary contraction (MVC) force (N) of BB and TB; both P < 0.001. SMA (solid symbols); controls (open symbols). (C) Linear correlations between MVC force (N) and Δ capillary blood lactate ([La]) (mmol/l) of arm-cycling to exhaustion for BB (gray) and TB (black) muscles of patient with 5qSMA; P < 0.001 and P = 0.002, respectively. Dashed line indicates Δ[La] = 0. (D) Linear correlations between Δ [La] (mmol/l) of arm-cycling to exhaustion and fractional peak area of Pi in intermediate and white myofibers (% of total Pi peak area) in the *in vivo* ^{31}P MR spectrum recorded at exhaustion from BB (gray) and TB (black) muscles of patients with 5qSMA; P = 0.040 and P = 0.039, respectively. (E) Association of the 95% recovery time (RT) of P_i in white myofibers and ratio of fractional peak area of P_i in red versus intermediate (IM) + white myofibers in the *in vivo* ^{31}P MR spectrum recorded at exhaustion from BB muscle of patients with 5qSMA (solid symbols). Open symbol: median and IQR of these parameters for BB muscle of healthy controls. Gray area indicates IQR domains. * = P < 0.05, ** = P < 0.01, *** = P < 0.001.

Discussion

The notion that 5qSMA is a pure motor neuron disease has in recent years been overtaken by the observation that many cell types and tissues are affected by depletion of survival motor neuron protein.[18,53] Specifically, extensive evidence for intrinsic defects of muscle and the neuromuscular junction that are central to 5qSMA pathogenesis has been identified in recent years in both SMA mouse models as well as clinical investigations in patients.[6,10,11,14,17–20,22,54,55] Examples of intrinsic muscular abnormalities in 5qSMA include maladaptive phenotypic remodeling,[8,9] mitochondrial dysfunction and abnormal sarcomeric

calcium handling.[17,19,20] Investigative platforms to further detail these observations in muscle of patients with 5qSMA type 3 and 4 performing a physical task have, however, not yet been available. Here, we exploited quantitative MRI and dynamic *in vivo* ^{31}P MRS methods in combination with a voluntary exercise paradigm to examine muscle morphology and metabolic phenotypic traits in relation to muscle function in adolescent and adult 5qSMA type 3 and 4 *in situ*. Below, we discuss our findings and how they may impact understanding of the clinical presentation of 5qSMA and may guide design and delivery of emergent therapies for this disease.

Understanding muscle weakness in adolescent and adult 5qSMA

Muscle weakness is the main symptom in 5qSMA.[6,7] In our patient cohort, weakness of the proximal arm muscles that were studied here was likewise significant. However, median residual strength of the TB muscle of these individuals was only 15% of controls compared to 55% for the antagonist BB muscle (Fig. 1C). The observation of selective muscle sparing in SMA has previously been reported including in other patients with 5qSMA seen in our centre but remains poorly understood.[6,23–25,27,56,57] Our morphological MRI studies of the upper arm musculature in this cohort offer only a partly explanation of the almost fourfold difference in decline of strength between the TB and BB muscles in these individuals. Specifically, the residual mean contractile cross-sectional area of the TB muscle in patients was only 40% of controls whereas there was no significant evidence for atrophy of their BB muscle (Fig. 2C). Closer inspection of these data shows that in a subpopulation of patients atrophy of the TB muscle had progressed even further, to the point that signal degradation in our dynamic in vivo ^{31}P MRS recordings from this muscle in some of these individuals prohibited their analysis (Fig. 3D and 4D). Regardless, atrophy in and by itself cannot account for the almost 90% decline in strength of the TB muscle in our patients. This is evident when comparing the force per unit contractile cross-sectional area which was 1.4-fold lower in patients (Supplementary Fig. 7). Therefore, altered mechanical properties of the muscle itself must also contribute to this decline.

The comparison of *in vivo* ^{31}P MRS metabolic fingerprints of the BB and TB muscles at exhaustion between patients and controls support this conclusion (Fig. 3C and D). In patients, almost 50% of total P_i accumulated in contracting myofibers of the TB muscle at exhaustion originated from red myofibers on basis of a corresponding myocellular pH of 7, whereas in healthy controls this percentage was only 20% both TB and BB muscles (Fig. 3D). In the latter the percentage in patients was 40% (Fig. 3C). These results strongly suggest that both the BB and TB muscles in these patients underwent a white-to-red shift with respect to their fiber-type composition. Various labs have previously reported similar conclusions on basis of *in vitro* studies on 5qSMA muscle biopsies from different patients with various types of 5qSMA.[4,8,9,58–62] However, these studies typically examine ~20 µl volumes of muscle

causing potential bias. Our *in vivo* ^{31}P MR spectra were obtained from a ~30,000 µl volume of muscle thus mitigating any such concerns.[63] Given the fact that both speed and peak force of red myofiber contractions are substantially lower than for intermediate and white myofibers,[4] this now provides a mechanistic explanation for the 1.4-fold decline in strength per contractile cross-sectional area of both proximal arm muscles of the patients in this study.

Shifts in fiber-type composition have previously been described in patients with neuromuscular diseases including a red-to-white shift in a fat oxidation defect and are considered to reflect adaptation to the underlying defect.[40,64] Based on what has been learned about 5qSMA pathophysiology, it is more likely that a white-to-red shift in myofiber-type composition in this disease is rather the result of a higher vulnerability of fast motor neurons and their associated white musculature to survival motor neuron protein depletion.[23] In this light, we asked if the latter may be in any way mechanistically linked to the decreased oxidative capacity of white fibers first described in a mouse model of mild SMA by Deguise et al.[17] and captured here in patients (Fig. 4C). For this limited cohort we lacked statistical power to test any correlation but we found that the majority of patients scored above-average on both white-to-red shift and an index of mitochondrial oxidative impairment for the BB muscle (Fig. 5E). Future studies in larger patient cohorts will be needed to rigorously test such a correlation.

Understanding muscle fatigability in adolescent and adult 5qSMA

Abnormal muscular fatigability is also a prominent symptom in the clinical presentation of adolescent and adult patients with 5qSMA.[14] In the present study patients likewise presented with premature fatigue during execution of a physical task, lasting on average less than half the amount of time of their controls during arm-cycling. This was associated with both near maximal perceived fatigue scores as well as near maximal PCr depletion at the end of exercise, similar to controls. While survival motor neuron 2 copy number is generally accepted as the most important modifier for disease severity in 5qSMA,[65] we found no trend between cycling time and survival motor neuron 2 copy number (Supplementary Fig. 10). A previous study from our group in a cohort of 61 patients with 5qSMA type 2, 3 and 4 employing a different endurance task likewise found no such association.[14]

In healthy individuals, onset of fatigue during physical work typically reflects failing muscular ATP balance resulting in failing calcium cycling between the myoplasm and the sarcoplasmic reticulum.[15] Based on considerations of ATP-cost per twitch and mitochondrial density,[4] white and intermediate myofibers are at higher risk than red fibers to develop a mismatch between ATP demand and supply during muscular work. Our *in vivo* finding that post-exercise recovery of P_i in white but not intermediate or red fibers with functional innervation in proximal arm muscle of patients was 40% slower than in healthy controls (Fig.

4C) indicates that mitochondrial ATP synthetic function is compromised specifically in this particular fiber type in 5qSMA type 3 and 4. Houdebine et al.[22] came to the same conclusion in a recent study of an SMA mouse model on basis of biochemical analyses of hindlimb muscles. As a consequence, white fibers of skeletal muscle in this neuromuscular disease are more vulnerable to onset of cellular fatigue mechanisms during physical work.

While this particular outcome of our investigation furthers understanding of abnormal fatigability in 5qSMA, it cannot in and by itself quantitatively explain either our present finding of a 60% reduction in cycling time compared to healthy individuals or previous reports of abnormal fatigability in patients with 5qSMA performing low-intensity endurance tasks.[14,66] First and foremost, white myofibers typically make up only 15-20% of total myofiber content in healthy individuals including BB and TB.[4,45,47] In the present study, we found evidence in proximal arm muscle that this percentage may be even lower in 5qSMA (Fig. 3C). Secondly, post-exercise P_i 95% recovery time in red and intermediate fibers in BB and TB muscles of patients (Fig. 4C) indicated that in vivo mitochondrial ATP synthetic capacity in these fiber types is not affected by the disease. This finding also renders any role of muscular capillary defects previously reported in 5qSMA type 1 [18,67,68] unlikely in the clinical presentation of 5qSMA type 3 and 4.[69,70] Secondly, it could be argued that, per unit contractile cross-sectional area, the BB and TB muscles of the patients should have been more, not less resistant than their healthy controls to onset of fatigue mechanisms associated with insufficient ATP supply during arm-cycling. In fact, total contractile cross-sectional area of the BB muscle did not differ significantly between patients and controls (Fig. 2B). Together, these considerations point to other factors than common myocellular fatigue mechanisms associated with ATP supply-demand imbalance as primary cause of abnormal fatigability in adolescent and adult 5qSMA type 3 and 4.[15]

In light of the accumulated knowledge of 5qSMA pathophysiology,[71] progressive failure of excitation-contraction coupling during task execution at the neuromuscular junction itself is an obvious candidate. Indeed, Deguise et al.[17] reported evidence of such neurotransmission impairment in a pioneering mouse model of adult SMA. Using elegant experiments on *ex vivo* nerve- soleus muscle preparations, they found that the force of contractions elicited by nerve versus direct muscle stimulation was up to 25% lower in the former and exhibited a progressive decline not observed in direct muscle stimulation.[17] Notably, the soleus muscle in mice is primarily composed of intermediate (60%) and red (35%) fibers.[50] Their findings suggests that future research to further understanding of the mechanistic basis of abnormal fatigability in 5qSMA should perhaps focus on neuromuscular junction functionality.[55] A further clue pointing towards a primary role of the neuromuscular junction in this matter comes from a recent clinical trial in 5qSMA studying the efficacy of pyridostigmine to enhance neuromuscular signal transmission.[72] Oral administration of this drug reduced fatigability

on endurance shuttle tests with 70% but did not affect muscle strength in adolescent and adult patients with 5qSMA type 2-4.[73]

Impact on clinical management and therapy guidance in adolescent and adult 5qSMA

Molecular therapy aimed at rescuing survival motor neuron protein availability in patients with 5qSMA has become available in recent years.[18,74] Both *SMN1* gene replacement therapy (i.e. on DNA level) and *SMN2*-mRNA splicing modification therapies (i.e. on mRNA level) are now available and approved for use in humans.[75] The effect of one of such agents, nusinersen,[76] in children with severe disease (5qSMA type 1) has been promising.[77] However, therapy outcomes in adult patients with comparatively less severe phenotypes (5qSMA types 2 and 3) have been much more variable, with responder rates of 40-50% at best.[78–81] Here, it is important to note that nusinersen delivery in these trials has been done by injection into cerebrospinal fluid.[77] As such, its target was exclusively motor neuron populations. However, the notion has been emerging that 5qSMA is not strictly a motor neuron disease and that systemic delivery of these drugs should also be considered.[18] Our present findings do not in and by themselves further this debate, as it remains to be established whether they are the result of a primary muscle defect associated with ubiquitous survival motor neuron depletion or rather secondary to neuromuscular transmission impairment. The latter, however, seems more likely, since any primary muscle defect affecting mitochondrial ATP synthetic capacity may be expected to impact post-exercise P_i recovery across all myofiber types, including red and intermediate myofibers. Our results do suggest thatadditional use of pharmaceuticals that directly target the muscle and neuromuscular junction, such as pyridostigmine,[73,82] may also benefit these patients, specifically by rescuing excitation-contraction coupling to restore mechanical function and, in its wake, rebuild mitochondrial capacity. In this light, the finding of promising effects of high intensity training in a mild SMA mouse model suggests that such non-pharmaceutical therapy approaches should also be explored in care for adolescent and adult patients with 5qSMA type 3 and 4.[10,22] Specifically, Houdebine et al.[22] found that high intensity exercise training over a period of ten months not only reduced fatigability and protected the integrity of the neuromuscular junction, but it also reduced intermediate and white motor neuron death and enhanced CSA of large myofibrils.[10] Translating this approach to our present findings in our particular patient cohort, such exercise training could thus potentially improve muscle strength and halt, if not reverse, white-to-red muscle remodeling.[83] Moreover, if the reduced oxidative capacity of white myofibers that we identified in our patients is indeed a consequence of failing neuromuscular transmission aggravated by a state of detraining [84] associated with disuse, then combinatorial treatment of exercise training and pharmaceutical neuromuscular transmission enhancement may reverse also this pathophysiology.[85] The ^{31}P MRS methodology presented here offers various quantitative measures including time to PCr depletion during exercise and 95%

recovery time post-exercise that may be used to investigate and tailor the efficacy of such exercise therapy regimens in individual patients. Future studies focusing on development and validation of effective yet safe training programs for patients with 5qSMA are needed.[86]

This study also provides complementary *in vivo* biomarkers and a read-out platform to guide and monitor therapy in 5qSMA and other neuromuscular diseases including sarcopenia.[87] A recent review of the literature on this subject matter concluded that new techniques and biomarkers are needed to improve adult 5qSMA patient stratification, diagnosis and treatment.[81] Current methodologies available to this aim include examination of functional motor unit innervation (i.e. electrophysiological tests)[88–90], morphology (e.g. MRI)[24,27] and functional and physical performance tests (e.g. HFMSE, muscle strength and endurance shuttle tests)[13,91]. While each of these methods has its own particular strengths and weaknesses,[81] the *in vivo* ^{31}P MRS methodology presented here may provide added insights such as the nature of the residual functional motor units determined by electrophysiological tests. Moreover, while the latter type of examination is typically not well tolerated, the examination in the present study was very well received and tolerated by all subjects. Our work has identified the *in vivo* ^{31}P MRS phenotypic fingerprint of muscle at the point of exhaustion and post-exercise P_i recovery time in white myofibers as potential novel complementary biomarkers towards this aim. For example, the latter parameter may be particularly useful to investigate which therapy and delivery strategy may prove most effective to restore mitochondrial function in white fibers. With respect to the platform itself, musculoskeletal *in vivo* ^{31}P MRS is a widely used biomedical imaging modality supported by the major MRI vendors.[16] ^{31}P RF coils and MR compatible cycle-ergometers are likewise commercially available.[16] As such, the arm-cycling MR platform used in this study may be assembled without too much difficulty.

Conclusion

This study provides first *in vivo* evidence in patients that degeneration of motor neurons and associated musculature causing atrophy and muscle weakness in 5qSMA type 3 and 4 is aggravated by disproportionate depletion of myofibers that contract fastest and strongest. Our finding of decreased mitochondrial ATP synthetic function selectively in residual white myofibers provides both a possible clue to understanding the apparent vulnerability of this particular fiber type in 5qSMA type 3 and 4 as well as a new biomarker and target for therapy.

Abbreviations

BB	M. biceps brachii
PCr	Phosphocreatine
P_i	Inorganic phosphate
^{31}P MRS	^{31}Phosphorus magnetic resonance spectroscopy
5qSMA	5q spinal muscular atrophy
TB	M. triceps brachii

Declarations

Competing interests

WLP is a member of the scientific advisory board of SMA Europe and has served as an ad hoc member of the scientific advisory boards of Biogen and Avexis and as a member of a data monitoring committee for Novartis. The other authors report no conflicts of interest.

Funding

This work was supported by Prinses Beatrix Spierfonds (W.OR17-05), Stichting Spieren voor Spieren and Zwaluwen Jeugd Actie.

Acknowledgements

We thank all participants in this study for their willingness and commitment. We thank E.J.N. Groen for critical revision of the manuscript.

References

1. Chaytow H, Huang YT, Gillingwater TH, Faller KME. The role of survival motor neuron protein (SMN) in protein homeostasis. Cell Mol Life Sci. 2018;75(21):3877-3894.
2. Lefebvre S, Brglen L, Reboullet S, et al. Identification and characterization of a spinal muscular atrophy-determining gene. Cell. 1995;80(1):155-165.
3. Boyer JG, Bowerman M, Kothary R. The many faces of SMN: Deciphering the function critical to spinal muscular atrophy pathogenesis. Future Neurol. 2010;5(6):873-890.
4. Schiaffino S, Reggiani C. Fiber types in Mammalian skeletal muscles. Physiol Rev. 2011;91(4):1447-1531.
5. Glancy B, Balaban RS. Protein composition and function of red and white skeletal muscle mitochondria. Am J Physiol - Cell Physiol. 2011;300(6):1280-1290.
6. Wadman RI, Wijngaarde CA, Stam M, et al. Muscle strength and motor function throughout life in a cross-sectional cohort of 180 patients with SMA types 1c-4. Eur J Neurol. 2018;25(3):512-518.
7. Munsat TL, Davies KE. International SMA Consortium Meeting (26-28 June 1992, Bonn, Germany). Neuromuscul Disord. 1992;2(5-6):423-428.
8. Anderson JR. Atlas of skeletal muscle pathology. In: Gresham GA, ed. Atlas of Skeletal Muscle Pathology. 9th ed. MTP Press Limited; 1985:46-52.
9. Johnson MA, Kucukyalcin DK. Patterns of abnormal histochemical fibre type differentiation in human muscle biopsies. J Neurol Sci. 1978;37:159-178.
10. Chali F, Desseille C, Houdebine L, et al. Long-term exercise-specific neuroprotection in spinal muscular atrophy-like mice. J Physiol. 2016;594(7):1931-1952.
11. Stam M, Wadman RI, Bartels B, et al. A continuous repetitive task to detect fatigability in spinal muscular atrophy. Orphanet J Rare Dis. 2018;13(1):1-7.
12. Bartels B, Habets LE, Stam M, et al. Assessment of fatigability in patients with spinal muscular atrophy: Development and content validity of a set of endurance tests. BMC Neurol. 2019;19(1):1-10.
13. Bartels B, Groot JF De, Habets LE, et al. Fatigability in spinal muscular atrophy : validity and reliability of endurance shuttle tests. Orphanet J Rare Dis. 2020;2:1-9.
14. Bartels B, de Groot JF, Habets LE, et al. Correlates of fatigability in patients with spinal muscular atrophy. Neurology. 2021;96(6):845-852.
15. Cheng AJ, Place N, Westerblad H. Molecular Basis for Exercise-Induced Fatigue : The Importance of Strictly Controlled Cellular Ca2+ Handling. Cold Spring Harb Perspect Med. 2018;8((2)).
16. Meyerspeer M, Boesch C, Cameron D, et al. 31P magnetic resonance spectroscopy in skeletal muscle: Experts' consensus recommendations. NMR Biomed. 2020;(August 2019):1-22.
17. Deguise MO, De Repentigny Y, Tierney A, et al. Motor transmission defects with sex differences in a new mouse model of mild spinal muscular atrophy. EBioMedicine. 2020;55:102750.
18. Yeo CJJ, Darras BT. Overturning the Paradigm of Spinal Muscular Atrophy as just a Motor Neuron Disease. Pediatr Neurol. 2020;109:12-19.

19. Miller N, Shi H, Zelikovich A., Ma Y-C. Motor Neuron Mitochondrial Dysfunction in Spinal Muscular Atrophy. Hum Mol Genet. 2016;25(16):3395-3406.
20. Ripolone M, Ronchi D, Violano R, et al. Impaired Muscle Mitochondrial Biogenesis and Myogenesis in Spinal Muscular Atrophy. JAMA Neurol. 2015;72(6):1-10.
21. Shababi M, Lorson CL, Rudnik-Schöneborn SS. Spinal muscular atrophy: A motor neuron disorder or a multi-organ disease? J Anat. 2014;224(1):15-28.
22. Houdebine L, D'Amico D, Bastin J, et al. Low-Intensity Running and High-Intensity Swimming Exercises Differentially Improve Energy Metabolism in Mice With Mild Spinal Muscular Atrophy. Front Physiol. 2019;10(October):1-21.
23. Boyd PJ, Tu WY, Shorrock HK, et al. Bioenergetic status modulates motor neuron vulnerability and pathogenesis in a zebrafish model of spinal muscular atrophy. PLoS Genet. 2017;13(4):1-27.
24. Otto LAM, van der Pol WL, Schlaffke L, et al. Quantitative MRI of skeletal muscle in a cross-sectional cohort of patients with spinal muscular atrophy types 2 and 3. NMR Biomed. 2020;(March):1-13.
25. Chabanon A, Seferian AM, Daron A, et al. Prospective and longitudinal natural history study of patients with Type 2 and 3 spinal muscular atrophy: Baseline data NatHis-SMA study. PLoS One. 2018;13(7):1-28.
26. Bonati U, Holiga Š, Hellbach N, et al. Longitudinal characterization of biomarkers for spinal muscular atrophy. Ann Clin Transl Neurol. 2017;4(5):292-304.
27. Brogna C, Cristiano L, Verdolotti T, et al. MRI patterns of muscle involvement in type 2 and 3 spinal muscular atrophy patients. J Neurol. 2020;267(4):898-912.
28. Mizuno M, Justesen LO, Bedolla J, Friedman DB, Secher NH, Quistorff B. Partial curarization abolishes splitting of the inorganic phosphate peak in 31P-NMR spectroscopy during intense forearm exercise in man. Acta Physiol Scand. 1990;139(4):611-612.
29. Mizuno M, Horn A, Secher NH, Quistorff B. Exercise-induced 31P-NMR metabolic response of human wrist flexor muscles during partial neuromuscular blockade. Am J Physiol - Regul Integr Comp Physiol. 1994;267(2 36-2):408-414.
30. D'Amico A, Mercuri E, Tiziano FD BE. Spinal muscular atrophy. Orphanet J Rare Dis. 2011;6(71). doi:10.1186/1750-1172-6-71
31. Beenakker EAC, Van der Hoeven JH, Fock JM, Maurits NM. Reference values of maximum isometric muscle force obtained in 270 children aged 4-16 years by hand-held dynamometry. Neuromuscul Disord. 2001;11(5):441-446.
32. Juel C. Lactate/proton co-transport in skeletal muscle: Regulation and importance for pH homeostasis. Acta Physiol Scand. 1996;156(3):369-374.
33. Juel C. Lactate-proton cotransport in skeletal muscle. Physiol Rev. 1997;77(2):321-358.
34. Vegter RJ, Brink S van den, Mouton L, Sibeijn-Kuiper A, Woude L, Jeneson J. Magnetic Resonance-Compatible Arm-Crank Ergometry: A New Platform Linking Whole-Body Calorimetry to Upper-Extremity Biomechanics and Arm Muscle Metabolism. Front Neurol. 2021;12(February):1-13.
35. Jeneson JAL, Schmitz JPJ, Hilbers PAJ, Nicolay K. An MR-compatible bicycle ergometer for in-magnet whole-body human exercise testing. Magn Reson Med. 2010;63(1):257-261.

36. Henneman E, Clamann HP, Gillies JD, Skinner RD. Rank order of motoneurons within a pool: law of combination. J Neurophysiol. 1974;37(6):1338-1349.
37. Schlaffke L, Rehmann R, Rohm M, et al. Multi-center evaluation of stability and reproducibility of quantitative MRI measures in healthy calf muscles. NMR Biomed. 2019;32(9):1-14.
38. Yushkevich PA, Piven J, Hazlett HC, et al. User-guided 3D active contour segmentation of anatomical structures: Significantly improved efficiency and reliability. Neuroimage. 2006;31(3):1116-1128.
39. Rzanny R, Stutzig N, Hiepe P, Gussew A, Thorhauer HA, Reichenbach JR. The reproducibility of different metabolic markers for muscle fiber type distributions investigated by functional 31P-MRS during dynamic exercise. Z Med Phys. 2016;26(4):323-338.
40. Diekman EF, Visser G, Schmitz JPJ, et al. Altered energetics of exercise explain risk of rhabdomyolysis in very long-chain acyl-coa dehydrogenase deficiency. PLoS One. 2016;11(2):1-19.
41. Werkman M, Jeneson J, Helders P, et al. Exercise oxidative skeletal muscle metabolism in adolescents with cystic fibrosis. Exp Physiol. 2015;3:1-35.
42. Vandenborne K, McCully K, Kakihira H, et al. Metabolic heterogeneity in human calf muscle during maximal exercise. Proc Natl Acad Sci U S A. 1991;88(13):5714-5718.
43. Vegter RJK, Hartog J, De Groot S, et al. Early motor learning changes in upper-limb dynamics and shoulder complex loading during handrim wheelchair propulsion. J Neuroeng Rehabil. 2015;12(1):1-14.
44. Schmitz JPJ, van Riel NAW, Nicolay K, Hilbers PAJ, Jeneson JAL. Silencing of glycolysis in muscle: experimental observation and numerical analysis. Exp Physiol. 2010;95(2):380-397.
45. Johnson MA, Polgar J, Weightman D ADD. Data on the distribution of fibre types in thirty-six human muscles. J Neurol Sci. 1973;18(1):111-129.
46. E. Nygaard, M. Houston, Y. Suzuki KJ and BS. Morphology of the brachial biceps muscle and elbow flexion in man. Acta Physiol Scand. 1983;117:287-292.
47. Klitgaard H, Mantoni M, Schiaffino S, et al. Function, morphology and protein expression of ageing skeletal muscle: a cross-sectional study of elderly men with different training backgrounds. Acta Physiol Scand. 1990;140(1):41-45.
48. Meyer RA. A linear model of muscle respiration explains monoexponential phosphocreatine changes. Am J Physiol - Cell Physiol. 1988;254(4):C548–553.
49. Glancy B, Hsu LY, Dao L, et al. In Vivo microscopy reveals extensive embedding of capillaries within the sarcolemma of skeletal muscle fibers. Microcirculation. 2014;21(2):131-147.
50. Ciapaite J, van den Berg SA, Houten SM, Nicolay K, Willems van Dijk K, Jeneson JA. Fiber-type-specific sensitivities and phenotypic adaptations to dietary fat overload differentially impact fast- versus slow-twitch muscle contractile function in C57BL/6J mice. J Nutr Biochem. 2015;26(2):155-164.
51. Kemp G., Thompson CH, Barnes PRJ, Radda G. Comparisons of ATP turnover in human muscle during ischemic and aerobic exercise using 31P magnetic resonance spectroscopy. Magn Reson Med. 1994;31(3):248-258.
52. Bendahan D, Confort-Gouny S, Kozak-Reiss G, Cozzone PJ. Heterogeneity of metabolic response to muscular exercise in humans. New criteria of invariance defined by in vivo phosphorus-31 NMR spectroscopy. FEBS Lett. 1990;272(1-2):155-158.

53. Hamilton G, Gillingwater TH. Spinal muscular atrophy: Going beyond the motor neuron. Trends Mol Med. 2013;19(1):40-50.
54. Khayrullina G, Moritz KE, Schooley JF, et al. SMN-deficiency disrupts SERCA2 expression and intracellular Ca2+ signaling in cardiomyocytes from SMA mice and patient-derived iPSCs. Skelet Muscle. 2020;10(1):16.
55. Wadman RI, Vrancken AFJ, Van den Berg LH, Van der Pol WL. Dysfunction of the neuromuscular junction in patients with spinal muscular atrophy type 2 and 3. Neurology. 2012;79:2050-2055.
56. Piepers S, Van Den Berg LH, Brugman F, et al. A natural history study of late onset spinal muscular atrophy types 3b and 4. J Neurol. 2008;255(9):1400-1404.
57. Deymeer F, Serdaroglu P, Parman Y, Poda M. Natural history of SMA IIIb: muscle strength decreases in a predictable sequence and magnitude. Neurology. 2008;71(9):644 LP - 649.
58. Dubowitz V. Pathology of experimentally re-innervated skeletal muscle. J Neurol Neurosurg Psychiatry. 1967;30(2):99-110.
59. Dubowitz V. Enzyme histochemistry of skeletal muscle. 3. Neurogenic muscular atrophies. J Neurol Neurosurg Psychiatry. 1966;29(1):23-28.
60. Hausmanowa-Petrusewicz I, Askanas W, Badurska B, et al. Infantile and juvenile spinal muscular atrophy. J Neurol Sci. 1968;6(2):269-287.
61. Mastaglia FL, Walton JN. Histological and histochemical changes in skeletal muscle from cases of chronic juvenile and early adult spinal muscular atrophy (the Kugelberg-Welander syndrome). J Neurol Sci. 1971;12(1):15-44.
62. Scott W, Stevens J, Binder–Macleod SA. Human Skeletal Muscle Fiber Type Classifications. Phys Ther. 2001;81(11):1810-1816.
63. Jeneson JAL, van Dobbenburgh JO, van Echteld CJA, et al. Experimental design of 31P MRS assessment of human forearm muscle function: Restrictions imposed by functional anatomy. Magn Reson Med. 1993;30(5):634-640.
64. Imoto C, Nonaka I. The significance of type 1 fiber atrophy (hypotrophy) in childhood neuromuscular disorders. Brain Dev. 2001;23(5):298-302.
65. Wadman RI, Jansen MD, Stam M, et al. Intragenic and structural variation in the SMN locus and clinical variability in spinal muscular atrophy. Brain Commun. 2020;2(2):1-13.
66. Montes J, Dunaway S, Garber CE, Chiriboga CA, De Vivo DC, Rao AK. Leg muscle function and fatigue during walking in spinal muscular atrophy type 3. Muscle Nerve. 2014;50(1):34-39.
67. Zhou H, Ying H, Scoto M, Brogan P, Parson S, Muntoni F. Microvascular abnormality in spinal muscular atrophy and its response to antisense oligonucleotide therapy. Neuromuscul Disord. 2015;25(2015):S193.
68. Somers E, Lees RD, Hoban K, et al. Vascular Defects and Spinal Cord Hypoxia in Spinal Muscular Atrophy. Ann Neurol. 2016;79(2):217-230.
69. Van Brussel M, van Oorschot JWM, Schmitz JPJ, et al. Muscle Metabolic Responses During Dynamic In-Magnet Exercise Testing: A Pilot Study in Children with an Idiopathic Inflammatory Myopathy. Acad Radiol. 2015;22(11):1443-1448.
70. Cea G, Bendahan D, Manners D, et al. Reduced oxidative phosphorylation and proton efflux suggest reduced capillary blood supply in skeletal muscle of patients with dermatomyositis and polymyositis : a quantitative 31 P-magnetic resonance spectroscopy and MRI study. Published online 2002.

71. Faravelli I, Nizzardo M, Comi GP, Corti S. Spinal muscular atrophy—recent therapeutic advances for an old challenge. Nat Rev Neurol. 2015;11(6):351-359.
72. Stam M, Wadman RI, Wijngaarde CA, et al. Protocol for a phase II, monocentre, double-blind, placebo-controlled, cross-over trial to assess efficacy of pyridostigmine in patients with spinal muscular atrophy types 2-4 (SPACE trial). BMJ Open. 2018;8(7):1-9.
73. Stam M, Wijngaarde C, Bartels B, et al. Space trial. A phase 2, monocenter, double-blind, placebo-controlled, cross-over trial to assess efficacy of pyridostigmine in patients with spinal muscular atrophy types 2,3 and 4. In: Cure SMA June 30 2019; 2019.
74. Bowerman M, Becker CG, Yáñez-Muñoz RJ, et al. Therapeutic strategies for spinal muscular atrophy: SMN and beyond. DMM Dis Model Mech. 2017;10(8):943-954.
75. Wirth B, Karakaya M, Kye MJ, Mendoza-Ferreira N. Twenty-Five Years of Spinal Muscular Atrophy Research: From Phenotype to Genotype to Therapy, and What Comes Next. Annu Rev Genomics Hum Genet. 2020;21:231-261.
76. Passini M a, Bu J, Richards AM, et al. Antisense Oligonucleotides Delivered to the Mouse CNS Ameliorate Symptoms of Severe Spinal Muscular Atrophy. Sci Transl Med. 2011;3(72).
77. Finkel RS, Mercuri E, Darras BT, et al. Nusinersen versus sham control in infantile-onset spinal muscular atrophy. N Engl J Med. 2017;377(18):1723-1732.
78. Walter MC, Wenninger S, Thiele S, et al. Safety and treatment effects of nusinersen in longstanding adult 5q-SMA type 3 – A prospective observational study. J Neuromuscul Dis. 2019;6(4):453-465.
79. Hagenacker T, Wurster CD, Günther R, et al. Nusinersen in adults with 5q spinal muscular atrophy: a non-interventional, multicentre, observational cohort study. Lancet Neurol. 2020;19(4):317-325.
80. Jochmann E, Steinbach R, Jochmann T, et al. Experiences from treating seven adult 5q spinal muscular atrophy patients with Nusinersen. Ther Adv Neurol Disord. 2020;13:1-11.
81. Smeriglio P, Langard P, Querin G, Biferi MG. The identification of novel biomarkers is required to improve adult SMA patient stratification, diagnosis and treatment. J Pers Med. 2020;10(3):1-23.
82. Riker WF, Wescoe WC. The direct action of prostigmine on skeletal muscle; its relationship to the choline esters. J Pharmacol Exp Ther. Published online 1946:58-66.
83. Fitts RH. Cellular mechanisms of skeletal muscle fatigue. Pysiological Rev. 1994;74(1):49-81.
84. Wibom R, Hultman E, Johansson M, Matherei K, Constantin-Teodosiu D, Schantz PG. Adaptation of mitochondrial ATP production in human skeletal muscle to endurance training and detraining. J Appl Physiol. 1992;73(5):2004-2010.
85. Westerblad H, Bruton JD, Katz A. Skeletal muscle: Energy metabolism, fiber types, fatigue and adaptability. Exp Cell Res. 2010;316(18):3093-3099.
86. Bartels B, Montes J, Van Der Pol WL, De Groot JF. Physical exercise training for type 3 spinal muscular atrophy. Cochrane Database Syst Rev. 2019;2019(3).
87. Larsson L, Degens H, Li M, et al. Sarcopenia: Aging-related loss of muscle mass and function. Physiol Rev. 2019;99(1):427-511.
88. Sleutjes BTHM, Wijngaarde CA, Wadman RI, et al. Assessment of motor unit loss in patients with spinal muscular atrophy. Clin Neurophysiol. 2020;131(6):1280-1286.

89. Querin G, Lenglet T, Debs R, et al. The motor unit number index (MUNIX) profile of patients with adult spinal muscular atrophy. Clin Neurophysiol. 2018;129(11):2333-2340.
90. Verma S, Forte J, Ritchey M, Shah D. Motor unit number index in children with later-onset spinal muscular atrophy. Muscle and Nerve. 2020;(March):633-637.
91. Glanzman AM, O'Hagen J, McDermott M, et al. Validation of the Expanded Hammersmith Functional Motor Scale in Spinal Muscular Atrophy Type II and III. J Child Neurol. 2011;26(12):1499-1507.

Supplementary material

Supplementary Table 1. Individual patient results

Baseline characteristics						Upper arm muscle morphology			
						BB		TB	
Case no.	Sex	Age (y)	SMA type	SMN copy no.	HFMSE	Fat (%)	cCSA (cm^3)	Fat (%)	cCSA (cm^3)
1.	M	63	3b	4	11	57.6	9.40	77.9	3.83
2.	F	58	3b	4	34	10.3	13.90	72.0	1.96
3.	M	26	3b	4	62	7.1	24.60	7.4	16.68
4.	F	57	3a	3	34	23.5	9.20	46.3	5.14
5.	F	55	3b	4	43	7.6	19.00	19.9	13.97
6.	M	35	3a	4	29	23.7	7.00	34.3	4.51
7.	F	57	4	4	65	10.4	12.70	10.4	14.44
8.	M	54	3b	4	42	14.8	17.30	36.9	5.82
9.	F	12	3a	3	27	40.2	2.90	51.7	2.17
10.	F	19	3b	4	62	14.9	11.10	52.4	7.36
11.	F	35	3a	3	8	a	a	a	a
12.	F	18	3a	4	38	a	a	a	a
13.	F	47	3b	4	58	9.4	13.40	8.2	17.14
14.	M	36	3b	4	58	13.7	6.50	18.4	6.88
15.	F	26	3a	4	29	46.7	3.50	35.3	2.75

BB = m. biceps brachii; TB = m. triceps brachii; SMA = spinal muscular atrophy; SMN = survival motor area; IM = intermediate myofibers; RT = recovery time; a = contra-indication MRI scan; b = no dyna-

Metabolic phenotypic profile and mitochondrial function					
BB			**TB**		
Metabolic fingerprint (%) $P_{i\ red/IM/white}$	**95% RT (min.) $P_{i\ red/IM/white}$**	**95% RT (min.) PCr**	**Metabolic fingerprint (%) $P_{i\ red/IM/white}$**	**95% RT (min.) $P_{i\ red/IM/white}$**	**95% RT (min.) PCr**
b	b	b	b	b	b
28.4/10.2/61.4	1.93-1.13/ n.a./10.15-0.95	6.78-0.90	0/8.8/91.2	0.62-0.38/ n.a./4.9-2.6	2.31-2.95
39.2/48/12.8	n.a./.a./ 15.40-2.70	15.0-1.9	3.8/30.6/65.6	0.95-0.83/ n.a./10.4-5.3	2.75-0.15
41.6/58.4/0	0.35-1.42/ n.a./6.88-5.10	6.51-2.03	n.a.	n.a./n.a./n.a.	n.a.
100/0/0	0.38-0.15/-/-	0.80-0.25	80.2/19.8/0	2.60-3.02/2.60-3.02/-	2.50-1.35
58.7/15.5/25.8	n.a./n.a./n.a.	0.26-0.03	58/42/0	0.57-0.47/ n.a./-	1.18-0.03
16.7/46.2/37.1	n.a./0.58-0.23/9.15-0.56	4.53-0.23	26.6/41/32.4	n.a./1.35-0.97/4.2-1.8	3.48-0.33
18/0/82	n.a./-/n.a.	2.30-0.51	n.a.	n.a./n.a./n.a.	n.a.
70.7/29.3/0	0.50-0.98/0.50-0.98/-	1.10-0.11	100/0/0	1.38-0.68/-/-	6.76-0.61
35.3/0/64.7	0.77-0.22/-/10.02-0.95	5.36-0.70	19.2/0/80.8	3.35-0.58/-/9.6-1.5	4.86-0.35
n.a.	n.a./n.a./n.a.	n.a.	n.a.	n.a/n.a./n.a..	n.a.
48.7/52.3/0	1.38-2.83/1.38-2.83/-	5.33-0.43	80.9/0/19.1	0.42-0.28/-/n.a.	1.21-0.11
23.2/45.4/31.4	n.a./0.30-0.08/4.67-0.48	3.00-0.36	45.6/54.4/0	2.52-0.97/2.52-0.97/-	4.35-0.05
32/42.6/25.4	n.a./1.58-0.62/ n.a.	1.38-0.48	65.3/25.5/9.2	1.17-0.33/n.a./ n.a.	3.16-0.80
64.8/0/35.2	n.a./-/n.a.	1.16-0.66	46.6/24.8/28.6	n.a./n.a./n.a.	0.77-0.43

neuron; HFMSE = Hammersmith Functional Motor Scale Expanded; cCSA = contractile cross-sectional

mic exercise data due to technical considerations; n.a. = not available due to low signal to noise.

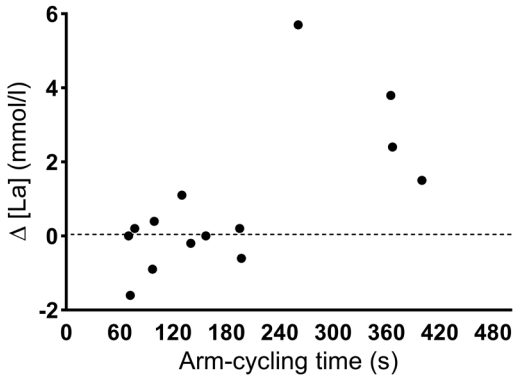

Supplementary Figure 1. Association of Δ capillary blood lactate ([La]; mmol/l) of arm-cycling to exhaustion and total arm-cycling time to exhaustion (s) for the m. biceps brachii of 5qSMA patients. Dashed line indicates Δ [La] = 0.

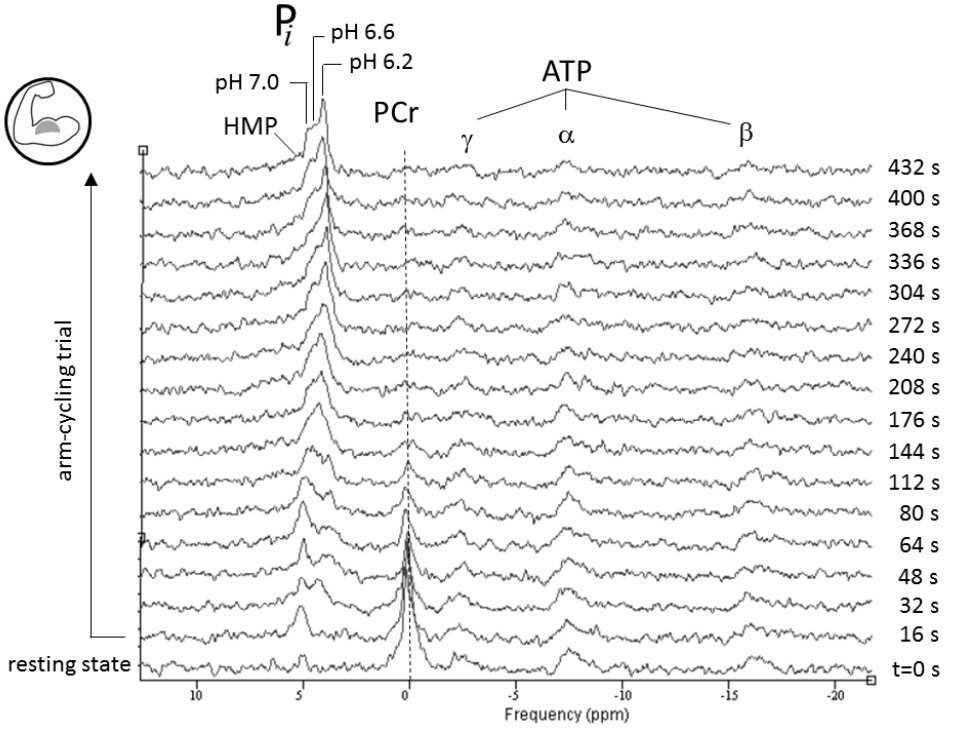

Supplementary Figure 2. Stack plot of *in vivo* ^{31}P NMR spectra acquired serially from m. biceps brachii in a healthy control subject at rest (t=0) and during subsequent arm-cycling at 90 rpm until exhaustion (t=432). Peak assignments: hexose-monophosphate (HMP), inorganic phosphate (P_i), phosphocreatine (PCr), and α-, β-, γ- Adenosine triphosphate (ATP). Dashed line indicates the reference resonance frequency of PCr (set at 0 ppm).

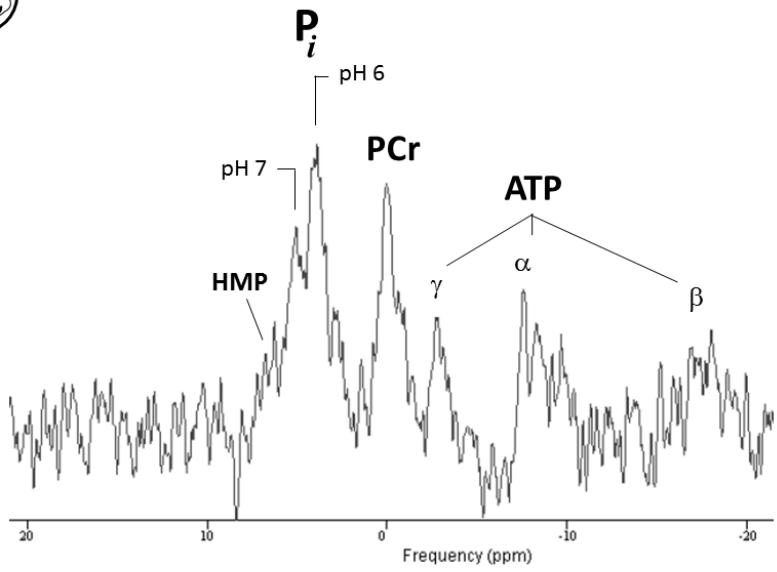

Supplementary Figure 3. *In vivo* ^{31}P MR spectrum acquired from m. triceps brachii of a healthy control subject, 60 seconds after onset of supine arm-cycling exercise at 90 rpm. Peak assignments: hexosemono-phosphates (HMP), inorganic phosphate (P_i), phosphocreatine (PCr), and α-, β-, γ-Adenosine triphosphate (ATP).

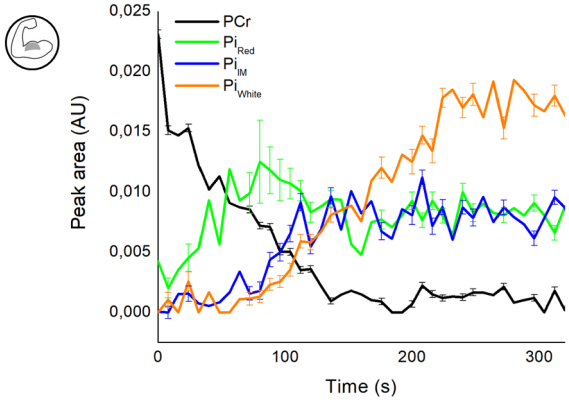

Supplementary Figure 4. Time course of PCr (black), P_i in red myofibers operating at pH 7 (green), P_i in intermediate (IM) myofibers operating at pH 6.6 (blue) and P_i in white fiber operating at pH 6 (orange) of the m. biceps brachii of an individual patient with 5qSMA performing the arm-cycling at 90 rpm until exhaustion (Table S1 Case no. 10). Error bars represent Cramer-Rao bounds of AMARES fit of ^{31}P MR spectra and inform on goodness of fit.

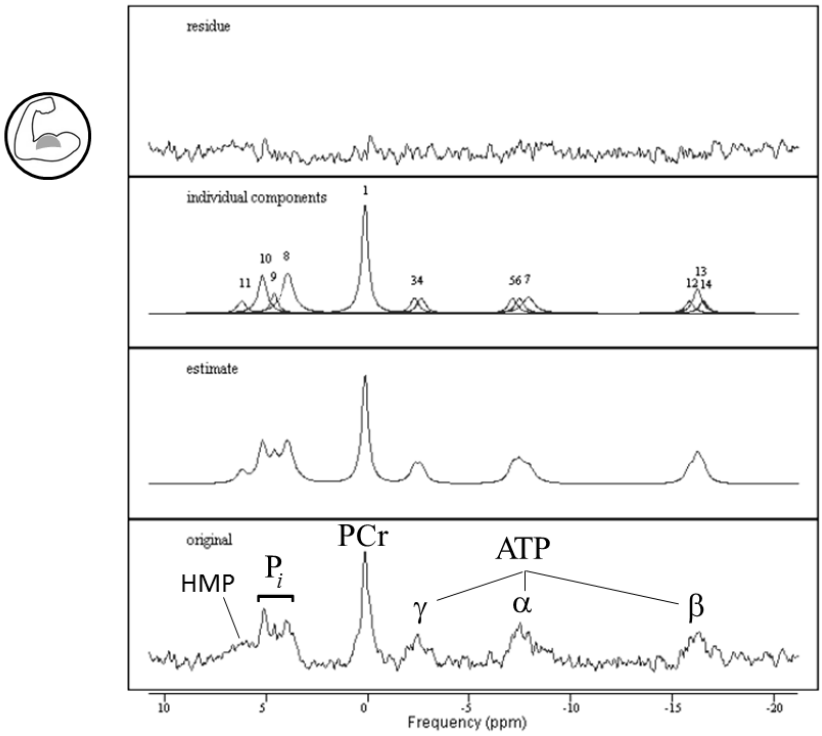

Supplementary Figure 5. Typical example of output of spectral fitting of an individual *in vivo* ^{31}P NMR spectrum from the time series dataset acquired from m. biceps brachii of a healthy control subject during arm-cycling exercise at 90 rpm using the JMRUI software platform (www.jmrui.eu). Here, we used the AMARES time domain fitting algorithm in combination with custom-built starting values (.sv) and prior know-ledge (.pk) files. Model lineshape: Lorentzian. Lower trace: input dataset = *in vivo* ^{31}P NMR spectrum. Peak assignments: hexosemonophosphates (HMP), inorganic phosphate (P_i), phosphocreatine (PCr), and α-, β-, γ- Adenosine triphosphate (ATP). The two middle traces show the converged best fit to the original data (composite and individual peak components, respectively) within the set of hard- and soft constraints provided in the .pk file. The upper trace shows the residuals of subtraction of the original spectrum and the fitted estimate. Visual inspection shows absence of any residual correlated signal with significant amplitude. On this basis, the fitted estimate was deemed 'acceptable'. The quantitative information on resonance frequency and peak area of each component of the fit was then used for estimation of P-metabolite concentrations and pH domains as described elsewhere (Materials and Methods).

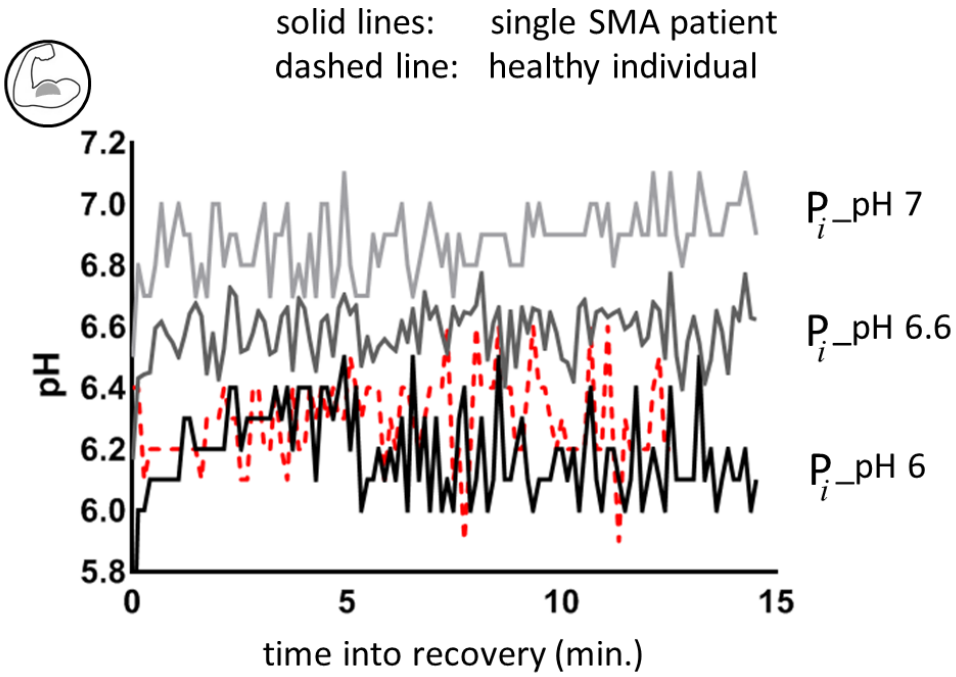

Supplementary Figure 6. Time course of myoplasmic pH in red (light gray), intermediate (dark gray) and white (black) myofibers of m. biceps brachii of a patient with 5qSMA after arm-cycling was halted due to exhaustion. For comparison the time course is shown of myoplasmic pH in white myofibers of m. biceps brachii of a healthy control (dashed red line). Myoplasmic pH in each fiber type was determined from the chemical shift of the corresponding inorganic phosphate (P_i) peak relative to the reference frequency of phosphorcreatine (PCr) (set at 0 ppm) as described in Materials and Methods.

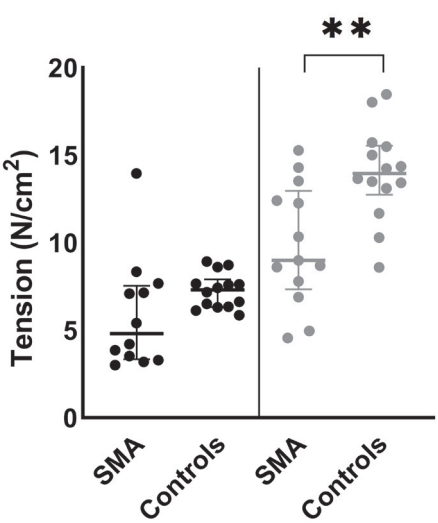

Supplementary Figure 7. Median and interquartile range of force per contractile cross-sectional area (cCSA) (tension; N/cm^2) of the m. triceps brachii (TB) (black) and m. biceps brachii (BB) (gray) muscles in patients with 5qSMA versus healthy controls; ** = P < 0.01. This parameter was calculated for each individual using maximal voluntary contraction force (N) and cCSA (cm^2) measured using a handheld dynamometer and quantitative MRI as described in Materials and Methods. Median values for the BB muscle in patients were 9.9 N/cm^2 versus 14.0 N/cm^2 in controls. For the TB muscle these values were 4.8 N/cm^2 versus 7.3 N/cm^2 in controls, respectively.

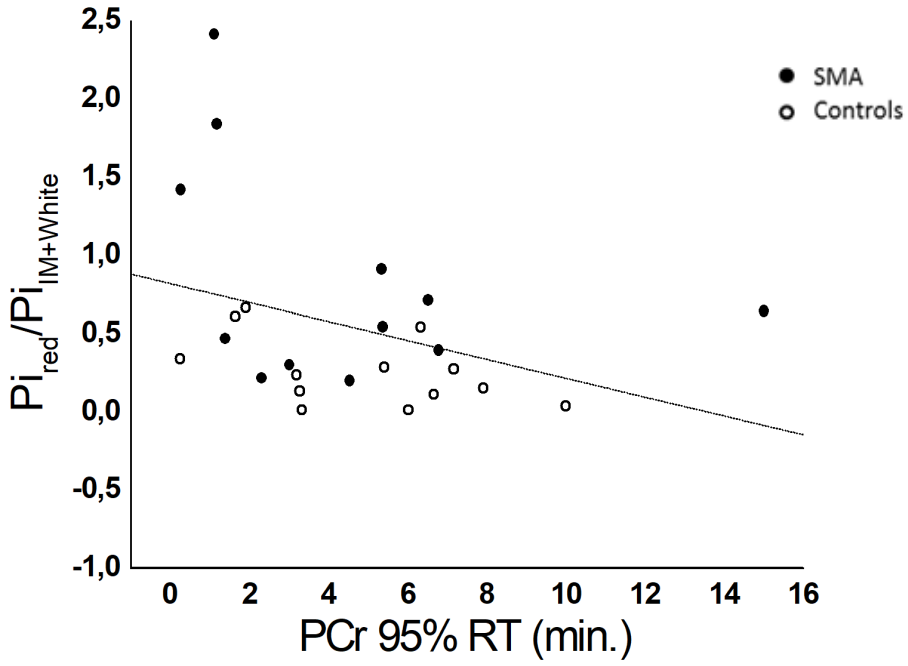

Supplementary Figure 8. Plot of 95% recovery time (RT) (min.) of phosphorcreatine (PCr) and ratio of fractional peak area of inorganic phosphate (P_i) in red versus intermediate (IM) + white myofibers in the *in vivo* ^{31}P MR spectrum recorded at exhaustion in m. biceps brachii for 5qSMA patients (solid symbols) and healthy controls (open symbols). Solid line: fit of a linear function to the pooled data of patients and controls. No significant correlation was found; P > 0.1.

Supplementary Figure 9. Picture showing the adjustable glove (Leki, Italy) of the handle of one of the carbon poles (Leki, Italy) of the arm-cycling ergometer fitted on to the hand of a healthy subject. This configuration minimizes any involvement of hand and forearm muscles in push and pulling action of the arm during execution of the arm-cycling task.

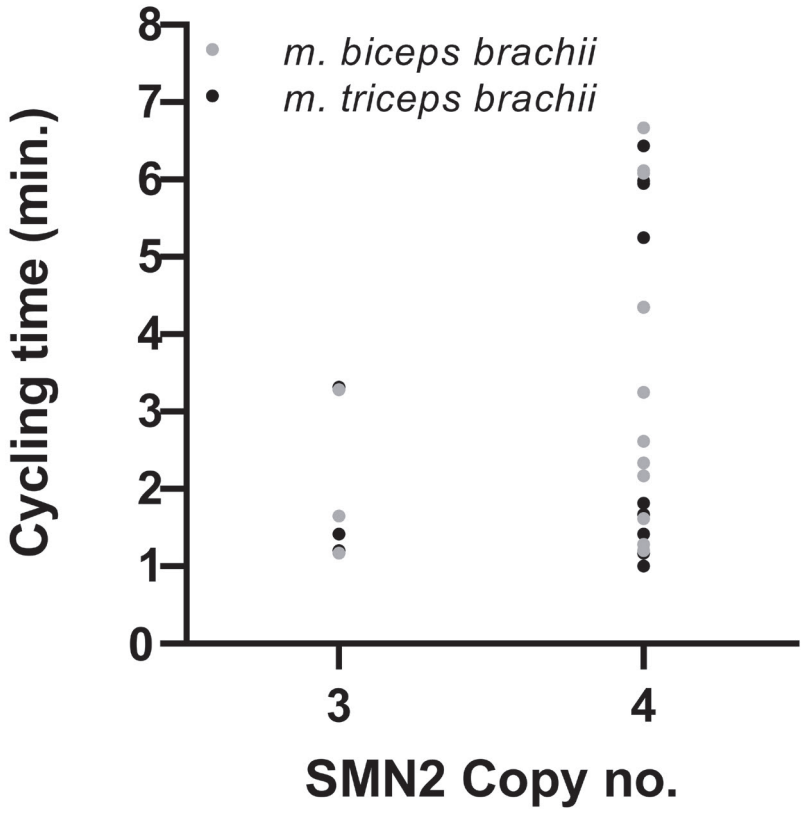

Supplementary Figure 10. Association of arm-cycling time to exhaustion (min.) during measurement of the m. biceps brachii (gray dots) and m. triceps brachii (black dots) and *SMN2* copy number (n) of patients with 5qSMA.

Chapter 7

Motor unit- and capillary recruitment during fatiguing arm-cycling exercise in spinal muscular atrophy types 3 and 4

L.E. Habets
B. Bartels
F. Asselman
H.J. Hulzebos
D.F. Stegeman
J.A.L. Jeneson
W.L. van der Pol

Submitted

Abstract

Background

Exercise intolerance is an important impairment in patients with SMA, but little is known about the mechanisms underlying this symptom.

Objective

To investigate if reduced motor unit- and capillary recruitment capacity in patients with SMA contribute to exercise intolerance.

Methods

Adolescent and adult patients with SMA types 3 and 4 (n=15) and age- and gender matched controls (n=15) performed a maximal upper body exercise test. We applied respiratory gas analyses, non-invasive surface electromyography (sEMG) and continuous wave near-infrared spectroscopy (CW-NIRS) to study oxygen consumption, arm muscle motor unit- and capillary recruitment, respectively.

Results

Maximal exercise duration was twofold lower ($p < 0.001$) and work of breathing and ventilation was 1.6- and 1.8-fold higher ($p < 0.05$) in patients compared to controls, respectively. Regarding motor unit recruitment, we found higher normalized RMS amplitude onset values of sEMG signals from all muscles and the increase in normalized RMS amplitudes was similar in the m. triceps brachii, m. brachioradialis and m. flexor digitorum in SMA compared to controls. Median frequency, onset values were similar in patients and controls. We found a similar decrease in median frequencies of sEMG recordings from the m. biceps brachii, a diminished decrease from the m. brachioradialis and m. flexor digitorum, but a larger decrease from the m. triceps brachii. With respect to capillary recruitment, CW-NIRS recordings in m. biceps brachii revealed dynamics that were both qualitatively and quantitatively similar in patients and controls.

Conclusions

We found no evidence for the contribution of motor unit- and capillary recruitment capacity of the upper arm muscles in adolescent and adult patients with SMA types 3 and 4 as primary limiting factors to premature fatigue during execution of a maximal arm-cycling task.

Introduction

Hereditary proximal spinal muscular atrophy (SMA) is a progressive neuromuscular disease caused by the homozygous loss of function of the survival motor neuron 1 (*SMN1*) gene.[1] This results in α-motor neuron degeneration and neuromuscular junction abnormalities, but also affects other tissues including skeletal muscle.[2–4] SMA is characterized by progressive muscle atrophy and fatty replacement of muscle tissue and life-long deteriorating muscle strength.[5–7] Reduced endurance during repetitive motor task is an additional and disabling dimension of physical impairment in SMA.[4,8–11]

Evidence has been mounting that neurogenic abnormalities are not the sole cause of muscle dysfunction and exercise intolerance in SMA.[3] Amongst other factors, mitochondrial abnormalities have been found in muscle in SMA mouse models and patient biopsy material.[3,12–16] We recently reported the first in vivo evidence for mitochondrial dysfunction in muscle in a cohort of adolescent and adult patients with SMA.[17] However, we found oxidative mitochondrial dysfunction in residual white, but not red or intermediate, myofibers of the upper arm muscles similar to previous findings in a mild SMA mouse model. This finding was associated with a white-to-red shift in myofiber type composition and, as a consequence, a reduced specific force of the arm muscles.[17]

Other peripheral factors that have been implicated in exercise intolerance in SMA include truncated motor unit recruitment capacity and vascular abnormalities, respectively. Specifically, decreased muscle capillary density has been documented in mouse SMA models and patients.[18–21] Lack of residual motor unit recruitment capacity during execution of a submaximal motor task has been reported to limit performance during a six minute walk test[22] and was identified in some, but not all, patients with SMA during submaximal endurance tests.[23]

Here, we further investigate these matters in a cohort of adolescent and adult patients with SMA types 3 and 4. We collected surface electromyographical (sEMG)[22–26] and continuous wave near-infrared spectroscopic (CW-NIRS) data[27–29] from arm muscles together with respiratory gas analyses during a maximal arm-cycling task to study motor unit and capillary recruitment dynamics in relation to exercise performance and bodily oxygen consumption.

Materials and Methods

Participants

Subjects participated in a cross-sectional study of two visits, aiming to examine muscle morphology and oxidative mitochondrial function in SMA.[17] We obtained data described here during the first visit at the Spieren voor Spieren Inspanningslab of the University Medical Center Utrecht, The Netherlands. The local Medical Ethics Committee approved our study (NL62792.041.17). We obtained informed consent from all participants (and their parents in case of minors). We included treatment-naïve patients, ambulant and non-ambulant, with an initial genetically confirmed diagnosis of SMA types 3a, 3b and 4 registered in the Dutch SMA database.[30] We recruited age and gender matched control participants via the patient's social network of family and friends. All participants met the following inclusion criteria: 1) age ≥ 12, 2) ability to perform active supine arm cycling movements, 3) ability to follow test instructions, 4) m. biceps brachii Medical Research Council (MRC) score for muscle strength ≥ 4 and m. triceps brachii MRC score ≥ 2. Exclusion criteria were: 1) contraindications concerning MR assessment, 2) risk factors for exercise testing registered by a Dutch version of the Preparticipation Questionnaire (American College of Sports Medicine and American heart Association), 3) mental retardation, 4) comorbidities affecting exercise tolerance, 5) being under examination for non-diagnosed disease at the time of investigation.

Study design

We collected baseline characteristics (e.g. anthropometry (lean body mass using a bodystat scan (Quadscan 4000® Euromedix, Leuven, Belgium)). We assessed motor function (Hammersmith Functional Motor Scale Expanded), Medical Research Council (MRC) scores for muscle strength and patients performed a supine arm-cycling test to exhaustion.

Supine arm cycling test

A custom-built mechanically braked bicycle ergometer for arm-cycling described elsewhere[17,31] was used in the study. Participants were positioned supine on a bed with an angle of 90º elbow flexion and vertical cranks (Figure 1). After five minutes of rest for baseline recordings, participants were asked to start cycling until exhaustion at a desired pace of 90 rpm indicated by audio cues. Between minutes 0 and 6, the workload was 5 W. At min 6, a mechanical brake was applied raising the workload to 10 W. From min 7 on, the workload was increased every min by adding weight (0.2 kg for women and 0.3 kg for men) (Figure 2). Exercise duration in each subject was documented.

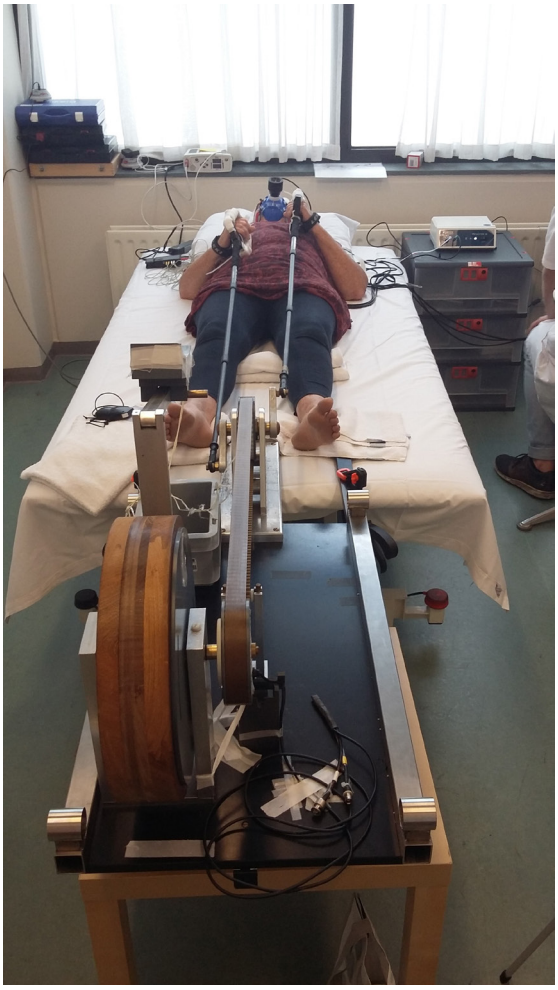

Figure 1. Overview of the experimental set up of the incremental arm-cycling test to exhaustion. The participant is wearing sEMG equipment on the right arm, CW-NIRS equipment on the left arm and a respiratory gas exchange mask. The participant depicted in the photo granted permission for publication.

Respiratory gas exchange data collection and processing

We measured breath-by-breath gas exchange (CORTEX Biophysik GmbH, Leipzig, Germany) and heart rate (HR) (Polar, Kempele, Finland) during rest, exercise and recovery. Participants with an exercise duration lower than three minutes were excluded from the analyses. Recorded data was time-aligned and interpolated second-by-second in Metasoft® and averaged over 10 second periods. Mean rest (HR and RER) and end recovery values (HR, VO_2, VCO_2, VE , RER) were calculated over the last three minutes of period, respectively. We calculated peak values (HR, VO_2 peak, VCO_2 peak, VE peak, RER peak) over the last 30 seconds of exercise. Mean values of VO_2, VCO_2, VE and RER over the last 30 seconds of every minute during constant load cycling were calculated for participants with an exercise duration between six and nine minutes. We corrected VE, VO_2 and VCO_2 for lean body mass.

sEMG data collection and processing

We continuously measured muscle activation of four muscles with bipolar sEMG, using the four-channel wireless Bio Radio system (Great Lakes Neurotechnologies, Cleveland, Ohio, USA). If necessary, we removed hair and we cleaned the skin with alcohol (70% denatured ethanol incl. 5% isopropanol). We placed standard self-adhesive Ag/AgCl Discs (3M™Red Dot™, 9 mm electrode, 18 mm gel, 50 mm disc) with 34 mm center-to-center inter-electrode distance on the right side of the body: m. biceps brachii (1/3 on the line from fossa cubit to medial acromion), m. triceps brachii (1/2 on the line between posterior crista of the acromion and olecranon at 2 fingers width medial to the line), m. brachioradialis (4 cm distally from lateral epicondyle of the elbow on the medial fleshy mass) and m. flexor digitorum (1/4 between wrist and elbow on the area where the greatest movement is felt while the subject flexes his/her fingers). Reference electrodes were placed on the manubrium. We taped all wires to the skin to prevent cable movement artifacts.

We recorded muscle electrical activation (sampling rate of 1000 Hz, sampling resolution of 6 μV per least significant bit, 250 Hz anti-aliasing filter) using Biocapture software. We used custom programs written in MATLAB R2016b to process raw sEMG data (detrend, 20 Hz high pass bi-directional 4th order butterworth filter, 50 Hz notch filter). Outcome variables were median frequencies (Fast Fourier Transformation) and root mean square (RMS) amplitudes, calculated over 10 sec windows. RMS amplitudes were normalized to maximal voluntary contractions (MVC); measured before arm-cycling using a handheld dynamometer (MicroFET2, Hoggan Health Industries, Salt Lake City, UT, USA) following standardized procedures.[32]

NIRS data collection and processing

We continuously measured capillary recruitment by [766+859] nm and [766-859] nm signals using a two-channel single distance wave photometer (OXYMON, Artinis, Zetten, The Netherlands) during rest and arm-cycling. We placed light emitting fibers with an interoptode distance between 30 – 50 mm,[29,33] depending on skinfold and adipose tissue thickness measured with a Harpender Skinfold Caliper (93/42/EEC), on the left m. biceps brachii and m. triceps brachii according to described procedures. We taped the optodes on the skin to prevent movement and used a black cloth to reduce stray light intrusion and loss of transmitted light from the field of examination.

We recorded NIRS signals (sampling rate of 50 Hz) using Oxysoft software (diffusion path length factor (DPF) = 4)[34]. We used a Gaussian filter and custom programs written in MATLAB R2016b for data down sampling to 2Hz. Datasets were excluded based on high percentages of fatty infiltration in the m. triceps brachii and the absence of an appropriate reference DPF. Datasets with a high signal to noise ratio, drift, high adipose tissue thickness or an instable resting period were excluded from analyses. Signals were normalized to

the highest value of the [766+859] nm signal measured in controls. We visually inspected the match between the [766+859] nm signal and [766-859] nm signal. A mismatch was determined individually by visual inspection of the NIRS signals in combination with sEMG parameters and exercise duration.

Statistical analysis

We used quantitative descriptive statistics (independent samples t-test: mean (SD) or Wilcoxon singed rank test: median (IQR)) to present between group differences in demographics, clinical characteristics, respiratory gas analyses and NIRS. We used linear mixed effect statistical models (LMM) (fixed effects: group, time, interaction; random effects: intercept per individual; unstructured covariance) to examine the difference over time, during the first six minutes, on VO_2, VCO_2, VE and RER between patients and controls. We used LMM (fixed effects: group, time, interaction; random effects: intercept per individual; unstructured covariance) to examine the difference over time on sEMG normalized RMS amplitudes and median frequencies between patients and controls. A simple linear regression was fitted on individual HR and NIRS parameters over time to calculate slopes. We used SPSS (IBM SPSS Statistics version 24; IBM, Inc., Chicago, IL) for statistical analyses. Level of significance was set on $p < 0.05$.

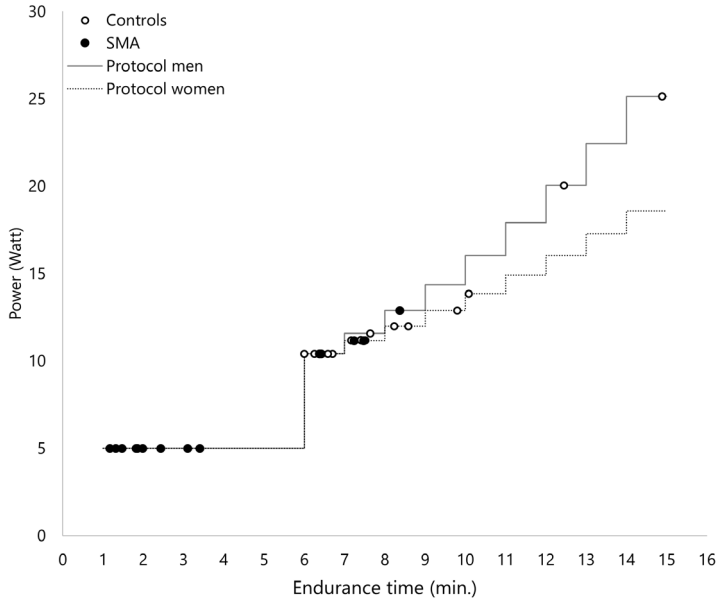

Figure 2. Schematic overview of the incremental arm-cycling protocol and individual performances during the first visit.

Results

Subject characteristics and arm-cycling exercise performance

We included 15 patients with SMA types 3 and 4 (type 3a: n=6, type 3b: n= 8, type 4: n=1) and 15 age and gender matched controls in the study. Participant baseline characteristics are summarized in Table 1. Lean body mass was significantly lower in patients compared to controls (table 1). Patients prematurely fatigued during execution of the arm-cycling task. Mean (SD) exercise duration (min) was twofold lower in patients (4.1 (2.6)) compared to controls (8.4 (2.5)), $p < 0.001$. Individual exercise performances are shown in Figure 2.

Respiratory gas exchange during arm-cycling

Basal and post-exercise values of respiratory gas exchange variables in patients and controls were not significantly different (Table 2). In response to arm-cycling exercise, minute ventilation (VE) and oxygen uptake (VO_2) scaled to maximal power output was significantly higher in patients with SMA compared to controls (Figure 3). Absolute values of VE, VO_2, VCO_2 and RER were not significantly different between patients and controls (Table 2, Figure 4 and Supplementary Table 1). The median incremental change in heart rate per minute in response to arm-cycling was 2.1-fold larger in patients with SMA than controls ($p = 0.016$). This result was closely correlated with arm-cycling duration and lower total upper arm muscle strength ($r2 = 0.86$; Supplementary Figure 1). The temporal change in HR per minute in response to exercise was not correlated with arm muscle activity (Supplementary Figure 2).

Table 1. Baseline characteristics

Variable	SMA (mean±SD)	Controls (mean±SD)	p-value
Age (y)	40.2 ± 17.1	39.5 ± 16.6	0.915
Height (cm)	168.3 ± 16.6	175.2 ± 10.0	0.054
Weight (kg)	67.1 ± 18.5	79.5 ± 15.0	0.176
Lean body mass (kg)	46.8 ± 16.4	59.5 ± 11.9	0.022*
FEV1 (L/min)	3.4 ± 0.9 (n=14)	2.9 ± 0.9	0.236
FVC (L)	4.6 ± 1.5 (n=14)	4.5 ± 1.7	0.894
Gender (m/f)	5/10	5/10	n.a.

SMA = spinal muscular atrophy, FEV1 = forced expiratory volume in 1 s, FVC = forced vital capacity, * = level of significance $p < 0.05$.

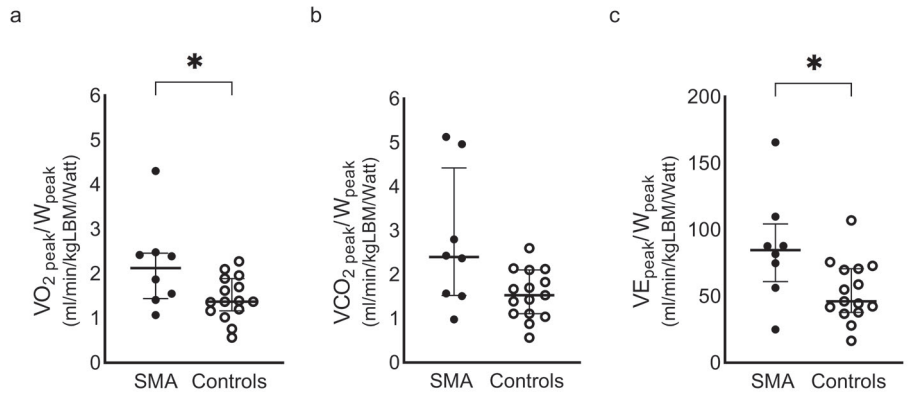

Figure 3. Peak oxygen consumption, carbon dioxide exhalation and ventilation normalized to peak workload in patients with SMA (n=8) and controls (n=15). a) Median (IQR) and individual oxygen consumption per Watt in patients with SMA (solid dots) and controls (open dots), p = 0.040. b) Median (IQR) and individual carbon dioxide exhalation per Watt in patients with SMA (solid dots) and controls (open dots), p = 0.056. c) Median (IQR) and individual ventilation per Watt in patients with SMA (solid dots) and controls (open dots), p = 0.023.* p < 0.05.

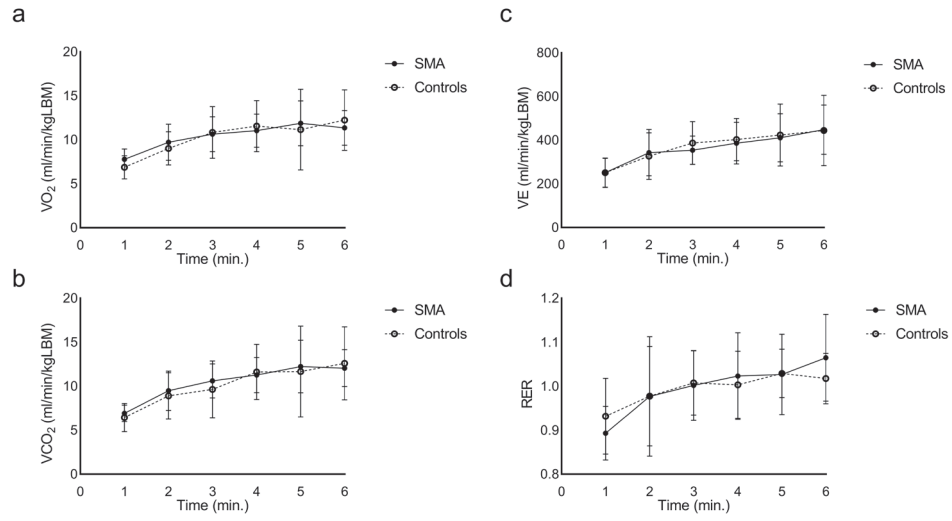

Figure 4. Respiratory gas exchange in patients with SMA (n=6; closed symbols, solid lines) and controls (n=12; open symbols, dotted lines) during the constant load phase of arm-cycling. a) Mean (SD) oxygen uptake per minute, corrected for lean body mass (LBM), in patients with SMA and controls. b) Mean (SD) carbon dioxide exhalation per minute, corrected for lean body mass (LBM), patients with SMA and controls. c) Mean (SD) ventilation per minute, corrected for lean body mass (LBM), patients with SMA and controls. d) Mean (SD) respiratory exchange ratio per minute in patients with SMA and controls.

Table 2. Respiratory gas exchange during exercise

Rest		**SMA (n=15)**	**Controls (n=15)**	**p-value**
mean ± SD	HR (bpm)	74 ± 17 (n=14)	66 ± 10	0.127
(last 3 minutes)	VO_2 (ml/min/LBM)	5.85 (2.10)	5.06 (0.92)	0.193
	RER	0.86 ± 0.06	0.88 ± 0.05	0.286
End exercise		**SMA (n=8)**	**Controls (n=15)**	**p-value**
median (IQR)	HR peak (bpm)	111 (38) (n=7)	123 (31)	0.535
	VE peak (ml/min/LBM)	584.1 (526.3)	545.2 (285.5)	0.776
	VO_2 peak (ml/min/LBM)	13.7 (12.9)	14.5 (5.2)	0.825
	VE/VO_2	32.8 (11.63)	29.5 (5.82)	0.636
	VE/VCO_2	28.4 (12.15)	28.7 (5.96)	0.925
	RER peak	1.10 (0.28)	1.04 (0.13)	0.548
	W peak (Watt/LBM)	0.15 (0.11)	0.19 (0.05)	0.065
Recovery		**SMA (n=7)**	**Controls (n=15)**	**p-value**
median (IQR)	HR (bpm)	64 (12) (n=6)	71 (18)	0.470
(last 3 minutes)	VE (ml/min/LBM)	185.8 (100.4)	164.5 (72.1)	0.581
	VO_2 (ml/min/LBM)	4.99 (1.49)	5.15 (0.89)	1
	VE/VO_2	26.1 (8.39)	26.0 (5.41)	0.490
	VE/VCO_2	27.4 (9.06)	27.7 (4.74)	0.630
	RER	0.89 (0.10)	0.92 (0.07)	0.091

SMA = spinal muscular atrophy, HR = heart rate, RER = respiratory exchange ratio (VCO_2/VO_2), VE peak = peak ventilation, VO_2 peak = peak oxygen uptake per kilogram lean body mass, W peak = peak workload per kilogram lean body mass.

Surface EMG dynamics during arm-cycling

We obtained sEMG datasets from 15 patients with SMA and their controls. Two m. flexor digitorum and one m. biceps- and triceps brachii datasets from one patient and control were excluded due to invalid normalization. Normalized RMS amplitudes of sEMG recordings immediately after onset of arm-cycling were increased in patients with SMA compared to controls in all sampled muscles (m. biceps brachii, m. triceps brachii and m. brachioradialis: $p < 0.001$, m. flexor digitorum: $p < 0.05$ (Figure 5a, b and Supplementary Table 2). Normalized RMS amplitudes of sEMG recordings from the m. triceps brachii, m. brachioradialis and m. flexor digitorum increased identically in patients and controls as exercise progressed (Figure 5a, c and Supplementary Table 3). The increase in normalized RMS amplitude for the m. biceps brachii as exercise progressed was significantly higher in patients than in controls ($p < 0.01$). The median frequency of the sEMG recordings immediately after onset of arm-cycling were not different between patients and controls for all sampled muscles (Figure 5d, e and Supplementary Table 2). As exercise progressed, this parameter decreased identically (m. biceps brachii), less (m. brachioradialis and m. flexor digitorum, $p < 0.05$) or more (m. triceps brachii, $p < 0.05$) in patients compared to controls, respectively (Figure 5d, f and Supplementary Table 3).

NIRS dynamics during arm-cycling

We obtained 10 complete datasets from the m. biceps brachii in patients with SMA and 8 complete datasets in controls. In the patient group we had one missing dataset and excluded four datasets (three due to insufficient signal to noise ratio and one due to drift, respectively). In the control group, we excluded seven datasets (one due to high skinfold thickness, five due to unstable baseline and one due to movement artefacts, respectively). Upon onset of arm-cycling we observed in all participants a steady increase in [766+859] nm signal with a response time of approximately 10 seconds, except in one patient with SMA (Figure 6a and Supplementary Figure 3). The decrease in [766+859] nm signal in this particular patient (exercise duration 502s) was the result of an initial increase and a steep decrease in the last 50 seconds of exercise. In comparison, the [766-859] nm signal dynamics were much more variable than the [766+859] nm signal dynamics (Supplementary Figure 3). Regardless, we found no differences between groups in temporal change in [766+859] nm signals (Figure 6a) and [766-859] nm signals (Figure 6b), $p > 0.05$ respectively.

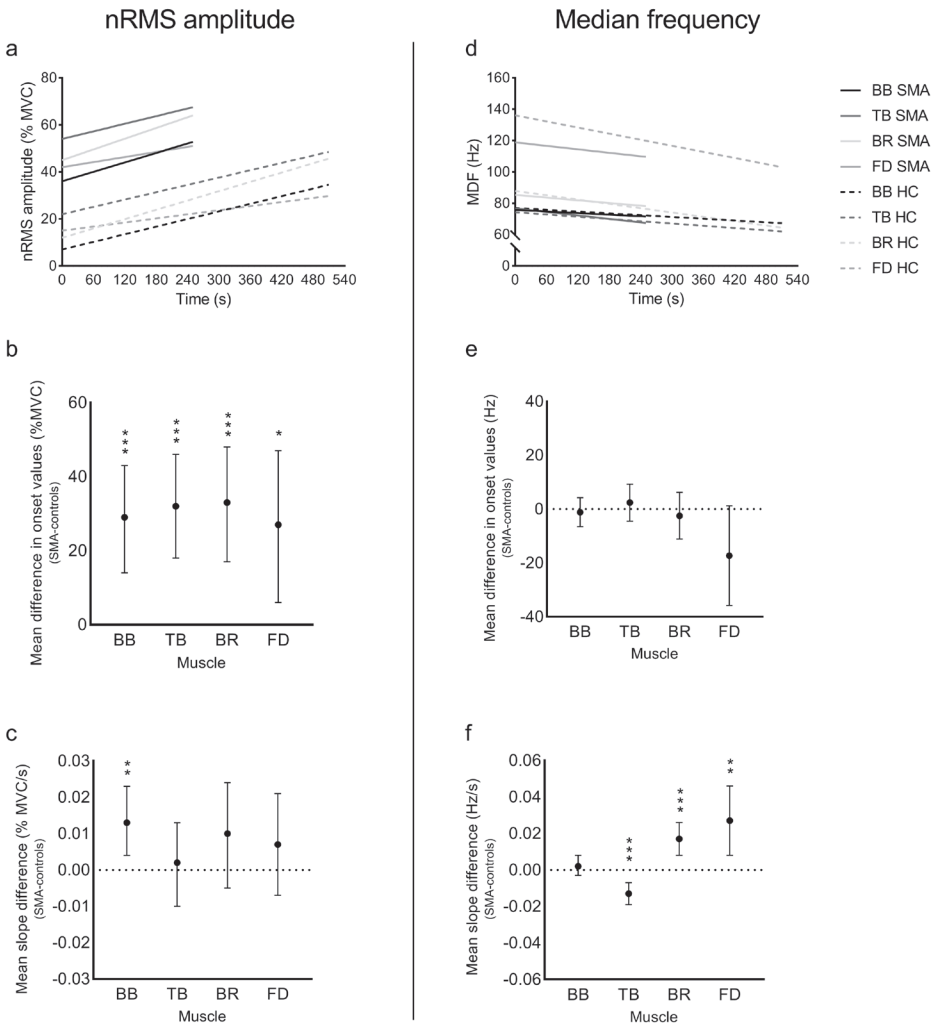

Figure 5. Linear mixed effect statistical models on sEMG variables in patients with SMA and controls. Linear mixed statistical models on normalized RMS amplitude (a) and median frequency (d) per muscle in patients with SMA (solid lines) and controls (HC: dotted lines) extrapolated to the mean cycle time to exhaustion. (b) Mean difference in normalized RMS amplitude values at onset of four muscles between patients with SMA and controls. (c) Mean differences in normalized RMS amplitude slopes of four muscles between patients with SMA and controls (e) Mean difference in median frequency at onset of four muscles between patients with SMA and controls. (f) Mean difference in median frequency slopes of four muscles between patients with SMA and controls. Error barrs indicate 95% confidence interval. BB = m. biceps brachii, TB = m. triceps brachii, BR = m. brachioradialis, FD = m. flexor digitorum, */**/*** = $p < 0.05/ 0.01/ 0.001$.

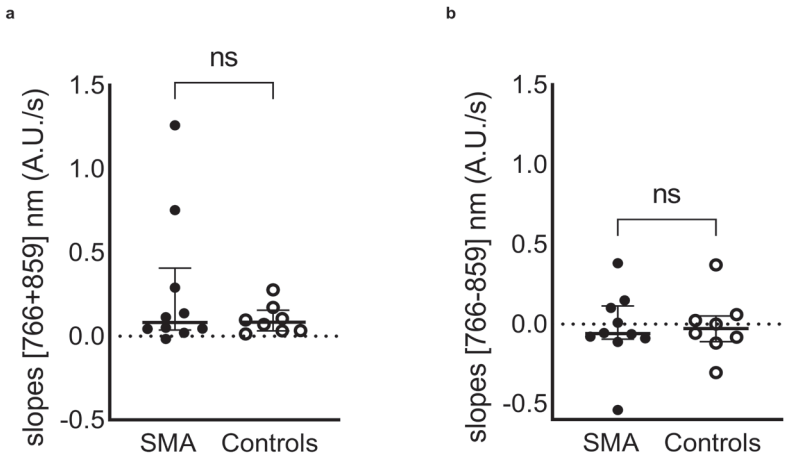

Figure 6. Non-significant differences in capillary recruitment between groups, indicated by slopes of the [766+859] nm and [766-859] nm continuous wave near-infrared spectroscopy signals, respectively. a) Median (IQR) and individual [766+859] nm slopes in patients with SMA (solid dots) and controls (open dots). b) Median (IQR) and individual [766-859] nm slopes in patients with SMA (solid dots) and controls (open dots).

Discussion

Patients with SMA in our cohort prematurely fatigued during execution of a maximal arm-cycling task, evidencing the symptoms of muscle weakness and exercise intolerance known for this disease. Below, we discuss what may be learned from our breath-by-breath gas exchange, sEMG and CW-NIRS measurements about the underlying mechanisms of premature mechanical failure of the arm muscles in the patients.

Cardiac and ventilatory work during arm-cycling

Our analysis revealed an association between exercise duration, muscle weakness and change in HR (Supplementary Figure 1). Specifically, in weak patients the change in HR in response to arm-cycling against the initially stationary workload of 5 W was more pronounced than in less affected patients or controls. Ventilatory work and work of breathing during maximal arm-cycling in patients was 1.8-fold and 1.6-fold higher than in controls (Figure 3). In light of the fact that patients have lower arm muscle mass than controls this was a surprising finding. Our results may be explained two ways. Patients may have additionally recruited other muscles than strictly upper- and lower arm muscles during arm-cycling to compensate weakness of their arm musculature. Indeed, inspecting recorded videos we observed compensatory movements of the trunk and legs at the occurrence of fatigability

(data not shown). This observation may also explain the higher change in HR in response to this heavy arm-cycling exercise task. Conversely, our results may also be explained by a white-to-red shift in myofiber type composition.[17] Since red myofibers rely on oxidative metabolism a shift towards this myofiber type may result in higher ventilatory work. However, during constant load arm-cycling we found no such pattern (figure 4) which provides no conclusive evidence on this matter. Here, we found, in fact, similar respiratory gas exchange findings between patients and controls. This may suggest limited sensitivity of whole body measurements to examine gas exchange at the level of the muscle when using an upper body exercise paradigm.[31,35]

A previous investigation in patients with SMA employing breath-by-breath gas analyses during exercise reported decreased peak oxygen uptake compared to controls.[28] This particular study employed a lower-body exercise paradigm. The authors suggested that the lack of a larger increase in oxygen uptake was a consequence of muscle atrophy and provided evidence for a mitochondrial dysfunction in SMA.[28] However, VO_2 peak corrected for peak workload during exercise in patients compared to controls in that particular study was threefold higher in patients than in controls [28] similar to our present finding in patients with SMA using an arm-cycling exercise task. This suggests that oxidative work capacity of the muscles in adolescent and adult patients with SMA normalized to peak work is, in fact, intact if not enhanced in these studied cohorts. Again, this hypothesis is supported by our previous finding of evidence for a white-to-red shift in myofiber type composition of upper arm muscles of the patients in our cohort .[17] In light of future studies on training interventions in SMA, our results suggest no energetic limitations in muscle of adolescent and adult patients with SMA types 3 and 4.

Motor unit recruitment capacity during arm cycling

Motor unit (MU) recruitment during a submaximal voluntary exercise task in patients with SMA has been investigated in two previous studies using sEMG.[22,23] Any increase in firing frequency, recruitment of MUs, and/or MU synchronization during exercise may be reflected by an increase of the normalized RMS amplitude of the sEMG signal.[25,26,36] We previously reported increasing RMS amplitudes and decreasing median frequencies in some, but not all, patients with SMA performing a submaximal endurance shuttle task involving shoulder and arm muscles, suggesting the presence of motor unit reserve capacity in individual patients.[23] Here, we observed in all patients a temporal increase of normalized RMS amplitudes during arm-cycling similar to controls (Figure 5). This suggests residual motor unit recruitment capacity in upper extremity muscles in patients with SMA (Figure 5). In comparison, an overall decrease of RMS amplitude of sEMG signals recorded from leg muscles during a six minute walk test in patients with SMA type 3 has been recorded previously.[22] Walking velocity, however, decreased during the test which may have confounded this observation.[22]

As described above, we previously found evidence for a white-to-red shift in myofiber composition in upper arm muscles in this same cohort of patients.[17] Since muscle fiber conduction velocity correlates with muscle acidification [37] we therefore hypothesized to observe a diminished decrease in median frequency of the sEMG signal.[24–26,38] Our present results on temporal changes in median frequencies testing this hypothesis are, however, inconclusive. Specifically, we found a 0.6-fold smaller decrease in median frequency of the sEMG signal from the m. brachioradialis and m. flexor digitorum in patients compared to controls, but not in the m. biceps- and m. triceps brachii. Further studies are needed to test the hypothesis, preferably using simultaneous ^{31}Phosphorus Magnetic Resonance Spectroscopy and sEMG data acquisition. In principle such measurements are feasible.[39]

This study has provided no new insight into the underlying mechanisms of premature mechanical failure of the arm muscles of our cohort of patients with SMA during execution of a maximal arm-cycling task. Based on sEMG data we suggest that muscle function was, at least, not the primary limiting factor. As presented in figure 5, the linear mixed effect models on RMS amplitudes and median frequencies extrapolated to the mean cycle time to exhaustion in patients seem to end abruptly. While the patients performed the exercise task at higher percentages of MCV, we did not observe any abnormal sEMG dynamics compared to controls. Therefore, we suggest that future investigations should perhaps focus on another link in the chain, i.e. failure of neuromuscular transmission at the neuromuscular junction itself, previously associated with exercise intolerance and located proximal to the muscle, which may primarily affect exercise duration.[40–47.]

Comparison of our results to observations in other neuromuscular diseases such as Duchenne Muscular Dystrophy and Amyotrophic Lateral Sclerosis reveals similar observations, i.e. higher normalized RMS amplitude onset values and a reduced shift in median frequencies.[48–50] To the best of our knowledge no observations of temporal changes of normalized RMS amplitudes providing insight into any residual motor unit recruitment capacity during dynamic exercise in neuromuscular diseases other than SMA have been reported. Further research on the latter is needed in this patient population since the availability of any residual MU recruitment capacity suggest an opportunity for training interventions.

Capillary recruitment capacity during arm-cycling

Studies in SMA mouse models have reported evidence for local vascular system defects which may affect skeletal muscle oxygen supply.[18–21] To provide insight into muscle capillary recruitment in vivo, we used non-invasive CW-NIRS. This technique uses specific wavelengths, [766] nm and [859] nm, of infrared light and the difference in absorption characteristics of oxygenated and deoxygenated hemoglobin.[51–53] A normal physiological response during exercise shows an overall increase in the sum of the two signals as a

consequence of exercise-induced capillary recruitment in the active muscle.[54–56] Montes and colleagues first applied NIRS to study vascular functional abnormalities in upper leg muscle in a cohort of 19 adolescent and adult patients with SMA and reported inadequate capillary recruitment.[28] Here, we found no such evidence in upper arm muscles in a similar but different cohort of patients. Specifically, we found an overall increase in [766+859] nm signals and decrease in [766-859] nm signals with no differences between the patient and control group (Figure 6 and Supplementary Figure 3) also suggesting that capillary recruitment was not the primary limiting factor of premature mechanical failure. Importantly, these NIRS findings are consistent with our previous finding of normal, if not faster, aerobic recovery of phosphocreatine stores in these muscles following arm-cycling in this same cohort of patients.[17] Whereas NIRS, in particular when using a continuous wave light source, is a technique with a number of methodological limitations [29,57–59] no such methodological concerns apply to in vivo [31]Phosphorus Magnetic Resonance Spectroscopy assay of muscular oxidative ATP synthesis capacity.[60]

Limitations and outlook

The arm-cycling exercise set-up used in the present study has some technological limitations that should be considered when assessing the results. First of all, the minimal workload of the arm-cycling ergometer at 90 rpm is 5 W.[31] As such, seven patients with SMA were unable to perform arm-cycling for more than three minutes against the minimal workload as a result of muscle weakness (Figure 2). Consequently, data of these patients had to be excluded for analysis of breath-by-breath gas exchange. Secondly, atrophy of the m. triceps brachii was much more pronounced than its antagonist m. biceps brachii in this patient cohort,[17] lowering its contribution to the cycling movement. This may have contributed to the 1.2-fold higher increase in RMS amplitudes found in the m. biceps brachii of patients compared to controls. Third, the factors examined in this study in mildly affected patients with SMA may possibly still contribute to exercise intolerance in severely affected patients. As, such, future studies employing a voluntary arm-cycling exercise paradigm, for example to evaluate the outcome of exercise training, should use ergometers with even lower 'idle' workloads than the ergometer used here (~5W). This would additionally provide the opportunity to study exercise intolerance in more severely affected patients with SMA. Preserving, if not expanding motor unit- and capillary recruitment capacity of arm muscles, may present a potential therapeutic target. Specifically, high intensity exercise training in a mouse SMA model reduced fatigability, protected the integrity of the NMJ and additionally reduced motor neuron death and enhanced cross sectional area of large myofibrils.[16] Furthermore, as suggested above, beneficial effects of pharmaceuticals that directly target the NMJ, such as pyridostigmine, may also be investigated using this platform in future studies.

Abbreviations

CW-NIRS	Continuous wave near infrared spectroscopy
DPF	Differential pathlength factor
HR	Heart rate
MRC	Medical research council
MU	Motor unit
MVC	Maximal voluntary contraction
RER	Respiratory exchange ratio
RMS	Root mean square
sEMG	Surface electromyography
SMA	Spinal muscular atrophy
SMN	Survival motor neuron
VE	Ventilation
VO_2	Oxygen uptake
VCO_2	Carbon dioxide exhalation

Declarations

Conflict of Interest Statement

WLP is a member of the scientific advisory board of SMA Europe and has served as an ad hoc member of the scientific advisory boards of Biogen and Avexis and as a member of a data monitoring committee for Novartis. BB is a member of the scientific advisory board of Scholar Rock. Their employer receives fees for SMA-related consultancy activities. WLP, BB and JALJ obtained research grants from non-profit foundations Prinses Beatrix Spierfonds and Stichting Spieren voor Spieren. The other authors have no conflict of interest to report.

Human and animal rights

"We confirm that we have read the Journal's position on issues involved in ethical publication and affirm that this report is consistent with those guidelines."

Funding

This work was supported by grants from Prinses Beatrix Spierfonds (W.OR17-05), Stichting Spieren voor Spieren and Zwaluwen Jeugd Actie. The Spieren voor Spieren Inspanningslab at the University Medical Center Utrecht was funded by Stichting Spieren voor Spieren.

Acknowledgment

The authors would like to thank all participants who participated in this study.

References

1. Lefebvre S, Brglen L, Reboullet S, et al. Identification and characterization of a spinal muscular atrophy-determining gene. Cell. 1995;80(1):155-165.
2. Hamilton G, Gillingwater TH. Spinal muscular atrophy: Going beyond the motor neuron. Trends Mol Med. 2013;19(1):40-50.
3. Yeo CJJ, Darras BT. Overturning the Paradigm of Spinal Muscular Atrophy as just a Motor Neuron Disease. Pediatr Neurol. 2020;109:12-19.
4. Mercuri E, Bertini E, Iannaccone ST. Childhood spinal muscular atrophy: Controversies and challenges. Lancet Neurol. 2012;11(5):443-452.
5. Otto LA., Froeling M, van Eijk RP., et al. Quantification of disease progression in spinal muscular atrophy with muscle MRI – a pilot study. NMR Biomed. 2021:1-11.
6. Otto LAM, van der Pol WL, Schlaffke L, et al. Quantitative MRI of skeletal muscle in a cross-sectional cohort of patients with spinal muscular atrophy types 2 and 3. NMR Biomed. 2020;(March):1-13.
7. Wijngaarde CA, Stam M, Otto LAM, et al. Muscle strength and motor function in adolescents and adults with spinal muscular atrophy. Neurology. 2020;95(14):e1988-e1998.
8. Bartels B, Habets LE, Stam M, et al. Assessment of fatigability in patients with spinal muscular atrophy: Development and content validity of a set of endurance tests. BMC Neurol. 2019;19(1):1-10.
9. Bartels B, Groot JF De, Habets LE, et al. Fatigability in spinal muscular atrophy : validity and reliability of endurance shuttle tests. Orphanet J Rare Dis. 2020;2:1-9.
10. Montes J, McDermott MP, Martens WB, et al. Six-minute walk test demonstrates motor fatigue in spinal muscular atrophy. Neurology. 2010;74(10):833-838.
11. Stam M, Wadman RI, Bartels B, et al. A continuous repetitive task to detect fatigability in spinal muscular atrophy. Orphanet J Rare Dis. 2018;13(1):1-7.
12. Cheng AJ, Place N, Westerblad H. Molecular Basis for Exercise-Induced Fatigue : The Importance of Strictly Controlled Cellular Ca2+ Handling. Cold Spring Harb Perspect Med. 2018;8((2)).
13. Miller N, Shi H, Zelikovich A., Ma Y-C. Motor Neuron Mitochondrial Dysfunction in Spinal Muscular Atrophy. Hum Mol Genet. 2016;25(16):3395-3406.
14. Ripolone M, Ronchi D, Violano R, et al. Impaired Muscle Mitochondrial Biogenesis and Myogenesis in Spinal Muscular Atrophy. JAMA Neurol. 2015;72(6):1-10.
15. Shababi M, Lorson CL, Rudnik-Schöneborn SS. Spinal muscular atrophy: A motor neuron disorder or a multi-organ disease? J Anat. 2014;224(1):15-28.
16. Houdebine L, D'Amico D, Bastin J, et al. Low-Intensity Running and High-Intensity Swimming Exercises Differentially Improve Energy Metabolism in Mice With Mild Spinal Muscular Atrophy. Front Physiol. 2019;10(October):1-21.
17. Habets LE, Bartels B, Asselman F-L, et al. Magnetic resonance reveals mitochondrial dysfunction and muscle remodelling in spinal muscular atrophy. Brain. November 2021.
18. Nobutoki T, Ihara T. Early disruption of neurovascular units and microcirculatory dysfunction in the spinal cord in spinal muscular atrophy type I. Med Hypotheses. 2015;85(6):842-845.

19. Shababi M, Habibi J, Ma L, Glascock JJ, Sowers JR, Lorson CL. Partial restoration of cardio-vascular defects in a rescued severe model of spinal muscular atrophy. J Mol Cell Cardiol. 2012;52(5):1074-1082.
20. Somers E, Stencel Z, Wishart TM, Gillingwater TH, Parson SH. Density, calibre and ramification of muscle capillaries are altered in a mouse model of severe spinal muscular atrophy. Neuromuscul Disord. 2012;22(5):435-442.
21. Zhou H, Ying H, Scoto M, Brogan P, Parson S, Muntoni F. Microvascular abnormality in spinal muscular atrophy and its response to antisense oligonucleotide therapy. Neuromuscul Disord. 2015;25(2015):S193.
22. Montes J, Dunaway S, Garber CE, Chiriboga CA, De Vivo DC, Rao AK. Leg muscle function and fatigue during walking in spinal muscular atrophy type 3. Muscle Nerve. 2014;50(1):34-39.
23. Habets LE, Bartels B, de Groot JF, et al. Motor unit reserve capacity in spinal muscular atrophy during fatiguing endurance performance. Clin Neurophysiol. 2021;132(3):800-807.
24. Fitts RH. Cellular mechanisms of skeletal muscle fatigue. Pysiological Rev. 1994;74(1):49-81.
25. Dimitrova NA, Dimitrov G V. Interpretation of EMG changes with fatigue: Facts, pitfalls, and fallacies. J Electromyogr Kinesiol. 2003;13(1):13-36.
26. Konrad P. The ABC of EMG: A Practical Introduction to Kinesiological Electromyography. Noraxon INC. USA; 2005. http://www.noraxon.com/docs/education/abc-of-emg.pdf.
27. Hamaoka T, McCully KK, Quaresima V, Yamamoto K, Chance B. Near-infrared spectroscopy/imaging for monitoring muscle oxygenation and oxidative metabolism in healthy and diseased humans. J Biomed Opt. 2007;12(6):062105.
28. Montes J, Goodwin AM, McDermott MP, et al. Diminished muscle oxygen uptake and fatigue in spinal muscular atrophy. Ann Clin Transl Neurol. 2021:1-10.
29. Perrey S, Ferrari M. Muscle Oximetry in Sports Science: A Systematic Review. Sport Med. 2017:1-20.
30. Wadman RI, Stam M, Gijzen M, et al. Association of motor milestones, SMN2 copy and outcome in spinal muscular atrophy types 0-4. J Neurol Neurosurg Psychiatry. 2017;88(4):364-367.
31. Vegter RJ, Brink S van den, Mouton L, Sibeijn-Kuiper A, Woude L, Jeneson J. Magnetic Resonance-Compatible Arm-Crank Ergometry: A New Platform Linking Whole-Body Calorimetry to Upper-Extremity Biomechanics and Arm Muscle Metabolism. Front Neurol. 2021;12(February):1-13.
32. Beenakker EAC, Van der Hoeven JH, Fock JM, Maurits NM. Reference values of maximum isometric muscle force obtained in 270 children aged 4-16 years by hand-held dynamometry. Neuromuscul Disord. 2001;11(5):441-446.
33. Hamaoka T, McCully KK, Niwayama M, Chance B. The use of muscle near-infrared spectroscopy in sport, health and medical sciences: Recent developments. Philos Trans R Soc A Math Phys Eng Sci. 2011;369(1955):4591-4604.
34. Duncan A, Meek J, Clemence M, et al. Optical pathlength measurements on adult head, calf and forearm and the head of the newborn infant using phase resolved optical spectorscopy. Phys Med Biol. 1995;(40):295-304.
35. Martin TW, Zeballos RJ, Weisman IM. Gas exchange during maximal upper extremity exercise. Chest. 1991;99(2):420-425.
36. Henneman E, Clamann HP, Gillies JD, Skinner RD. Rank order of motoneurons within a pool: law of combination. J Neurophysiol. 1974;37(6):1338-1349.

37. Schmitz JPJ, Van Dijk JP, Hilbers PAJ, Nicolay K, Jeneson JAL, Stegeman DF. Unchanged muscle fiber conduction velocity relates to mild acidosis during exhaustive bicycling. Eur J Appl Physiol. 2012;112(5):1593-1602.
38. Jones D, Round J, de Haan A. Skeletal Muscle from Molecules to Movement. Elsevier Ltd; 2005.
39. Vestergaard-Poulsen P, Thomsen C, Sinkjaer T, Hendriksen O. Simultaneous 31P NMR spectroscopy and EMG in exercising and recovering human skeletal muscle: Technical aspects. Magn Reson Med. 1994;31(2):93-102.
40. Wadman RI, Vrancken AFJ, Van den Berg LH, Van der Pol WL. Dysfunction of the neuromuscular junction in patients with spinal muscular atrophy type 2 and 3. Neurology. 2012;79:2050-2055.
41. Goulet B, Kothary R, Parks R. At the "Junction" of Spinal Muscular Atrophy Pathogenesis: The Role of Neuromuscular Junction Dysfunction in SMA Disease Progression. Curr Mol Med. 2013;13(7):1160-1174.
42. Kong L, Wang X, Choe DW, et al. Impaired synaptic vesicle release and immaturity of neuromuscular junctions in spinal muscular atrophy mice. J Neurosci. 2009;29(3):842-851.
43. Kariya S, Park GH, Maeno-Hikichi Y, et al. Reduced SMN protein impairs maturation of the neuromuscular junctions in mouse models of spinal muscular atrophy. Hum Mol Genet. 2008;17(16):2552-2569.
44. Murray LM, Comley LH, Thomson D, Parkinson N, Talbot K, Gillingwater TH. Selective vulnerability of motor neurons and dissociation of pre- and post-synaptic pathology at the neuromuscular junction in mouse models of spinal muscular atrophy. Hum Mol Genet. 2008;17(7):949-962.
45. Bowerman M, Murray LM, Beauvais A, Pinheiro B, Kothary R. A critical smn threshold in mice dictates onset of an intermediate spinal muscular atrophy phenotype associated with a distinct neuromuscular junction pathology. Neuromuscul Disord. 2012;22(3):263-276.
46. Stam M, Wadman RI, Wijngaarde CA, et al. Protocol for a phase II, monocentre, double-blind, placebo-controlled, cross-over trial to assess efficacy of pyridostigmine in patients with spinal muscular atrophy types 2-4 (SPACE trial). BMJ Open. 2018;8(7):1-9.
47. Bartels B, de Groot JF, Habets LE, et al. Correlates of fatigability in patients with spinal muscular atrophy. Neurology. 2021;96(6):845-852.
48. Janssen MMHP, Harlaar J, Koopman B, De Groot IJM. Dynamic arm study: Quantitative description of upper extremity function and activity of boys and men with duchenne muscular dystrophy. J Neuroeng Rehabil. 2017;14(1).
49. Meekins GD, So Y, Quan D, Vavricek J. American Association of Neuromuscular & Electrodiagnostic Medicine evidenced-based review: Use of surface electromyography in the diagnosis and study of neuromuscular disorders. Muscle and Nerve. 2008;38(4):1219-1224.
50. Lindeman E, Spaans F, Reulen JPH, Leffers P, Drukker J. Surface EMG of proximal leg muscles in neuromuscular patients and in healthy controls. Relations to force and fatigue. J Electromyogr Kinesiol. 1999;9(5):299-307.
51. Mancini DM, Bolinger L, Li H, Kendrick K, Chance B, Wilson JR. Validation of near-infrared spectroscopy in humans. J Appl Physiol. 1994;77(6):2740-2747.
52. Piantadosi CA. Near infrared spectroscopy: Principles and application to noninvasive assessment of tissue oxygenation. J Crit Care. 1989;4(4):308-318.
53. Jöbsis FF. Noninvasive , Infrared Monitoring of Cerebral and Myocardial Oxygen Sufficiency and Circulatory Parameters Author (s): Frans F . Jöbsis. Am Assoc Adv Sci. 1977;198(4323):1264-1267.

54. Thomas GD, Segal SS. Neural control of muscle blood flow during exercise. J Appl Physiol. 2004;97(2):731-738.
55. Segal SS, Kurjiaka DT. Coordination of blood flow control in the resistance vasculatur of skeletal muscle. Med Sci Sports Exerc. 1995;27(8):1158-1164.
56. Fuglevand AJ, Segal SS. Simulation of motor unit recruitment and microvascular unit perfusion: Spatial considerations. J Appl Physiol. 1997;83(4):1223-1234.
57. Grassi B, Quaresima V. Near-infrared spectroscopy and skeletal muscle oxidative function in vivo in health and disease: a review from an exercise physiology perspective. J Biomed Opt. 2016;21(9):091313.
58. McCully KK, Hamaoka T. NIRS - what can it tell us about oxygen saturation in skeletal muscle. Exerc Sport Sci Rev. 2000;28(3):123-127.
59. McCully KK, Iotti S, Kendrick K, et al. Simultaneous in vivo measurements of HbO2 saturation and PCr kinetics after exercise in normal humans. J Appl Physiol. 1994;77(1):5-10.
60. Meyerspeer M, Boesch C, Cameron D, et al. 31P magnetic resonance spectroscopy in skeletal muscle: Experts' consensus recommendations. NMR Biomed. 2020;(August 2019):1-22.

Supplementary material

Supplementary Table 1. Linear mixed effect models respiratory gas analyses during constant load arm-cycling

Variable	Slope SMA	Slope Controls	Mean difference in slopes	95% CI Lower bound	95% CI Upper bound	p-value
VE (ml/min/kgLBM)	34.090	32.627	1.463	-12.209	15.136	0.832
VO_2 (ml/min/kgLBM)	0.706	0.441	0.265	-0.122	0.652	0.178
VCO_2 (ml/min/kgLBM)	0.988	0.801	0.186	-0.354	0.726	0.495
RER	0.029	0.042	-0.013	-0.030	0.004	0.141

CI = confidence interval, RER = respiratory exchange ratio, SMA=spinal muscular atrophy, VE = ventilation, VO_2 = oxygen uptake, VCO_2 = carbon dioxide exhalation.

Supplementary Table 2. Linear mixed effect models sEMG recordings - onset values

Muscle	Onset SMA	Onset Controls	Mean difference in onset	95% CI Lower bound	95% CI Upper bound	p-value
Median frequency (Hz)						
BB	75.7	76.9	-1.2	-6.5	4.2	0.652
TB	76.7	74.3	2.4	-4.5	9.2	0.486
BR	85.3	87.8	-2.5	-11.1	6.2	0.566
FD	118.8	136.1	-17.3	-35.8	1.2	0.065
nRMS amplitude (%MVC)						
BB	36	7	29	14	43	0.000
TB	54	22	32	18	46	0.000
BR	45	12	33	17	48	0.000
FD	42	15	27	6	47	0.014

CI = confidence interval, BB = m. biceps brachii, BR = m. brachioradialis, FD = m. flexor digitorum nRMS = normalized root mean square, SMA=spinal muscular atrophy, TB = m. triceps brachii.

Supplementary Table 3. Linear mixed effect models sEMG recodings - slopes

Muscle	Slope SMA	Slope Controls	Mean difference in slopes	95% CI		p-value
				Lower bound	Upper bound	
Median frequency (Hz/s)						
BB	-0.017	-0.019	0.002	-0.003	0.008	0.438
TB	-0.037	-0.024	-0.013	-0.019	-0.007	0.000
BR	-0.029	-0.046	0.017	0.008	0.026	0.000
FD	-0.038	-0.065	0.027	0.008	0.046	0.005
nRMS amplitude (%MVC/s)						
BB	0.067	0.054	0.013	0.004	0.023	0.005
TB	0.054	0.052	0.002	-0.010	0.013	0.756
BR	0.076	0.066	0.010	-0.005	0.024	0.184
FD	0.036	0.029	0.007	-0.007	0.021	0.347

CI = confidence interval, BB = m. biceps brachii, BR = m. brachioradialis, FD = m. flexor digitorum, nRMS = normalized root mean square, SMA=spinal muscular atrophy, TB = m. triceps brachii.

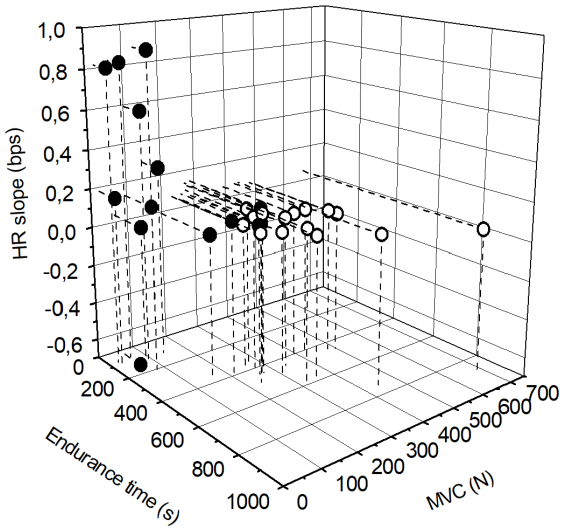

Supplementary Figure 1. Association between exercise duration (s), change in heart rate (HR) per minute in response to exercise and total upper extremity muscle strength (sum of m. biceps brachii (BB) and m. triceps brachii) in patients with SMA (solid dots) and controls (open dots).

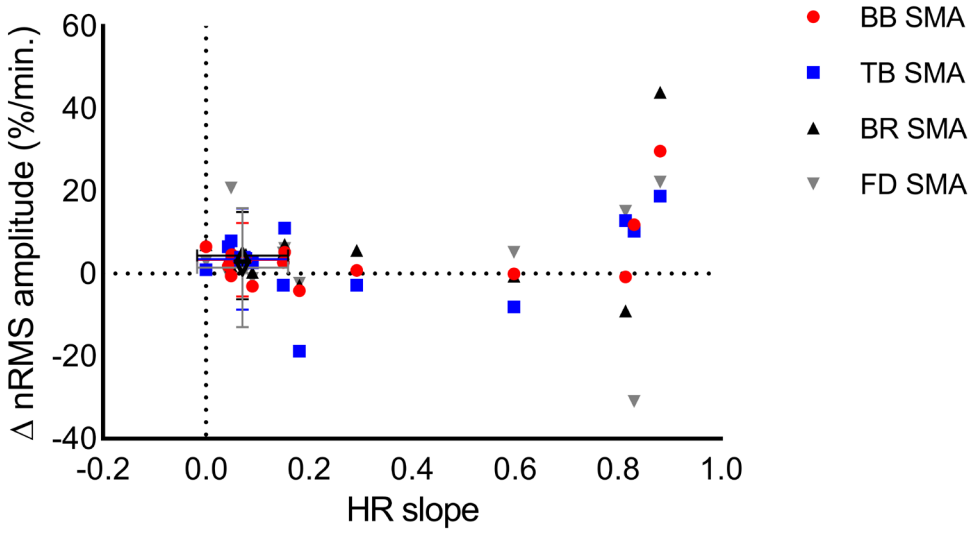

Supplementary Figure 2. Association between change in heart rate per minute in response to exercise and change in RMS amplitude per minute in patients with SMA (closed symbols) and controls (open symbols including 95% confidence intervals).

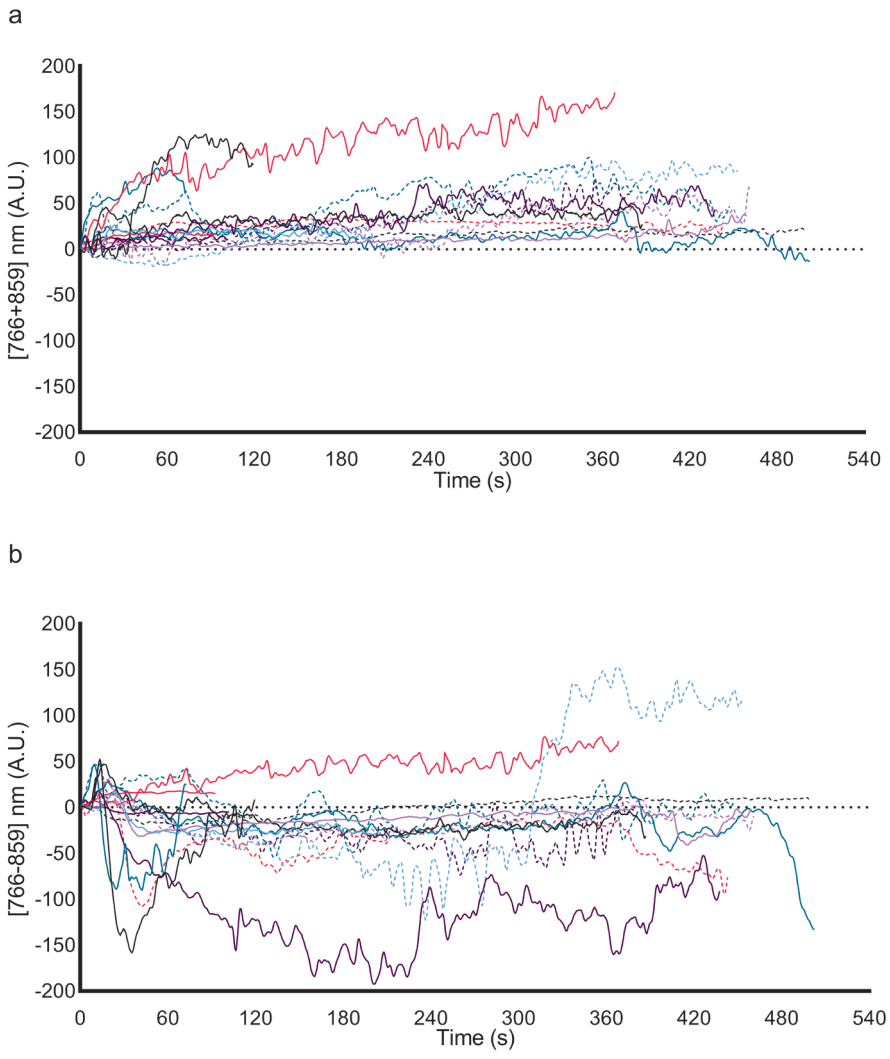

Supplementary Figure 3. Vascular oxygen supply and muscle oxygen demand indicated by [766+859] nm and [766-859] nm continuous wave Near Infrared Spectroscopy signals, respectively. a) [766+859] nm signals over time patients with SMA (solid lines) and controls (dotted lines). b) [766-859] nm signals over time in patients with SMA (solid lines) and controls (dotted lines). For clarity of presentation, we excluded two sets of control data with exercise durations over 540 s.

Chapter 8

General discussion

Since the first detailed clinical and post-mortem studies, published at the end of the 19th century,[1–6] spinal muscular atrophy (SMA) has been considered to be a prototype motor neuron disease. These early studies included descriptions of ventral nerve root and skeletal muscle atrophy as well as severe muscle weakness.[7–13] In the course of the 20th century it became clear that SMA varies widely in terms of disease severity with onset ranging from infantile to adult.[14–16] Eventually a clinical classification system was devised (1991), initially distinguishing three (i.e. types 1-3), and later five (i.e. type 0-4), SMA types based on the age at symptom onset and the acquisition of two motor milestones (independent sitting and walking).[14] Almost a century after the first reports, the genetic cause of SMA was finally discovered:[3] homozygous loss of function of the survival motor neuron 1 (*SMN1*) gene on chromosome 5q is found in all patients with SMA. Motor neurons are particularly vulnerable to SMN protein deficiency and it is likely that the level of residual SMN protein that can be produced through transcription of the second SMN gene in the human genome, *SMN2*, determines SMA severity. This is exemplified by the solid inverse association of *SMN2* copy number in patients and the severity of their disease.[17] How cellular SMN protein deficiency causes the α-motor neuron degeneration that underlies the symptoms of muscle weakness and atrophy is a matter of ongoing research and debate, because SMN contributes to a large number of cellular functions.

SMN protein is ubiquitously expressed and one of the puzzling aspects of the disease is the specific motor neuron vulnerability. Over the past twenty years, many studies have discovered abnormalities in many more tissues and organs, including vasculature tissue, brain, heart, bone, pancreas, liver, lung and intestine, suggesting that SMA is a motor neuron-dominant, multi-system disease.[1,2,4,18,19] This has been demonstrated both in animal models for SMA as well as in patients. Studies have also shown that motor unit abnormalities in SMA are not confined to motor neurons, but extend to muscle and the neuromuscular junction.[1,2,4] For example, the discovery of smaller myotubes in skeletal muscle of fetuses with SMA type 1 indicated a cell maturation lag, independent of motor neuron degeneration.[20] As a result, the current perspective on SMA treatment has shifted from solely addressing the genetic defect of a motor neuron disease towards an attempt to support all systems that are dysfunctional or at risk of dysfunction.

In the recent past, there has been renewed interest in symptoms of SMA.[21–25] In addition to muscular atrophy and weakness, reduced stamina when performing submaximal repetitive tasks (a.k.a. 'fatigability') is recognized as an additional significant aspect of the SMA phenotype.[21,22,24–26] Patients often spontaneously mention that their disability is not only caused by what they cannot do, but also by a lack of endurance for any physical tasks they can perform. When asked, up to 80% of patients mention symptoms of fatigability. Fatigability is specific to SMA, i.e. it is not seen to a similar extent in other neuromuscular disorders, and does not only occur secondary to weakness.[25] Although fatigability was first

linked to SMA more than three decades ago (1989),[26] surprisingly little research has been dedicated to the subject or its causes. Neuromuscular junction (NMJ) dysfunction plays an important role in fatigability in SMA.[27,28] Histological studies revealed abnormal anatomy of the NMJ and importantly suggested that not all NMJs are similarly susceptible to low levels of SMN protein in SMA.[27,29,30] *In vivo* findings from electromyography (EMG) studies in patients with SMA types 2 and 3,[27,31] using repetitive nerve stimulation (RNS), revealed neuromuscular transmission failure, i.e. a pathological amplitude decrement, in half the patients with SMA types 2 and 3.[27] This may, however, be an underestimation of the true prevalence of NMJ dysfunction, as although RNS is specific, it lacks sensitivity. However, the finding of neuromuscular transmission failure in a subgroup of patients may also indicate that mechanisms other than NMJ dysfunction contribute to fatigability in SMA.

The studies presented in this thesis were designed to advance the understanding of factors, other than NMJ dysfunction, which contribute to the symptom of fatigability in SMA. Identifying such factors might lead to therapeutic interventions. The first step was to design and validate new clinical instruments to quantify fatigability in both ambulant and non-ambulant patients with SMA (Chapter 2). Next, we used these clinical instruments to investigate potential underlying mechanisms of fatigability (Chapters 3-7). In this general discussion, I will address methodological considerations of the exercise tests and summarize our results on skeletal muscle function and their contribution to fatigability. I will end with recommendations for future research.

Methodological considerations of the exercise tests

In order to be able to examine factors of fatigability in patients with SMA types 2 to 4, we used two different tests: endurance shuttle tests and an arm-cycling platform.[32] These vary in their effect on fatigability by stressing different sites of the neuromuscular system. Both exercise tests have been developed to investigate specific peripheral factors which possibly contribute to fatigability in SMA.

Endurance shuttle tests

We developed a new set of clinical outcome measures to be able to assess fatigability in patients with SMA representing a wide range of disease severity (Chapter 2). The clinical tests had to represent the cyclic dynamic character of everyday movements, paced on a pre-set frequency, in order to stress the NMJ. Exercise intensity during endurance shuttle test (EST) performance was low to submaximal. During endurance performance at submaximal exercise intensities, NMJ failure may initially be averted by additional motor unit recruitment

to maintain the crucial force output. Therefore, maximal time to exercise was set at 20 minutes. We previously showed that time to limitation on the ESTs was significantly shorter in patients with SMA compared to controls,[24] indicating usefulness for clinical trials.[24]

After EST development (Chapter 2), we used these tests to investigate factors contributing to fatigability (Chapters 3 and 4). We used surface electromyography (sEMG) to measure motor unit reserve capacity and thus indirectly examine signal transmission from the axon to the myofibers (figure 1).

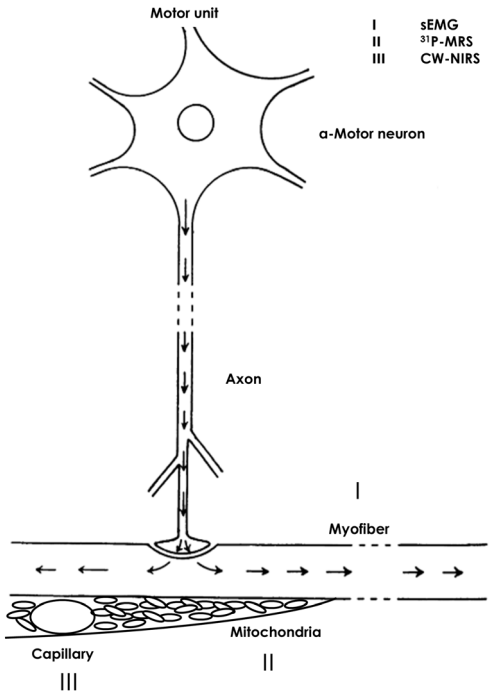

Figure 1. Schematic representation of the motor unit (figure adapted from Buller et al. [33,34]). The techniques (I,II,III) used in the studies described in this thesis examine different components of the motor unit. I = surface electromyography, II = ^{31}P-magnetic resonance spectroscopy, III = continuous wave-near infrared spectroscopy.

We encountered several methodological limitations in the use of sEMG. In Chapters 3 and 4, we discuss the possibility that compensational strategies during the ESTs may affect sEMG results. Furthermore, difficulties in determining the maximal voluntary contraction (MVC) of human leg muscle and the absence of time-related reference values of sEMG parameters complicated data interpretation. Another methodological limitation of the ESTs in relation to sEMG data interpretation deserves mention. In Chapter 3, we used sEMG recordings to examine the level of exercise intensity at onset of the ESTs. Here, exercise intensity was defined as a percentage of an individual's maximal voluntary contraction (MVC) force. As we chose to scale the newly developed ESTs according to muscle power, i.e. at 75% of an individual's maximal speed to perform one cycle of an EST (Chapter 2), we saved time during a clinical appointment which usually involves the lengthy process of taking into account an individual's maximal predicted oxygen uptake, as in the original endurance

shuttle walk test.[35] Consequently, we hypothesized that this decision could possibly result in difficulties when comparing fatigability of mild and more severely affected patients (Chapter 2). Specifically, the relative muscle force required to perform an EST might differ between mild and more severely affected patients.

Indeed, we showed that there is a difference in the level of MVC force at which patients with SMA types 2 and 3 start to perform the ESTs. Lowest percentages were measured in controls while the highest percentages were measured in patients with SMA type 2. A similar association has been found previously in work on trunk muscle activity.[36] These data show that patients use a larger proportion of the available muscle capacity to generate necessary power compared to controls.[36]

Additionally, based on this association and the fact that the residual motor unit recruitment capacity decreases with higher exercise intensities,[32] we expected to find a similar though inverse relation between motor unit reserve capacity and SMA phenotype, i.e. less motor unit reserve capacity in more severely affected patients. Surprisingly, we found considerable variability; indicating that some, but not all, patients showed motor unit reserve capacity. There are several explanations for this heterogeneity. First, these results may be due to the variability in NMJ dysfunction found both within and between patients with SMA.[27,31] NMJ dysfunction explains fatigability in a percentage of the patients, but further research is required to determine additional factors contributing to fatigability in the remaining part of the patient population. Another explanation may be that in some patients, motor function was relatively spared. The analyses of the endurance shuttle nine hole peg test (ESNHPT) in Chapter 3 included recordings from both patients for whom the ESNHPT was the highest achievable test, and patients who were also able to perform a more difficult test, i.e. endurance shuttle-box and block (ESBBT). We were thus able to perform analyses on a larger dataset, but this approach may have affected our results by underestimating the time-related effects of motor unit recruitment. Indeed, as described in Chapter 4, more consistent results on recruitment capacity have been found: exercise intensities at onset of the ESTs were similar in all patients.

Arm-cycling platform

The first chapters of this thesis contribute to a better understanding of the NMJ function in SMA during submaximal fatiguing dynamic exercise. However, the fact that individual patients showed different sEMG patterns and responded differently to pyridostigmine, a neuromuscular transmission enhancer, suggests that factors other than motor unit recruitment reserve and NMJ failure may also contribute to fatigability. Animal and human muscle biopsy studies reported on morphological, biochemical and mitochondrial content abnormalities as well as on, among other things, reduced capillary density in skeletal muscles.[37–45] Our next step was to investigate mitochondrial function (Chapter 6) and

capillary recruitment (Chapter 7) *in vivo* in patients with SMA types 3 and 4 during dynamic arm-cycling exercise.

A magnetic resonance (MR) compatible arm-cycling ergometer[46] provided the opportunity to perform upper-body exercise testing inside an MR-scanner with concomitant *in vivo* ^{31}phosphorus-magnetic resonance spectroscopy (^{31}P-MRS) interrogation of the upper arm musculature. In comparison with the ESTs, the character of the movements in the arm-cycling test are also cyclic, dynamic and paced on a pre-set frequency. By contrast, exercise load was the most important difference between the two performance tests. Whereas the ESTs were performed against a submaximal constant load, the workload of arm-cycling was progressively increased until exhaustion. Though fatigability is not a phenomenon which manifests at maximal workloads, a maximal exercise protocol was needed in order to stress the mitochondrial function inside the muscle (figure 1) and investigate its possible effect on fatigability. A maximal protocol ensured phosphocreatine (PCr) depletion by the end of exercise, which was necessary to examine muscle mitochondrial function during subsequent post-exercise recovery (Chapter 6).

However, pilot testing in the exercise laboratory revealed that the 'idle' workload of the ergometer (i.e., ~5W as a result of its particular mechanical properties) was already relatively high for many of the patients (Chapters 6 and 7). As at least 3 minutes of arm-cycling were needed to ensure the validity of the measured response time of the respiratory gas analyses datasets, the load was kept constant during the first six minutes of the test. It should be noted that it is more likely that the arm-cycling exercise results are a mixture of both maximal and endurance performances.

Furthermore, it should be noted that the actual mechanical workload of arm-cycling exercise tests, performed inside versus outside the MR-scanner, may not be identical, due to possible interaction of the 3 Tesla strong static magnetic field with moving non-ferrous metal components of the ergometer (e.g. brass bearings and aluminum cranks). Indeed, participants reported that cycling inside the MR-scanner was harder compared to the test outside the scanner. This was also reflected in the performance times (figure 2). Mean (SD) cycle time (min.) was significantly longer during the first visit (4.1 (2.6)) compared to both the m. biceps brachii (3.1 (1.9)) and m. triceps brachii (3.0 (2.1)) measurements during the second visit in patients with SMA, $p < 0.05$ (figure 2). Similarly, significantly longer cycling times were measured in controls (8.4 (2.5)) during the first visit compared to the m. triceps brachii (7.3 (2.3)) measurement during the second visit, $p < 0.05$. Consequently, we decided not to compare the outcomes of the different measurements during these two separate visits.

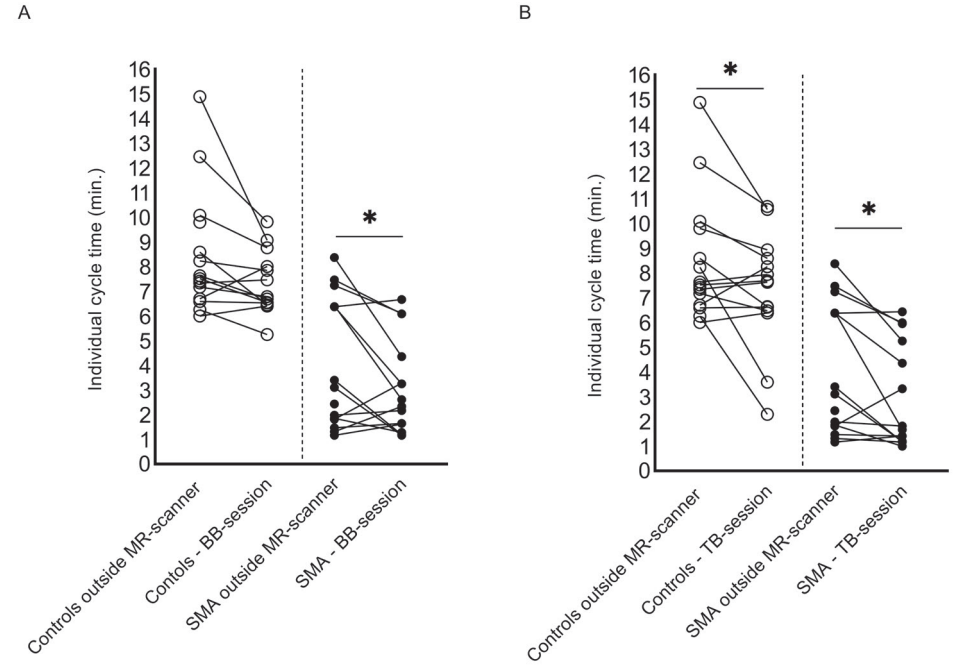

Figure 2. Paired individual cycle times of controls (open dots) and patients with SMA (solid dots) outside the MR-scanner during the first visit and inside the MR-scanner during both the m. biceps brachii (BB) session (A) and the m. triceps brachii (TB) session (B).

Another limitation of our present measurement set-up is that we were not able to measure high energy phosphate kinetics in the m. biceps brachii and m. triceps brachii simultaneously. This would have provided information on individual contributions of the muscles to the movement and, possibly, on which muscle primarily limited test performance. Additionally, simultaneous recordings of both muscles would have limited patients' burden since a second measurement session would not have been necessary.

Lastly, participants experienced some difficulties performing the arm-cycling test, particularly outside the scanner. Specifically, the respiratory gas exchange mask obstructed the view of the crank of the ergometer, resulting in difficulties with coordination dynamics at the start (Chapter 7). During execution of a first time activity, coordination dynamics might be less efficient compared to a frequently performed act.[47] For example, muscle co-contraction of antagonists may have affected sEMG signals and complicated their interpretation. We think that this factor was present more often during the arm-cycling task compared to the ESTs which reflected activities of daily life. We did not examine coordination dynamics quantitatively during the two tests, but future research might investigate this topic using sEMG recordings. Inefficient coordination dynamics may also contribute to fatigability.[47] On

the other hand, we performed qualitative examination of muscle co-contraction in order to interpret correctly the continuous wave near infrared spectroscopy (CW-NIRS) signals, as co-contraction or constant muscle activation may cause occlusion which consequently affects capillary recruitment. Individual post-exercise verbal feedback on the contribution of specific muscle groups during the exercise task and perceived fatigue of specific muscle groups also helped in the interpretation of sEMG and CW-NIRS signals. A short practice session and adequate verbal coaching during arm-cycling also helped to overcome this problem, at least in some of the participants.

Platform recommendations

With regard to future research, one question that needs to be asked is whether to recommend ESTs and arm-cycling exercise for the examination of factors of fatigability in patients with SMA. First and foremost, we were able to record high-quality data using different techniques described in the studies included in this thesis. Participants rated the acceptability of the two tests to lie between a mean of 8.3 (controls) and 9.6 (patients with SMA) on a scale from 0 (low) to 10 (high). These factors endorse the feasibility of the measurement set-ups of our experimental observational studies to investigate peripheral factors of fatigability in patients with SMA.

However, the issues regarding sEMG data interpretation, e.g. compensational strategies and coordination dynamics, seem to suggest that ESTs and the arm-cycling exercise test, as applied in Chapters 6 and 7, should be avoided in future studies, when solely investigating motor unit recruitment using sEMG. The patterns described should only be interpreted as a component of execution of a complex motor task, rather than as an indication of isolated muscle performance. A simplified exercise protocol of single muscle group activation may be sufficient to investigate motor unit recruitment capacity or NMJ function in future studies. For example, isokinetic movements with a constant speed on a Biodex® or Cybex® device may be an appropriate alternative.[48,49] The advantage of this system is that the range of motion of specific muscle groups can be established in advance and maintained during multiple contractions. Similarly, future studies should focus on the design of a surface coil which is able to measure both muscles simultaneously. An important adaptation to an - as yet to be developed - MR-compatible ergometer, is the option to stress only one muscle during isolated movements and to decrease the idle workload to ~0W. A submaximal protocol would then be possible and more severely affected patients with lower muscle strength could then also be included.

Peripheral factors of muscle strength and fatigability in SMA

Fatigability correlates with but is not equivalent to muscle weakness.[25] The results of our studies on the underlying mechanisms of fatigability in SMA have provided new insights into the correlations between fatigability, muscle strength and peripheral factors (figure 3). Below I will discuss the most important correlates and factors that remain to be studied.

Neuromuscular transmission failure increases fatigability

At the start of this project, we assumed that progressive failure of excitation-contraction coupling at the NMJ during task execution was an obvious candidate to explain fatigability. Since the NMJ is crucial for transmission of action potentials from the axon to myofibers, we hypothesized that neuromuscular transmission failure in a context of diminished motor unit capacity would cause fatigability because it would further limit the recruitment of motor units needed to prevent task failure. Our hypothesis is supported by the differences in sEMG results when patients used pyridostigmine or placebo (Chapter 4). Patients with SMA using pyridostigmine performed the task for a longer time at the same power output, while motor unit recruitment reserve was available. This might indicate that there is either less recruitment of higher-threshold motor units or that there is no need to increase firing rates of active motor units. Since pyridostigmine is a neuromuscular transmission enhancer, these results would tend to indicate a primary limiting factor of fatigability localized at the NMJ of upper extremity muscles, at least in some of the patients.

In line with our findings, previous work reported a reduction in tetanic force measured in SMA mice.[51] Specifically, these authors studied a milder phenotypic SMA mouse model and found inability to recruit 26% of the fibers while using neuronal stimulation compared to direct muscle stimulation.[51] This finding also points in the direction of axonal or NMJ abnormalities, but distinguishing between these locations was, at that time, not possible.

Future studies on the contribution of the NMJ function on fatigability may benefit from the MR-platform using ^{31}P-MRS combined with simultaneous sEMG measurements. Our sEMG recordings during ESTs revealed motor unit recruitment reserve by increasing amplitudes and decreasing median frequencies. The latter was additionally substantiated by similar patterns found during maximal arm-cycling exercise. At some point in time, however, patients were not able to continue the task; this stage was reached significantly earlier than in controls. Our hypothesis is that neuromuscular transmission failure is the underlying cause of this observation. This can best be investigated by developing an MR-compatible exercise platform with an idle workload of ~0W. If neuromuscular transmission fails, the MR spectrum at the end of exercise will reveal a substantial residual concentration of PCr in muscle fibers, while excitation contraction coupling failure at the level of the sarcoplasmic reticulum would cause >90% PCr depletion.

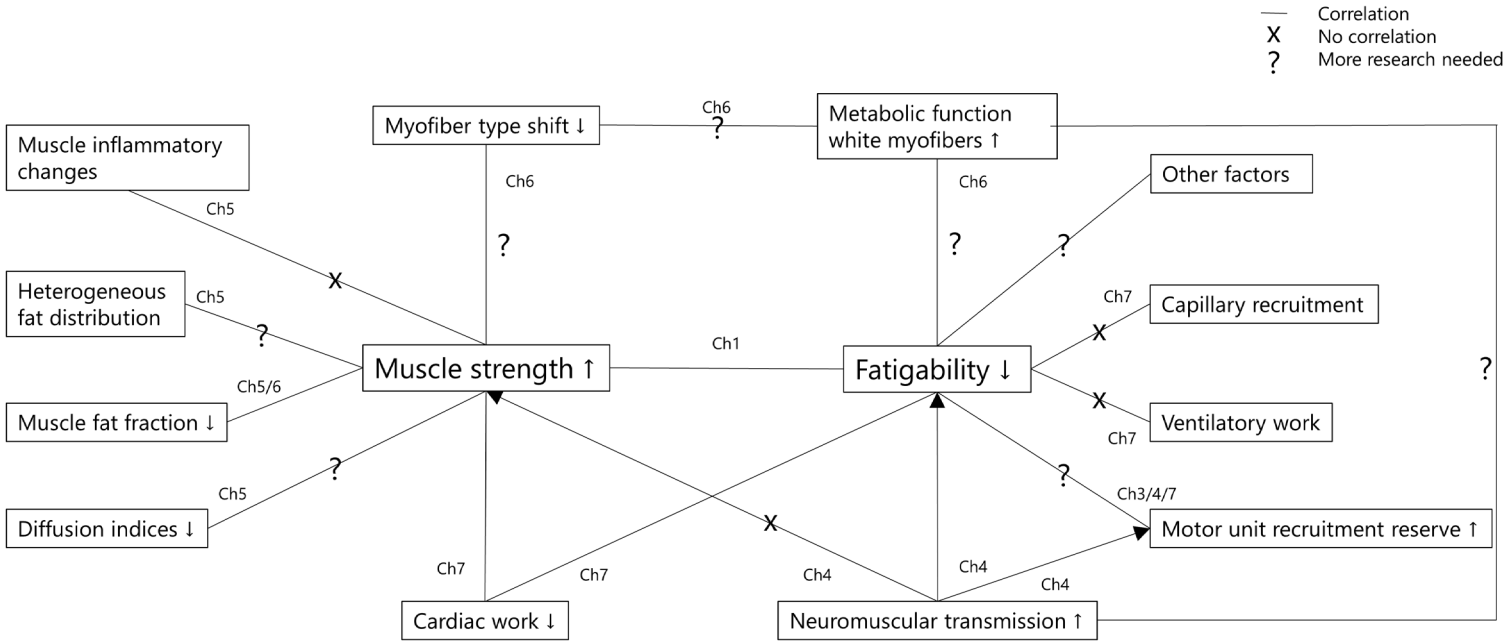

Figure 3. Updated overview of the correlates of fatigability[50] and muscle strength in patients with spinal muscular atrophy based on the studies described in this thesis. An arrow indicates the directional change. Ch = chapter in which the correlation has been investigated or suggested, X = investigated non-significant correlation, ? = possible contributing factor that should be investigated in future research.

Capillary recruitment does not limit performance in SMA types 3 and 4

Previous studies have reported vascular defects in muscle in (models of) SMA, including 'capillary rarefaction' which increases diffusion distances to myofibers and the NMJ.[45] All of these studies were conducted in severe SMA phenotypes, either in mouse models or patient muscle biopsies.[45,52] We investigated capillary recruitment *in vivo* in patients with SMA types 3 and 4. Using two different techniques, we provided evidence for an intact capillary recruitment.

First of all, relevant capillary defects in the patient cohort that we studied using the arm-cycling platform would have been detected using ^{31}P-MRS (Chapter 6). Previous *in vivo* ^{31}P-MRS studies in adolescents diagnosed with Juvenile Dermatomyositis, an inflammatory disease associated with capillary defects, demonstrated how the PCr, inorganic phosphate (P_i) and pH dynamics during exercise differed, both qualitatively and quantitatively, from what we currently observed in our cohort of patients with SMA.[53,54] Specifically, one might expect to observe pronounced acidification of red and intermediate fibers due to hypoxia, most probably associated with some mechanical malfunction requiring accelerated recruitment of white fibers and, as a consequence, an accelerated increase in P_i and drop in PCr. Conversely, during the metabolic recovery from exercise, capillary defects might be expected to manifest as slower, if not fundamentally altered kinetics (i.e., linear versus exponential kinetics) depending on severity. As red and intermediate fibers have more capillary contact points than white fibers,[34] associated with corresponding differences in oxidative metabolic capacity, the impact of capillary defects would have been most prominently observed in the P_i dynamics corresponding to these oxidative myofiber types.

Secondly, as described in Chapter 7, we used CW-NIRS to examine capillary recruitment in the m. biceps brachii (figure 1). If present, capillary defects would presumably have resulted in a decline in the [766-859] nm signal indicating a decrease in oxygenated hemoglobin,[55] but recordings in both patients and controls showed similar responses during maximal arm-cycling exercise. In contrast to these findings, a diminished change in deoxygenated hemoglobin during lower extremity exercise has previously been found in 19 patients with SMA, indicative of muscle oxygen uptake abnormalities.[56] This is the only other study in which CW-NIRS has been used in patients with SMA.[56] We suggest that the discordance in results between their findings and ours can be explained in two ways. First, we used the sum of two, instead of a single wavelength, to examine changes in deoxygenated hemoglobin concentrations. The downside of the single wavelength method is that hemoglobin, oxygenated hemoglobin, as well as oxidized cytochrome-c absorb light of this specific wavelength, and are thus all represented in the results.[57] By using the sum of two wavelengths, the contribution of oxygenated hemoglobin and oxidized cytochrome-c will be reduced. Second, it would not be inconceivable that the - in general - severely atrophied m. vastus lateralis of patients with SMA[8] contributed minimally to the cycling movement. This

might explain the minimal response in signals associated with deoxygenated hemoglobin.[56] In conclusion, our findings suggest capillary recruitment during dynamic exercise in patients with SMA types 3 and 4 is not a limiting factor of endurance performance (figure 3).

Muscle strength could correlate with non-uniform fat distribution

Quantitative magnetic resonance imaging (MRI) is being used increasingly to study muscle anatomy and to identify muscle specific biomarkers when monitoring treatment and disease progression in neuromuscular diseases including SMA.[31,58–64] Initial qualitative scales for fatty infiltration[60] were followed by quantitative approaches to determine fatty infiltration of muscle in SMA.[31,58,61] While increased fat fractions in both lower and upper extremity muscles are correlated with a decrease in muscle strength (figure 3), a non-symmetrical heterogeneous distribution of fat within the muscle (Chapter 5) has not previously been reported in SMA and is a factor which requires further research (figure 3).

In other neuromuscular diseases, including Duchenne muscular dystrophy and facioscapulohumeral muscular dystrophy, similar heterogeneous distributions of fatty infiltration have been described and linked to stretch-induced muscle damage.[65–67] Whereas these findings in Duchenne muscular dystrophy and facioscapulohumeral muscular dystrophy have been explained by a greater mechanical strain at the muscle end regions compared to the muscle belly,[65–67] such a mechanism can only partially explain our observation in patients with SMA, as higher percentages of fat were found in the proximal part of the m. triceps brachii and m. brachialis compared to the distal part.

Since mechanical strain at the tendinous regions of a muscle is determined by contraction force and the penation angle of the myofibers,[68] a difference in penation angle between the proximal and distal ends of the muscle may help explain the non-uniformity in fatty infiltration between the origin and insertion of a muscle.[65] The proximal penation angle in healthy m. biceps brachii has been reported to be larger than the distal penation angle,[69] but we found no non-uniform distribution of fatty infiltration in this muscle in our patient population. Further research on penation angles in SMA muscle, e.g. using MRI or ultrasonography, is needed to test the correlation with our MRI observations. Compared to MRI, 2D or 3D ultrasound imaging may be an alternative bedside or complementary in vivo technique.[70–72] Ultrasound imaging is potentially a faster and more cost-effective way of measuring skeletal muscle morphology.[70–72]

The question is: do mechanical factors provide any answers? It would also be interesting to investigate whether the pattern of fatty infiltration is, in any way, associated with functional muscle-specific vulnerability in SMA and/or SMN depletion. Further research is needed to examine the fat distribution in other muscles of patients with SMA to verify our results. If verified, heterogenic fat distributions may have important clinical implications for diagnostic MR examinations. For example, when comparing a longitudinal series of MR images to study

disease progression, the finding of a heterogeneous fat distribution in skeletal muscle implies that the precise location of the image should be exactly reproduced, for example using a mask alignment strategy.[59]

Low muscle strength could correlate with a white-to-red shift in myofiber type distribution

Another factor that could explain lower muscle strength in patients with SMA is the shift in myofiber type distribution (figure 3). In Chapter 6, we described our finding of a white-to-red shift in myofiber distribution in the m. biceps brachii muscle of patients with SMA types 3 and 4 which was indirectly correlated, using changes in capillary blood lactate, with a decrease in muscle strength.

A similar shift in myofiber composition has been reported in a study with SMA mice.[51] This phenomenon was worse in animals with lower SMN protein levels, suggesting an SMN-dependent relationship. Based on what has been learned about SMA pathophysiology, it is likely that a white-to-red shift in myofiber type composition is the result of a higher vulnerability of fast motor neurons and their associated white musculature to SMN depletion.[73] Follow-up research using ^{31}P-MRS techniques during a maximal exercise paradigm in patients treated with SMN enhancing therapies may clarify this issue. If associated with SMN depletion, the effect of such therapies may be found in a blunted shift in myofiber distribution in adolescent and adult patients with SMA types 3 and 4 during longitudinal follow-up measurements.

Fatigability could correlate with myofiber-selective mitochondrial dysfunction

Previous work suggested that mitochondrial dysfunction may be an important characteristic of SMA. At the start of the work described in this thesis, we regarded mitochondrial dysfunction as an important candidate to explain fatigability. We used ^{31}P-MRS to investigate the mitochondrial function in upper arm musculature of patients with SMA types 3 and 4 *in vivo* (Chapter 6). Patients with SMA showed rapid PCr depletion in combination with a blunted muscle acidification during arm-cycling exercise. Interestingly, we found no significant differences in post-exercise PCr recovery in patients with SMA compared to controls.

Though similar results of a rapid PCr depletion and blunted muscle acidification during exercise were found in patients with metabolic myopathies, e.g. mitochondrial myopathy and Mc Ardle disease,[74–79] we did not find abnormally slower PCr recovery times. The latter is indicative of normal mitochondrial function in our patient cohort. Similarly, post-exercise PCr recovery in other patients with a neuromuscular disease, i.e. Becker muscular dystrophy, was similar to controls, as described in previous studies.[80,81] Based on our findings, we concluded that oxidative phosphorylation in upper arm musculature is not

inhibited and does not, therefore, primarily limit endurance performance in adolescent and adult patients with SMA. However, this conclusion must be interpreted with caution since we did find myofiber-specific slower P_i recovery times. Specifically, slower P_i recovery times corresponding to white myofibers, that produce higher forces and are easily fatigable, indicated mitochondrial abnormalities. While these slower recovery times indicated some metabolic defects, they could not by themselves explain fatigability in SMA (Chapter 6). The relationship between myofiber selective mitochondrial dysfunction and fatigability requires further study (figure 3).

What could be the origin of white myofiber mitochondrial dysfunction?

At the start of the study on mitochondrial function in skeletal muscle of patients with SMA, we questioned whether mitochondrial dysfunction is a primary disease defect or secondary to denervation. Based on our findings, we favor the hypothesis that the origin of the observed mitochondrial ATP synthetic dysfunction in white myofibers is a secondary, rather than primary, muscle defect in patients with SMA types 3 and 4. If mitochondrial ATP synthetic dysfunction in white myofibers in SMA were the result of a primary muscle defect associated with failing expression of the ubiquitous SMN gene, it would be more likely that recovery of P_i (and PCr) levels post-exercise would be delayed across all myofiber types present in the interrogated arm muscles of the patients. Since cellular ATP supply in red and intermediate myofibers relies much more heavily on functional mitochondrial oxidative ADP phosphorylation than in white fibers,[82] our *in vivo* ^{31}P-MRS methodology is even more sensitive to detecting the consequence of mitochondrial dysfunction in the former. The fact that we did not find any delay of P_i recovery in red or intermediate myofibers post-exercise in the patients argues strongly against a primary muscle defect underlying mitochondrial dysfunction in white fibers of the arm muscles of our patients. A secondary origin would, therefore, seem more likely. For example, detraining of muscles has previously been shown to result in a decline in mitochondrial ATP synthetic capacity.[83] In patients, lack of regular voluntary recruitment (disuse) or failing neuromuscular transmission during recruitment of high-threshold motor units may effectively induce a state of detraining of the associated white myofibers. Future investigations into the efficacy of various proposed therapies in SMA, including both pharmaceutical as well as exercise therapies, may help clarify this issue. Here, the ^{31}P-MRS parameter, 95% recovery time of P_i in white myofibers, may be a particularly useful biomarker for evaluating which therapy and which delivery proves to be most effective in restoring mitochondrial function in white fibers.

Lastly, myofibers in motor neuron diseases, such as SMA, may undergo re-innervation after motor neuron death.[84,85] It would be interesting to be able to link our findings of mitochondrial dysfunction in white myofibers to neuromuscular transmission instability (figure 3). A literature search revealed that only a few studies have investigated this aspect.[86]

Most were conducted in relation to aging; we found only one investigation that explicitly set out to induce mitochondrial dysfunction in muscle and subsequently study its impact on neuromuscular transmission.[87] Unfortunately, the particular mechanism that was used to inflict mitochondrial dysfunction in muscle – i.e. overexpression of uncoupling protein 1 in a mouse model – also caused loss of a significant fraction of the motor neuron pool. No clear picture emerged, as mitochondrial dysfunction itself might in fact accelerate degeneration. A recent review, discussing current knowledge on this subject in the field of aging, reports that "most evidence suggests that mitochondrial dysfunction of muscle is secondary to denervation" but that "This is clearly an issue requiring additional study".[86] We suggest that NMJ model systems[88] may offer a solution for studying these issues in the future. Currently, there are no techniques for examining NMJ function in detail or *in vivo* in humans.

Techniques and methods to guide and evaluate treatment interventions

Techniques to investigate fatigability in SMA

Simultaneous recordings of multiple techniques

The view that fatigability is a very complex phenomenon is supported by the evidence of underlying mechanisms presented so far. In addition to the concept of using multiple biomarkers to examine these mechanisms in SMA, the heterogeneity in results is also indicative of a personalized approach in clinical therapy. For an even better understanding of SMA skeletal muscle function in relation to fatigability, I would suggest that further research be carried out using simultaneous recordings of multiple techniques, i.e. ^{31}P-MRS and sEMG, on individual muscles during isolated movements.[89–91] Theoretically, these experiments are possible.

Another suggestion for future research would be to take force measurements during ^{31}P-MRS exercise activities using an MR compatible ergometer. For example, a load cell can be incorporated in the carbon ski poles of the MR-compatible arm-cycling ergometer.[46] Combined with sEMG measurements, this may provide additional insight into coordination dynamics.

As the use of CW-NIRS in patients with a neuromuscular disease like SMA is accompanied by several significant limitations, I would not recommend the use of this technique, with its current restrictions. In addition to the above-mentioned disadvantages, high quality signal acquisition and signal interpretation remain difficult and depend on multiple factors, e.g. adipose tissue thickness, predefined differential pathlength factors, motion artifacts and light stray, which also impede signal quantification.[55,92,93] This may also explain why this technique has not frequently been applied in a clinical setting.

Non-voluntary electrodiagnostics

So far, the studies described in this thesis have focused on voluntary muscle activation. The following section will discuss the possibility of an inconsistency between this and electrically provoked activation. As we expect NMJ function to be a primary factor of fatigability, such a discrepancy may not be inconceivable. Motor unit number estimation (MUNE) is an electrodiagnostic tool to track motor unit loss during non-voluntary activation using nerve conduction studies.[94–96] Motor unit number index (MUNIX) and Mscan uses mathematical models based on compound motor unit action potentials (CMAP) and sEMG interference patterns.[95] These techniques can detect differences at an asymptomatic stage of SMA, while a reduction of at least 50% of motor neurons results in significant differences measured in muscle strength.[97] Hence, these techniques are feasible as new biomarkers with a high sensitivity.[98–100] An important advantage of these techniques is the lower dependency of daily subjective variations compared to voluntary functional outcome measures.[97] In future studies it would be interesting to combine electrodiagnostics, sEMG and ^{31}P-MRS when examining the differences between the existing number of motor units and dynamic maximal voluntary myofiber recruitment. This could ultimately help in assessing the opportunity to increase motor unit recruitment capacity using therapies with a training or pharmaceutical approach.

Metabolomics

Besides the non-invasive techniques used in our studies, blood spot samples for exploratory metabolomics may provide additional information on muscle metabolism in SMA.[101,102] Global quantitative analysis of the metabolome using high resolution mass spectroscopy involves comparing relative abundances of metabolites in multiple samples without prior identification.[102] Therefore, it is highly suitable for clinical populations with unidentified metabolic errors such as SMA.[103,104] Blood spot samples for exploratory metabolomics will be obtained prior to and directly following exercise. Next, a bioinformatics pipeline lists and visualizes which of the thousands of identified metabolites are deviating from a control situation. Our finding of mitochondrial dysfunction in white myofibers suggests the implementation of metabolomics prior to and after maximal exercise to investigate metabolites involved in post-exercise mitochondrial oxidative ADP phosphorylation. As such, abnormalities of specific metabolite concentrations may inform on the affected mitochondrial pathway in white myofibers. It is, however, important to bear in mind the possible bias in these analyses, since metabolites in the blood are not solely derived from active skeletal muscles.

Methods to evaluate early effects of pharmaceutical therapies

Since SMA phenotypes will change as a result of the newly available treatments, it is important that further research investigates their effect on the -possible- underlying mechanisms of fatigability.[105] Currently available molecular therapies aim for upregulation of SMN protein by either modulating *SMN2* gene or by *SMN1* gene therapy in patients with SMA.[1,18,106] These treatment strategies achieved impressive effects on survival in severe SMA (type 1).[107,108] However, the effects on motor function were more variable in patients with SMA types 1, 2 and 3.[108–114]

These differences may be explained by baseline differences, such as disease duration. The window of opportunity in which SMN-augmenting therapies may exert maximal effect probably differ between SMA types and even individual patients. A complicating factor for the near future is the application of different treatment strategies. Tissue distribution of *SMN2* splicing modifying drugs differs. Nusinersen is administered through intrathecal injections, whilst Risdiplam is administered orally. Systemic delivery of SMN enhancing drugs may eventually exert direct effects on multiple organs, including muscle.[1] The use of complementary pharmaceuticals that directly target the muscle and the NMJ, such as pyridostigmine (Chapter 4),[115,116] is currently under investigation. Analysis of efficacy of multi-drug treatment may become increasingly complicated. The studies described in this thesis provided biomarkers for the investigation of such combinational therapies. For example, it would be interesting to measure the effect of the SMN enhancing therapy nusinersen and pyridostigmine on motor unit recruitment. While nusinersen generally increases motor function,[117] i.e. muscle strength, our findings suggested that pyridostigmine specifically targets lower-threshold motor units, thereby decreasing fatigability (Chapter 4). Here, we mention several interesting biomarkers to be included in future research on the efficacy of this combined treatment. First of all, functional motor scales should be combined with endurance testing to investigate the therapeutic effect on both muscle strength and endurance performance, e.g. Hammersmith functional motor scale expanded with the ESTs. To examine the effect of both therapies on motor unit recruitment, sEMG signals could be recorded during both muscle specific maximal voluntary contractions and during repeated low-intensity isokinetic muscle contractions. Additionally, ^{31}P-MRS measurements may also provide insight into the effect of combination therapies. Specifically, P_i dynamics corresponding to red, intermediate or white myofibers, during dynamic exercise may inform on time-related myofiber recruitment.

Methods to guide and evaluate training interventions

Non-pharmaceutical therapies, such as exercise therapy, may also benefit patients with SMA types 3 and 4. Positive effects of exercise therapy have previously been reported in SMA mouse studies.[118,119] Based on the literature, high intensity training (HIT) may be expected to predominantly target fast-twitch myofibers, including white fibers.[119] As it may be hypothesized that disuse – and so 'detraining' – at least contributed to our finding of reduced mitochondrial ATP synthetic functionality in this particular myofiber type in our cohort of adolescent and adult patients with SMA types 3 and 4 (Chapter 6), our ^{31}P-MRS protocol would allow quantifying and tracking the effect of HIT on the basis of the rate of post-exercise recovery of the P_i signal, 4 ppm upfield of the PCr resonance compared to pre-training. In addition, positive effects on capacity for power-output and energy balance, respectively, may be expected to translate into a tractable altered time course of PCr depletion during exercise compared to pre-training.

Low-to-moderate intensity exercise training targeting red and intermediate myofiber recruitment may, on the other hand, be expected to enhance overall function of these particular myofiber types. In terms of our ^{31}P-MRS protocol, this would manifest, compared to pre-training, as a delayed need for recruitment of white myofibers – detectable by appearance of P_i signal, 4 ppm upfield of the PCr resonance – to maintain power-output required to execute the arm-cycling task. The length of time of this delay (in s) can then be used to quantify and track the training efficacy in individual patients. Since oxidative metabolic function of red and intermediate myofibers in the upper arm muscles of the patients in our cohort was found to be excellent, we do not expect that post-exercise metabolic recovery rate will act as a sensitive index for training efficacy in this particular neuromuscular disease; however, it may be informative in other (neuromuscular) myopathies.

Importantly, a recent systematic review of exercise training in patients with SMA type 3 showed that the available evidence on the beneficial or harmful effects of strength and aerobic exercise training is inconclusive.[120] Too little research has been carried out in adequate numbers of patients to support exercise guidelines in SMA. Especially in the light of recent major developments in pharmaceutical therapies aiming to improve muscle strength, evidence on training interventions is needed more than ever. In terms of skeletal muscle adaptations, it seems irrational to strive for increased muscle function using only these pharmaceutical therapies when the gain in muscle strength will not be optimally used nor maintained. Exercise programs are, therefore, the natural complement of new genetic treatment strategies. A clear challenge for future studies in designing optimal training programs is the considerable heterogeneity in SMA phenotypes. The studies described in this thesis may help to identify the best training modalities for individual patients.

References

1. Yeo CJJ, Darras BT. Overturning the Paradigm of Spinal Muscular Atrophy as just a Motor Neuron Disease. Pediatr Neurol. 2020;109:12-19.
2. Hamilton G, Gillingwater TH. Spinal muscular atrophy: Going beyond the motor neuron. Trends Mol Med. 2013;19(1):40-50.
3. Lefebvre S, Brglen L, Reboullet S, et al. Identification and characterization of a spinal muscular atrophy-determining gene. Cell. 1995;80(1):155-165.
4. Shababi M, Lorson CL, Rudnik-Schöneborn SS. Spinal muscular atrophy: A motor neuron disorder or a multi-organ disease? J Anat. 2014;224(1):15-28.
5. Hoffmann J. Ueber chronische spinale Muskelatrophie im Kindesalter, auf familiärer Basis. Dtsch Z Nervenheilkd. 1893;3:427-471.
6. Werdnig G. Zwei fruhinfantile hereditare Falle von progressiver Muskelatrophie unter dem Bilde der Dystrophie, aber auf neurotischer Grundlage. Arch Psychiatr Nervenkr. 1891;22:437-480.
7. Mercuri E, Bertini E, Iannaccone ST. Childhood spinal muscular atrophy: Controversies and challenges. Lancet Neurol. 2012;11(5):443-452.
8. Wadman RI, Wijngaarde CA, Stam M, et al. Muscle strength and motor function throughout life in a cross-sectional cohort of 180 patients with SMA types 1c-4. Eur J Neurol. 2018;25(3):512-518.
9. Deymeer F, Serdaroglu P, Parman Y, Poda M. Natural history of SMA IIIb: muscle strength decreases in a predictable sequence and magnitude. Neurology. 2008;71(9):644 LP - 649.
10. Deymeer F, Serdaroglu P, Poda M, Gulsen-Parman Y, Ozcelik T, Ozdemir C. Segmental distribution of muscle weakness in SMA III: implications for deterioration in muscle strength with time. Neuromuscul Disord. 1997;7(8):521-528.
11. Zerres K, Rudnik-Schöneborn S, Forrest E, Lusakowska A, Borkowska J, Hausmanowa-Petrusewicz I. A collaborative study on the natural history of childhood and juvenile onset proximal spinal muscular atrophy (type II and III SMA): 569 patients. J Neurol Sci. 1997;146(1):67-72.
12. Piepers S, van der Pol WL, Brugman F, Wokke JH, van den Berg LH. Natural history of SMA IIIb: muscle strength decreases in a predictable sequence and magnitude. Neurology. 2009;72(23):2057-2058; author reply 2058.
13. Piepers S, Van Den Berg LH, Brugman F, et al. A natural history study of late onset spinal muscular atrophy types 3b and 4. J Neurol. 2008;255(9):1400-1404.
14. Munsat TL, Davies KE. International SMA Consortium Meeting (26-28 June 1992, Bonn, Germany). Neuromuscul Disord. 1992;2(5-6):423-428.
15. Dubowitz V. Chaos in the classification of SMA: A possible resolution. Neuromuscul Disord. 1995;5(1):3-5.
16. Wijngaarde CA, Stam M, Otto LAM, et al. Muscle strength and motor function in adolescents and adults with spinal muscular atrophy. Neurology. 2020;95(14):e1988-e1998.
17. Wadman RI, Jansen MD, Stam M, et al. Intragenic and structural variation in the SMN locus and clinical variability in spinal muscular atrophy. Brain Commun. 2020;2(2):1-13.

18. Wirth B, Karakaya M, Kye MJ, Mendoza-Ferreira N. Twenty-Five Years of Spinal Muscular Atrophy Research: From Phenotype to Genotype to Therapy, and What Comes Next. Annu Rev Genomics Hum Genet. 2020;21:231-261.
19. Boyer JG, Bowerman M, Kothary R. The many faces of SMN: Deciphering the function critical to spinal muscular atrophy pathogenesis. Future Neurol. 2010;5(6):873-890.
20. Martínez-Hernández R, Soler-Botija C, Also E, et al. The developmental pattern of myotubes in spinal muscular atrophy indicates prenatal delay of muscle maturation. J Neuropathol Exp Neurol. 2009;68(5):474-481.
21. Stam M, Wadman RI, Bartels B, et al. A continuous repetitive task to detect fatigability in spinal muscular atrophy. Orphanet J Rare Dis. 2018;13(1):1-7.
22. Montes J, McDermott MP, Martens WB, et al. Six-minute walk test demonstrates motor fatigue in spinal muscular atrophy. Neurology. 2010;74(10):833-838.
23. Bartels B, Habets LE, Stam M, et al. Assessment of fatigability in patients with spinal muscular atrophy: Development and content validity of a set of endurance tests. BMC Neurol. 2019;19(1):1-10.
24. Bartels B, Groot JF De, Habets LE, et al. Fatigability in spinal muscular atrophy : validity and reliability of endurance shuttle tests. Orphanet J Rare Dis. 2020;2:1-9.
25. Bartels B, de Groot JF, Habets LE, et al. Correlates of fatigability in patients with spinal muscular atrophy. Neurology. 2021;96(6):845-852.
26. Milner-Brown HS, Miller RG. Increased muscular fatigue in patients with neurogenic muscle weakness: quantification and pathophysiology. Arch Phys Med Rehabil. 1989;70(5):361-366.
27. Wadman RI, Vrancken AFJ, Van den Berg LH, Van der Pol WL. Dysfunction of the neuromuscular junction in patients with spinal muscular atrophy type 2 and 3. Neurology. 2012;79:2050-2055.
28. Pera MC, Luigetti M, Pane M, et al. 6MWT can identify type 3 SMA patients with neuromuscular junction dysfunction. Neuromuscul Disord. 2017;27(10):879-882.
29. Kariya S, Park GH, Maeno-Hikichi Y, et al. Reduced SMN protein impairs maturation of the neuromuscular junctions in mouse models of spinal muscular atrophy. Hum Mol Genet. 2008;17(16):2552-2569.
30. Goulet B, Kothary R, Parks R. At the "Junction" of Spinal Muscular Atrophy Pathogenesis: The Role of Neuromuscular Junction Dysfunction in SMA Disease Progression. Curr Mol Med. 2013;13(7):1160-1174.
31. Chabanon A, Seferian AM, Daron A, et al. Prospective and longitudinal natural history study of patients with Type 2 and 3 spinal muscular atrophy: Baseline data NatHis-SMA study. PLoS One. 2018;13(7):1-28.
32. Hunter SK. Performance fatigability: Mechanisms and task specificity. Cold Spring Harb Perspect Med. 2018;8(7):1-22.
33. Buller BYAJ, Eccles JC, Eccles RM. INTERACTIONS BETWEEN MOTONEURONES AND MUSCLES IN RESPECT OF THE CHARACTERISTIC SPEEDS OF THEIR RESPONSES From the Department of Physiology , Australian National University , presented which suggested that the differentiation of slow muscles of the cat hin. J Physiol. 1960:417-439.
34. Glancy B, Hsu LY, Dao L, et al. In Vivo microscopy reveals extensive embedding of capillaries within the sarcolemma of skeletal muscle fibers. Microcirculation. 2014;21(2):131-147.
35. Revill SM, Morgan MDL, Singh SJ, Williams J, Hardman AE. The endurance shuttle walk test: a new field exercise test for the assessment of endurance capacity in chronic obstructive pulmonary disease. Thorax. 1999;54:213-222.

36. Peeters LHC, Janssen MMHP, Kingma I, van Dieën JH, de Groot IJM. Patients with spinal muscular atrophy use high percentages of trunk muscle capacity to perform seated tasks. Am J Phys Med Rehabil. 2019:1.
37. Hausmanowa-Petrusewicz I, Vrbová G. Spinal muscular atrophy: A delayed development hypothesis. Neuroreport. 2005;16(7):657-661.
38. Boyer JG, Deguise MO, Murray LM, et al. Myogenic program dysregulation is contributory to disease pathogenesis in spinal muscular atrophy. Hum Mol Genet. 2014;23(16):4249-4259.
39. Hayhurst M, Wagner AK, Cerletti M, Wagers AJ, Rubin LL. A cell-autonomous defect in skeletal muscle satellite cells expressing low levels of survival of motor neuron protein. Dev Biol. 2012;368(2):323-334.
40. Bricceno K V., Martinez T, Leikina E, et al. Survival motor neuron protein deficiency impairs myotube formation by altering myogenic gene expression and focal adhesion dynamics. Hum Mol Genet. 2014;23(18):4745-4757.
41. Ripolone M, Ronchi D, Violano R, et al. Impaired Muscle Mitochondrial Biogenesis and Myogenesis in Spinal Muscular Atrophy. JAMA Neurol. 2015;72(6):1-10.
42. Miller N, Shi H, Zelikovich A., Ma Y-C. Motor Neuron Mitochondrial Dysfunction in Spinal Muscular Atrophy. Hum Mol Genet. 2016;25(16):3395-3406.
43. Nobutoki T, Ihara T. Early disruption of neurovascular units and microcirculatory dysfunction in the spinal cord in spinal muscular atrophy type I. Med Hypotheses. 2015;85(6):842-845.
44. Shababi M, Habibi J, Ma L, Glascock JJ, Sowers JR, Lorson CL. Partial restoration of cardio-vascular defects in a rescued severe model of spinal muscular atrophy. J Mol Cell Cardiol. 2012;52(5):1074-1082.
45. Somers E, Lees RD, Hoban K, et al. Vascular Defects and Spinal Cord Hypoxia in Spinal Muscular Atrophy. Ann Neurol. 2016;79(2):217-230.
46. Vegter RJ, Brink S van den, Mouton L, Sibeijn-Kuiper A, Woude L, Jeneson J. Magnetic Resonance-Compatible Arm-Crank Ergometry: A New Platform Linking Whole-Body Calorimetry to Upper-Extremity Biomechanics and Arm Muscle Metabolism. Front Neurol. 2021;12(February):1-13.
47. Osu R, Franklin DW, Kato H, et al. Short- and long-term changes in joint co-contraction associated with motor learning as revealed from surface EMG. J Neurophysiol. 2002;88(2):991-1004.
48. Tiffreau V, Ledoux I, Eymard B, Thévenon A, Hogrel JY. Isokinetic muscle testing for weak patients suffering from neuromuscular disorders: A reliability study. Neuromuscul Disord. 2007;17(7):524-531.
49. de Araujo Ribeiro Alvares JB, Rodrigues R, de Azevedo Franke R, et al. Inter-machine reliability of the Biodex and Cybex isokinetic dynamometers for knee flexor/extensor isometric, concentric and eccentric tests. Phys Ther Sport. 2015;16(1):59-65.
50. Bartels B. Fatigability in Spinal Muscular Atrophy.; 2020.
51. Deguise MO, De Repentigny Y, Tierney A, et al. Motor transmission defects with sex differences in a new mouse model of mild spinal muscular atrophy. EBioMedicine. 2020;55:102750.
52. Zhou H, Ying H, Scoto M, Brogan P, Parson S, Muntoni F. Microvascular abnormality in spinal muscular atrophy and its response to antisense oligonucleotide therapy. Neuromuscul Disord. 2015;25(2015):S193.
53. van Brussel M, van Oorschot JWM, Schmitz JPJ, et al. Muscle Metabolic Responses During Dynamic In-Magnet Exercise Testing: A Pilot Study in Children with an Idiopathic Inflammatory Myopathy. Acad Radiol. 2015;22(11):1443-1448.

54. Cea G, Bendahan D, Manners D, et al. Reduced oxidative phosphorylation and proton efflux suggest reduced capillary blood supply in skeletal muscle of patients with dermatomyositis and polymyositis : a quantitative 31 P-magnetic resonance spectroscopy and MRI study. 2002.
55. McCully KK, Hamaoka T. NIRS - what can it tell us about oxygen saturation in skeletal muscle. Exerc Sport Sci Rev. 2000;28(3):123-127.
56. Montes J, Goodwin AM, McDermott MP, et al. Diminished muscle oxygen uptake and fatigue in spinal muscular atrophy. Ann Clin Transl Neurol. 2021:1-10.
57. Piantadosi CA. Near infrared spectroscopy: Principles and application to noninvasive assessment of tissue oxygenation. J Crit Care. 1989;4(4):308-318.
58. Otto LAM, van der Pol WL, Schlaffke L, et al. Quantitative MRI of skeletal muscle in a cross-sectional cohort of patients with spinal muscular atrophy types 2 and 3. NMR Biomed. 2020;(March):1-13.
59. Otto LA., Froeling M, van Eijk RP., et al. Quantification of disease progression in spinal muscular atrophy with muscle MRI – a pilot study. NMR Biomed. 2021:1-11.
60. Brogna C, Cristiano L, Verdolotti T, et al. MRI patterns of muscle involvement in type 2 and 3 spinal muscular atrophy patients. J Neurol. 2020;267(4):898-912.
61. Bonati U, Holiga Š, Hellbach N, et al. Longitudinal characterization of biomarkers for spinal muscular atrophy. Ann Clin Transl Neurol. 2017;4(5):292-304.
62. Brogna C, Cristiano L, Verdolotti T, et al. Predominant distal muscle involvement in spinal muscular atrophy. Neuromuscul Disord. 2019;29(11):910-911.
63. Durmus H, Yilmaz R, Gulsen-Parman Y, et al. Muscle magnetic resonance imaging in spinal muscular atrophy type 3: Selective and progressive involvement. Muscle and Nerve. 2017;55(5):651-656.
64. Strijkers GJ, Araujo ECA, Azzabou N, et al. Exploration of new contrasts, targets, and MR imaging and spectroscopy techniques for neuromuscular disease-A workshop report of working group 3 of the biomedicine and molecular biosciences COST action BM1304 MYO-MRI. J Neuromuscul Dis. 2019;6(1):1-30.
65. Shin DD, Hodgson JA, Edgerton VR, Sinha S. In vivo intramuscular fascicle-aponeuroses dynamics of the human medial gastrocnemius during plantarflexion and dorsiflexion of the foot. J Appl Physiol. 2009;107(4):1276-1284.
66. Morgan DL, Proske U. Popping Sarcomere Hypothesis Explains Stretch-Induced Muscle Damage. Clin Exp Phamacology Physiol. 2004;(31):541-545.
67. Hooijmans MT, Niks EH, Burakiewicz J, et al. Non-uniform muscle fat replacement along the proximodistal axis in Duchenne muscular dystrophy. Neuromuscul Disord. 2017;27(5):458-464.
68. Wisdom KM, Delp SL, Kuhl E. Use it or lose it: Multiscale skeletal muscle adaptation to mechanical stimuli. Biomech Model Mechanobiol. 2015;14(2):195-215.
69. Asakawa DS, Pappas G., Drace JE, Delp SL. Aponeurosis Length and Fascicle Insertion Angles of the Biceps Brachii. J Mech Med Biol. 2002;02(03n04):449-455.
70. Weide G, Van Der Zwaard S, Huijing PA, Jaspers RT, Harlaar J. 3D ultrasound imaging: Fast and cost-effective morphometry of musculoskeletal tissue. J Vis Exp. 2017;2017(129):1-10.
71. Wu JS, Darras BT, Rutkove SB. Assessing spinal muscular atrophy with quantitative ultrasound. Neurology. 2010;75(6):526-531.

72. Nakamura R, Kitamura A, Tsukamoto T, et al. Spinal muscular atrophy type 3 showing a specific pattern of selective vulnerability on muscle ultrasound. Intern Med. 2021;60(12):1935-1939.
73. Boyd PJ, Tu WY, Shorrock HK, et al. Bioenergetic status modulates motor neuron vulnerability and pathogenesis in a zebrafish model of spinal muscular atrophy. PLoS Genet. 2017;13(4):1-27.
74. Tonon C, Gramegna LL, Lodi R. Magnetic resonance imaging and spectroscopy in the evaluation of neuromuscular disorders and fatigue. Neuromuscul Disord. 2012;22(SUPPL. 3):S187-S191.
75. Diekman EF, Visser G, Schmitz JPJ, et al. Altered energetics of exercise explain risk of rhabdomyolysis in very long-chain acyl-coa dehydrogenase deficiency. PLoS One. 2016;11(2):1-19.
76. Ross BD, Radda GK. Application of 31P n.m.r. to inborn errors of muscle metabolism. Biochem Soc Trans. 1983;11(6):627-630.
77. Arnold DL, Taylor DJ, Radda GK. Investigation of human mitochondrial myopathies by phosphorus magnetic resonance spectroscopy. Ann Neurol. 1985;18(2):189-196.
78. Argov Z, Bank WJ, Maris J, Peterson P, Chance B. Bioenergetic heterogeneity of human mitochondrial myopathies. Neurology. 1987;37(2):257.
79. Bakker HD, Scholte HR, Jeneson JAL. Vitamin E in a mitochondrial myopathy with proliferating mitochondria. Lancet. 1993;342:175-176.
80. Lodi R, Kemp GJ, Muntoni F, et al. Reduced cytosolic acidification during exercise suggests defective glycolytic activity in skeletal muscle of patients with Becker muscular dystrophy. An in vivo 31P magnetic resonance spectroscopy study. Brain. 1999;122(1):121-130.
81. Tosetti M, Linsalata S, Battini R, et al. Muscle metabolic alterations assessed by 31-phosphorus magnetic resonance spectroscopy in mild becker muscular dystrophy. Muscle Nerve. 2011;44(5):816-819.
82. Schiaffino S, Reggiani C. Fiber types in Mammalian skeletal muscles. Physiol Rev. 2011;91(4):1447-1531.
83. Wibom R, Hultman E, Johansson M, Matherei K, Constantin-Teodosiu D, Schantz PG. Adaptation of mitochondrial ATP production in human skeletal muscle to endurance training and detraining. J Appl Physiol. 1992;73(5):2004-2010.
84. Holloszy JO, Larsson L. Motor Units: Remodeling in Aged Animals. Journals Gerontol Ser A. 1995;50A(Special_ Issue):91-95.
85. Johnson MA, Kucukyalcin DK. Patterns of abnormal histochemical fibre type differentiation in human muscle biopsies. J Neurol Sci. 1978;37:159-178.
86. Anagnostou ME, Hepple RT. Mitochondrial Mechanisms of Neuromuscular Junction Degeneration with Aging. Cells. 2020;9(1).
87. Dupuis L, Gonzalez de Aguilar JL, Echaniz-Laguna A, et al. Muscle mitochondrial uncoupling dismantles neuromuscular junction and triggers distal degeneration of motor neurons. PLoS One. 2009;4(4).
88. De Jong R, Spijkers XM, Paseuning-Vuhman S, Vulto P, Pasterkamp RJ. Journal of Neurochemistry - 2021 - Jongh - Neuromuscular junction on a chip ALS disease modeling and read out development.pdf. J Neurochem. 2021;(157):393-412.
89. Vestergaard-Poulsen P, Thomsen C, Sinkjaer T, Hendriksen O. Simultaneous 31P NMR spectroscopy and EMG in exercising and recovering human skeletal muscle: Technical aspects. Magn Reson Med. 1994;31(2):93-102.

90. Ryan TE, Southern WM, Reynolds MA, McCully KK. A cross-validation of near-infrared spectroscopy measurements of skeletal muscle oxidative capacity with phosphorus magnetic resonance spectroscopy. J Appl Physiol. 2013;115(12):1757-1766.
91. Kemp GJ, Roberts N, Bimson WE, et al. Mitochondrial function and oxygen supply in normal and in chronically ischemic muscle: A combined 31P magnetic resonance spectroscopy and near infrared spectroscopy study in vivo. J Vasc Surg. 2001;34(6):1103-1110.
92. Perrey S, Ferrari M. Muscle Oximetry in Sports Science: A Systematic Review. Sport Med. 2017:1-20.
93. Hamaoka T, McCully KK, Quaresima V, Yamamoto K, Chance B. Near-infrared spectroscopy/imaging for monitoring muscle oxygenation and oxidative metabolism in healthy and diseased humans. J Biomed Opt. 2007;12(6):062105.
94. Bostock H. Estimating motor unit numbers from a CMAP scan. Muscle and Nerve. 2016;53(6):889-896.
95. Gooch CL, Doherty TJ, Chan KM, et al. Motor unit number estimation: A technology and literature review. Muscle and Nerve. 2014;50(6):884-893.
96. Kariyawasam D, D'silva A, Howells J, et al. Motor unit changes in children with symptomatic spinal muscular atrophy treated with nusinersen. J Neurol Neurosurg Psychiatry. 2021;92(1):78-85.
97. Neuwirth C, Weber M. MUNIX in children with spinal muscular atrophy: An unexpected journey. Muscle and Nerve. 2020;(July):565-566.
98. Verma S, Forte J, Ritchey M, Shah D. Motor unit number index in children with later-onset spinal muscular atrophy. Muscle and Nerve. 2020;(March):633-637.
99. Querin G, Lenglet T, Debs R, et al. The motor unit number index (MUNIX) profile of patients with adult spinal muscular atrophy. Clin Neurophysiol. 2018;129(11):2333-2340.
100. Sleutjes BTHM, Wijngaarde CA, Wadman RI, et al. Assessment of motor unit loss in patients with spinal muscular atrophy. Clin Neurophysiol. 2020;131(6):1280-1286.
101. Zhang XW, Li QH, Xu Z Di, Dou JJ. Mass spectrometry-based metabolomics in health and medical science: A systematic review. RSC Adv. 2020;10(6):3092-3104.
102. Schranner D, Kastenmüller G, Schönfelder M, Römisch-Margl W, Wackerhage H. Metabolite Concentration Changes in Humans After a Bout of Exercise: a Systematic Review of Exercise Metabolomics Studies. Sport Med - Open. 2020;6(1).
103. Denes J, Szabo E, Robinette S, et al. Metabonomics of newborn screening dried blood spot samples – a novel approach in the screening and diagnostics of inborn errors of metabolism. Anal Chem. 2012;(84):10113-10120.
104. Takats Z. Analysis of dried blood spot samples by high resolution mass spectrometry - From newborn screening to cancer diagnostics. Clin Biochem. 2014;47(9):699.
105. Smeriglio P, Langard P, Querin G, Biferi MG. The identification of novel biomarkers is required to improve adult SMA patient stratification, diagnosis and treatment. J Pers Med. 2020;10(3):1-23.
106. Bowerman M, Becker CG, Yáñez-Muñoz RJ, et al. Therapeutic strategies for spinal muscular atrophy: SMN and beyond. DMM Dis Model Mech. 2017;10(8):943-954.
107. Passini M a, Bu J, Richards AM, et al. Antisense Oligonucleotides Delivered to the Mouse CNS Ameliorate Symptoms of Severe Spinal Muscular Atrophy. Sci Transl Med. 2011;3(72).

108. Finkel RS, Mercuri E, Darras BT, et al. Nusinersen versus sham control in infantile-onset spinal muscular atrophy. N Engl J Med. 2017;377(18):1723-1732.
109. Walter MC, Wenninger S, Thiele S, et al. Safety and treatment effects of nusinersen in longstanding adult 5q-SMA type 3 – A prospective observational study. J Neuromuscul Dis. 2019;6(4):453-465.
110. Hagenacker T, Wurster CD, Günther R, et al. Nusinersen in adults with 5q spinal muscular atrophy: a non-interventional, multicentre, observational cohort study. Lancet Neurol. 2020;19(4):317-325.
111. Jochmann E, Steinbach R, Jochmann T, et al. Experiences from treating seven adult 5q spinal muscular atrophy patients with Nusinersen. Ther Adv Neurol Disord. 2020;13:1-11.
112. Mercuri E, Darras BT, Chiriboga CA, et al. Nusinersen versus sham control in later-onset spinal muscular atrophy. N Engl J Med. 2018;378(7):625-635.
113. Finkel R, Day J, Darras B, et al. Phase 1 study of intrathecal administration of AVXS-101 gene-replacement therapy (GRT) for spinal muscular atrophy type 2 (SMA2) (STRONG). Neurology. 2019;92(15 Supplement):P1.6-059.
114. Mendell JR, Al-Zaidy S, Shell R, et al. Single-dose gene-replacement therapy for spinal muscular atrophy. N Engl J Med. 2017;377(18):1713-1722.
115. Riker WF, Wescoe WC. The direct action of prostigmine on skeletal muscle; its relationship to the choline esters. J Pharmacol Exp Ther. 1946:58-66.
116. Stam M, Wijngaarde C, Bartels B, et al. Space trial. A phase 2, monocenter, double-blind, placebo-controlled, cross-over trial to assess efficacy of pyridostigmine in patients with spinal muscular atrophy types 2,3 and 4. In: Anaheim, California: Cure SMA June 30; 2019.
117. Hoy SM. Nusinersen: A Review in 5q Spinal Muscular Atrophy. CNS Drugs. 2018;32(7):689-696.
118. Chali F, Desseille C, Houdebine L, et al. Long-term exercise-specific neuroprotection in spinal muscular atrophy-like mice. J Physiol. 2016;594(7):1931-1952.
119. Houdebine L, D'Amico D, Bastin J, et al. Low-Intensity Running and High-Intensity Swimming Exercises Differentially Improve Energy Metabolism in Mice With Mild Spinal Muscular Atrophy. Front Physiol. 2019;10(October):1-21.
120. Bartels B, Montes J, Van Der Pol WL, De Groot JF. Physical exercise training for type 3 spinal muscular atrophy. Cochrane Database Syst Rev. 2019(3).

Appendices

Nederlandse samenvatting

Spinale musculaire atrofie, kortweg SMA, is een autosomaal recessieve neuromusculaire aandoening. Jaarlijks worden in Nederland 15-20 kinderen geboren met SMA. Dit zorgt ervoor dat SMA, tot de komst van therapieën in 2017, een van de belangrijkste genetische oorzaken van kindersterfte was. De oorzaak van SMA ligt in het ontbreken van een genetische code op beide exemplaren van het vijfde chromosoom, het *SMN1* gen. Door de afwezigheid van het *SMN1* gen wordt onvoldoende SMN-eiwit aangemaakt. Het menselijke erfelijke materiaal bevat een tweede SMN gen, *SMN2*, dat slechts geringe hoeveelheden SMN-eiwit produceert. SMN-eiwit wordt door alle cellen gebruikt voor een aantal basale functies zoals de celontwikkeling, de vorm en opbouw van het cytoskelet, bio-energetische processen en de afgifte van synapsblaasjes. De gevolgen van een tekort aan het SMN-eiwit zijn voor cellen heel verschillend. De alfa-motor neuronen die vanuit het ruggenmerg de hersenen met de spieren verbinden, functioneren niet goed bij een tekort. Het ontbreken van voldoende SMN-eiwit zorgt daarom in deze alfa-motor neuronen voor degeneratie. Hierdoor ontstaan de spieratrofie (verschrompelen van spierweefsel) en progressieve spierzwakte die kenmerkend zijn voor SMA en die aan het einde van de 19e eeuw voor het eerst werden beschreven. Tegenwoordig zijn er steeds meer aanwijzingen dat ook andere cellen en weefsels gevoelig zijn voor een tekort aan SMN-eiwit.

Er bestaat bij SMA een grote variatie in de ernst van ziekteklachten. SMA wordt, op basis van de leeftijd waarop de klachten ontstaan en de behaalde motorische mijlpalen, onderverdeeld in vier verschillende types (1-4) die een spectrum van ziekte-ernst weergeven (zie tabel 1). In dit proefschrift worden onderzoeken beschreven waaraan mensen met SMA type 2 tot 4 hebben deelgenomen. SMA type 2 wordt gekenmerkt door een debuut van klachten op een leeftijd tussen de 6 en 18 maanden en het behalen van de motorische mijlpaal van het zelfstandig kunnen zitten. Bij mensen met SMA type 3 is het debuut van klachten op een leeftijd van >18 maanden. Zij zijn (op enig moment in hun leven) in staat (geweest) zelfstandig te lopen. Het mildere SMA type 4 komt tot uiting op de volwassen leeftijd waarbij de ambulante functie vaak lang behouden blijft.

Spieren van de romp en onderste ledematen zijn over het algemeen het meest ernstig aangedaan, maar spierzwakte komt ook voor in de armen en ademhalingsspieren. Naast spierzwakte is snel optredende vermoeibaarheid bij repeterende bewegingen een belangrijk symptoom van SMA. Met 'vermoeibaarheid' tijdens bijvoorbeeld het lopen, schrijven, kauwen of haren kammen wordt het niet langdurig kunnen volhouden van de handeling op een zelfde intensiteit bedoeld, terwijl iemand wel fysiek in staat is om de handeling op zich uit te voeren.

Tabel 1. SMA klassificatiesysteem

SMA type	**1 (Werdnig-Hoffman syndroom)**	**2**	**3 (Kugelberg-Welander syndroom)**	**4**
Debuut van klachten	0-6 maanden	6-18 maanden	3a: 1,5-3 jaar 3b: >3 jaar	>30 jaar
Incidentie	50%	30%	20%	<1%
Zelfstandig zitten	nee	ja	ja	ja
zelfstandig lopen	nee	nee	ja	ja
Mediane leeftijdsverwachting	overlijdt prenataal of overleeft een aantal dagen tot 17 jaar	afhankelijk van beademing wordt het overgrote deel volwassen	normale levensver-wachting	normale levensver-wachting

Om te begrijpen hoe een beweging uitgevoerd wordt, is kennis van spiervezels nodig. Menselijke spieren zijn grofweg opgebouwd uit drie verschillende spiervezels met elk verschillende eigenschappen. Rode spiervezels hebben veel mitochondria – de energiefabrieken van een cel – , hebben zuurstof nodig om te werken, leveren relatief weinig kracht en zijn minder gevoelig voor vermoeibaarheid. Witte spiervezels hebben daarentegen relatief weinig mitochondria, kunnen snel, zonder zuurstof energie opwekken en kunnen voor korte tijd veel kracht leveren. Intermediaire spiervezels functioneren, zoals de naam al aangeeft, tussen de rode en witte spiervezels in. Uitkomsten van onderzoeken met spierbiopten zijn niet eenduidig met betrekking tot de kwetsbaarheid van verschillende spiervezeltypes als gevolg van SMA. Over het algemeen wordt een grotere kwetsbaarheid van witte spiervezels vermeld als oorzaak voor de afname van de maximaal leverbare kracht. Echter, de spiervezelsamenstelling is niet eerder bij patiënten gemeten tijdens inspanning. Wanneer inspanning geleverd wordt, zullen rode spiervezels altijd het eerst geactiveerd worden om een bepaalde kracht te leveren. Daarna zullen de intermediaire en witte spiervezels bijspringen. De alfa-motor neuron (zenuw), de neuromusculaire (van zenuw naar spier) overgang en de spier vormen samen een motor unit. De hoeveelheid motor units die er nog is om bij te springen nadat een activiteit is ingezet, bepaalt de reservecapaciteit van de spier. Mogelijk speelt een kleinere reservecapaciteit een rol bij vermoeibaarheid maar de onderliggende oorzaak van vermoeibaarheid is voor een deel nog onbekend.

Een van de factoren die wel al in verband is gebracht met vermoeibaarheid bij SMA, is een verstoring in de signaaloverdracht van de zenuw naar de spier, via de neuromusculaire overgang. Dit symptoom werd bij ongeveer de helft van de patiënten waargenomen met behulp van EMG onderzoek door middel van repeterende stimulatie van de zenuwen. Verondersteld wordt dat dit percentage een onderschatting is van de werkelijkheid omdat repetitieve zenuwstimulatie niet sensitief genoeg is om alle verstoringen goed te kunnen meten. Het medicijn pyridostigmine, dat de signaaloverdracht via de neuromusculaire overgang verbetert, helpt vermoeibaarheid te verminderen in een deel van de patiënten met SMA. Daarom is het belangrijk om ook onderzoek te doen naar andere factoren die mogelijk bijdragen aan vermoeibaarheid.

Een mogelijke andere factor van vermoeibaarheid is een verandering in de mitochondriële functie in spiercellen. Mitochondria kunnen worden gezien als de batterijen van een cel. Ze zorgen voor de energiehuishouding waarbij zuurstof betrokken is. Rode en intermediaire spiervezels hebben een grote hoeveelheid mitochondria. Een abnormale functie van de mitochondria kan daarom vooral in deze spiervezels mogelijk leiden tot snelle vermoeibaarheid omdat ze dan niet genoeg energie hebben om langdurig kracht te leveren. Studies in SMA diermodellen en in spierbiopten van mensen met SMA lijken hierop te wijzen, maar dit is niet eerder bij patiënten tijdens het leveren van inspanning onderzocht.

Ook een abnormale doorbloeding van spieren kan invloed hebben op vermoeibaarheid bij mensen met SMA. Wanneer onvoldoende zuurstof naar de spieren getransporteerd wordt, heeft dat een negatief effect op de energiehuishouding van voornamelijk de rode en intermediaire spiervezels. Eerdere studies bij mensen met een meer ernstig aangedane vorm van SMA geven aanwijzing voor zo'n abnormale doorbloeding van de spieren.

Hoofddoelen van dit proefschrift

Bij de start van het schrijven van dit proefschrift stond een belangrijke vraag centraal: wat zijn de onderliggende oorzaken van vermoeibaarheid bij SMA? Dit heeft geleid tot het formuleren van een aantal kernvragen en hoofddoelen die ten grondslag liggen aan het werk in dit proefschrift.

1. Het ontwikkelen van motorische testen om vermoeibaarheid bij alle mensen met SMA objectief, valide en betrouwbaar te kunnen meten.
2. Het onderzoeken of sprake is van reservecapaciteit in de aansturing van motor units in spieren van mensen met SMA, en of die capaciteit verbeterd kan worden.
3. Het onderzoeken of een disfunctie van de mitochondriën in, en een abnormale doorbloeding van spieren van mensen met SMA een onderliggende oorzaak kan zijn van vermoeibaarheid.

De belangrijkste bevindingen van dit proefschrift

In **hoofdstuk 2** van dit proefschrift beschrijven we het onderzoek dat is gedaan naar de ontwikkeling van motorische testen voor mensen met SMA waarmee vermoeibaarheid gemeten kan worden. Met behulp van COSMIN (COnsensus-based Standards for the selection of health Measurement INstruments) richtlijnen en bestaande literatuur heeft een groep experts de belangrijkste kenmerken van de te ontwikkelen testen samengesteld. Eén van die kenmerken was dat de handelingen moeten lijken op dagelijkse bewegingen. Op basis hiervan zijn de volgende drie duurtesten ontwikkeld: de Endurance Shuttle Walk Test voor de loopfunctie, de Endurance Shuttle Box and Block Test voor de grove motorische armfunctie en de Endurance Shuttle Nine Hole Peg Test voor de fijne motorische armfunctie. Deze duurtesten (ESTs) bestaan uit herhalende cycli van het lopen over een afstand van 10 meter tussen twee pionnen, het verplaatsen van tien blokjes vanuit de ene bak, over een schotje naar de aangrenzende bak en het plaatsen en terugleggen van negen pinnetjes. Een audiosignaal geeft het tempo aan binnen welke tijd een cyclus afgerond moet zijn. Deze tijd wordt ingesteld op 75% van iemands eigen maximale snelheid om een cyclus af te ronden. De maximale duur van de ESTs was 20 minuten. Hoewel er in de literatuur een duidelijk onderscheid is tussen ervaren vermoeidheid (subjectief) en vermoeibaarheid (hier onderzocht) zullen beide fenomenen samen het duurvermogen van een persoon beïnvloeden. Bij de interpretatie van testresultaten moet dit dan ook altijd in acht genomen worden.

In **hoofdstuk 3** hebben we bij 70 patiënten en 19 controles (mensen zonder SMA) gekeken naar de intensiteit waarop de ESTs werden uitgevoerd. In vergelijking met de controles voerden mensen met SMA alle ESTs uit op een hoger, maar wel sub-maximaal, percentage van hun maximale spierkracht. Hiermee hebben we het sub-maximale karakter van de ESTs bevestigd voor mensen met SMA type 2 tot 4. Ook onderzochten we de spieractiviteit tijdens het uitvoeren van de drie ESTs. Oppervlakte elektromyografie (EMG) registratie is een methode om spieractiviteit tijdens inspanning te meten. Aan de hand hiervan hebben we onderzocht of mensen met SMA over reservecapaciteit beschikken om zo de test nog wat langer vol te kunnen houden. Deze studie wees uit dat een deel van de mensen met SMA inderdaad beschikt over reservecapaciteit tijdens het uitvoeren van een duurtest. In een ander onderzoek werd eerder verondersteld dat mensen met SMA deze reservecapaciteit niet hebben. Onze bevinding is belangrijk voor de ontwikkeling van toekomstige training- of medicatiestudies.

Het feit dat niet alle patiënten over reservecapaciteit beschikken tijdens de uitvoering van de ESTs heeft ertoe geleid dat we hebben onderzocht of de inname van het medicijn pyridostigmine hier verandering in kan brengen. Dit is een veelgebruikt medicijn bij mensen met Myasthenia Gravis. Myasthenia Gravis is een spierziekte waarbij signalen van de zenuwen niet of onvoldoende overgedragen worden aan de spieren waardoor deze

niet goed functioneren. In **hoofdstuk 4** hebben we opnieuw oppervlakte EMG gebruikt tijdens ESTs. Door middel van deze placebo gecontroleerde, dubbelblinde cross-over studie hebben we ontdekt dat pyridostigmine selectief zorgt voor extra reservecapaciteit in motor units met rode en intermediaire spiervezels waardoor het duurvermogen toeneemt. Omdat we geen effect vonden op de geleverde maximale kracht concludeerden we dat pyridostigmine waarschijnlijk niet werkt op de motor units met witte spiervezels. We vonden positieve effecten van pyridostigmine op een deel van de motor units wat aangeeft dat de werking van de neuromusculaire overgang, waar dit medicijn op werkt, afwijkend is. Wat er precies anders is bij deze spiervezels bij mensen met SMA en hoe pyridostigmine precies werkt, moet verder worden onderzocht.

In **hoofdstuk 5** hebben we met MRI-scans de anatomie van drie bovenarmspieren onderzocht. In het verleden is voornamelijk onderzoek gedaan naar de vervetting van beenspieren bij mensen met SMA. Nu is het ook gelukt om kwalitatief goede data van bovenarmspieren te verkrijgen. Met behulp van drie verschillende kwantitatieve MRI-technieken (DIXON, DTI en T2 sequentie analyses) hebben we onder andere de vervetting en ontstekingswaardes van de biceps-, triceps- en brachialisspier onderzocht. De belangrijkste bevinding was dat we een grotere vervetting van de triceps vonden in vergelijking met de brachialis en biceps. Ook was de vervetting niet gelijkmatig verdeeld over de spier. Dit gold voor zowel de triceps als de brachialis en is niet eerder gerapporteerd bij mensen met SMA. In de toekomst kunnen kwantitatieve MRI-analyses van bovenarmen mogelijk gebruikt worden om ziekteprogressie of therapierespons te meten. Verder onderzoek in grotere groepen is nog wel noodzakelijk om deze hypothese te toetsen.

De opvatting dat SMA meer is dan een ziekte van zenuwcellen wint terrein. Onderzoek in dierstudies en spierbiopten gaf aanleiding om ook de mitochondriële functie (batterijen van de cel) in skeletspieren tijdens inspanning te onderzoeken. In **hoofdstuk 6** bestudeerden we de mitochondriële functie van twee bovenarmspieren bij mensen met SMA. Dit hebben we gedaan met behulp van 31-fosfor magnetische resonantie spectroscopie (^{31}P-MRS). Bij deze techniek wordt gebruik gemaakt van een MR-scanner. In plaats van het maken van afbeeldingen zoals bij een MRI-scan, wordt met deze techniek de concentratie van verschillende stoffen in de spier gemeten. We kunnen deze concentraties meten tijdens rust, inspanning en het herstel. Vijftien patiënten en veertien controles hebben liggend een inspanningstest uitgevoerd waarbij de weerstand werd opgevoerd tot de armspieren volledig uitgeput waren. Bijzonder aan deze studie is het gebruik van een aangepaste ergometer zodat met de armen gefietst kon worden. Een beenfietstest zou voor de overgrote meerderheid van mensen met SMA onmogelijk zijn geweest door spierzwakte die het ernstigst is in de benen. We vonden dat mensen met SMA, in vergelijking met de controlegroep, bij een maximale inspanning meer rode en minder witte spiervezels hadden geactiveerd. Deze verschuiving in de spiervezelsamenstelling past goed bij de verminderde

spierkracht van deze mensen. Daarnaast konden we, aan de hand van het herstel van bepaalde stoffen, de mitochondriële functie in kaart brengen. Het energieherstel in rode en intermediaire spiervezels, verantwoordelijk voor duurvermogen, was bij mensen met SMA en de controles gelijkwaardig. Het energieherstel in witte spiervezels, verantwoordelijk voor grote kracht, was daarentegen wel vertraagd bij mensen met SMA. De conclusie van deze studie was dat mitochondriële disfunctie in witte spiervezels gedeeltelijk kan bijdragen aan vermoeibaarheid bij mensen met SMA maar dat het geen limiterende factor is.

In **hoofdstuk 7** beschrijven we het onderzoek naar de spieractiviteit en doorbloeding van spieren tijdens maximale inspanning om meer inzicht te krijgen in deze factoren in relatie tot vermoeibaarheid. Met deze reden hebben we ademgasanalyse, oppervlakte EMG en near infrared spectroscopie (NIRS) toegepast tijdens dezelfde test als beschreven in hoofdstuk 6, maar dan buiten de MR-scanner. Patiënten hielden de inspanningstest met de armen, net als bij de metingen in de scanner, minder lang vol dan de controles. We vonden een verhoogde ademarbeid en ventilatie bij mensen met SMA vergeleken met de controles. Oppervlakte EMG resultaten wezen uit dat mensen met SMA, net als bij de sub-maximale EST (hoofdstuk 3 en 4), ook reservecapaciteit hebben en dat inzetten bij het uitvoeren van een maximale inspanningstest. Opvallend is dat er op basis van de oppervlakte EMG data geen aanwijzing gevonden kan worden waarom patiënten stoppen met het uitvoeren van de taak. We concludeerden daarom dat reservecapaciteit in spieren geen limiterende factor is. Wanneer een spier actief wordt is daar zuurstofrijk bloed voor nodig. De haarvaten van een spier worden wijder zodat er voldoende zuurstof overgedragen kan worden aan de spier. Met behulp van NIRS hebben we geen aanwijzingen gevonden voor een probleem in de verwijding van deze haarvaten. Verwijding van haarvaten, met als gevolg een toename van de toevoer van zuurstofrijk bloed tijdens inspanning, vindt dus plaats bij zowel gezonde mensen als bij mensen met SMA. We concludeerden dat de toevoer van zuurstofrijk bloed naar de spieren geen beperkende factor is. De oorzaak voor vermoeibaarheid bij mensen met SMA type 3 en 4 lijkt dus, zoals ook gevonden in hoofdstuk 4, vooral de gestoorde functie van de neuromusculaire (van zenuw naar spier) overgang te zijn.

Conclusies van dit proefschrift

- Vermoeibaarheid is een functionele beperking tijdens het uitvoeren van dagelijkse activiteiten van kinderen en volwassenen met SMA en kan gemeten worden met de nieuwe uitkomstmaten: Endurance Shuttle Walk Test, Endurance Shuttle Box and Block Test en Endurance Shuttle Nine Hole Peg Test.

- Een deel van de mensen met SMA heeft de beschikking over een reservecapaciteit van motor units die ingezet kunnen worden wanneer vermoeibaarheid optreedt tijdens duurinspanning.

- Behandeling met pyridostigmine lijkt selectief effect te hebben op de reservecapaciteit van motor units met rode en intermediaire spiervezels wat verklaart waarom vermoeibaarheid wel vermindert maar spierkracht niet toeneemt.

- Kwantitatieve MRI-analyses van bovenarmspieren kunnen in de toekomst mogelijk bijdragen aan het in kaart brengen van ziekteprogressie en therapierespons.

- Spierzwakte in de bovenarmen van mensen met SMA kan worden verklaard door vervetting van de spieren en een verschuiving in spiervezelsamenstelling van witte naar meer rode spiervezels.

- ^{31}P-MRS is een veelbelovende niet invasieve methode om spieranatomie en mitochondriële functie tijdens dynamische inspanning bij mensen met SMA, maar ook andere neuromusculaire ziekten, in kaart te brengen.

- Op basis van bovenstaande studies is geen aanwijzing gevonden voor een energetische ('mitochondriële') component of probleem in de doorbloeding van spieren die primair bijdraagt aan de gemeten vermoeibaarheid bij mensen met SMA.

A

Dankwoord

Allereerst bedank ik alle kinderen en volwassenen die, met veel interesse en enthousiasme, door hun deelname aan de onderzoeken ervoor gezorgd hebben dat dit proefschrift inhoud heeft gekregen. Vaak ook zonder er zelf direct baat bij te hebben. Ik heb veel geleerd van jullie unieke verhalen en ik vond het op mijn beurt heel waardevol dat ik tijdens de onderzoeken de tijd kreeg om uit te leggen wat het onderzoek inhoudt en daarmee hopelijk ook kennis aan jullie over kon dragen. Een mooie balans tussen experts en specialisten!

Prof. dr. W.L. van der Pol, beste Ludo, bedankt voor de kans die je mij hebt geboden om direct na mijn afstuderen op zo'n inspirerende plek te mogen komen werken. Je hebt een onderzoeksteam samengesteld bestaande uit veel verschillende disciplines. Gedurende mijn promotietraject heb ik gezocht naar mijn plek binnen de groep, een voor mij ingewikkeld proces waarin ik vooral heel kritisch was op mezelf. Gelukkig kan de wetenschap, als het aan jou ligt, wel wat meer bescheiden onderzoekers gebruiken. Daarnaast heb je me ook geleerd trots te zijn op de unieke onderzoeken die we met het SMA-team uitvoeren. Ik zal de ontwikkelingen in de SMA-wereld met veel interesse blijven volgen!

Prof. dr. E.E.S. Nieuwenhuis, beste Edward, ik wil je graag bedanken voor de fijne gesprekken die we de afgelopen jaren, maar vooral in de laatste twee jaar, gevoerd hebben. Jij wist me steeds heel goed een spiegel voor te houden. Hiermee leerde je mij dat dit hele traject draait om het leren omgaan met … mijzelf. Het verhaal van de man, de slang en het touw zal ik in ieder geval nooit meer vergeten. Waar kan ik de titel psycholoog voor je aanvragen?

Dr. B. Bartels, beste Bart, toen ik in 2015 voor een kennismakingsgesprek het WKZ in liep had ik geen vermoeden dat ik hier een jaar later ook echt de eerste stappen in mijn carrière zou zetten. Wat ik wel wist is dat je een heel interessant verhaal vertelde, met aandacht voor details, over de rationale van de studie die je opgezet had over vermoeibaarheid bij patiënten met SMA. Als er iets is dat je mij de afgelopen jaren geleerd hebt, is het dat het formuleren van een rationale, nog voordat de studie, analyse of wat dan ook uitgevoerd wordt, een hele belangrijke stap is. Een stap in het proces dat vaak tekort gedaan wordt, maar waarvan je mij de noodzaak hebt laten inzien. Je hebt me ook geleerd te staan voor 'ons' onderzoek waarbij het belang van de patiënt hoog in het vaandel staat. Ik denk dat deze twee onderdelen van het wetenschappelijk onderzoek in een klinische omgeving hebben gemaakt dat ik dit traject heb kunnen volbrengen op een manier waar ik trots op ben. Dank je wel!

Dr. J.A.L. Jeneson, beste Jeroen, als er iemand is die mij geleerd heeft met mezelf om te gaan ben jij het wel. Want wat zijn wij elkaars 'opposite' qua karakter en werkstijl. Maar het mooie daarvan vind ik dat we een hele goede modus gevonden hebben om met elkaar samen te werken en hele mooie resultaten hebben neergezet! Daar ben ik heel trots op! Ik heb genoten van jouw tomeloze enthousiasme en passie voor de wetenschap. Bedankt voor het vertrouwen dat je mij, als beginnend onderzoeker, gegeven hebt.

Beste leden van de beoordelingscommissie, **prof. dr. C. Veenhof**, **prof. dr. K.P.J. Braun**, **prof. dr. D.W.J. Klomp**, **dr. S. Fuchs** en **prof. dr. N.L.U. Van Meeteren**, hartelijk dank voor de tijd en bereidheid dit proefschrift kritisch te lezen en te beoordelen.

Prof. dr. ir. D.F. Stegeman, beste Dick, hartelijk dank voor je gastvrijheid, geduld en interesse in de studies die we uitgevoerd hebben. We hebben een aantal middagen bij jou thuis, samen met een kop thee en een bak kruidnootjes, intensief de verzamelde sEMG-data geanalyseerd om zo een grote stap te kunnen maken in de interpretatie van deze data. Ik heb veel van je kunnen leren en ik vond het erg fijn om samen te kunnen werken!

Dr. J van der Net en **dr. T. Takken**, beste Janjaap en Tim, graag wil ik jullie als (voormalig) hoofd van de afdeling en hoofd van het onderzoek op de afdeling bedanken voor jullie hulp bij mijn promotietraject. De afgelopen jaren heb ik mij door jullie gesteund gevoeld en hebben jullie mij op de juiste momenten begeleid om dit traject tot een succes te maken.

Mijn dank gaat ook uit naar de beste paranimfen Marcella en Rosa. Lieve **Marcella**, dank je wel voor de leuke jaren samen op het Kinderbewegingscentrum! De maandagen waren altijd net wat leuker en gezelliger dan de rest van de week. Het was fijn om elkaars promotietraject te volgen, van elkaar te leren en samen bij te kletsen met een kop thee of koffie! Ik kijk ook uit naar jouw promotie en hoop dat we ook na deze tijd contact blijven houden. Lieve **Rosa**, een paar jaar geleden omschreef jij onze vriendschap al heel goed. Ik citeer: "Nothing compears to you. You're the apple to my eye. Jou met anderen vergelijken zou net zo onnozel zijn als appels met peren. Ik vind je een toffe peer en je bent de kers op mijn spreekwoordelijke taart. Ik zou het niet kunnen pruimen als ons mooie duo uit elkaar zou vallen." Tsja, daar is bijna alles wel mee gezegd, toch?! Ik kan altijd bij je terecht en alles is bespreekbaar. Dat is me heel dierbaar!

Beste collega's van het **SMA expertisecentrum**, bedankt voor de mooie leerzame tijd in deze multidisciplinaire omgeving. Ik heb veel geleerd van al jullie inzichten en presentaties op de donderdagochtend. Ik heb ook genoten van het SMA Europe congres in Evry waarin ik een aantal van jullie nog beter heb leren kennen. **Fay-Lynn**, **Christa** en **Angela**, jullie

wil ik graag bedanken voor al jullie werkzaamheden om het SMA onderzoek mogelijk te maken. Jullie zijn de spin in een soms ingewikkeld en groot SMA web! Zonder jullie hulp en overzicht is het niet mogelijk om zulke mooie onderzoeken te realiseren. **Renske**, **Camiel** en **Marloes**, jullie zijn, op onderzoeksgebied, mijn voorbeelden geweest de afgelopen jaren. Zeker in het begin was ik vaak onder de indruk van de discussies die tijdens het SMA-overleg gevoerd werden om zo het uiterste uit de studies en onszelf te halen. Ik heb veel van jullie geleerd en het was erg leuk om daarin ook jullie traject te kunnen volgen. Beste **Louise**, we zijn ongeveer tegelijk gestart met onze studie en ik heb steeds met bewondering geluisterd en gekeken naar jouw passie voor het MRI werk. Ik hoop dat je je op je plek voelt in je volgende uitdaging! Beste **Ewout**, bedankt voor het delen van je kennis om zo onze onderzoeken nog beter te maken. Ik heb jouw interesse en inzet voor diverse onderzoeken zeer gewaardeerd! Beste **Ruben**, dank voor alle statistische hulp! Maar vooral ook voor het geduld toen ik het in mijn hoofd haalde (want hoe moeilijk kon het nou zijn?) om R te gaan gebruiken voor de statistische analyses. Aan alle andere collega's binnen het SMA team wil ik graag kwijt dat jullie heel mooi werk afleveren! Ik ben benieuwd wat de toekomst nog meer gaat brengen.

Collega's van het **Kinderbewegingscentrum**, jullie wil ik graag bedanken voor de gezelligheid op de afdeling en jullie interesse in het onderzoek dat ik uitvoerde. Ik heb veel van jullie geleerd. Vooral toen ik mijn werkplek in de grote ruimte had en ik een hoop voor mij onbekende termen (stiekem) googlede om te weten te komen wat er allemaal speelde bij de kinderen op de poli en in de kliniek. Ik heb me steeds onderdeel van het team gevoeld. Dank daarvoor! Wie weet, hopelijk, komen we elkaar nog eens tegen in de toekomst! Beste **Erik** en **Janke**, dank jullie wel voor de fijne samenwerking en begeleiding. Beste **Annemiek**, **Sonja** en **Suzanne**, jullie wil ik graag bedanken voor alles wat jullie geregeld hebben om mijn onderzoek op de afdeling zo soepel mogelijk te laten verlopen. Maar dat niet alleen, wanneer andere collega's druk in de weer zijn, zijn jullie altijd in voor een fijn kletspraatje! Ik vond het altijd erg gezellig bij jullie!

Alle studenten, Tom, Lonneke, Isa, Luca en Heleen, dank je wel voor jullie inzet en enthousiasme tijdens het uitvoeren van metingen voor de MRS studie! Zonder jullie bijdrage was het een stuk moeilijker geweest alle data te verzamelen. Ik wens jullie een hele mooie toekomst waarin je jezelf nog meer kan ontwikkelen!

Collega's van het Amsterdam UMC, locatie AMC, afdeling Radiologie, beste **prof. dr. ir. A. J. Nederveen** en **dr. Melissa Hooijmans**, dank jullie wel voor de mooie tijd en voor jullie gastvrijheid. Niet alleen voor mij als externe onderzoeker, maar ook voor onze studenten en het belangrijkste, de onderzoeksdeelnemers! We hebben mooie dingen bereikt en ik ben

trots op onze samenwerking! Lieve **Sandra**, wat heb ik het naar mijn zin gehad in het AMC en wat was het gezellig om met jou samen te werken! Wat heb jij mooie plaatjes gemaakt (maar echt!), wat waren jouw zakjes thee lekker, wat hebben we tussendoor lekker gekletst, wat waren we een geoliede machine en wat zou de fiets zonder jou buurman-en-buurman-instinkt hebben gemoeten?! Dank je wel!

Eenieder die ik mogelijk vergeten ben, hartelijk dank voor jullie bijdrage aan alle studies waaraan we samen hard gewerkt hebben.

Lieve **teamies van VollinGo dames 1**, plezier hebben in wat je doet is het belangrijkste wat er is en jullie weten dat als geen ander! Ik kan me geen leven voorstellen zonder volleybal (Oké, na afgelopen tijd wel, maar dat bevalt me niet). Dank je wel voor jullie enthousiasme in het veld en voor jullie interesse in, en soms zelfs deelname aan mijn onderzoeken!

Lieve vrienden en familie, dank jullie wel voor de interesse in mijn promotietraject. Ook sommigen van jullie zijn daadwerkelijk een onderdeel van de data in dit proefschrift. De laatste loodjes duurden lang maar nu is het dan echt klaar! Dank je wel voor jullie support en afleiding tussendoor! Vooral de gezellige (spelletjes)avonden zijn mijn favoriet!

Lieve **Marcel** en **Anja**, lieve papa en mama, ik kan me nog goed herinneren dat jullie in augustus 2016 vertelden dat een promotietraject volgens mijn scriptiebegeleider wel eens goed bij mij zou passen. "Echt niet!", was daarop mijn antwoord... En zie hier wat de toekomst mij heeft gebracht. Jullie hebben de afgelopen jaren met veel belangstelling mijn ontwikkelingen in mijn eerste 'grote-mensen-baan' gevolgd en ik ben heel blij met jullie steun en adviezen! Het laatste jaar vond ik zwaar maar jullie hebben me er doorheen geholpen met lekkere kopjes thee en koffie en (stiekeme) knuffels! Lieve **Maurice**, jij bent een ster in doen wat je hart je ingeeft, vooral als dat precies het tegenovergestelde is van wat ik zou doen. Man, wat kan ik dat irritant vinden ;) Maar hé, je gaat hartstikke lekker en ik vind het leuk om jouw ontwikkelingen vanaf een afstandje te volgen. Ik wens je alle goeds en heel veel plezier en succes in het voltooien van de studie accountancy die je bent begonnen!

Lieve **Frank**, de belangrijkste persoon komt in een dankwoord vaak als laatst. Jij bent mijn beste maatje, knuffel, partner in crime, voice-over, bandlid, psycholoog, collega, vertaalmachine en ICT service desk. Ik ben heel dankbaar voor alle mogelijke manieren waarop je me altijd steunt als ik weer eens stress, aan het piekeren ben of geen keuze kan maken. "Andere mensen doen ook maar wat!" is een zin die je dan vaak herhaalde. Nu is het tijd voor nieuwe uitdagingen! Ik kijk er heel erg naar uit deze samen met jou aan te gaan!

About the author

Laura Eline Habets was born in Gouda on November 3rd, 1992. She grew up in Gouda and in 2011 she graduated from the Goudse Scholen Gemeenschap (GSG) Leo Vroman in Gouda. Already during high school, she became interested in the wonderful world of the human body, in particular the musculoskeletal system. She started the study Human Movement Sciences in 2011 at the Vrije Universiteit Amsterdam. A Minor psychomotor therapy, including a clinical internship at the department of personality disorders and eating disorders at PsyQ Haaglanden substantiates her broad interest in the human body. Laura obtained her bachelor's degree in 2014.

Right after this achievement, she started the Master Human Movement Sciences: Sport, Exercise and Health in 2014. Under supervision of dr. Bart Bartels, she did her research internship regarding fatigability in spinal muscular atrophy at the Center for Child Development, Exercise and Physical Literacy. This internship sparked the interest of Laura in neuromuscular disorders, especially spinal muscular atrophy. When the Masters programme of Musculoskeletal Physiotherapy Sciences was first accredited in 2015, she did not hesitate to continue her study. With a research project regarding ultrasound imaging of nerves in the upper arm of women with a history of breast cancer, she deviated from neuromuscular diseases but still explored the musculoskeletal system. She developed a special interest in working on the edge of clinical and basic science.

After completing both Masters in 2016, she returned to the Center for Child Development, Exercise and Physical Literacy at the Wilhelmina Children's Hospital to assist Bart Bartels for 14 months in his doctoral research regarding fatigability in spinal muscular atrophy. In 2017 she combined this position with her own PhD-project under the successful supervision of prof. dr. W.L. van der Pol and prof. dr. E.E.S. Nieuwenhuis. Her doctoral research focused on the working mechanisms of the skeletal muscle during exercise in patients with spinal muscular atrophy. Besides her research project, she enjoyed supervising Master students in their research internship.

Laura lives in Gouda. Quality time with friends and family is important for her. But above all, playing volleyball is her passion. The feeling of pleasure and freedom while playing volleyball perhaps is the driving force behind her fascination with the human musculoskeletal system.

A

List of publications

Bartels, B., de Groot, J. F., Habets, L. E., Wadman, R. I., Asselman, F.-L., Nieuwenhuis, E. E. S., van Eijk, R. P. A., Goedee, H. S., & van der Pol, W. L. (2020). Correlates of fatigability in patients with spinal muscular atrophy. Neurology, 10.1212/WNL.0000000000011230.

Bartels, B., Groot, J. F. De, Habets, L. E., Wijngaarde, C. A., Vink, W., Stam, M., Asselman, F., Eijk, R. P. A. Van, & Pol, W. L. Van Der. (2020). Fatigability in spinal muscular atrophy : validity and reliability of endurance shuttle tests. Orphanet Journal of Rare Diseases, 2, 1–9.

Bartels, B., Habets, L. E., Stam, M., Wadman, R. I., Wijngaarde, C. A., Schoenmakers, M. A. G. C., Takken, T., Hulzebos, E. H. J., Van Der Pol, W. L., & De Groot, J. F. (2019). Assessment of fatigability in patients with spinal muscular atrophy: Development and content validity of a set of endurance tests. BMC Neurology, 19(1), 1–10.

Habets, L. E., Bartels, B., de Groot, J. F., Ludo van der Pol, W., Jeneson, J. A. L., Asselman, F.-L., van Eijk, R. P. A., & Stegeman, D. F. (2021). Motor unit reserve capacity in spinal muscular atrophy during fatiguing endurance performance. Clinical Neurophysiology, 132(3), 800–807.

Stam, M., Wadman, R. I., Wijngaarde, C. A., Bartels, B., Asselman, F. L., Otto, L. A. M., Goedee, H. S., Habets, L. E., De Groot, J. F., Schoenmakers, M. A. G. C., Cuppen, I., Van Den Berg, L. H., & Van Der Pol, W. L. (2018). Protocol for a phase II, monocentre, double-blind, placebo-controlled, cross-over trial to assess efficacy of pyridostigmine in patients with spinal muscular atrophy types 2-4 (SPACE trial). BMJ Open, 8(7), 1–9.

Habets, L. E., Bartels, B., Asselman, F., Hooijmans, M. T., van den Berg, S., Nederveen, A. J., van der Pol, W. L., & Jeneson, J. A. L. (2021). Magnetic resonance reveals mitochondrial dysfunction and muscle remodelling in spinal muscular atrophy. Brain.

Melissa T. Hooijmans, Laura E. Habets, Sandra van den Berg, Fay-Lynn Asselman, Gustav J. Strijkers, Jeroen A.L. Jeneson, Aart J. Nederveen, Bart Bartels, W. Ludo van der Pol (2022). Multi-modal MR imaging of the upper arm muscles of patients with spinal muscular atrophy. NMR in Biomedicine.

Forthcoming

Marloes Stam, Camiel A. Wijngaarde, Bart Bartels, Fay-Lynn Asselman, Louise A.M. Otto, Laura E. Habets, Ruben P.A. van Eijk, Bas M. Middelkoop, H. Stephan Goedee, Janke F. de

Groot, Kit. C.B. Roes, Marja A.G.C. Schoenmakers, Edward E.S. Nieuwenhuis, Inge Cuppen, Leonard H. van den Berg, Renske I. Wadman, W. Ludo van der Pol. Randomized, double-blind, cross-over, phase 2 trial of pyridostigmine versus placebo in spinal muscular atrophy types 2,3 and 4.

Laura E. Habets, Bart Bartels, Jeroen A.L. Jeneson, Fay-Lynn Asselman, Ruben P.A. van Eijk, Dick F. Stegeman, W. Ludo van der Pol. Increased motor unit reserve capacity during endurance performance in spinal muscular atrophy patients treated with pyridostigmine.

Laura E. Habets, Bart Bartels, Fay-Lynn Asselman, Erik H.J. Hulzebos, Dick F. Stegeman, Jeroen A.L. Jeneson, W. Ludo van der Pol. Motor unit and capillary recruitment during fatiguing arm-cycling exercise in spinal muscular atrophy types 3 and 4.

Kim Kant-Smits, Erik H.J. Hulzebos, Laura E. Habets, Fay-Lynn Asselman, Esther S. Veldhoen, Ruben P.A. van Eijk, Janke F. de Groot, W. Ludo van der Pol, Bart Bartels. Respiratory muscle fatigability in patients with spinal muscular atrophy.

Presentations

International scientific conferences and presentations

Habets, L.E., Bartels, B., De Groot, J.F. Fatigability in children with neuromuscular diseases. Oral presentation. European Collage of Sport Science, July 4-7th 2018, Dublin, Ireland.

Habets, L.E., Mast, I.H., Hulzebos, H.J., Jeneson, J.A.L., Bartels, B., Van der Pol, W.L. Dynamic exercise muscle oxygenation in Spinal Muscular Atrophy. Poster presentation. ARTscientific, May 9-11th 2019, Egmond aan Zee, the Netherlands.

Habets, L.E., Bartels, B., Asselman, F., Hulzebos, H.J., Hooijmans, M.T., Van den Berg-Faay, S.A., Van der Pol, W.L., Jeneson, J.A.L. In vivo muscle ATP metabolism in SMA type 3 – Dynamic 31Phosphorus Magnetic Resonance Spectroscopy during exercise. Poster presentation. CureSMA, June 28-30th 2019, Orlando, United States of America.

Habets, L.E., Bartels, B., Asselman, F., Hulzebos, H.J., Hooijmans, M.T., Van den Berg-Faay, S.A., Van der Pol, W.L., Jeneson, J.A.L. Handbike platform for in vivo 31P MRS study of arm muscle ATP metabolism in Spinal Muscular Atrophy. Oral and poster presentation. MYO-MRI, November 17-19th 2019, Berlin, Germany.

Habets, L.E., Bartels, B., Asselman, F., Hulzebos, H.J., Hooijmans, M.T., Van den Berg-Faay, S.A., Van der Pol, W.L., Jeneson, J.A.L. In vivo upper arm ATP metabolism during dynamic exercise in SMA type 3 and 4. Oral and poster presentation. SMA Europe, February 5-7th 2020, Evry, France.

Habets, L.E., Bartels, B., Asselman, F., Hulzebos, H.J., Hooijmans, M.T., Van den Berg-Faay, S.A., Van der Pol, W.L., Jeneson, J.A.L. Fast-to-slow remodeling and lower oxidative capacity of upper arm muscles in SMA type 3 and 4. Oral presentation. CureSMA, June 11th 2020, Online.

Habets, L.E., Bartels, B., Asselman, F., Hulzebos, H.J., Hooijmans, M.T., Van den Berg-Faay, S.A., Van der Pol, W.L., Jeneson, J.A.L. In vivo mitochondrial dysfunction in white but not red muscle fibers of patients with SMA. Poster presentation. CureSMA, June 11th 2021, Online.

Habets, L.E., Bartels, B., Asselman, F., Hulzebos, H.J., Hooijmans, M.T., Van den Berg-Faay, S.A., Van der Pol, W.L., Jeneson, J.A.L. Increased motor unit reserve capacity during endurance performance in spinal muscular atrophy patients treated with pyridostigmine. Oral presentation. CureSMA, June 11th 2021, Online.

National scientific conferences and presentations

Habets, L.E., Bartels, B., Asselman, F., Van der Pol, W.L., Jeneson, J.A.L. Energiehuishouding tijdens inspanning – MRI-studie bij mensen met SMA type 3 en 4. Poster presentation. Spierziektencongres, September 15th 2018, Veldhoven, the Netherlands.

Otto, L.A.M., Habets, L.E., Van der Pol, W.L., Froeling, M., Jeneson, J.A.L., Bartels, B., Wadman, R.I., Wijngaarde, C., Stam, M., Scheijmans, F., Van der Woude, D., Asselman, F., Van Ekris, C. Onderzoek naar spieren bij SMA. Poster presentation. Spierziektencongres, September 14th 2019, Veldhoven, the Netherlands.

Presentations for professionals and other activities

Habets, L.E. Exercise-induced fatigue in young people: advances and future perspectives. Artikelbespreking. Wilhelmina Kinderziekenhuis, March 7th 2019, Utrecht, the Netherlands.

Habets, L.E. Exercise intolerance in SMA type 3 and 4 – In vivo upper arm ATP metabolism during dynamic exercise. Oral presentation. Biogen, September 14th 2020, Utrecht, the Netherlands.